TECHNICAL REPORT STANDARD TITLE PAGE

1. Report No.	2. Government Accession No.	3. Recipient's Catalog No.
FHWA/TX-87+459-1		

4. Title and Subtitle	5. Report Date
STABILIZED SUBBASE FRICTION STUDY FOR CONCRETE PAVEMENTS	April 1987
	6. Performing Organization Code

7. Author(s)	8. Performing Organization Report No.
James W. Wesevich, B. Frank McCullough, and Ned H. Burns	Research Report 459-1

9. Performing Organization Name and Address	10. Work Unit No.
Center for Transportation Research The University of Texas at Austin Austin, Texas 78712-1075	11. Contract or Grant No. Research Study 3-8-86-459
	13. Type of Report and Period Covered
12. Sponsoring Agency Name and Address Texas State Department of Highways and Public Transportation; Transportation Planning Division P. O. Box 5051 Austin, Texas 78763-5051	Interim
	14. Sponsoring Agency Code

15. Supplementary Notes

Study conducted in cooperation with the U. S. Department of Transportation, Federal Highway Administration. Research Study Title: "Development of Subbase Friction Information for Use in Design of Concrete Pavement"

16. Abstract

Previously, research and testing have been carried out on loose unbinded subbases to determine their frictional characteristics concrete pavement movements. Stabilizing agents, such as asphalt, cement, and lime, are now being added to subbases to prevent pumping of subbase material from under pavements under saturated conditions. This report includes past experimental work performed on these outdated subbases, along with experimental work performed within this project on stabilized subbases. A survey was carried out in order to determine the subbases most used presently and expected to be used in the future by the Texas State Department of Highways and Public Transportation. A theoretical explanation of subbase frictional behavior and its effect on concrete pavements is also given. Recommendations are given for additional investigation, to include additional stabilized subbases not tested and stabilized subbases at varying depths with different moistures and temperatures to observe their effect on subbase friction.

17. Key Words	18. Distribution Statement
subbase, friction, concrete pavements, induced movements	No restrictions. This document is available to the public through the National Technical Information Service, Springfield, Virginia 22161.

19. Security Classif. (of this report)	20. Security Classif. (of this page)	21. No. of Pages	22. Price
Unclassified	Unclassified	196	

Form DOT F 1700.7 (8-69)

STABILIZED SUBBASE FRICTION STUDY FOR CONCRETE PAVEMENTS

by

James W. Wesevich
B. Frank McCullough
Ned H. Burns

Research Report 459-1

Development of Subbase Friction Information for Use in Design of Concrete Pavement
Research Project 3-8-86-459

conducted for

Texas State Department of Highways
and Public Transportation

in cooperation with the
U.S. Department of Transportation
Federal Highway Administration

by the

Center for Transportation Research
Bureau of Engineering Research
The University of Texas at Austin

April 1987

The contents of this report reflect the views of the authors, who are responsible for the facts and the accuracy of the data presented herein. The contents do not necessarily reflect the official views or policies of the Federal Highway Administration. This report does not constitute a standard, specification, or regulation.

PREFACE

This report is part of Research Project 3-8-86-459, entitled "Development of Subbase Friction Information for Design of Concrete Pavement." The study described was conducted as a part of the overall research program for the Center for Transportation Research, Bureau of Engineering Research, at The University of Texas at Austin. The study was sponsored jointly by the Texas State Department of Highways and Public Transportation and the Federal Highway Administration under an agreement with The University of Texas and the Texas State Department of Highways and Public Transportation.

Special appreciation is expressed to Carl Bertrand, Lyn Gabbert, Josef Fabiar, and Todd Thurber for their help in experimentation and the organization of this report; and to all of the Center for Transportation Research staff members who assisted in the production of the final draft of this report.

LIST OF REPORTS

Report No. 459-1, "Stabilized Subbase Friction Study for Concrete Pavements," by James W. Wesevich, B. Frank McCullough, and Ned H. Burns, presents (a) a review of all available literature on subbase friction studies; (b) a theoretical explanation of subbase friction and its effect on concrete pavements; (c) results of experiments to determine concrete pavement behavior over several stabilized subbases; (d) results of push-off tests run on several stabilized subbases; and (e) results of a state–wide survey to determine the subbases most used under concrete pavements.

ABSTRACT

Previously, research and testing have been carried out on loose unbound subbases to determine their frictional characteristics concrete pavement movements. Stabilizing agents, such as asphalt, cement, and lime, are now being added to subbases to prevent pumping of subbase material from under pavements under saturated conditions. This report includes past experimental work performed on these outdated subbases, along with experimental work performed within this project on stabilized subbases. A survey was carried out in order to determine the subbases most used presently and expected to be used in the future by the Texas State Department of Highways and Public Transportation. A theoretical explanation of subbase frictional behavior and its effect on concrete pavements is also given. Recommendations are given for additional investigation, to include additional stabilized subbases not tested and stabilized subbases at varying depths with different moistures and temperatures to observe their effect on subbase friction.

KEYWORDS: Subbase, friction, concrete pavements, induced movements.

SUMMARY

The Center for Transportation Research of The University of Texas at Austin was commissioned in 1985, by the Texas State Department of Highways and Public Transportation, to gather friction information on stabilized subbases being used under concrete pavements. The culmination of this study is to provide subbase friction profiles for determining concrete and steel stresses due to horizontally induced movements over stabilized subbases. The designation given to this study was Project 459 and is under the direction of Dr. B. Frank McCullough and Dr. Ned H. Burns.

This report covers initial research performed on several frequently used stabilized subbases. A survey was also carried out to determine the most popular present and future subbases to be used throughout the state by the Texas State Department of Highways and Public Transportation. Past experimental results on outdated loose unbound subbase were reviewed, and are presented within this report, so that frictional magnitudes and behaviors could be compared with results obtained using stabilized subbases. Many friction-movement profiles were obtained and are illustrated in this report. It was determined that slab weight had a direct effect on frictional resistance for loose unbound subbases and only a slight effect for stabilized subbases. The sliding plane was observed to be at the slab-subbase interface for loose unbound subbases and to be within the subbase for stabilized subbases. The magnitude of frictional resistance was much higher for stabilized subbases than for unstabilized subbases. Higher frictional restraints cause higher concrete and steel stress, the very reason for obtaining subbase friction information for stabilized subbases as opposed to unstabilized subbases. Further experimention is recommended, to include all stabilized subbase used in the state and to further test for sensitivity of subbase friction on moisture, temperature, varying construction techniques, varying subbase depths, and varying subbase-subgrade combinations.

IMPLEMENTATION STATEMENT

This report provides the missing link of information on subbase resistance that may be used in concrete pavement design for estimating the amount of reinforcement, joint spacings and joint sealant design. The subbase resistance information presented in Table 7.3 may be used directly in the CRCP, JRCP, and PCP programs, as well as in the AASHTO Pavement Design Guides, to provide a more precise design.

TABLE OF CONTENTS

CHAPTER 1. BACKGROUND FOR SUBBASE FRICTION STUDY

This chapter gives a basic definition of subbase friction and its role in concrete pavement behavior. The scope of the research project presented in this report is also given.

INTRODUCTION

When a design engineer designs a structural member, a major part of its design lies in characterizing the loads that are applied to the member. If, for example, the member is a beam for a bridge, then the engineer accumulates information to use as the expected live and dead loads on the member. In most building codes, a safety factor is selected and the member is then sized. Whether the member is a beam for a bridge or a column in a building, it is highly unlikely that these members will ever experience stresses that exceed their limits and cause cracking or failure, because of the safety factor used during their design.

Concrete pavements offer the designer a greater challenge than beams and columns. Not only must the vehicle loads be derived, but environmental loads must also be determined. These environmental loads may also cause cracking, not only during the pavement's service life but also during its construction phase as the concrete gains strength. Therefore, the designer must consider the concrete's properties, starting at placement, along with the magnitude of the environmental stresses the pavement is subjected to.

SUBBASE FRICTION

Subbase friction is one component of these environmental loads. As the pavement experiences moisture and thermal changes, it will try to slide against the resistance being offered by its supporting subbase. The magnitude of this resistance must be accurately measured if the pavement is to behave as designed. If the pavement is jointed, then it should not experience any cracking. If it is a continuous pavement, where cracking is allowed, then it should have the designed crack spacing and crack width. The magnitude of subbase friction must therefore be estimated properly if the pavement's behavior is to achieve its designed purpose.

SCOPE OF PROJECT

Most subbase friction information known today has been outdated by the change in subbases used under concrete pavements. The subbases used many years ago were soft, loose, and unbound, such as sand, gravel, and clay. Many pavements experienced failure due to pumping of loose subbase material during saturated conditions. Subbase material would be shoved out to varying degrees after each passing vehicle caused an increase in pore-water pressure under saturated subbase conditions. This behavior created voids under the pavement, leaving the concrete unsupported and, thus, more susceptible to failure by flexure.

Today, stabilizing agents are added to the subbase materials to prevent this failure mechanism from occuring. These agents bind the material together to resist pumping. They also fill previous voids that were used as pathways for water entry, thus keeping the subbases drier. Subbase strengths are also increased by the addition of these stabilizing agents. Some of these agents are lime, cement, and asphalt.

Few studies have been performed on these stabilized subbases with respect to their frictional behavior. The only major experimental work performed in the past was on the out–dated subbases. Because the frictional resistance magnitude is a needed parameter in the design of a functional concrete pavement, a study was performed at the Center for Transportation Research to obtain subbase friction information on these stabilized subbases. It was sponsored by the Federal Highway Administration and the Texas State Department of Highways and Public Transportation. This report reveals the results of past experimental work on subbase friction and of the experimental work performed during this project. All experimental work was performed on actual field locations, which gave a better representation of actual pavement behavior over various stabilized subbases.

CHAPTER 2. INTRODUCTION TO SUBBASE FRICTION UNDER CONCRETE PAVEMENTS

This chapter gives a more in depth definition of subbase friction by defining all of its components. The chapter also discusses the effect of subbase friction on concrete pavements with respect to concrete stresses, steel stresses, and slab movements.

DEFINITION OF SUBBASE FRICTION

During the life of concrete pavements there is constant movement in the horizontal and vertical directions. These movements are caused by several variables. Daily and seasonal temperature and moisture variations cause both contraction and expansion in the horizontal plane of the slab. When temperature and moisture vary along the depth of the slab, vertical movements are experienced and these are termed curling effects in the slab. The slab's weight will always act to resist these curling effects. Horizontal movements are resisted by friction at the interface of the bottom of the slab and the surface of the subbase on which the slab lies. This resistance in the horizontal direction is termed subbase friction.

COMPONENTS OF SUBBASE FRICTION

Three components can be combined to represent the total effect of subbase friction. Figure 2.1 denotes these three components in a large scale view of the interface where the concrete slab and the subbase meet. The figure shows that adhesion, bearing, and shearing all play a role in the total resistance of the slab as it tries to move.

In traditional physics, the hypothesis is made that there is a linear relationship between the nominal weight of the object to be moved and the amount of friction that it encounters as it tries to slide. This holds true for an ideal system if two boundary conditions are met. The first is the elimination of all adhesion between the two surfaces, because adhesion will not behave linearly with the nominal weight of the slab. The secondary boundary condition is that there are no deformations in the subbase or concrete to alter the interface profile. If these two conditions are assumed, the shear component is linearly dependent on the nominal force, which is directly dependent on the weight of the slab.

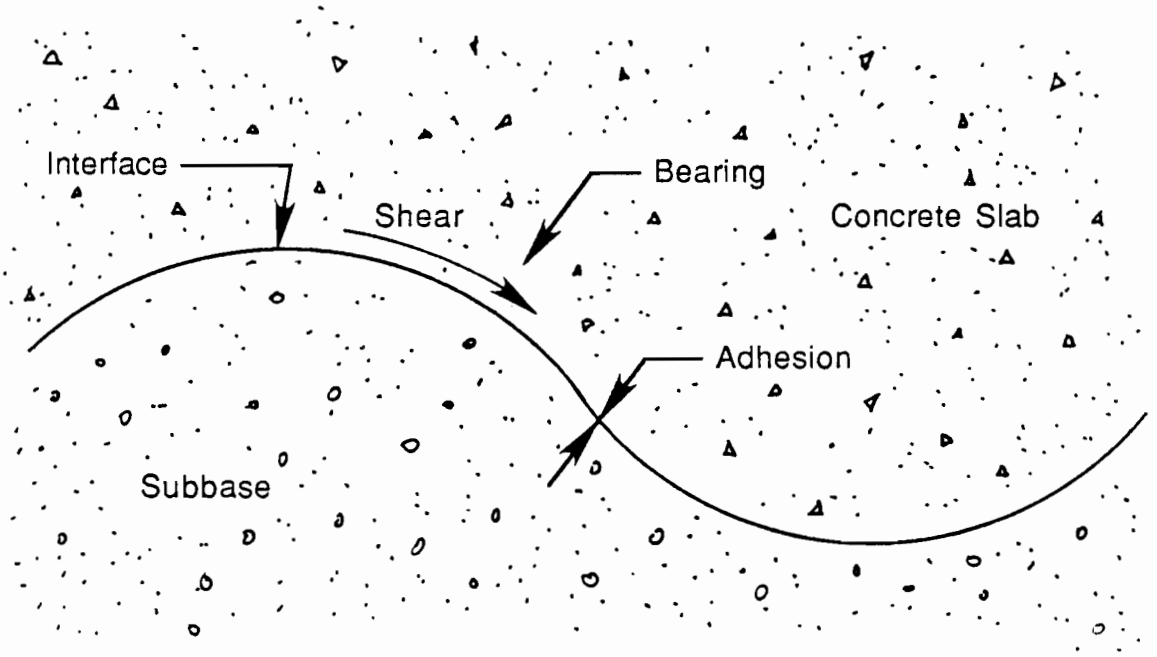

Fig 2.1. A conceptual illustration of the subbase friction components at interface of the concrete pavement slab and the subbase.

In everyday pavement construction, these boundary conditions do not hold. Asphalt is being introduced into several subbases, thus increasing the role of adhesion between the slab and its subbase. The pavement and subbase are not rigid materials; they are both elastic materials. The concrete and the subbase have different elastic properties so that for a given nominal force the two materials will deform in different proportions, therefore changing the interface profile. When these actual conditions are brought into focus, it is unrealistic to assume the hypothesis of linearity between nominal weight and the friction force between two materials.

As shown in Fig 2.1 three components make up the total effect of subbase friction. They are defined below.

Adhesion

Adhesion is the attraction the slab experiences relative to its subbase. This phenomenon can be thought of as a gluing action at the slab-subbase interface. Its magnitude is dependent on the components of the binder materials mixed into the subbase, and the moisture and temperature conditions. If the adhesion component is large enough, failure at sliding may be within the subbase itself.

Bearing

The bearing component is dependent on several parameters. Its direction is dependent on the roughness of the subbase surface at casting and can change depending on how the subbase reacts to the force that the slab is inducing. The subbase reaction to a given force is also dependent on the temperature and the moisture condition of the subbase.

Shear

The shear component is dependent on the rubbing characteristics of the two materials in contact when movement begins. This will vary along the interface due to the fact that different materials make up the concrete and different materials make up the subbase. It will also vary along points of contact because its magnitude is also dependent on the magnitude and

direction of the bearing component, or in other words, how much or in what way the two materials are being squeezed together at that particular location.

EFFECT OF SUBBASE FRICTION ON CONCRETE PAVEMENTS

The importance of understanding concrete pavement behavior, such as material stresses and movements, lies in the design and functional characteristics of the pavement. A parameter that plays a large role in the behavior of concrete pavements is subbase friction. Its impact will affect every material involved in the design. Its impact will also affect material movements which affect the riding quality of a pavement. The following gives a better explanation of how subbase friction affects concrete pavements with respect to (1) concrete stress, (2) steel stress, and (3) slab movements.

Concrete Stress

As a concrete pavement expands or contracts due to changing environmental conditions, such as moisture and temperature, the subbase frictional resistance will act in the direction opposite to the pavement's movement. This partial restraint will induce stresses into the concrete. If the pavement is expanding, the subbase friction will cause compressive stresses in the concrete. If it is contracting, the concrete will be in tension. Because concrete is strong in compression and weak in tension, its compressive strength will never be exceeded, due to this partial restraint, but tensile capacities are often exceeded and the pavement cracks.

Steel Stress

Steel reinforcement is added to jointed reinforced concrete pavements to help prevent midspan cracking. On the other hand, steel reinforcement is not used in continuously reinforced pavements to prevent cracking, but to control the crack width and crack spacing once cracks are formed. Since the reinforcement is bonded directly to the concrete, its stresses are largely affected by subbase friction. Prestressed concrete pavements are being introduced in today's pavements and the strands that keep the pavement in its compression region are affected in the same manner, as the slabs try to expand and contract. Subbase

friction will also affect the total effective jacking force that the strands are inducing on the concrete because the elastic shortening of the concrete during the jacking operations causes movements at the concrete-subbase interface.

Slab Movements

Concrete pavement movement refers to the movements at the joints for jointed, reinforced, and post-tensioned slabs. In other words, the design must consider the allowable opening of these joints over its service life with consideration of the riding quality of the vehicles passing over them. More importantly, the joint opening determines the amount of joint sealant needed and also the load transfer capacity of the joint. How much a joint opens up is dependent mostly on the joint spacing and the magnitude of the subbase friction that resists slab movements.

From a structural point of view, it is sometimes important to carry the shear and moment across the joint to reduce the impact load of the wheel as it passes from one slab to another. This is accomplished by using conventional reinforcement or various forms of dowel bars that permit movements at the joints. The bar sizes depend on the loads to be transferred across the expected joint opening. This expected joint opening is dependent on the joint spacing and the magnitude of its subbase friction against movements.

Continuously reinforced pavements must be designed to control crack spacing and crack widths to also insure their structural integrity. There is an upper limit for the crack width so that there is enough aggregate interlock between the two faces to transfer the load across the crack without pavement damage such as spalling. The subbase resistance will determine crack width and spacing with a given steel reinforcement percentage. If the magnitude of subbase resistance is overestimated, the crack spacing and crack width will be larger than expected. That would allow water penetration into the crack and result in improper aggregate interlock in transferring loads across the crack. If the magnitude of subbase resistance is underestimated, the crack spacing and crack width will be smaller than expected. The latter condition is of concern since the crack spacing may be so small that the transverse direction dominates the design, instead of the longitudinal direction. Cracks would then begin to form in the longitudinal direction and punchout failures would occur. And if a small steel percentage was used in the transverse direction, the crack widths might be large enough for water penetration.

In conclusion, the magnitude of resistance due to subbase friction is not a question of being above or below a certain amount; rather, its magnitude must be so that the predicted behavior of concrete pavements with relation to joint openings, crack widths, and crack spacings will be as observed in the field. Once a pavement designed with an erroneous estimated subbase frictional resistance has been constructed, it is too late to modify joint spacings and steel percentages.

FACTORS THAT INFLUENCE THE SUBBASE FRICTIONAL EFFECT

Given a certain type of subbase, there are many factors that can influence its effect on the overlying pavement. All of these factors influence pavement movements in which the subbase tries to resist. These parameters include the concrete coefficient of thermal expansion, the magnitude of daily temperature cycles, joint spacing, shrinkage, and moisture variations.

The first two parameters go hand-in-hand. How much a pavement tries to expand and contract due to temperature is dependent on the concrete's coefficient of thermal expansion and the magnitude of the change in daily temperature. The thermal coefficient of expansion is mostly dependent on the coarse aggregate type, because it is the major component in the mix design. Its values lie somewhere between three micro-strains per degree Farenheit and eight micro-strains per degree Farenheit (Ref 1). Daily slab temperature cycles can amount to as much as 20 to 30 degrees Farenheit or more. Slab temperatures are largely affected by the amount of cloud cover. Its heating is largely by absorption of solar radiation and can often exceed ambient temperatures for this very reason. Figure 2.2 shows slab and ambient temperature cycles for a 4-inch pilot slab used in conjunction with this project in Austin, Texas, on a clear and dry summer day. Note that the slab temperatures are far above ambient temperatures, with roughly a 25 to 30 degree Farenheit slab temperature differential for a 24–hour period.

The longer the slab is, the larger are the potential movements. Therefore, the joint spacing is an important parameter. Obviously a 30-foot joint spacing will experience smaller joint openings than a 50–foot joint spacing if equal temperature cycles are applied. The length of each individual slab will depend on how each of the other parameters that create pavement movements will be magnified.

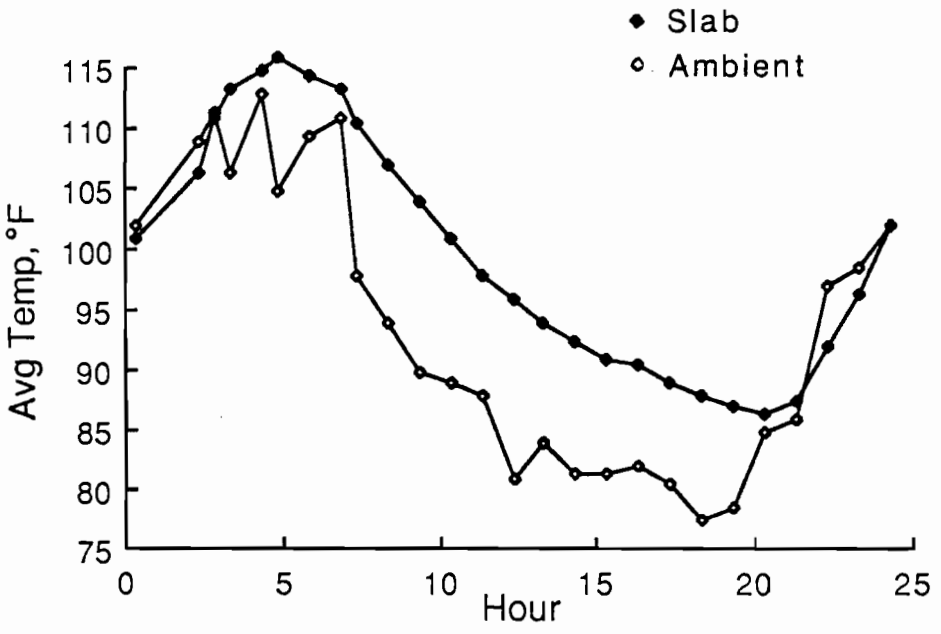

Fig 2.2. Slab and ambient temperature versus hour on pilot test slab in Austin, Texas.

The last two parameters also go hand-in-hand. From the time the concrete pavement is cast to the end of its service life, it will try and expel a portion of its original water content. This loss of water causes the concrete to shrink. Total concrete shrinkage with most of it occurring within the first month after casting, can range from 300 to 800 micro-strains and is also largely dependent on the aggregate type. Its rate is also dependent on the rate of hydration and the ambient moisture conditions after casting (Ref 2). There can also be moisture variations during the life of the pavement that can cause expansion, or, in other words, reverse the shrinkage process. This is mostly typical of dry arid climates; when there are brief heavy rains the pavements start absorbing moisture.

SUMMARY

Subbase friction is the amount of resistance a pavement experiences as it trys to move over its underlying support. The magnitude of resistance is dependent on three components, namely adhesion, bearing, and shear at the slab-subbase interface. All three components are dependent on the bonding properties of the subbase and the surface conditions of the subbase at placement of the pavement. Subbase friction is an environmental factor that affects concrete stresses, steel stresses, and slab movements, which are all important to the behavior of a functional pavement. Because slab movements induce subbase friction, all factors that affect movements play a role in determining how much impact subbase friction is being applied to the pavement. These factors are the concrete's coefficient of thermal expansion, the magnitude of daily temperature cycles, joint spacing, shrinkage, and moisture variations. Not only these factors but also the magnitude of subbase friction must be evaluated accurately to predict the behavior of concrete pavements in the field.

CHAPTER 3. LITERATURE REVIEW

The objective of this chapter is to give a deeper explanation of subbase friction. It begins with an explanation of friction between two objects from the traditional statics and dynamics approach. The chapter also reviews all the important experimental work performed in the past. The results and hypotheses of each experiment performed are also discussed. Finally, as opposed to the traditional approach, an overview is made of past experiments to characterize subbase friction into general behaviors.

CLASSICAL FRICTIONAL MODEL

When one studies traditional statics and dynamics, the model used to describe frictional behavior is a block with a certain weight, W, resting on a flat surface being subjected to a horizontal force, P. The reactions to these forces are N, the nominal force equal to W, and F, the frictional force equal to or less than P. Figure 3.1 shows the orientation of these forces. As the P loading increases so does the frictional resistance, at the same rate, and they are said to be in equilibrium with each other until a maximum is reached. This maximum is usually referred to as the static coefficient of friction, which is the peak frictional force divided by the nominal weight of the object (F_m/N). As soon as the maximum frictional resistance force is exceeded, the block begins to move and the frictional resistance drops to its maximum dynamic frictional resistance, F_K. The dynamic coefficient of friction will always be less than the static coefficient of friction and can be computed in the same manner (F_K/N). The properties of these two coefficients, from Ref 3, are

(1) independent of the normal force,
(2) dependent on the nature of the surfaces in contact and the exact condition of the surfaces, and
(3) independent of the area of the surfaces in contact.

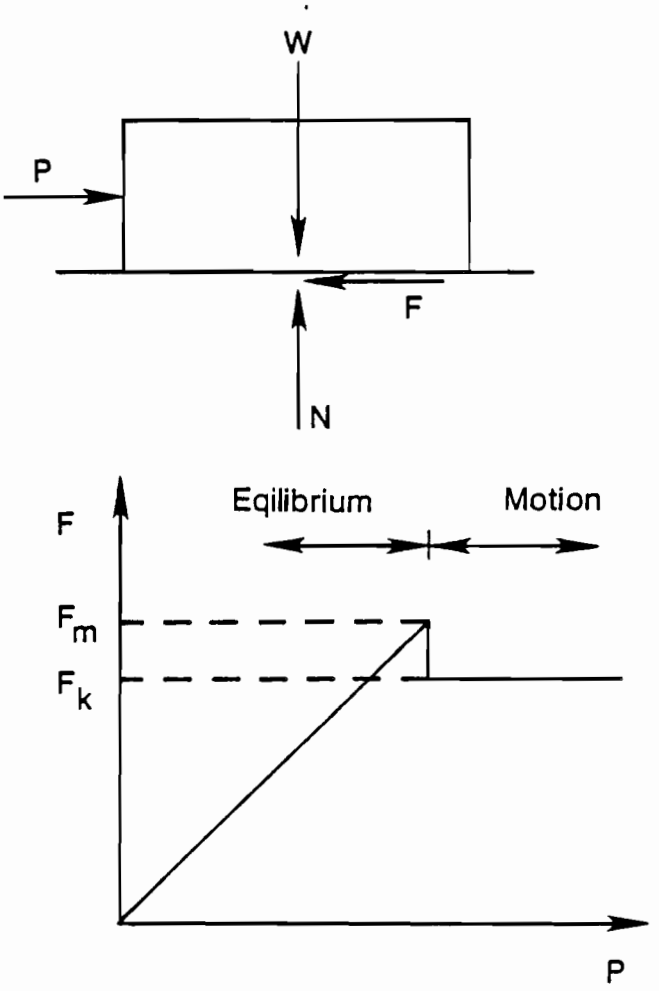

Fig 3.1. Classical friction model (Ref 3).

FRICTIONAL RESISTANCE UNDER CONCRETE PAVEMENTS

Frictional forces develop when a slab contracts as a result of a temperature drop, moisture reduction, concrete shrinkage, and creep. As the slab contracts, the movements are resisted by the friction at the interface. The resistance to movement produces a direct tensile stress in the concrete. The local movements of the slab increase from zero at the center to a maximum at the edges. The tensile stresses produced in the slab by the restraint decrease from a maximum at the geometric center to zero at the free edges since the frictional resistance to movements builds up from the slab ends. The higher the restraint, the higher will be the tensile stresses generated along the slab length. This situation is graphically presented in Fig 3.2 (Ref 4).

These tensile stresses are important since they may be added to those tensile stresses caused by traffic and restrained thermal warping to such an extent that the slab may crack. Also, in prestressed concrete road slabs, these tensile stresses will cancel some of the compressive stresses induced in the slab. The minimizing of subgrade restraint under prestressed concrete road slabs is usually sought because of the amount of prestress, hence the cost is directly related to these tensile stresses induced by the subbase restraint (Ref 5). The role of a friction reducing medium is to reduce the tensile stresses by reducing the frictional restraint between the slab and its underlying surface. This can lead to a reduction in steel for conventional jointed reinforced pavements and prestressed pavements. Also, with less frictional restraint the post-tensioning will work more effectively. Higher compressive prestress can be achieved at every point along the slab for a given post-tensioning force since loss due to restraint of the force applied at the ends through the tendon anchorages will be reduced. This condition is shown in Fig 3.3 (Ref 4). The decision to use a particular friction reducing medium is, from Ref 5, based on

(1) efficiency in reducing restraint,
(2) practicability for road construction, and
(3) economics.

Studies have been conducted since 1924 to study the nature of the frictional resistance under concrete pavements. Some of the observations and results during these tests are presented below.

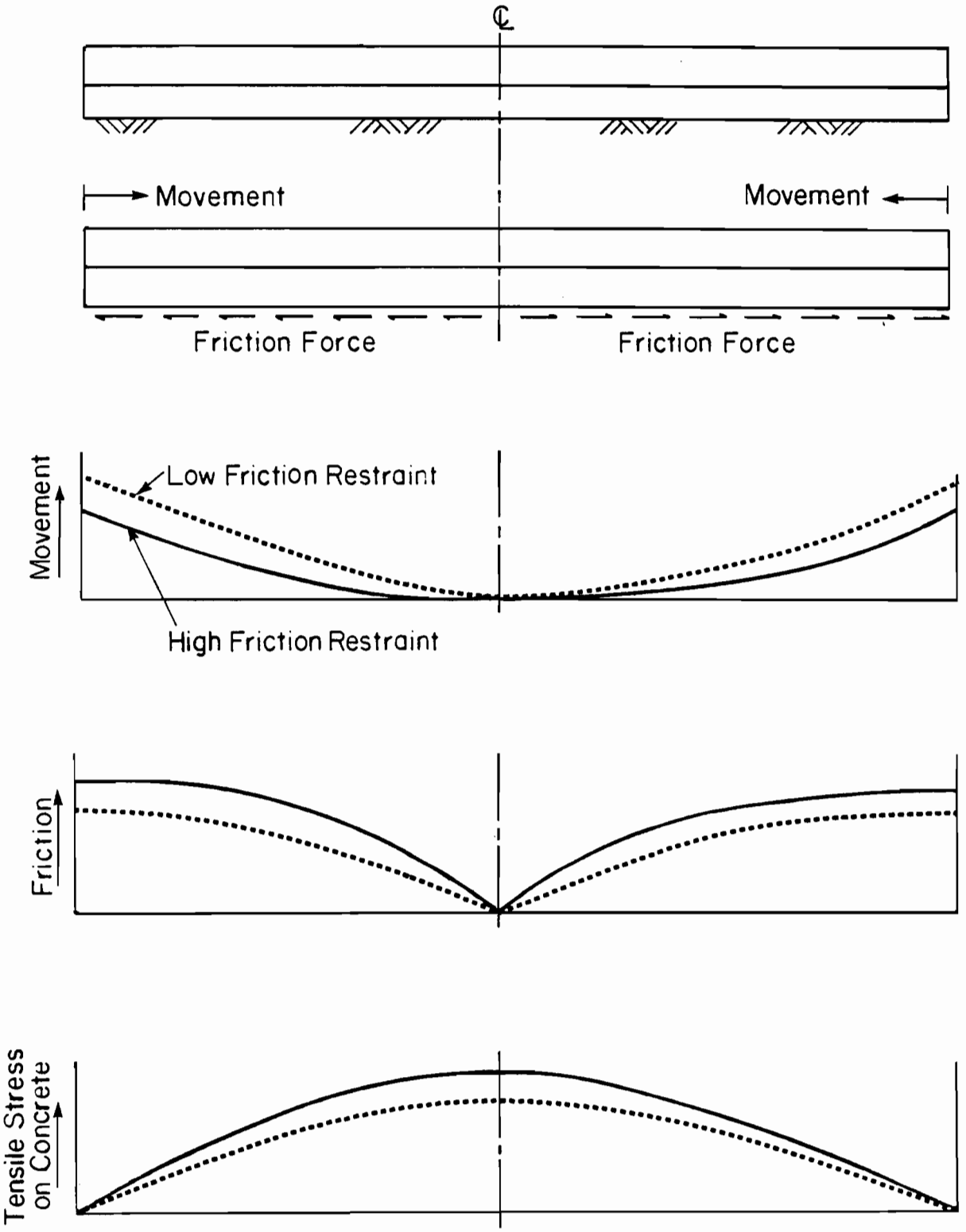

Fig 3.2. The effect of subbase restraint on the concrete's tensile stresses due to frictional resistance against movements.

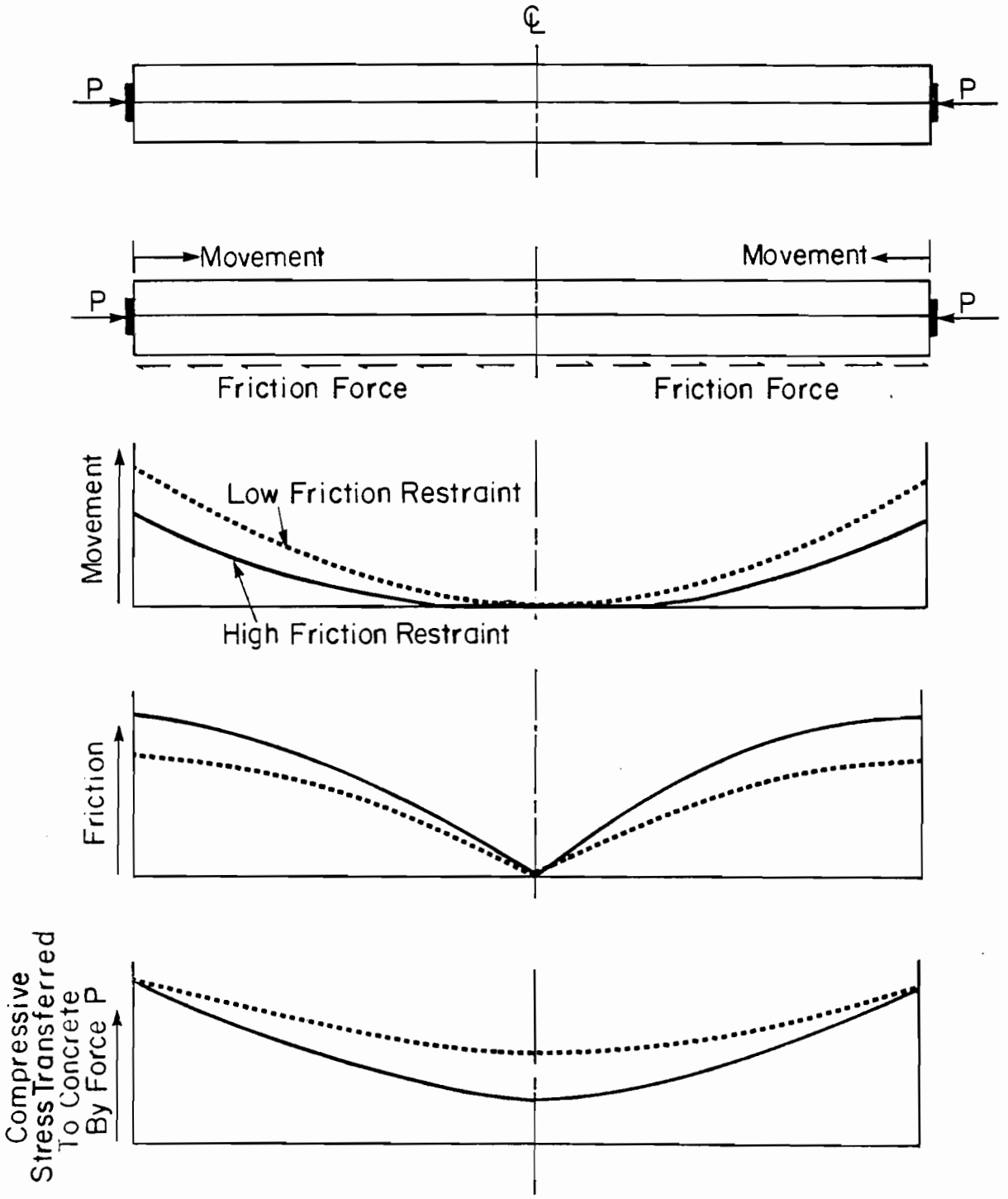

Fig 3.3. Effect of frictional restraint on the compressive stress transferred to the concrete by the post-tensioning for P.

Westergaard (Ref 10)

Westergaard shed additional light on subbase friction when he looked at it from a two dimensional point of view. In order to explain his analysis, it will be desirable to describe in general terms the behavior of a pavement when its temperature decreases uniformly. The immediate result is that there is a tendency for the slab to contract both longitudinally and transversely. The contraction is resisted by friction between the slab and subbase and as a result tensile stresses, both longitudinal and transverse, are set up in the concrete. From a mechanistics point of view, these stresses tend to elongate the slab in the two directions in which they act and to shorten it in the direction at right angles to their line of action. The longitudinal tensile stress, therefore, induces a longitudinal elongation and a transverse shortening, or necking. This transverse shortening is dependent on the magnitude of longitudinal elongation and Poisson's ratio. In addition, the transverse tensile stress induces a transverse elongation and a longitudinal shortening which is also dependent on the concrete's Poisson's ratio. In other words, because of the shortening due to Poisson's effect, there are additional slab movements that should be considered, especially for long narrow slabs. These additional movements due to the Poisson's effect will increase total movements due to thermal and moisture variations, thus causing the concrete to experience a higher frictional restraint, provided by the subbase.

Goldbeck (Ref 6)

Studies conducted in 1924 by the U.S. Bureau of Public Roads gave the first relevant insight into the nature of the frictional resistance offered by various materials to horizontal movements of concrete pavements. The materials tested reflected the types of subbases used in those times for supporting concrete pavements. These materials included loam, clay, old macadam, gravel, and sand. For the most part, loose materials were used as compared to the bound materials used in today's subbases. The only bound subbase tested was a concrete base with a troweled surface.

Shallow ditches 6 inches deep, 3 feet wide, and 7 feet long were dug in the soft clay soil of the Arlington experimental farm belonging to the U.S. Department of Agriculture. The subbases were deposited, tamped solidly, and smoothed. Then the slabs were cast 2 feet wide

by 6 feet long and 6 inches thick on top of the subbases. After a month, a 1/2-inch steel bar was wrapped around a slab and pulled by two men at the end of a lever, causing a constantly increasing force. Pulling force and slab displacements were recorded until sliding occurred. Table 3.1 and Fig 3.4 show the results of the first test taken when subbase conditions were damp but very firm. It can be seen that the coefficient of frictional resistance varied between one and two, which means some subbases offered twice as much resistance to movement as other subbases. The shapes of the force versus movement curves also leads to varying frictional behaviors between subbases. The rate of force required to movement in the early stages of the test was greater than towards the latter stages for all subbases tested. This behavior can then be characterized as being parabolic in nature, as all curves demonstrate.

Table 3.2 and Fig 3.5 show the results of the second series of tests taken under extremely wet and soft subbase conditions. It was obvious that less force was required to move the test slabs for equivalent subbase materials. For example, the level clay's maximum coefficient of friction dropped from 2.07 to 1.09, indicating the water acted as a lubricant at the slab-subbase interface and between clay particles to permit easier slippage. The concrete subbases were tested in this second series. It was impossible to slide the concrete specimen with respect to the concrete base without exceeding the capacity of the loading equipment. This is an important point because cement stabilized subbases are being used in present highway design. The coefficient of friction for a concrete subbase was above 2.9 for these particular tests.

There were also several other important factors learned from this early experimentation work. Oil was applied to several subbase surfaces before concrete casting, and the oil was not effective in decreasing the friction in any of the subbases tested. When the maximum load had been reached in some specimens it was slowly released. In some instances, this amounted to almost 1/4 inch. It thus becomes very plainly evident that when the concrete slides over the subbase there is a considerable amount of yielding of the subbase material, and therefore it is expected that, if the material were fairly homogeneous and the movement of the concrete took place slowly, the subbase material would gradually yield under this movement and would thereby offer less resistance than these tests seem to indicate.

In considering these friction results, the maximum resistances are naturally of greatest importance, since these create the greatest stresses. Those given in Table 3.1 are therefore of more interest than those in Table 3.2, and these results very clearly show that the friction varies considerably in the subbase, depending upon its character. The indications

TABLE 3.1. FRICTIONAL RESISTANCE OF CONCRETE ON VARIOUS SUBBASES (DAMP BUT VERY FIRM)(REF 6)

Kind of Base	Move-ment	Force	Coefficient	Move-ment	Force	Coefficient	Move-ment	Force	Coefficient
Level clay	0.001	480	0.55	0.01	1130	1.3	0.05	1800	2.07
Uneven clay	0.001	500	0.57	0.01	1120	1.29	0.05	1800	2.07
Loam	0.001	300	0.34	0.01	1030	1.18	0.05	1800	2.07
Level sand	0.001	600	0.69	0.01	1080	1.24	0.05	1200	1.38
3/4-in. gravel	0.001	450	0.52	0.01	960	1.10	0.05	1100	1.26
3/4-in. broken stone	0.001	380	0.44	0.01	800	0.92	0.05	950	1.09
3-in. broken stone	0.001	1060	1.84	0.01	1550	1.78	0.05	1900	2.18

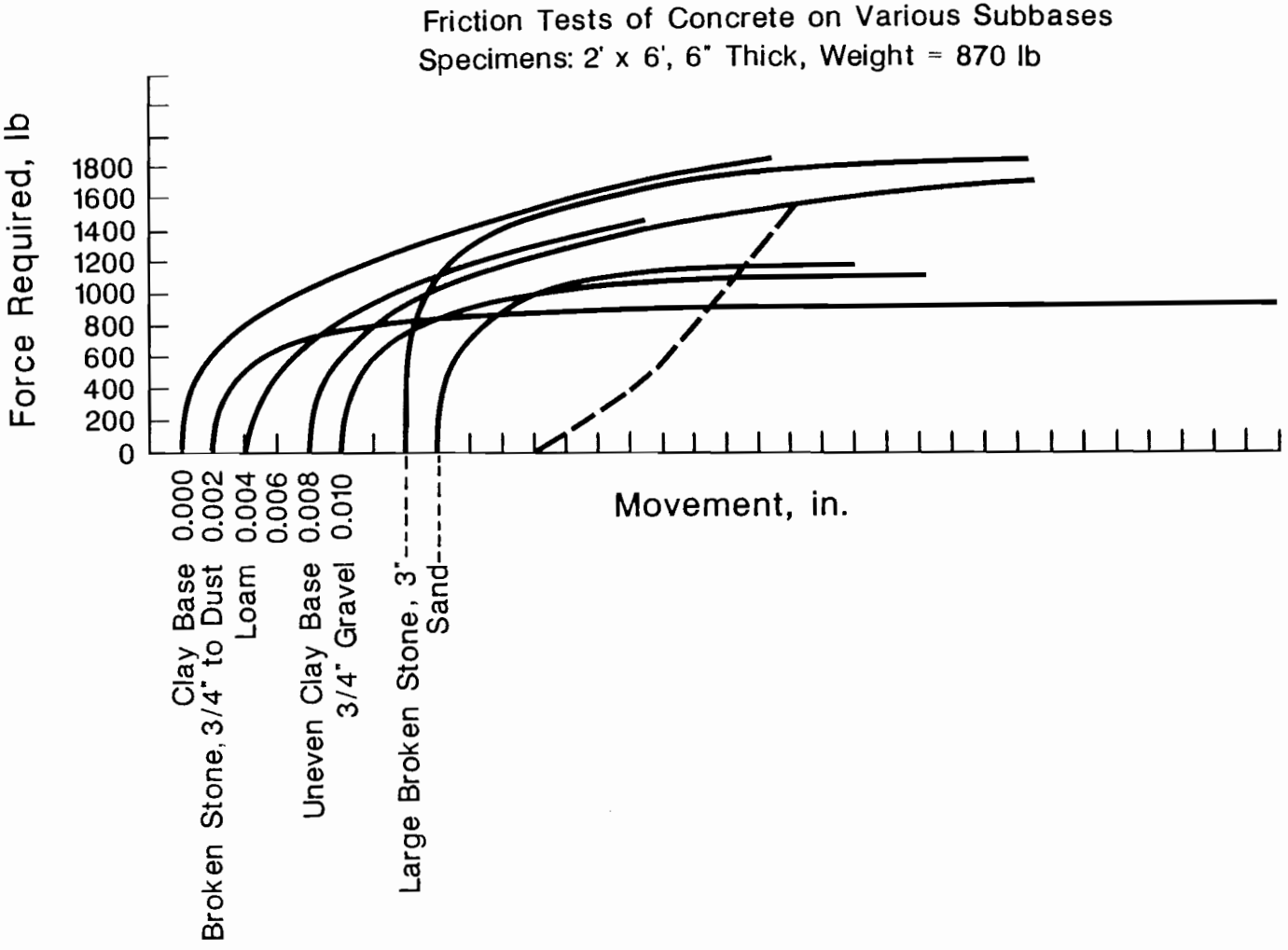

Fig 3.4. Curves showing movement versus force of test slabs on different subbases, from Goldbeck (Ref 6).

TABLE 3.2. FRICTIONAL RESISTANCE OF CONCRETE OF VARIOUS SUBBASES, (EXTREMELY WET AND SOFT) (REF 6)

Kind of Base	Move-ment	Force	Coefficient	Move-ment	Force	Coefficient
Level clay	0.001	120	0.14	0.01	300	0.35
Uneven clay	0.001	200	0.23	0.01	460	0.53
Loam	0.001	150	0.17	0.01	260	0.3
Level sand	0.001	140	0.16	0.01	280	0.32
3/4-in. gravel	0.001	510	0.58	0.01	640	0.73
3/4-in. broken stone	0.001	400	0.46	0.01	660	0.76
3-in. broken stone	0.001	240	0.28	0.01	630	0.73
Oiled clay	0.001	150	0.17	0.01	410	0.47
Clay and cobblestones	0.001	140	0.16	0.01	410	0.47
Concrete base	0.000	2500+	2.9+	0.00	2500+	2.9+
Sand, oiled	0.001	180	0.21	0.01	280	0.32
Concrete, oiled	0.000	2500+	2.9+	0.00	2500+	2.9+

Kind of Base	Move-ment	Force	Coefficient	Move-ment	Force	Coefficient
Level clay	0.05	500	0.58	1.5	950	1.09
Uneven clay	0.05	620	0.71	1.4	925	1.06
Loam	0.05	410	0.47	0.75	925	1.06
Level sand	0.05	400	0.46	0.75	875	1.00
3/4-in. gravel	0.05	950	1.1	0.5	1050	1.2
3/4-in. broken stone	0.05	940	1.08	2.0	1160	1.33
3-in. broken stone	0.05	900	1.04	0.875	1625	1.87
Oiled clay	0.05	850	0.98	1.25	1425	1.64
Clay and cobblestones	0.05	710	0.82	1.75	1260	1.45
Concrete base	0.00	2500+	2.9+	0.00	2500+	2.9+
Sand, oiled	0.05	480	0.55	0.375	800	0.92
Concrete, oiled	0.00	2500+	2.9+	0.00	2500+	2.9+

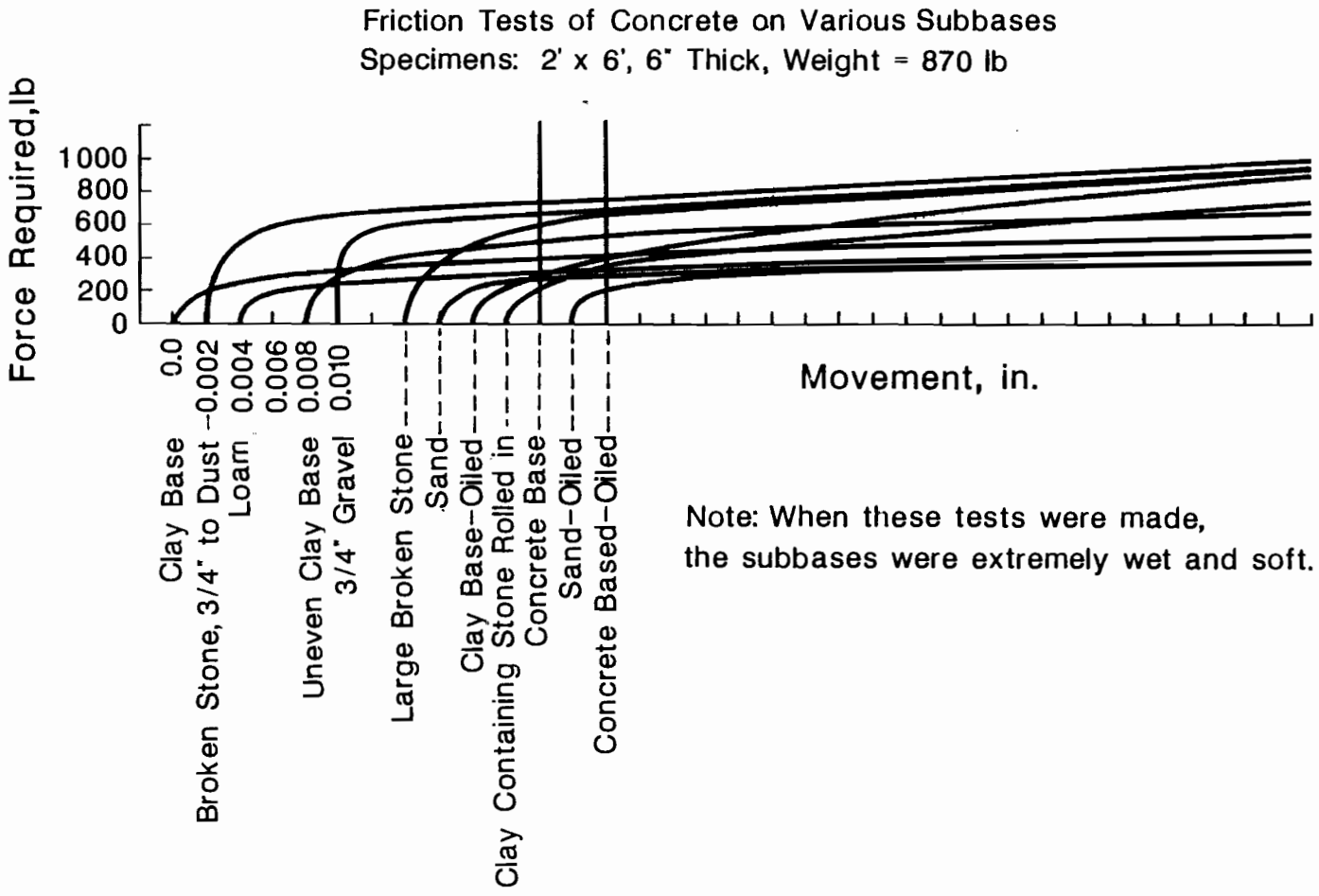

Fig 3.5. Curves showing movement versus force of test slabs on different subbases, from Goldbeck (Ref 6).

are that the friction can be greatly decreased if proper care is given to the preparation of the subbase. Every ridge or depression that is in the subbase surface before the concrete is deposited furnishes an additional grip for the concrete, thereby tending to deform a larger amount of base material and offering greater resistance to concrete sliding.

These test results indicate the coefficient of friction can vary from zero to something over two or more, depending upon the movement of the concrete and the character of the subbase. The problem comes when stabilizing agents are added to these materials. There has been no experimental work to determine their impact on the coefficient of friction. However, these experimental results can serve as bases for comparison with experimental work performed on these present day stabilized subbases.

Timms (Ref 7)

Relevant results were also obtained from a study conducted by the U.S. Bureau of Public Roads in 1963. More unbound subbases were tested, in addition to some modern subbases, such as asphalt and polyethylene sheeting. Figure 3.6 shows the results for some concrete slabs that were pushed over some of these subbases. The coefficient of friction varied, roughly between one and three. It was evident that the lowest coefficients of friction were obtained with double layers of polyethylene sheeting, followed by slabs placed on sand bases, granular bases, plastic clays, and emulsified and asphalt sheet layers consecutively. Slabs were then pushed at several later intervals. As also seen in Fig 3.6, the coefficient of friction was greater when the slabs were pushed initially and decreased for the average of subsequent movements. As addressed in Goldbeck's (Ref 6) study, it was again noticed that, upon release of the thrusting force, the slabs slightly tended to return toward their original position. This slight return is a small elastic recovery of the subbase material being tested.

The results of this experimentation clearly indicate that a bound subbase, such as asphalt, offers a higher degree of resistance when compared to loose subbases. Thus, higher coefficients of friction are expected during the testing of stabilized subbases.

Friberg (Ref 8)

After monitoring several 100-foot field slabs, several observations were made. A slight return of the slabs after release of the load indicated that the return was solely due to an

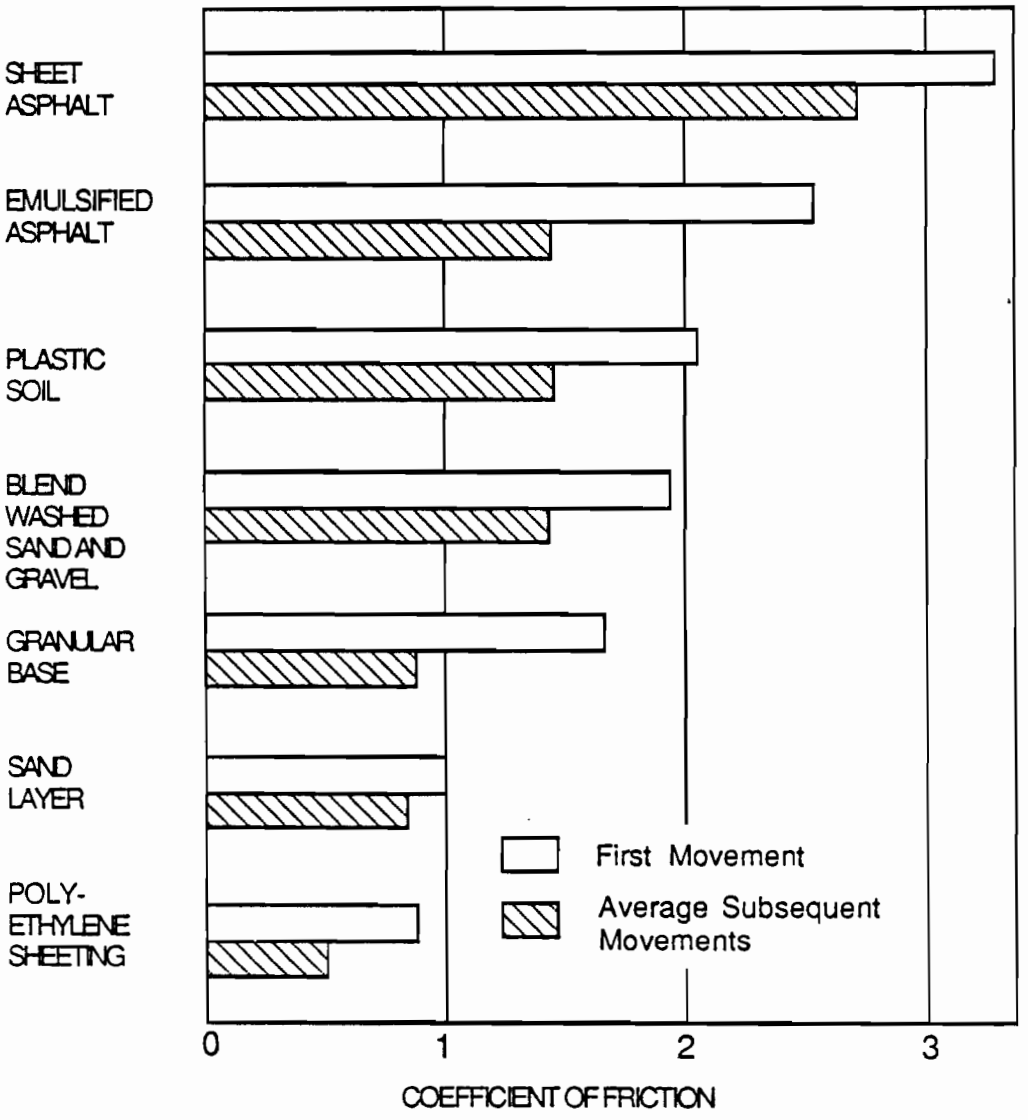

Fig 3.6. Summary of friction coefficients obtained by Timms (Ref 7).

elastic return of the subbases. The test data also showed a decrease in the coefficient of friction with increasing slab thickness. The subbase was found to participate in the movement to some degree up to 4-1/2 inches of depth for the long slabs. Hardly any subbase movement was encountered for smaller test slabs, due to soil resistance at the forward slab edge.

Stott (Ref 5)

In 1963, Stott of the Road Research Laboratories in Great Britain presented the results of a comprehensive laboratory investigation. This is the only experimental work involving the pushing of slabs back and forth until a steady state of frictional resistance was achieved. Table 3.3 and Fig 3.7 shows the results of the various subbases tested. The slab movement tests show that the force restraint increased from zero to a maximum with displacement, and the relationship varied with different materials. All materials gave curves showing hysteresis during cyclical movements, such as shown in Fig 3.8. A high initial force of restraint was generated by some materials and was reduced to a lower value after movement began. After several cycles of movement, a steady maximum force of restraint was observed, which ranged from 21 to 51 psf.

In tests on sands, aggregates, cement mortar, oil, paraffin wax, asphalt, paper, and polyethylene sheeting, this steady-state behavior is believed to be more representative of actual slab movement behavior. Usually, the initial frictional resistance curves are used in the design process, which is where the steady state frictional curves should be used instead.

A very important observation made during the testing of various subbase materials was that movement over loose granular material, such as sand or gravel, seemed to occur by rolling of the top particles whereas bound subbases failed by shear within the material. This observation should be kept in mind with push-off tests for stabilized subbases that are experimented on within this report. This was not the case for stablized subbases such as bitumen. It was shown that the force of restraint generated by a layer of bitumen varied with temperature, type of bitumen, rate of slab movement, and thickness of layer. This was in the theoretical expectation that the restraint of bitumen would be viscous, i.e., restraint per unit area. These factors must be kept in mind during the testing of asphalt stablized subbases.

TABLE 3.3. INITIAL AND STEADY STATE FRICTIONAL RESISTANCE FOR VARIOUS SUBBASES

Material Under Test	"Initial Peak Restraint"		"Steady" Value of Restraint After Several Displacements	
	Coefficient of Restraint	Force of Restraint (lb/sq. ft.)	Coefficient of Restraint	Force of Restraint (lb/sq. ft.)
Sand and aggregates				
Sharp sand A	0.74	50	0.62	42
Sharp sand B	- - -	- -	0.69	46
Dune sand	.78	54	0.69	48
Gravel	0.75	51	0.75	51
Limestone chippings	- - -	- -	0.56	37
(The above results are from 1-inch-thick layers covered with concreting paper before casting the concrete.)				
Sharp sand B	- - -	- -	0.64	43
(From 1/8-inch-thick layer covered with concreting paper.)				
Sharp sand B	1.05	79	0.64	50
(From 1-inch-thick layer and concrete cast directly on the sand.)				
Smooth mortar base	0.49	33	0.38	25
Waterproof paper on smooth mortar base	0.90	60	0.65	43
Hessian-backed paper on smooth mortar base	0.74	57	0.60	46

(continued)

TABLE 3.3. (CONTINUED)

Material Under Test	"Initial Peak Restraint"		"Steady" Value of Restraint After Several Displacements	
	Coefficient of Restraint	Force of Restraint (lb/sq. ft.)	Coefficient of Restraint	Force of Restraint (lb/sq. ft.)
Polyethylene				
Polyethylene on sand (Slab placed, not cast, on to polyethylene; sliding between concrete and polyethylene.)	- -	- -	0.43	29
Polyethylene on sand (Slab cast on to polyethylene; sliding between polyethylene and sand.)	- -	- -	0.55	38
Polyethylene on smooth mortar base	Impractical due to rapid water			
Paraffin wax on smooth mortar base	1.11	74	0.17-0.34	11-22
High-pressure lubricating oil (cardium compound D) on smooth mortar base	0.37	28	0.33-0.49	25-37
Asphalts - as base course				
1/8-inch-thick asphalt composed of 6 percent Shelphalt by weight to Thames Valley sand.	0.86	67	0.3-0.6	23-46
1/8-inch-thick asphalt composed of 10 percent Shelphalt by weight to Thames Valley sand.	0.64	48	- -	Similar results to previous asphalt

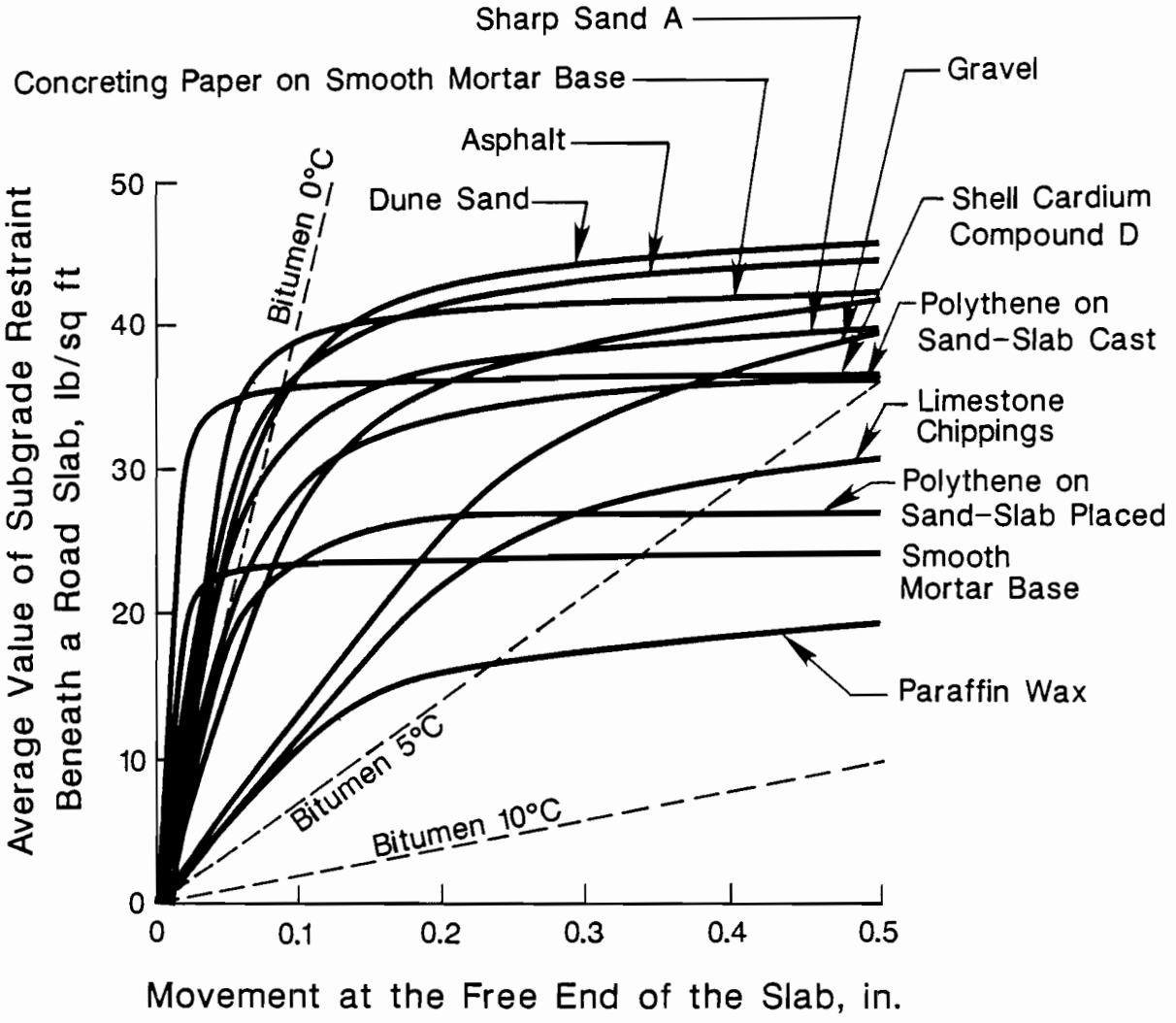

Fig 3.7. Frictional resistance for various subbases, from Stott (Ref 5).

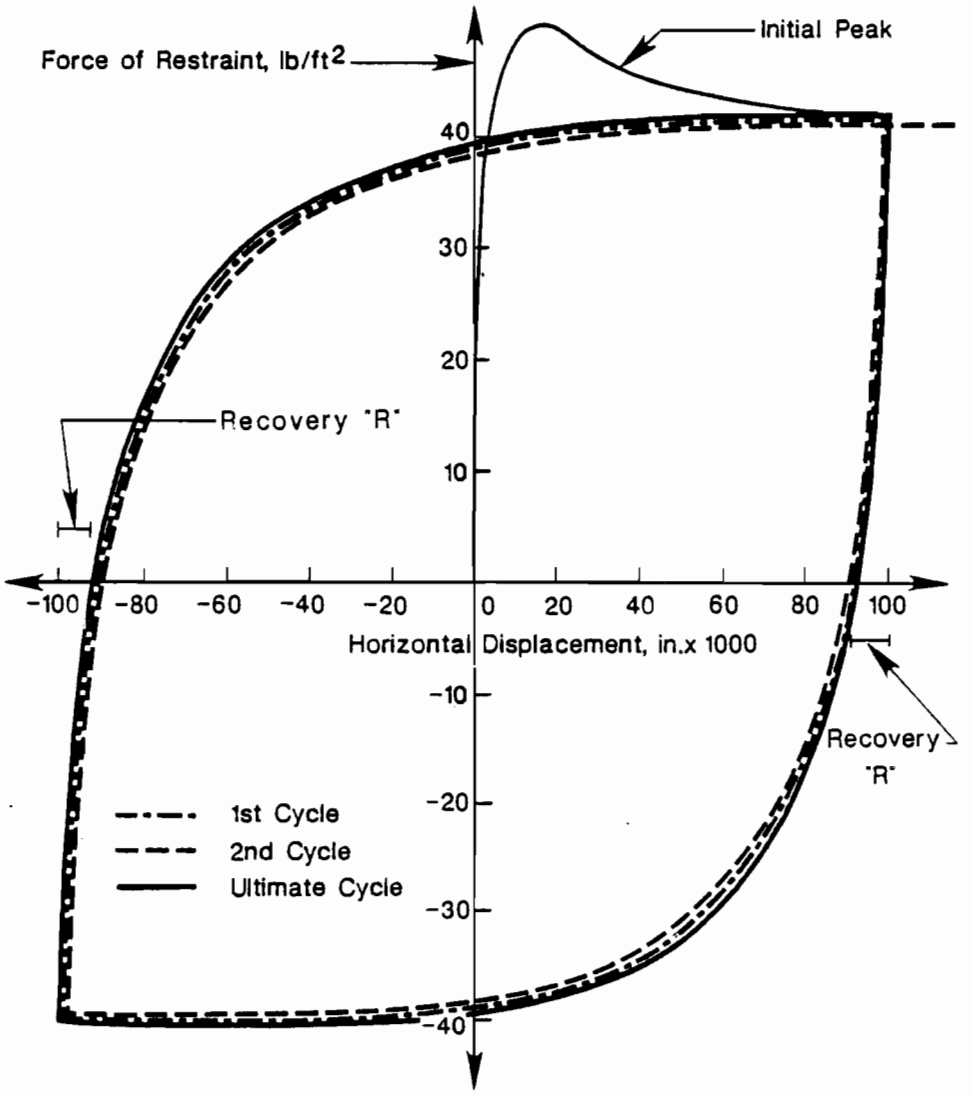

Fig 3.8. Hysteresis curve for cyclic slab movements, from Stott (Ref 5).

Center for Transportation Research Project 401 (Ref 4)

Several test slabs were subjected to push-off tests in Valley View, Texas, to determine the maximum coefficient of friction for three friction reducing mediums for future implementation of a prestressed pavement project in Cooke and McLennan counties, also located in the state of Texas. The three friction reducing mediums were

(1) a single layer of 6-mil polyethylene sheeting,
(2) a double layer of 6-mil polyethylene sheeting, and
(3) a spray-applied bond breaker consisting of white machine oil cut 1/3 with gasoline.

As discussed earlier in this chapter, the importance of reducing the resistance of the subbase was in reducing prestress losses and to prevent early cracking before stressing operations. Over a period of one year, three different push-off tests were run on each 6-inch test slab so that seasonal effects could be considered. The testing dates were June 1, 1984, August 22, 1984, and April 23, 1985. Table 3.4 and Fig 3.9 show the results of the averaging of the three push-off test dates. It was noted that the double layer of polyethylene sheeting began to act as one over time and that the spray-applied bond breaker was ineffective as a friction reducing medium.

Saudi Arabia (Ref 9)

The design of the apron zone of the King Fahd International Airport in Dhahran, Saudi Arabia, was conducted by Bechtel Engineers. The severe climatological conditions in Dhahran, where large daily temperature changes are characteristic, required that the frictional characteristics of different subbases be carefully assessed to avoid premature cracking of the pavement. Concrete cylinders 22.5 inches in diameter and 16 inches thick were cast over three types of subbases. These included

(1) an aggregate base coated with a medium curing asphalt cutback (MC70),
(2) a fine graded bituminous base course, and
(3) a one-sheet visqueen over a bituminous base course.

TABLE 3.4. SUMMARY OF AVERAGE MAXIMUM COEFFICIENT OF FRICTION AND MOVEMENTS FOR FRICTION RELEASING MEDIUMS (REF 4)

Test Slab Number	Friction Reducing Material	Maximum Coefficient of Friction U_{MAX}	Movement at Sliding (in.)
1	Double layer of polyethylene sheeting	0.467	0.0045
3	Single layer of polyethylene sheeting	0.824	0.01
4	Single layer of polyethylene sheeting	0.92	0.02
2	Spray-applied bond breaker	> 3.19	> 0.03

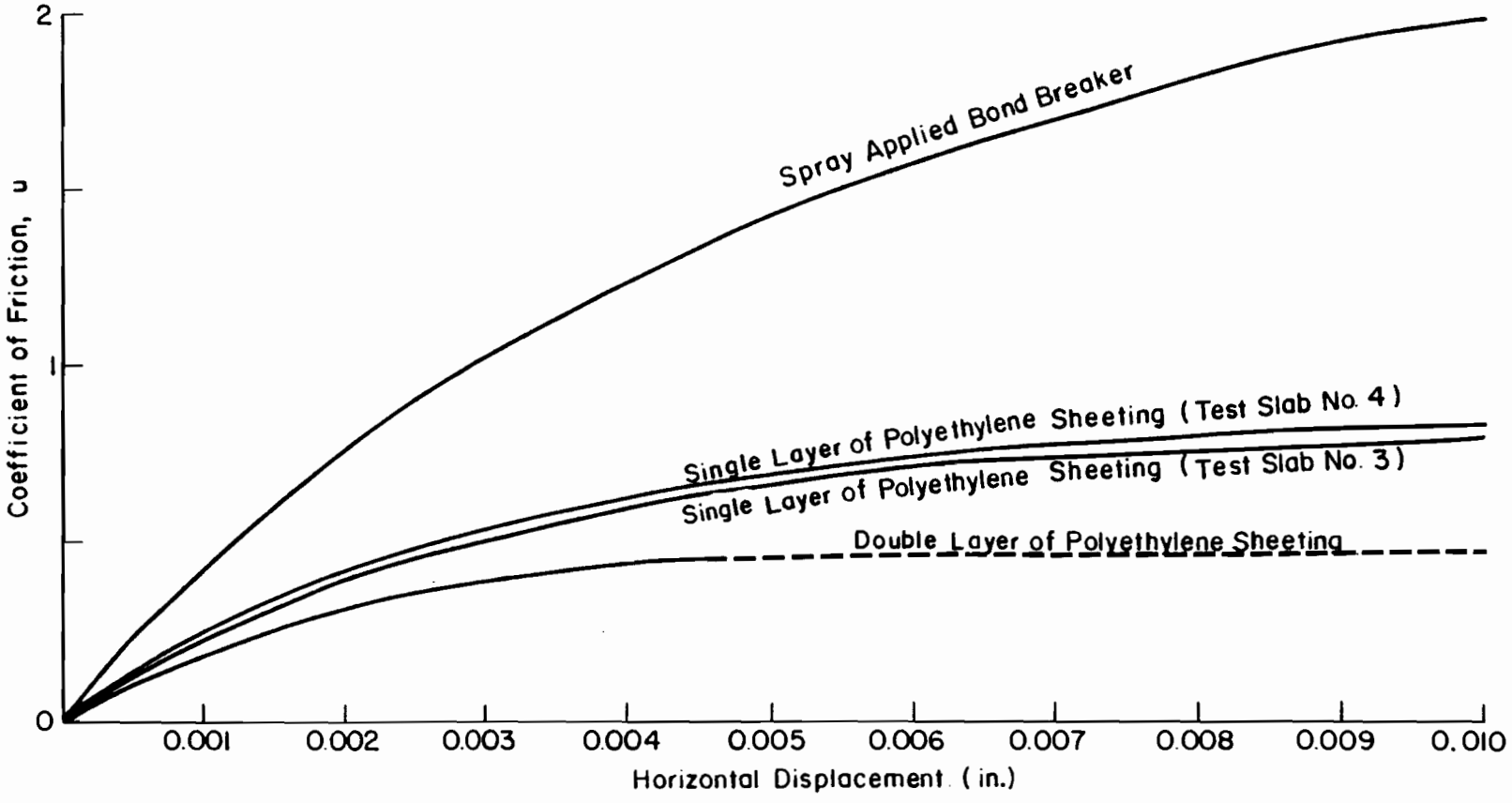

Fig 3.9. Average coefficient of friction versus horizontal displacement curves for friction reducing mediums (Ref 4).

The results of these push-off tests can be seen in Fig 3.10. It can be easily seen that the MC-70 in a granular subbase was inadequate as a friction reducing medium. It was noted that most of the failure was not at the concrete-subbase interface, but through the MC-70 and the granular subbase. In fact, for all push-off tests, there was some degree of failure within the subbase.

OVERVIEW OF PAST EXPERIMENTAL RESULTS

After reviewing the results above, it is clear that the relationship between frictional resistance and horizontal movements is inelastic. The resistance-movement curve for most subbase materials is defined by two major factors: (1) the elastic properties of the material beneath the slab, and (2) the condition of the sliding plane and the roughness of the materials either at the interface or within the subbase failure plane. The first defines the slope of the curve whether it is a linear relationship or parabolic relationship, as shown in Fig 3.11. The second factor defines the peak resistance and establishes the shape of the curve after sliding is reached. This region is also seen in Fig 3.11. Once a pavement section has reached this region, its recovery will be only semi-elastic, or, in other words, it will not be able to naturally slide back to its original position once the thermal and/or moisture variations have returned to their original state.

Other observations can be made from past experimental work. If the material beneath the slab is rigid and does not experience deformations due to friction related shear at the interface, the force-movement curve may look as illustrated in Fig 3.12(a). Obviously, no subbase is rigid; it is elastic to a varying degree. Figure 3.12(b) shows the curves for two subbases having different elastic properties, or, in other words shear stiffnesses. The sliding plane for the case depicted in Fig 3.12(b) is assumed to have surface characteristics similar to each other. Therefore the dynamic behavior at sliding follow the same curve. Only the point at which sliding is achieved is different. Figure 3.12(c) shows the effect of having two different sliding plane textures for the same subbase material; even though the subbase will react elastically equally and follow similar curves before sliding, the points where sliding is reached and the maximum frictional resistances will be different. This could also be applied to thin frictional reducing medium placed over a particular subbase. Subbases will react elastically

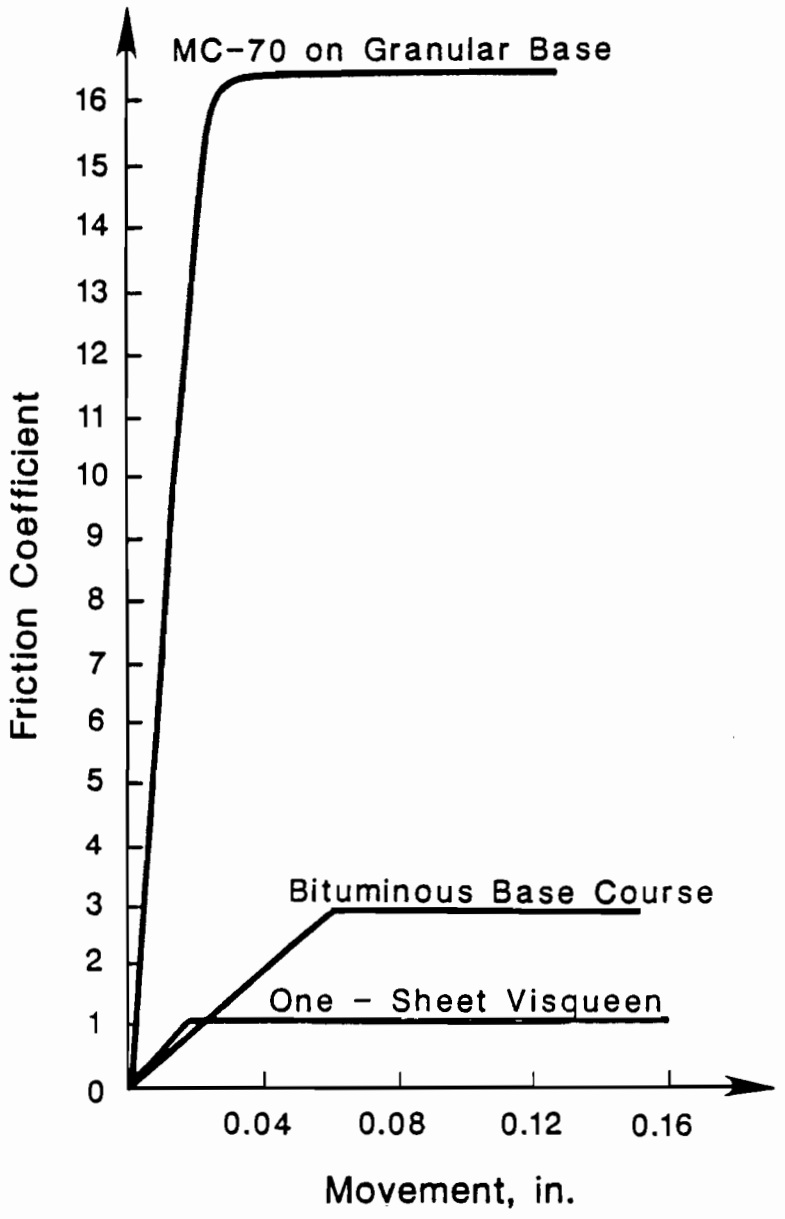

Fig 3.10. Friction coefficient versus movement for subbase tested in Saudi Arabia (Ref 9).

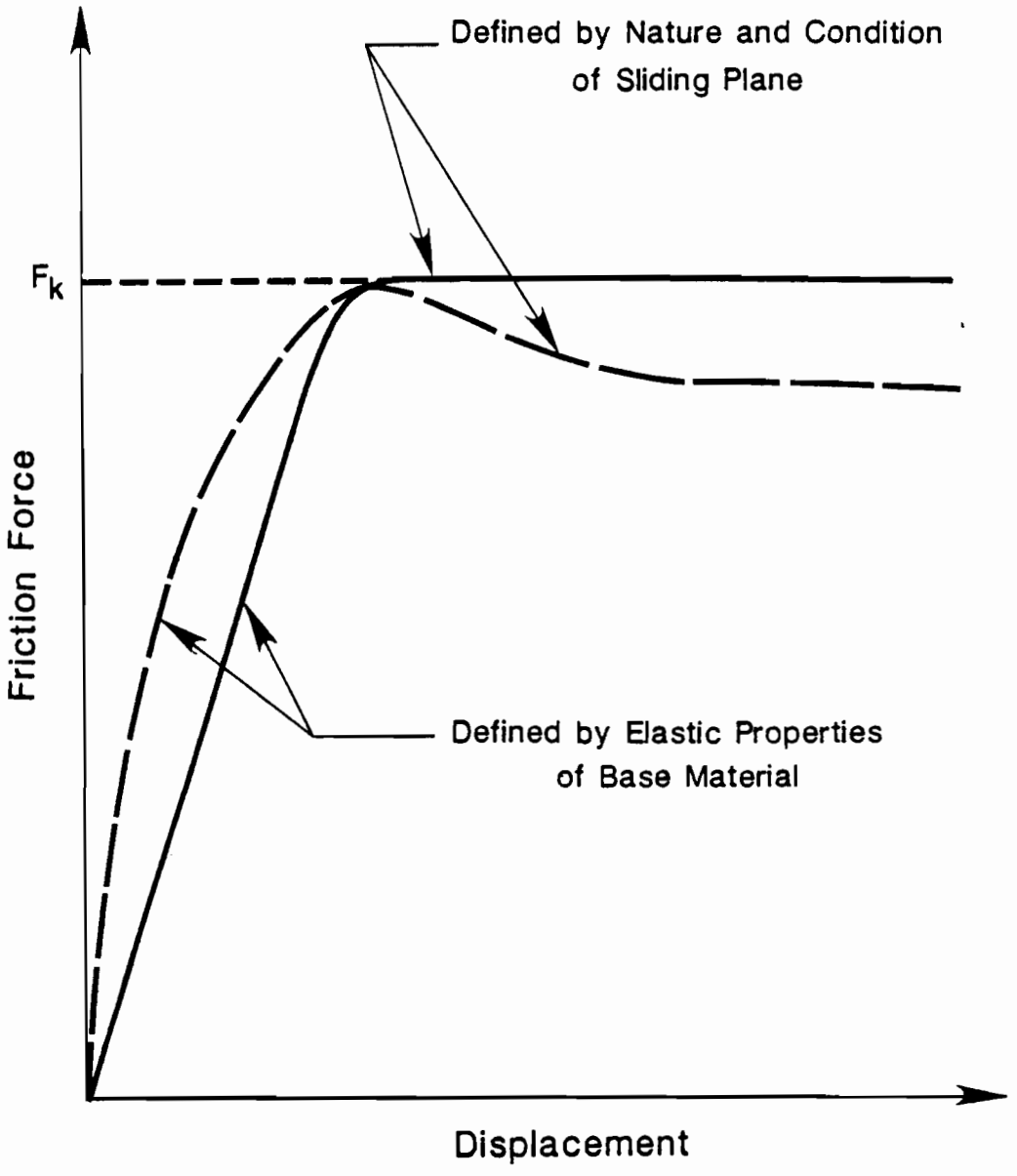

Fig 3.11. Factors affecting the shape of the force versus displacement curve.

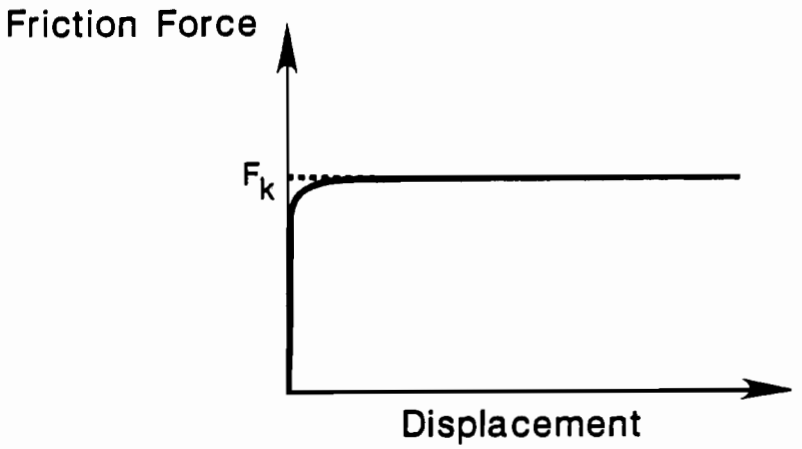

(a) Force–displacement curve for slab on infinitely rigid base.

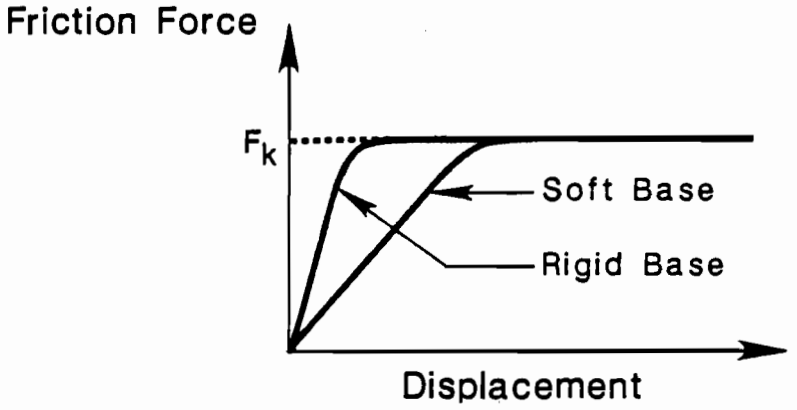

(b) Effect of stiffness of base material.

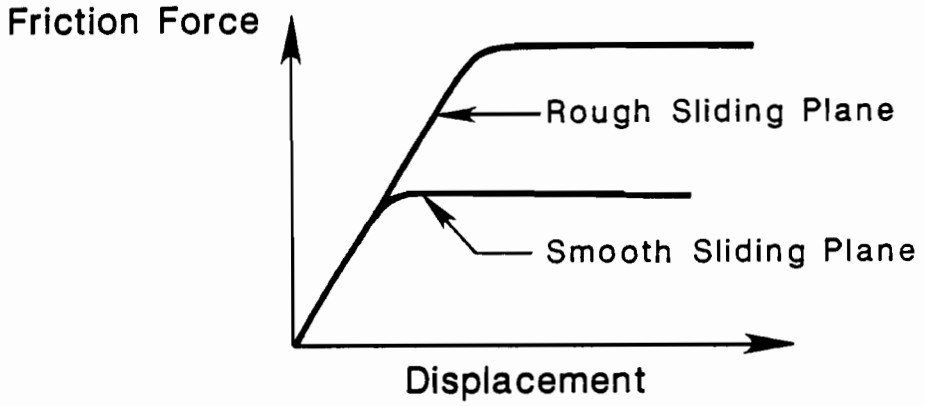

(c) Effect of texture of the sliding plane.

Fig 3.12. Effect of stiffness of subbase and texture of sliding plane on the frictional force versus movement curve.

the same to movements, but sliding will occur earlier if a thin friction reducing medium such as polyethylene is spread on top of the subbase.

CHAPTER 4. PRESENT NEED FOR FURTHER SUBBASE FRICTION INFORMATION

The objective of this chapter is to define a stabilized subbase and to determine which subbases are presently being used under concrete pavements at both the national and state level. Several federal sources provided information on what subbases are being used throughout the United States. This research project also performed a subbase survey within the Texas State Department of Highways and Public Transportation districts and the results are given in this chapter.

Since test specimens would have to be placed on these stabilized subbases, early cracking was possible due to the anticipated higher frictional resistances provided by these stabilized subbases. It was then necessary to make several computer runs, varying several slab parameters and dimensions so that cracking would most likely not be encountered in the field. These results are given in this chapter, not only to show how the test slabs were sized but also to give an opportunity for insight as to the importance and sensitivity of subbase friction on concrete stresses.

NATIONAL USE OF SUBBASES

The following list of stabilized subbases that are being used throughout the nation is based on Refs 11 and 12:

(1) asphalt stabilized subbase (black base),
(2) cement stabilized subbase,
(3) aggregate subbase (flexible base),
(4) lime treated subbase,
(5) fly-ash treated subbase,
(6) econocrete subbase course (primarily in California),
(7) asphalt pavement, and
(8) polyethylene (primarily for research).

All the subbases listed above have been used in varying degrees underneath concrete pavements. Excellent friction information should be gained so that proper concrete and steel stresses can be encompassed in the design.

STATE OF TEXAS SURVEY

After reviewing the various subbases being used throughout the nation it was also important to determine which types were being used within the State of Texas or, more importantly, the Texas State Department of Highways and Public Transportation. It was decided that a subbase survey would be sent out to the district offices within the state that primarily use rigid pavements in their particular highway network. Districts 1, 2, 3, 5, 12, 13, 17, and 20 were chosen and sent a survey. In order to encourage District support in filling out these surveys it was important to simplify them so that they required only a minimal effort. Providing a list of subbases used by the particular District allowed the highway engineer to make a simple ranking. Every list of subbases provided to each District was developed from the March 1, 1986, State Construction Report (Ref 10). This source provided control numbers where construction plans could be pulled to see typical cross-sections that showed the subbases being used in that particular District. Overall, 150 construction plans were reviewed until an adequate list of subbases for each District was arrived at. A letter was sent to each of these Districts stating the purpose of the survey and asking the list of subbases be ranked according to their importance, both present and future and that any subbases left out be included. Most engineers also included comments describing their District's typical cross-section under concrete pavements. Figure 4.1 is an example of a survey, the one sent to and returned by District 1. Table 4.1 shows the results of the survey for all Districts used. This survey suggests that a 2-inch to 6-inch asphalt stabilized subbase is the subbase most used in the state of Texas. Several common subbase-subgrade combinations were also noted from the survey. This is important because past experimental work showed that the subbase material participated in push-off tests several inches below the interface. Therefore, subgrade participation in subbase elastic deformations caused by pavement movements should be considered, especially if the subbase is very thin. If adhesion of the subbase to the concrete is high enough and the subbase is relatively thin, sliding may

occur at the subbase-subgrade interface. Therefore, it is suggested that not only should subbases be tested but various subbase-subgrade combinations should also be tested.

STABILIZED SUBBASES

Although many concrete pavements are being cast on various stabilized subbases, there is little to no friction information on them. Lime is being added to clay to cut down shrinkage and swelling due to moisture variations. Asphalt and cement are also being combined into granular subbases to eliminate pumping of loose material underneath pavements. Voids underneath rigid pavements have caused premature failures within the concrete. Some asphalts have been tested and show a noticeable increase in friction as compared to the loose subbases tested also. The failure plane was also shown to be contained within the subbase material as compared to loose subbases where sliding occurred at the interface of the slab and subbase. Therefore, it can be assumed that stabilized subbases would tend to give higher frictional characteristics as compared to the loose granular subbases used in the past. Thus, since higher stresses are anticipated, experimental work should be performed on stabilized subbases so their frictional characteristics can be determined for use in pavement design.

SUBBASES TESTED

Since a facility with a flexible subbase was already constructed at the Balcones Research Center, that subbase was tested to obtain friction information and to develop experimental techniques. After these experimental techniques were developed a site in Houston containing four different subbases was chosen for obtaining friction information. The Houston site was a state highway construction project where the typical cross-section was a 10-inch CRCP over 3/4-inch asphalt stabilized subbase (bond breaker), over 6-inch cement stabilized subbase, over 6-inch lime stabilized subbase. This is a very common cross-section in District 12. Therefore, the following subbases were tested for this report:

District 1

	Ranking*	
	Present Use	Future Use
2-inch asphalt concrete pavement (level up)	1	1
6-inch lime stabilized flexible b ase (TY A or B GR4 CL4)	2	2
6-inch flexible base (TY A or B GR4 CL4)	1	1

Reminder:

If any of the subbases above are out-dated for use under concrete pavement, please add the presently used subbases in your ranking scheme.

*Suggested Ranking System

1 = Top Choice

2 = Second Choice, etc.

One most common sub base for concrete pavement has been 2" ACP on 6" flexible base and this would be our first choice combination. Our second choice depending on the source of flexible base to be used would be 2" ACP on 6" lime treated flexible base.

Richard Stanley
5-9-86

Fig 4.1. Sample of subbase survey – District 1.

TABLE 4.1. TEXAS DISTRICT SURVEY OF PRESENTLY USED SUBBASES

Subbases	District 1	District 2	District 3	District 5	District 12	District 13	District 17	District 20
2 in ACP over 6 in Flexible Base (TY A or B GR4 CL4)	1							
2 in ACP over 6 in Lime-Treated Flexible Base (TY A or B GR4 CL4)	2							
2 to 6 in Asphalt Stabilized Base		1	1	1		1	1	
2 to 6 in ACP		2						
4 in Cement Stabilized Base			2					
1 in ACP			3					
6 in of Flexible Base Treated with 1 Percent Lime			4					
2 in Soil Asphalt Base			5					
3/4 in Asphalt Stabilized Base over 6 in of Cement Stabilized Base (TY A, B, C or E) over 6 in of Lime-Treated Subgrade (TY A Lime)					1			
6 in Cement Stabilized Base over 6 in Lime Stabilized Base (TY A, B, C, or E)					2			
6 in Lime Treated Subgrade					3			
Phosphogypsum Treated Base (Possible Future)					4			
6 In Cement Stabilized Base							2	1
6 in Cement Stabilized Subgrade							3	

Ranking System:
1 = Top Choice
2 = Second Choice, etc.

(1) 12-inch flexible subbase (aggregate subbase),
(2) 3/4-inch asphalt stabilized subbase (bond breaker) over 6-inch cement stabilized subbase, over 6-inch lime stabilized subbase,
(3) 6-inch cement stabilized subbase over 6-inch lime stabilized subbase,
(4) 6-inch lime stabilized over untreated clay, and
(5) untreated clay.

Although this list does not include all the subbases listed in the State District survey it is a starting place and provides insight for further experimental results on those not included. It does however represent a large majority of the subbases used for concrete pavements throughout the Texas highway system.

SIZING OF TEST SLABS

The first task for setting up experimental work for the subbases to be tested was to size the test slabs. Many simulated runs were made using the JRCP4 program developed by the Center for Transportation Research. Parameters that affect concrete stress due to frictional restraint were altered to test their sensitivity. Two lengths, 20 and 30 feet, were used at depths of 4 and 5 inches. As discussed in Chapter 2, the parameters tested were total shrinkage, maximum frictional restraint, total movement at sliding, maximum change in temperature, thermal coefficient of expansion, and concrete strength. All parameters were adjusted to a range of possible values in the field to see their impact on concrete tensile stresses at midspan. This analysis was carried out so that dimensions could be chosen for the test slabs with a low risk in cracking. As each parameter was altered, a ratio was made between the computed tensile stress over the available concrete tensile stress. If the ratio reached 100 percent then cracking would occur. This analysis not only serves as an aid in sizing the test slabs, but it is also an excellent example of how each parameter plays a role in frictional restraint. The expected maximum frictional restraint was set to be within 1.0 to 5.0 psi after review of past experimental values.

Figure 4.2 shows the impact of total shrinkage on slab length and slab depth as it is varied from 0.0004 in./in. to 0.0006 in./in. In both cases, there is little effect on the concrete's tensile stress. There is only an approximate 10 percent increase in tensile stress

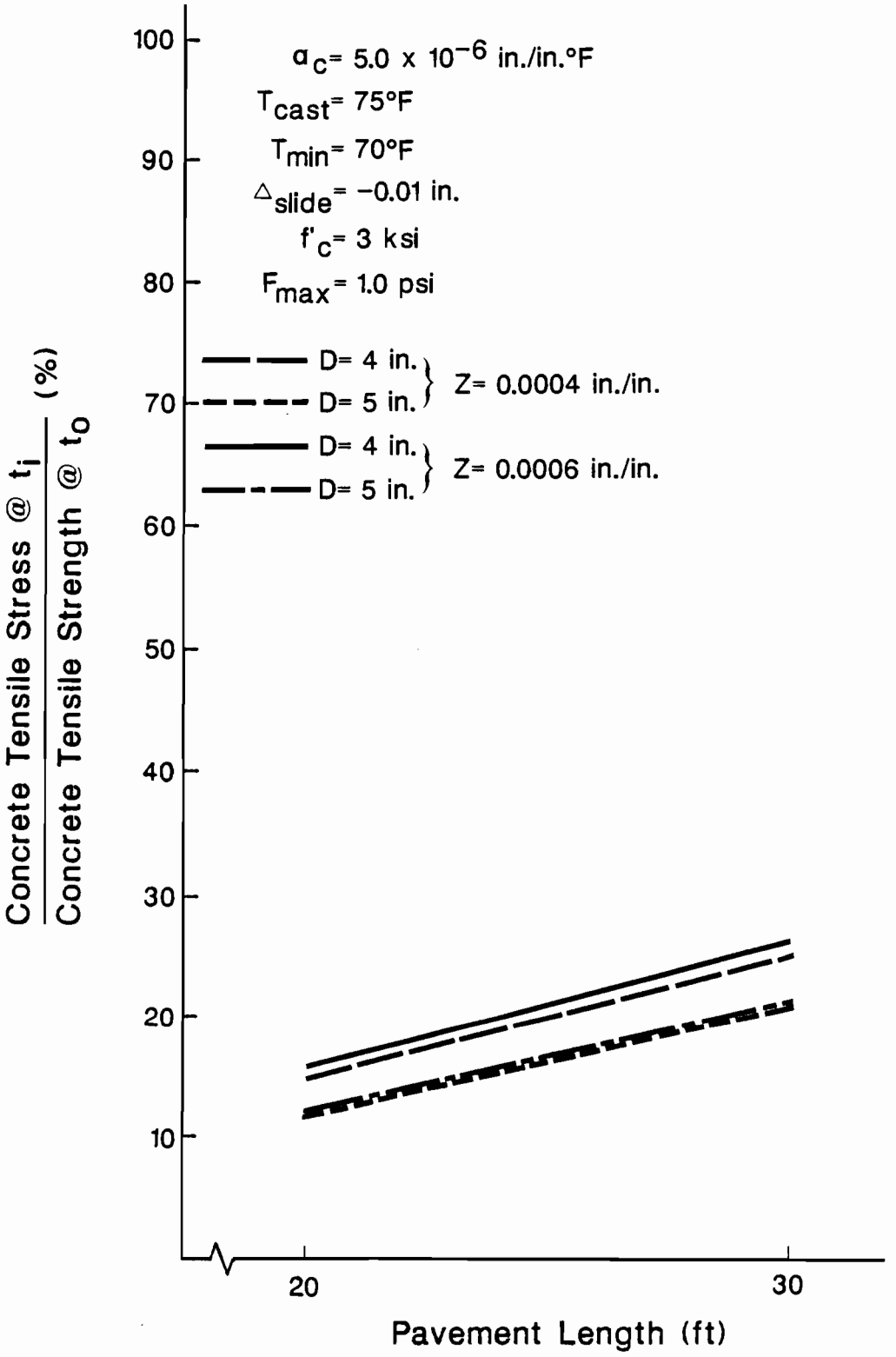

Fig 4.2. Shrinkage sensitivity study in sizing test slabs.

between the extreme cases, that being between a 5-inch slab 20 feet long experiencing 0.0004 in./in. in total shrinkage and a 4-inch slab 30 feet long experiencing 0.0006 in./in. in total shrinkage. Although shrinkage plays a role in increasing the concrete's tensile stress, its variability is not significant for this experiment.

Figure 4.3 tests the impact on concrete strengths. Notice that the higher the friction restraint, the higher the impact on concrete stresses. This is shown by the slopes of the graphs. The slopes for the maximum frictional restraint of 5.0 psi are higher than the slopes for the 1.0 psi maximum frictional restraint lines. Figure 4.3 also shows that if a weak concrete is used, cracking may be encountered if the wrong slab dimensions are chosen. This is shown by the 75 percent ratio computed for a slab 4 inches by 30 feet with 3 ksi compressive strength cast over a subbase which provides a maximum frictional restraint of 5 psi.

Figure 4.4 shows the impact of the point at which sliding occurs on concrete tensile stresses with the maximum frictional restraint held at 5 psi,. The results are significant. The stresses increase approximately 20 percent for a 20-foot slab and 30 percent for a 30-foot slab when the movement for sliding is varied from 0.10 inch to 0.01 inch. This is obviously true for short slabs, whose total movements lie within these magnitudes of movements. Only when total movements occur in the 1/2-inch range, as in long slabs, will this parameter not be of any significance, largely due to the fact that a majority of the slab will be past the point of sliding.

The coefficient of thermal expansion turns out to be very sensitive to the concrete's tensile stress, as seen in Fig 4.5. The coefficient of thermal expansion was varied between 0.000005 in./in.°F and 0.000007 in./in.°F; both are possible values that can be encountered in the field using a crushed limestone aggregate in the mix design. Cracking is almost encountered for a 4-inch by 30-foot slab using the higher coefficient of thermal expansion and maximum frictional restraint for the given conditions. As shown in Fig 4.3, Fig 4.5 reiterates that the larger the frictional resistance the more significant the role the parameter plays in determining the concrete's tensile stress. The slopes of the lines for the maximum frictional restraint of 5.0 psi are higher than the slopes of the lines of the 1.0 psi maximum frictional restraint. This sensitivity due to higher frictional restraints should be ingrained in every pavement design engineer after moving from loose granular subbases to stabilized subbases. The frictional restraint is not only increased by the switch to stabilized

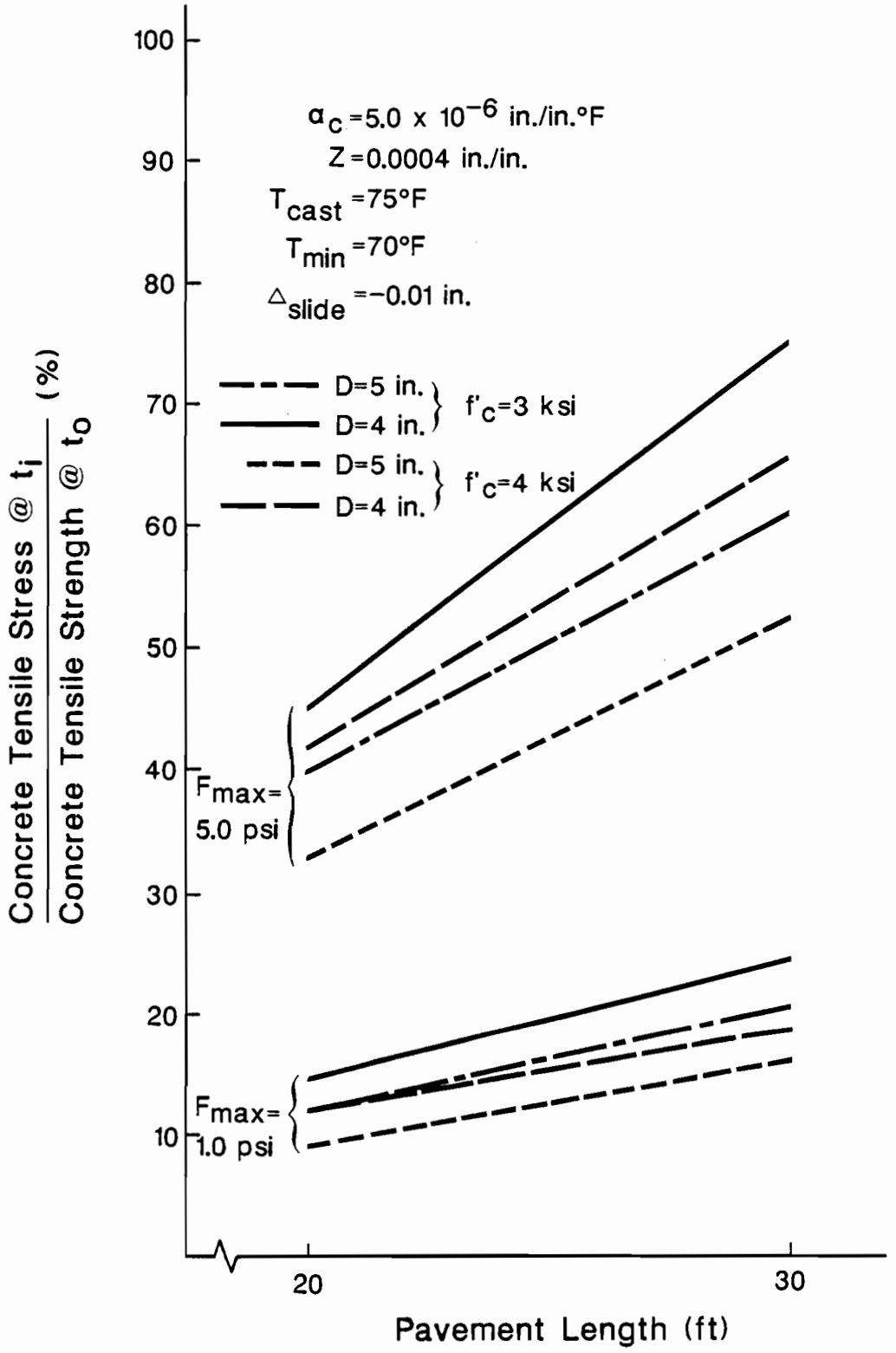

Fig 4.3. Compressive strength sensitivity study in sizing test slabs.

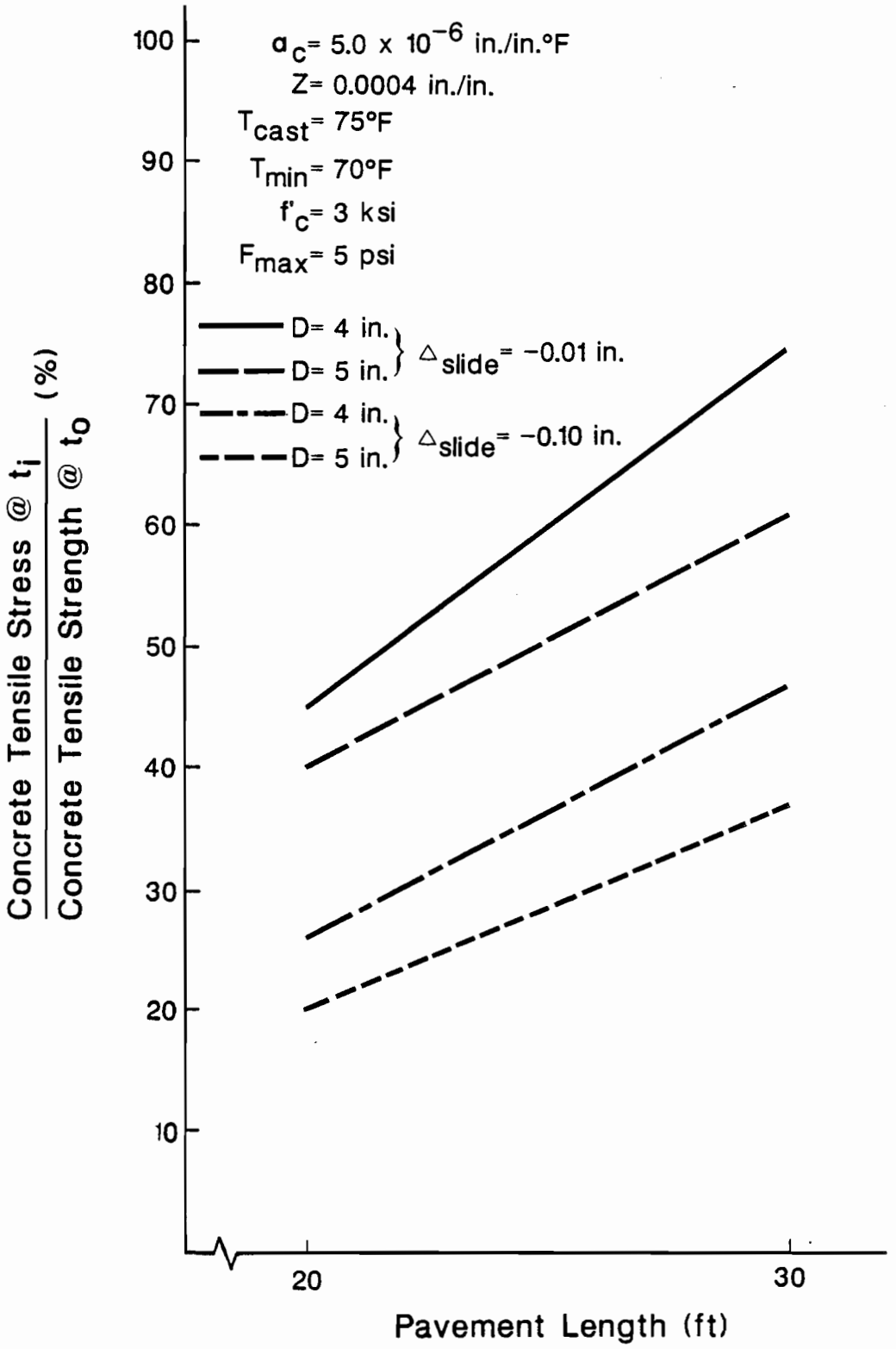

Fig 4.4. Movement at sliding sensitivity study for test slabs.

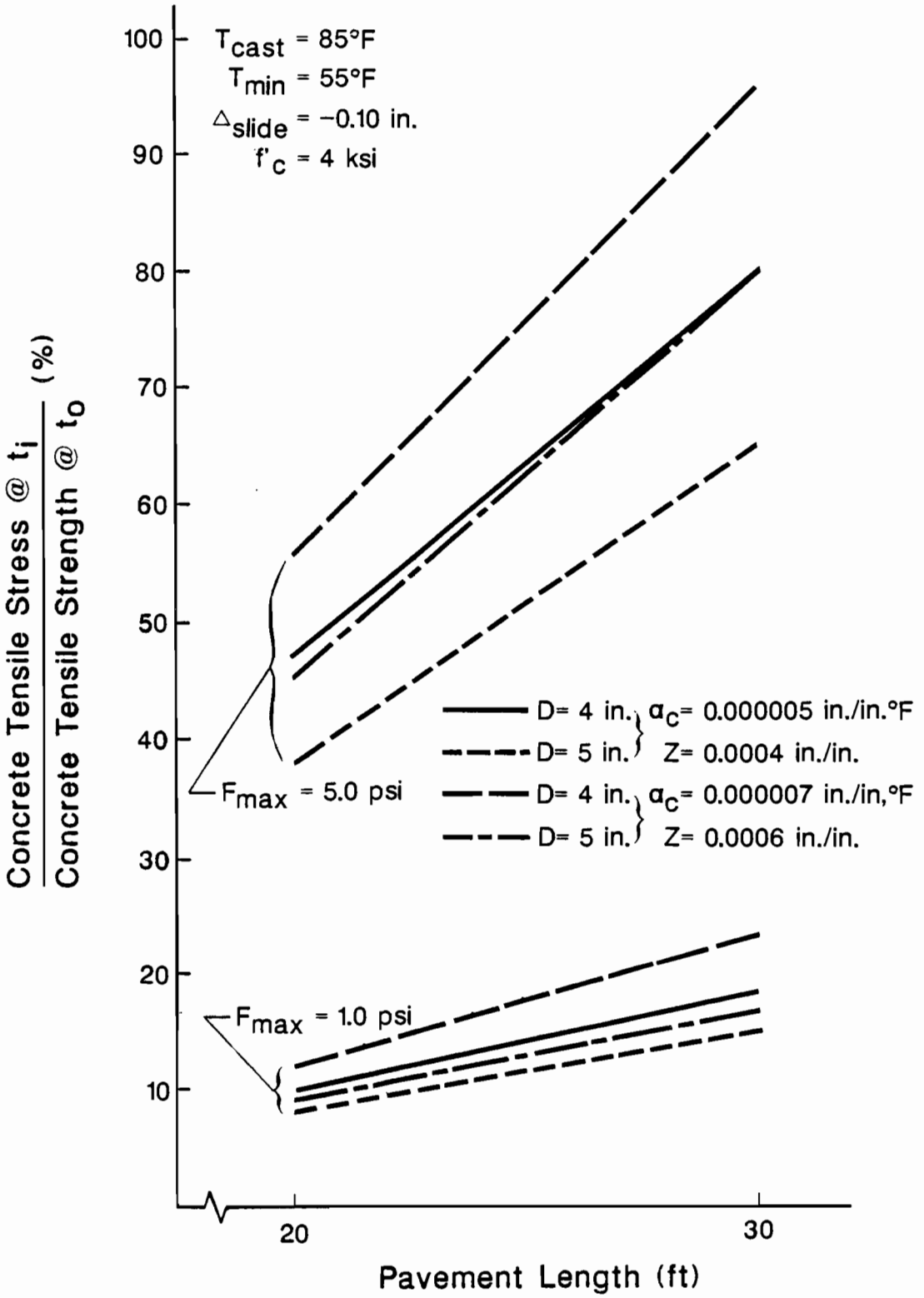

Fig 4.5. Coefficient of thermal expansion and shrinkage sensitivity study in sizing test slabs.

subbases, but the rate of increase is also more significant, thus causing concern over every parameter that induces movements into pavements.

Figure 4.6 shows the impact of drops in temperature after casting on concrete tensile stresses. The lowest pair of lines represent a 5°F drop, the next 15°F drop, and the last 20°F drop. There seems to be anywhere from a 20 percent increase for a 20-foot slab to a 30 percent increase in tensile stresses for a 30-foot slab when comparing 5°F and 20°F drops in temperatures. This last analysis proved that a 4-inch by 30-foot slab reached only 80 percent of its tensile strength for a 20°F drop in temperature after casting for the given expected parameters. One of these given parameters was a maximum frictional restraint of 5 psi. Therefore, after reviewing these results, it would be surprising to see cracking for a slab cast under these parameters.

These figures clearly show that a 4-inch by 30-foot test slab cast with moderate strength would be highly unlikely to experience cracking due to environmental stresses caused by the parameters investigated in this analysis. However, because the 5.0 psi maximum frictional restraint was only an upper estimated limit and curling effects were ignored in this analysis, the first test slab constructed was 4 inches by 22 feet. The width chosen was 2 feet and is irrelevant for this frictional experimentation. Cracking was never experienced in Austin. Thus, the test slabs placed in Houston were 3-1/2 inches by 2 feet by 32 feet because of expected higher concrete strengths due to a better concrete mix design.

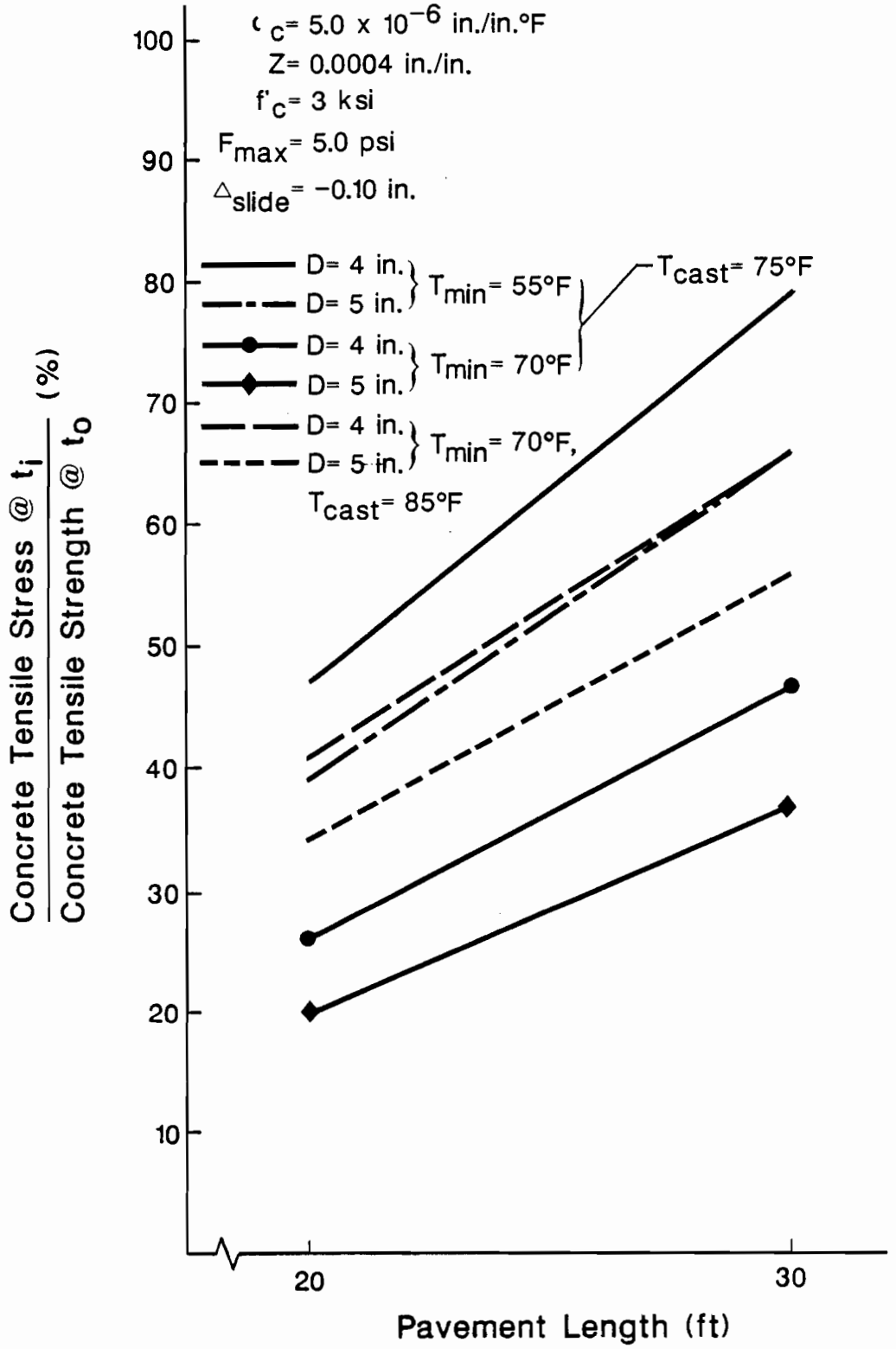

Fig 4.6. Temperature drop sensitivity study for sizing test slabs.

CHAPTER 5. CONSTRUCTION AND EXPERIMENTAL PROCEDURES

This chapter discusses construction and experimental procedures undertaken in this project. Illustrations of slab layouts and experimental set-ups are also provided. Construction of each test consisted of placing a concrete anchor into the particular subbase followed by placement of the slab. After the slab gained most of its strength, one end was pinned to the anchor with dowel bars. Therefore, all slab movements would theoretically be in one direction from the pinned anchor. Each slab was monitored between daily temperature peaks so that horizontal movements could be compared between subbases. This is considered to be Phase I of the experimentation. Phase II consisted of slicing the test slabs so that push-off tests could be run on them. Concrete specimens were cast at slab placement so that concrete properties of the mix could be monitored.

OVERVIEW OF TEST SLABS

A pilot experiment was performed at Balcones Research Center, in Austin, to determine if two major experimental procedures could be performed and to work out any bugs encountered during experimentation. After reviewing many computer-simulated runs, such as data presented in Chapter 4, with expected values for concrete properties and environmental parameters, a 22–foot by 2–foot by 4 inch–slab was constructed. The slab was placed on top of a previously prepared flexible subbase where other experimental projects with slabs were being tested. The slab did not encounter any cracking during the pilot study. The first phase monitored the slab's movements during a daily temperature cycle and the second phase involved breaking the slab into 9–foot by 2–foot sections and performing a push-off test on each section. Both phases involved complex hardware and software combinations. All problems were worked out and successful data were obtained from the pilot study.

Four test slabs were then cast on the West Beltway 8 project south of Westheimer in Houston, Texas. This project site was chosen for two reasons. The first reason was that the project was at a phase at which added subbase construction could be implemented. The second reason was that the subbase stratification used in the project matched major subbases suggested in the survey discussed in Chapter 4. Four major types of subbases could be tested

at this site. They are an asphalt stabilized base, a cement stabilized base, a lime-treated subbase, and an untreated clay subbase.

An island between two ramps and the southbound frontage road was chosen to be the location of the test site. It was chosen because of the ease of constructing the subbases, vehicle accessibility, and non-interference during construction of the roadways. Each subbase was constructed during each phase of the roadway construction. As each layer was constructed an additional roll-out from the edge of roadway was performed to include that subbase as a test section.

There is one major difference between the test slabs and the pilot test slab. The slab dimensions changed to 32 feet by 2 feet by 3-1/2 inches for Phase I of the testing. In Phase II a slab area of 14 feet by 2 feet was used for each push-off test.

CONSTRUCTION OF TEST SLABS

Each slab dimension was laid out on the ground first. A hole was then dug and filled with concrete to be used as an anchor for pinning one end of the slab in the future. The slabs were cast and then pinned to the anchor, using dowel bars, three weeks after casting. Four weeks after casting, the slabs were ready for all experimentation.

Layout of Subbases

The first slab was cast on top of an existing caliche flexible subbase that had a thin oil coating at its surface. The site had been constructed for research purposes by the Texas Department of Highways and Public Transportation several years ago at Balcones Research Center, located in Austin.

Four more subbases were constructed in Houston. They were constructed next to a ramp that was being constructed for the West Beltway 8 Project just south of Westheimer. Every time a subbase was laid for the ramp, the layer was extended outside of the ramp and into the test area. Therefore, all subbases tested would yield actual field results. Figures 5.1 and 5.2 show the construction configuration of the test site. Table 5.1 shows the compaction of three subbases through density tests. Each value represents the percentage of compaction written in the construction plans as the optimum compaction of each material. All three

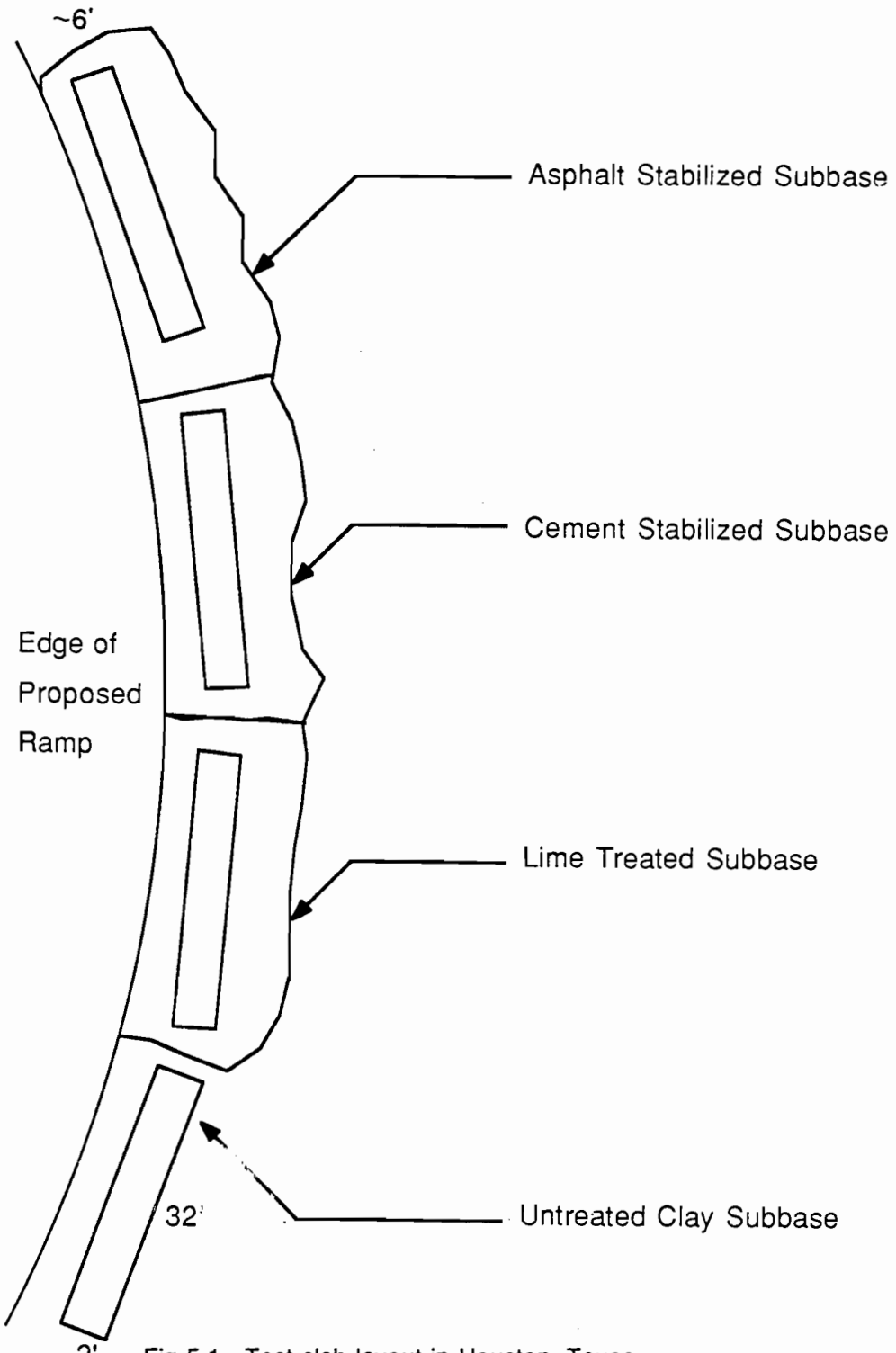

Fig 5.1. Test slab layout in Houston, Texas.

(continued)

Fig 5.2. Construction configuration of Houston test site.

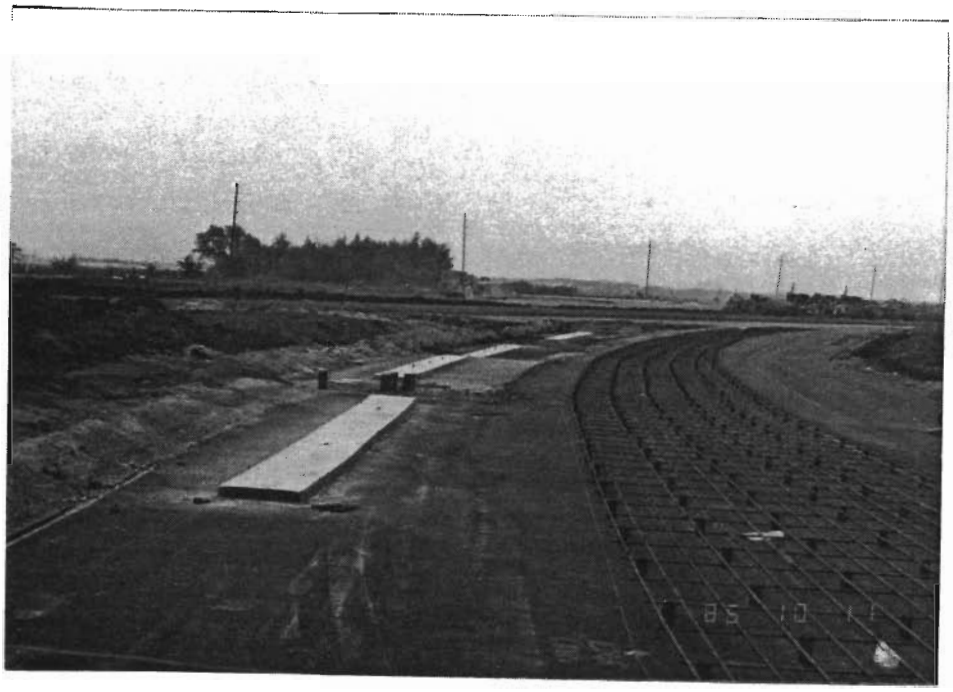

Fig 5.2. (continued)

TABLE 5.1. SUBBASE DENSITIES IN HOUSTON, TEXAS

Subbase Type	Percent Compactness
Cement Stabilized	98.5
Lime-Treated Clay	97.9
Untreated Clay	95.5

densities met specification requirements. Figure 5.3 shows a close-up view of each of the four subbases before construction of the anchors.

Anchors

After the test slab locations were established, holes were dug at one end of each test slab. The holes roughly measured one foot in the longitudinal direction of the slab, three feet in the transverse direction of the slab, and a foot and a half in depth. They were then filled with concrete until flush with the surface of the subbase. No steel reinforcement was added at this point. Figures 5.4 and 5.5 show a few of the holes dug and the cast anchors respectively.

Casting of Test Slabs

A couple of days after the anchors were cast, formwork was layed down and pinned to the ground to prevent sliding during concrete placement. Cut plywood was used to cast the 4-inch slab in Austin while finished 2 by 4's were used to cast the 3-1/2-inch slabs in Houston. Figure 5.6 shows the formwork ready for casting for the four test slabs in Houston. Figure 5.7 shows a close-up view of the condition of the subbases just before concrete placement.

Plastic inserts were placed during concrete placement. They measured 6 inches by 2 inches by 1/4-inch and were constructed for two purposes. The first was to be used as a reference point where the horizontal movements could be monitored. It also served to hold the thermocouple wire at mid-depth during casting operations. Figure 5.8 shows one of the plastic inserts before and after casting. Most of its surface was roughened with a wire-wheel grinder to enhance bonding to the concrete. Five plastic inserts were installed at different locations along every test slab. Slab dimensions and plastic insert locations are given in Fig 5.9.

Both test sites used roughly a five sack cement content with crushed limestone. The mix used in Houston was the same used for the pavements cast on the construction site. The slab in Austin was cured with wetted burlap sacks, while the test slabs in Houston were cured using a sprayed-on moisture barrier commonly used for curing concrete pavements. Figure 5.10 shows the Houston slabs after casting. All formwork was removed the very next day.

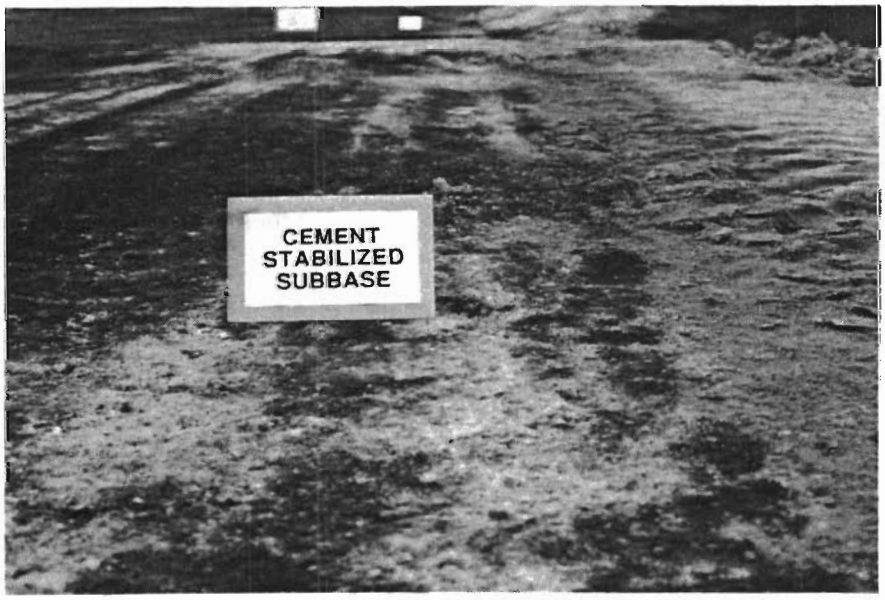

(continued)

Fig 5.3. Subbase types tested in Houston, Texas.

Fig 5.3. (continued).

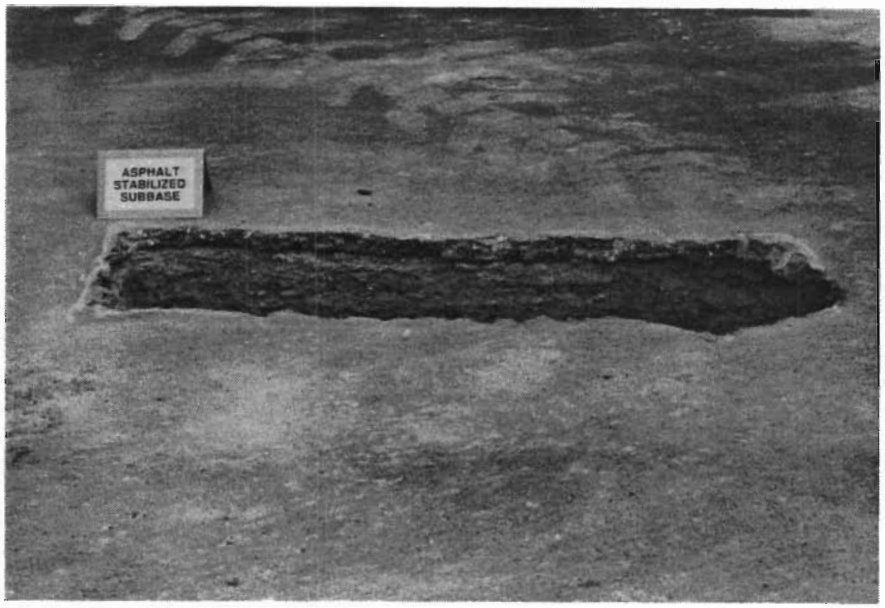

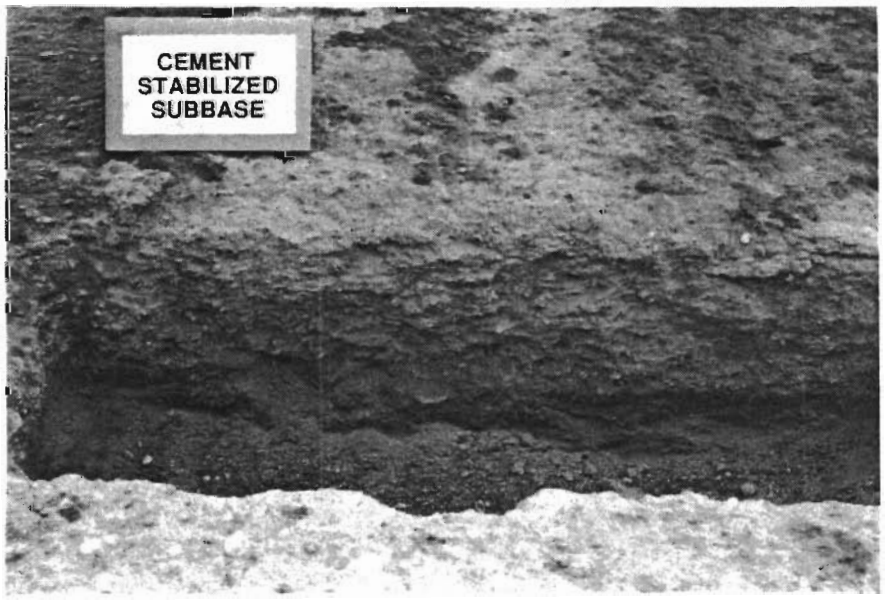

(continued)

Fig 5.4. Holes for anchors in Houston, Texas.

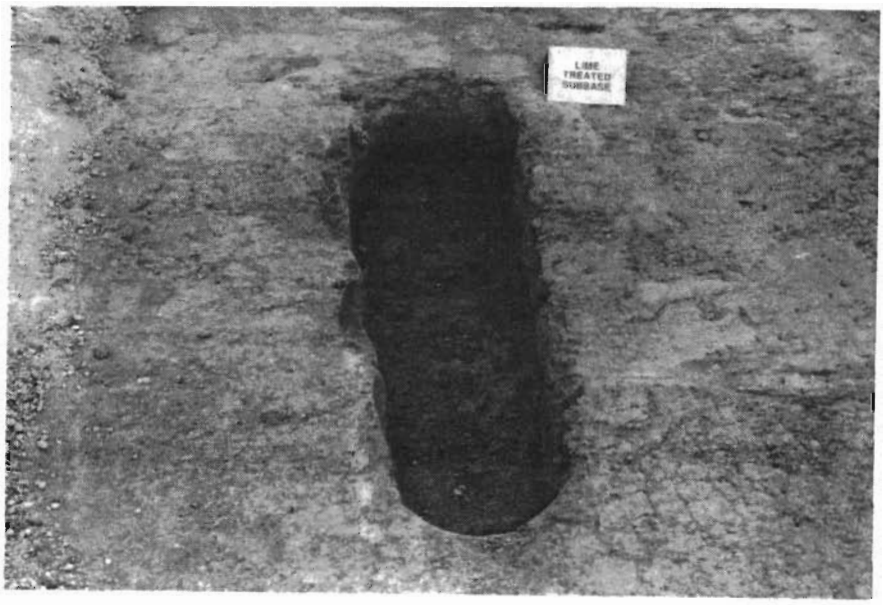

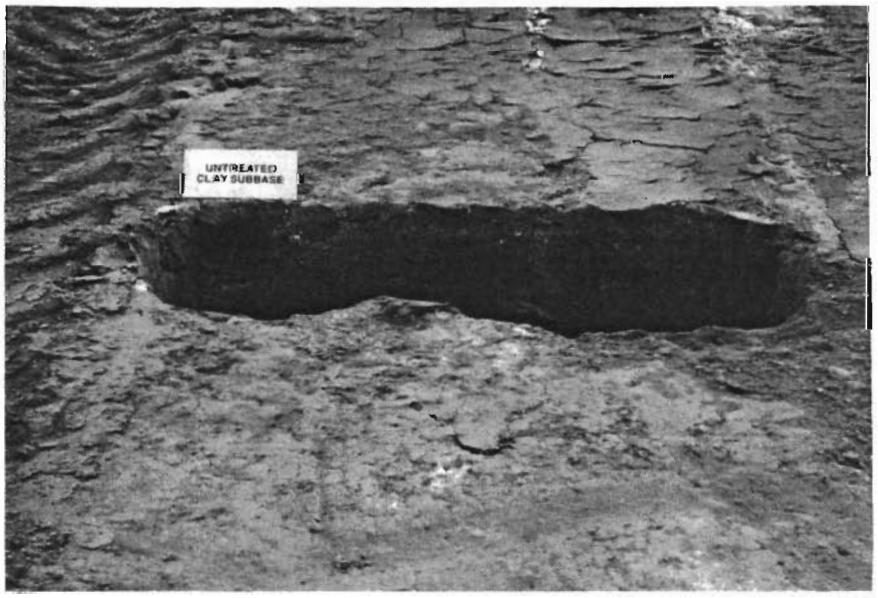

Fig 5.4. (continued).

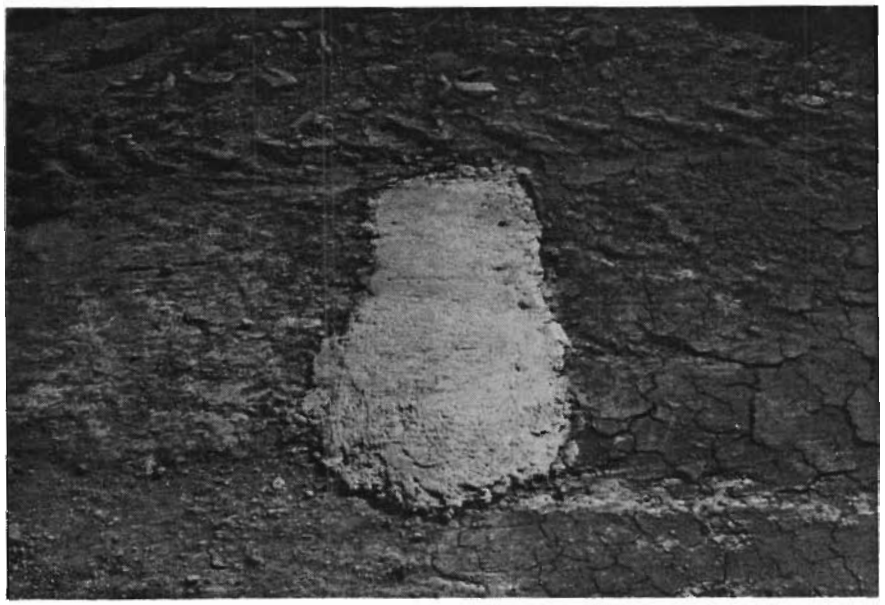

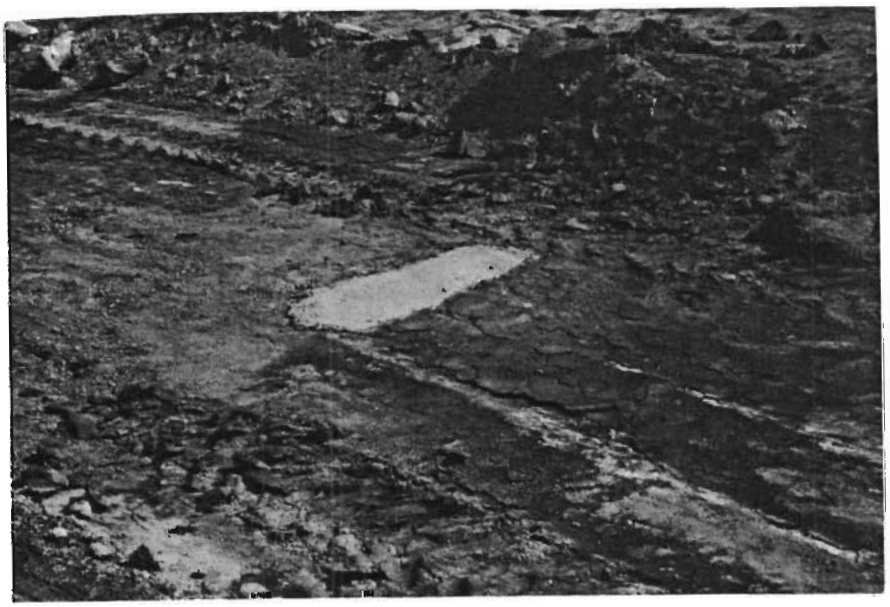

(continued)

Fig 5.5. Anchors for pinning test slabs.

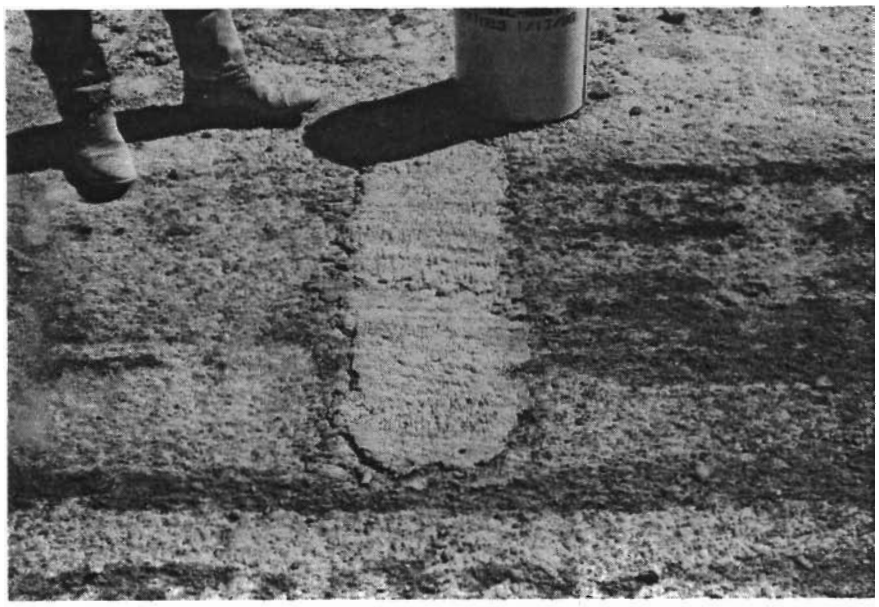

Fig 5.5. (continued).

Fig 5.6. Formwork for Houston test site.

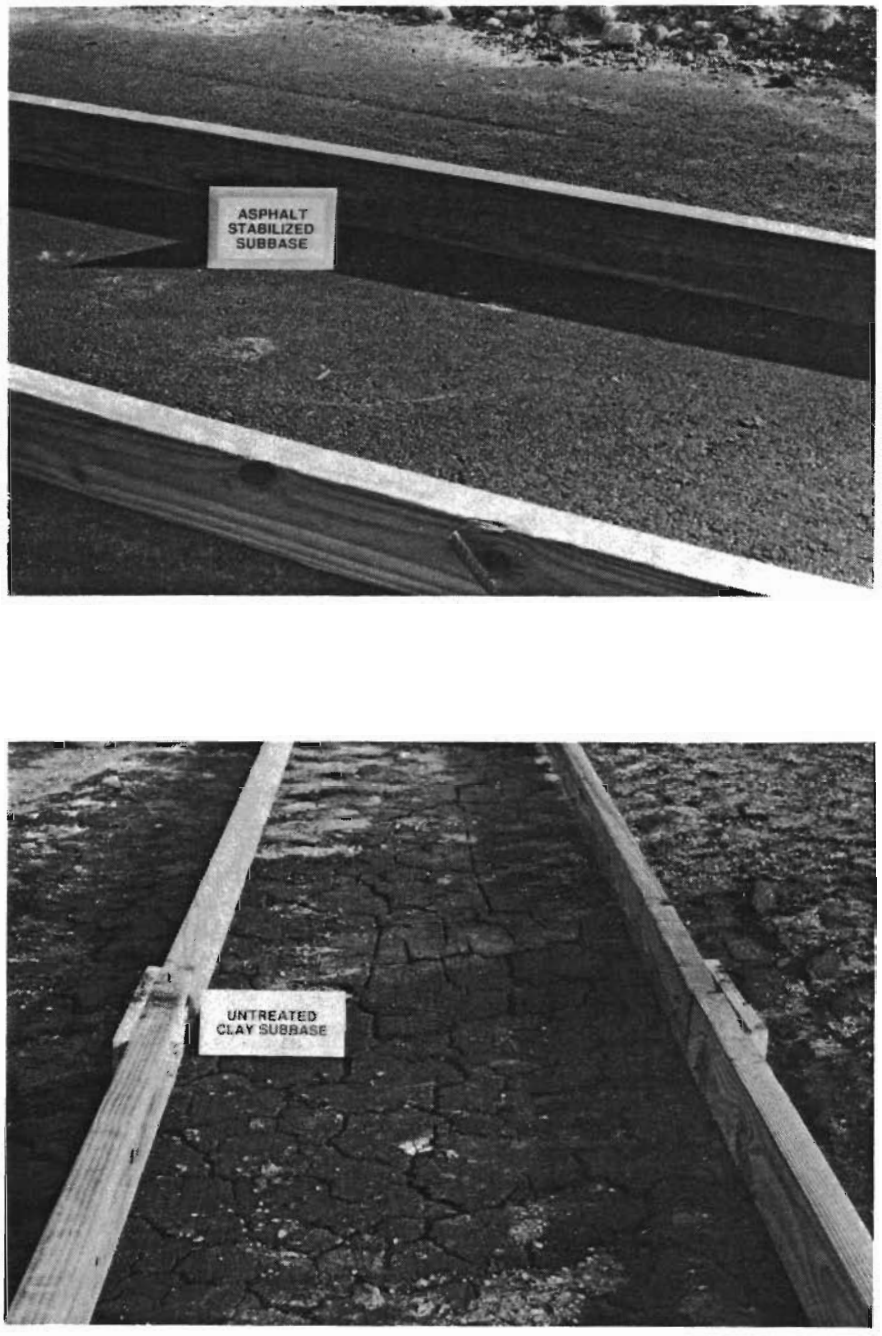

(continued)

Fig 5.7. Condition of Houston subbases just before casting.

Fig 5.7. (continued).

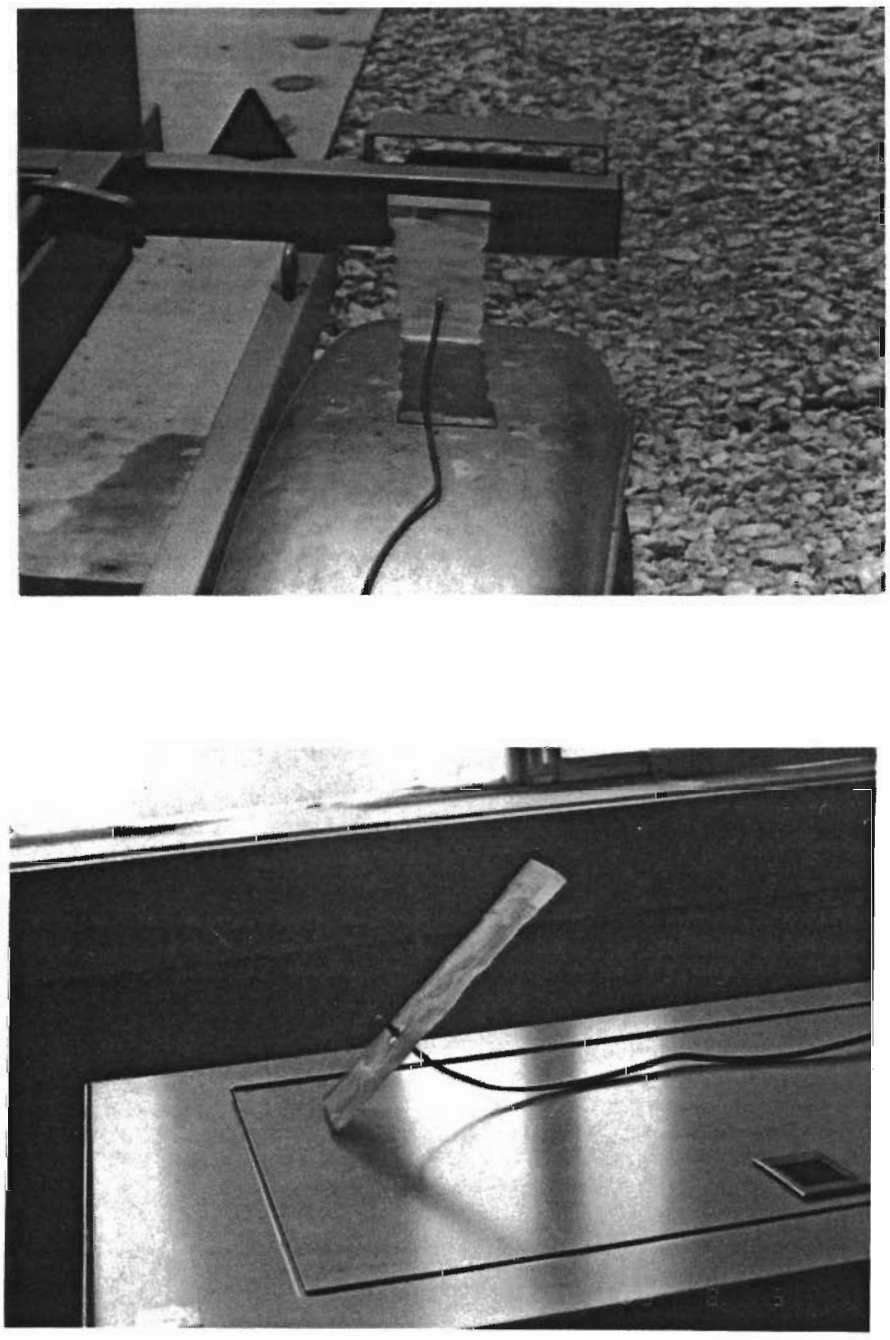

(continued)

Fig 5.8. Plastic inserts with mounted thermocouple wire before and after casting.

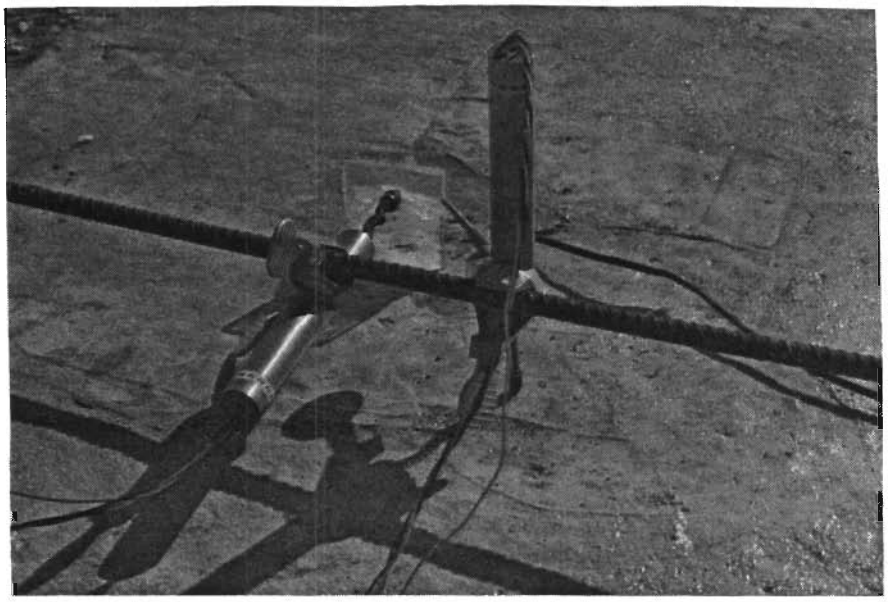

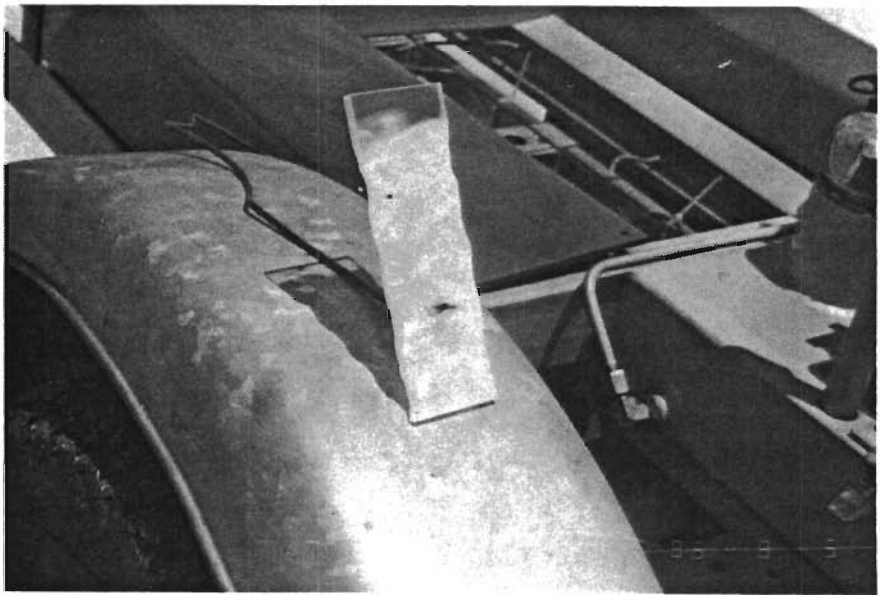

Fig 5.8. (continued).

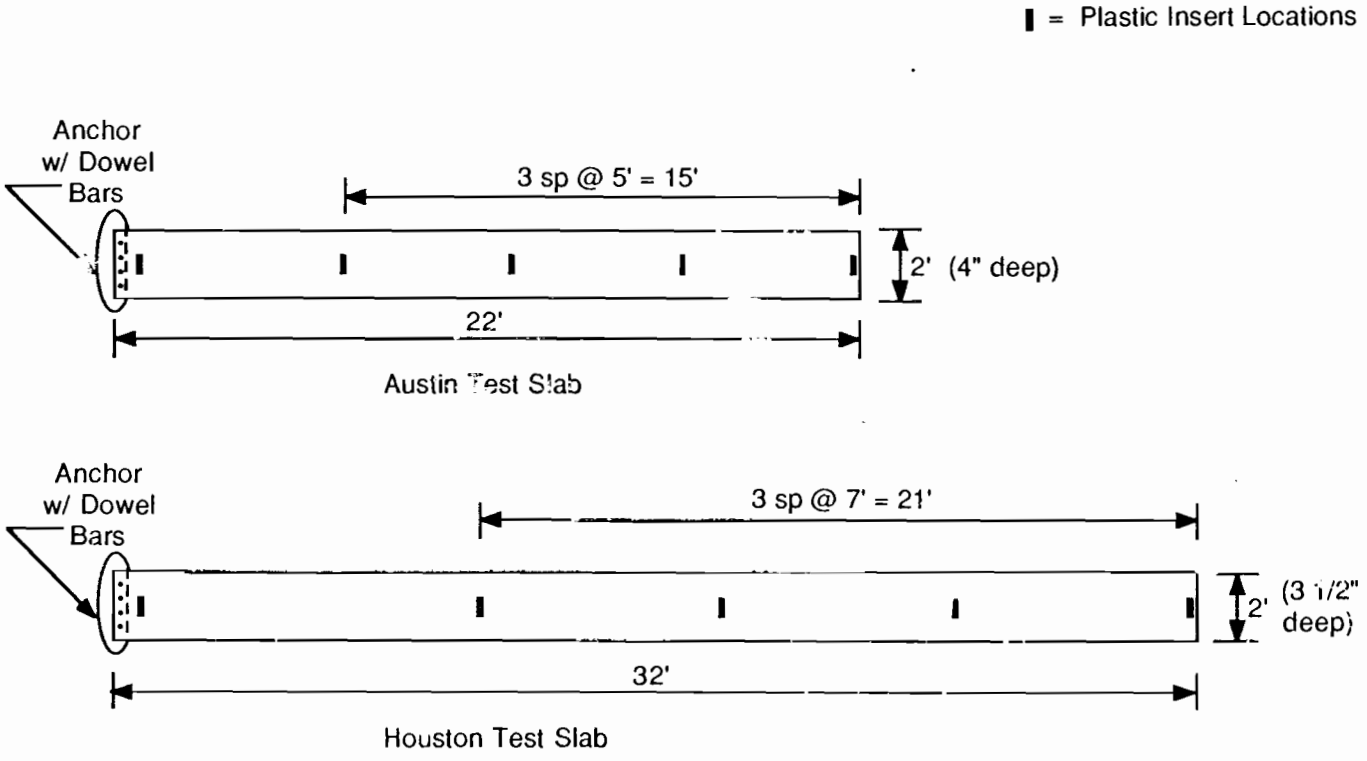

Fig 5.9. Test slab dimensions with plastic insert locations.

(continued)

Fig 5.10. Houston test slabs after casting.

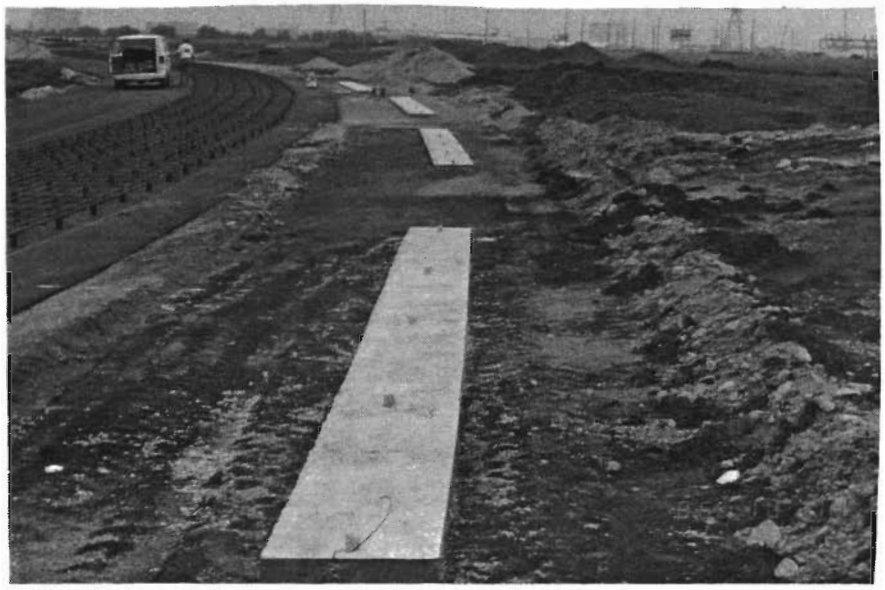

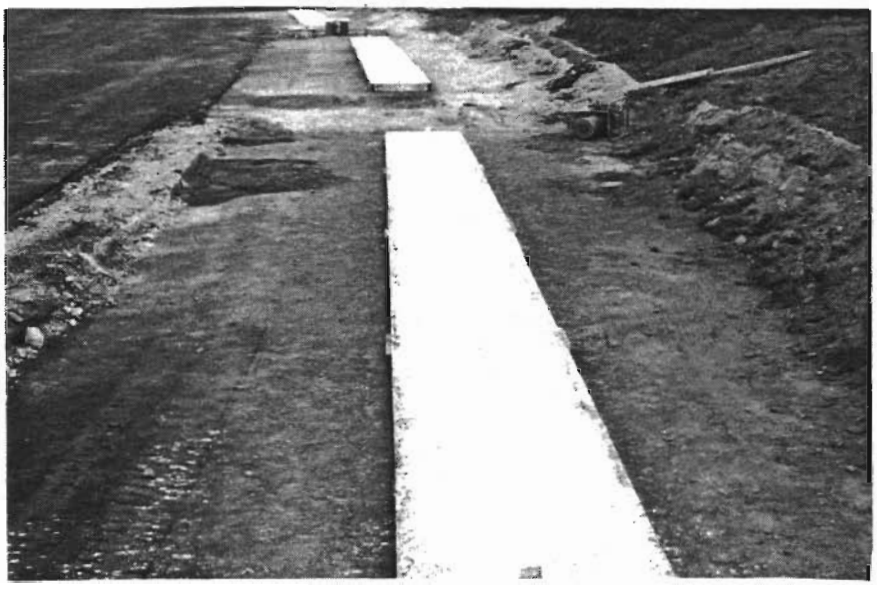

Fig 5.10. (continued).

Laboratory specimens were also cast during the two placements. They included standard cylinders for measuring the concrete's modulus of elasticity and compressive strength. Standard beams were also cast to measure the concrete's flexural strength. Smaller beams were cast for measuring the concrete's thermal coefficient of expansion. Each specimen was cured in the same environmental conditions as its partner slab(s) and remained on location before all testing began. Figure 5.11 shows the concrete specimens cast in Houston.

Pinning Slabs

Three weeks after casting, the slabs were pinned to their respective anchors. This delay permitted a three week concrete strength increase that could better handle the increased stresses induced by the larger movements since the slab's effective length would be doubled after being pinned at one end. If the slab(s) experienced cracking due to subbase resistance, the first phase of experimentation could not be performed. There are two reasons for pinning one end. The first, as mentioned before, is to effectively double the effective length of the slab for Phase I of the experimentation so that all movements will occur in one direction from the pinned end. The second reason is so that the pins can serve as a reaction for the push-off tests in Phase II of the experimentation.

The pinning process began by drilling four holes through one end of each slab down into its anchor. This required the use of an impact drill with a 1-3/8-inch–diameter drill bit. Eleven-inch–long No. 6, Grade 60 rebars were used as dowel bars. A fast-setting grout was mixed and placed inside the holes after they were vacuumed out and cleaned. The grout used was a non-ferrous, non-shrink grout produced and sold by the Burke Company. While the grout was still fluid, the dowel bars were slowly inserted in a clockwise rotation to prevent entrapped air from gathering around them. Figure 5.12 shows the holes being drilled down into the anchor while Fig 5.13 shows the dowel bars in place shortly after being grouted.

EXPERIMENTATION

All experimentation completed in this project can be summarized in three parts. The first two include Phase I and Phase II, which included monitoring of the constructed test slabs. The final part includes the testing of concrete specimens that were cast during both pours.

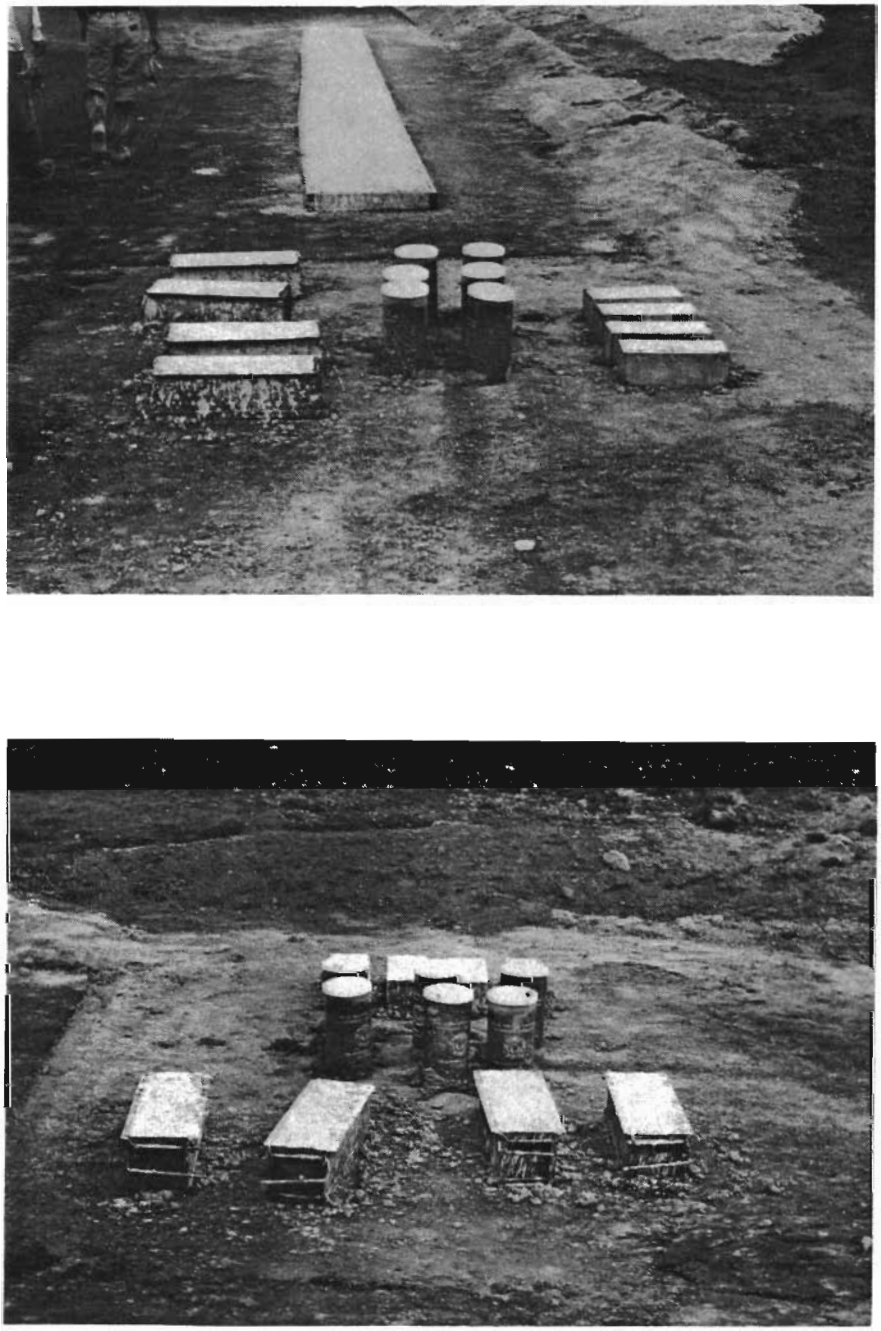

Fig 5.11. Concrete specimens cast for Houston test slabs.

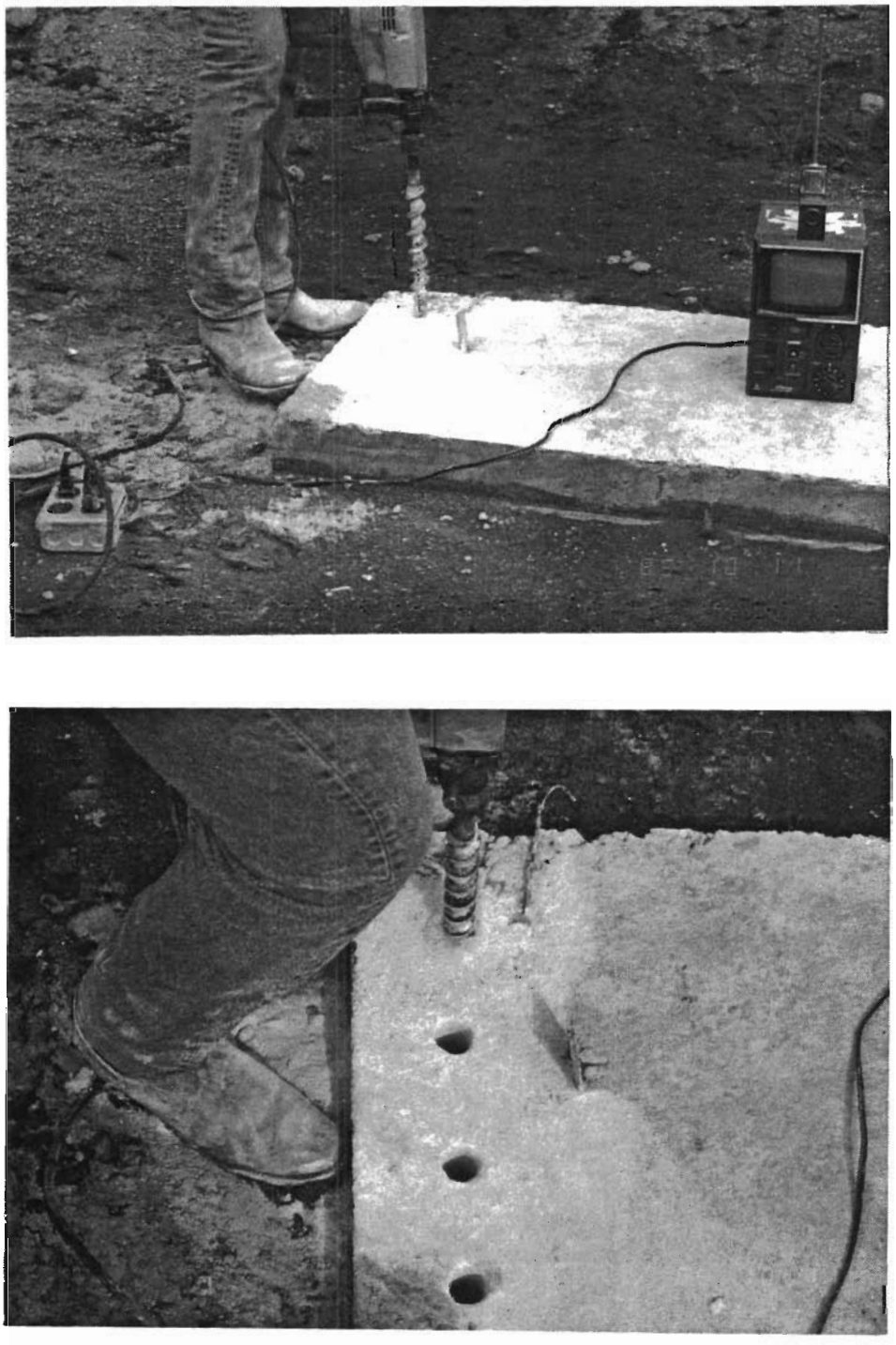

Fig 5.12. Drilling operation for pinning slab to anchor.

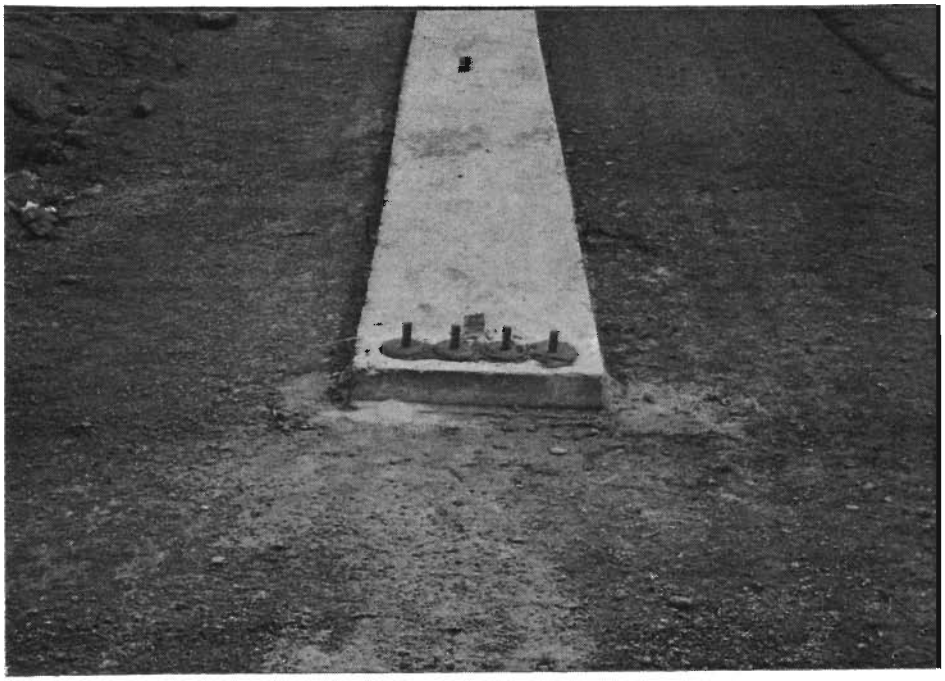

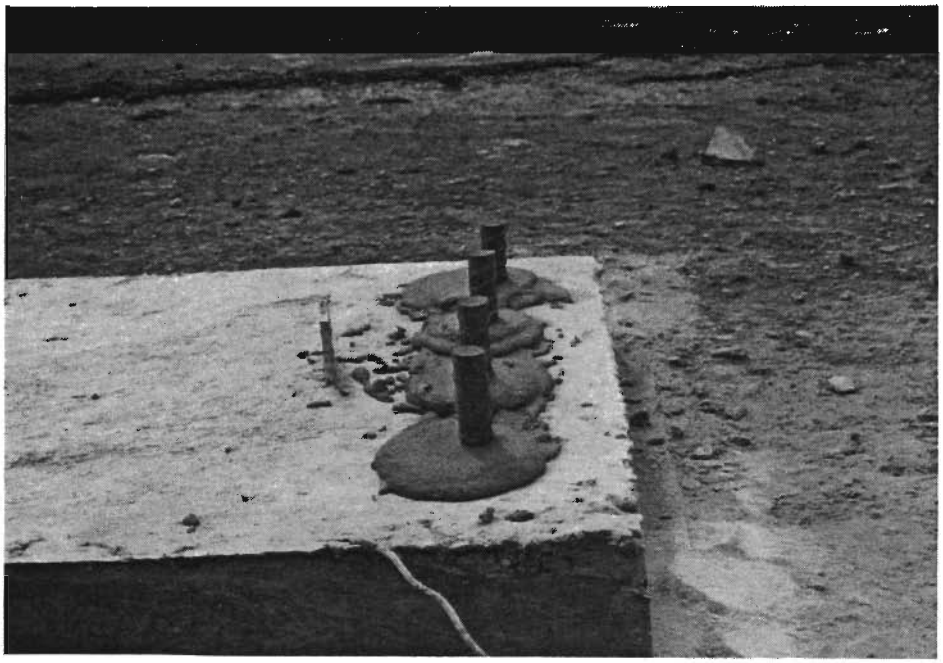

(continued)

Fig 5.13. Pinned anchors after grouting dowel bars.

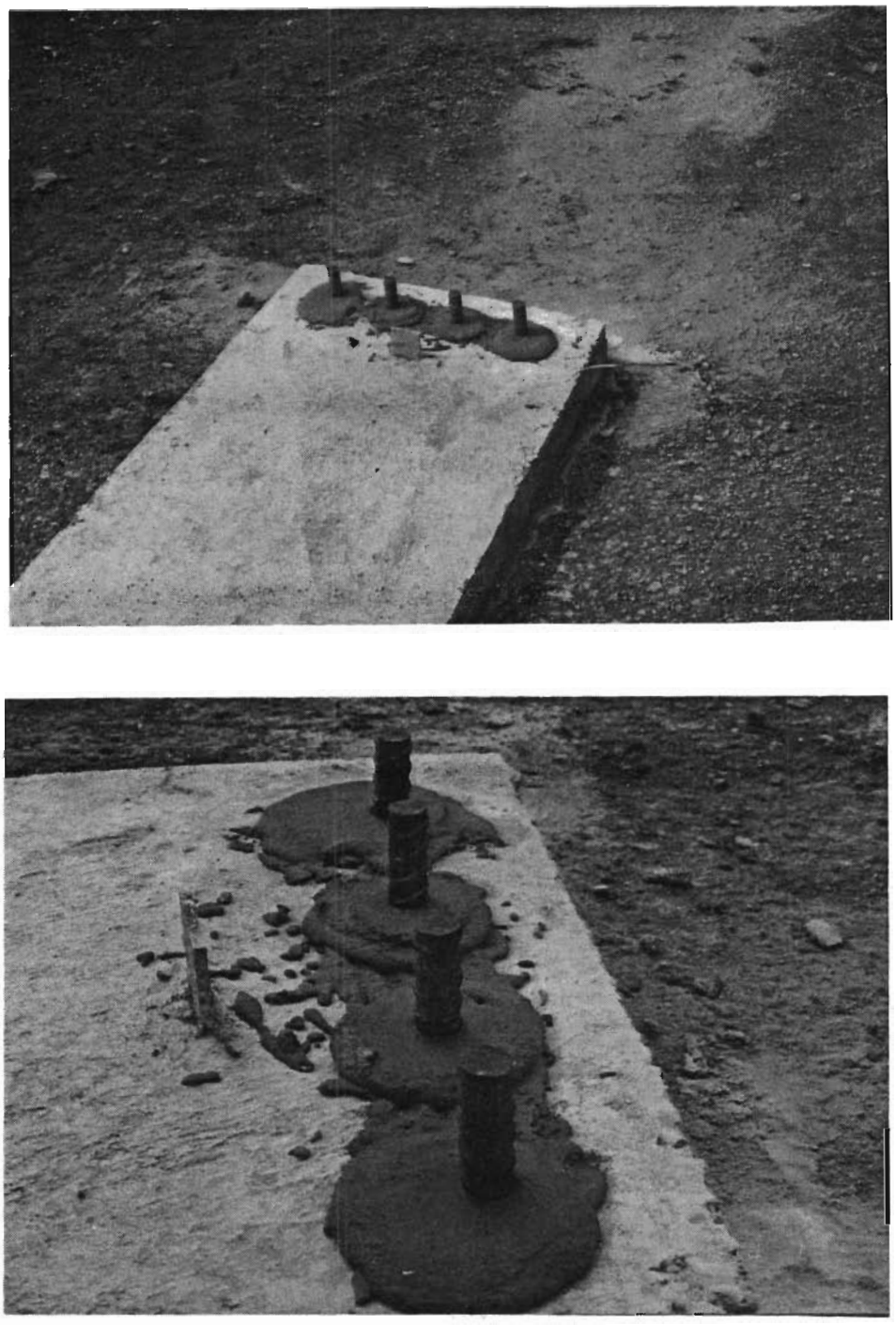

Fig 5.13. (continued).

Phase I was carried out to monitor the slab's actual movements over a particular subbase during a typical temperature cycle. Horizontal and vertical movements and mid-depth temperatures were recorded every 10 minutes between the peaks of the heating part of the day. Because of the pinned action at one end of each slab, all horizontal movements would yield positive values as the slab expands during the course of the day. Even though the test slabs were quite long, actual movements expected would not reach expected peak resistances also. Therefore, Phase II was to induce larger movements mechanically so that the peak resistance could be recorded and, thus, the entire friction profile would be established. The final part of the experiment included the measuring of needed parameters so that computed movements could be compared to the actual movements obtained in Phase I. These parameters included the concrete's compressive strength, modulus of elasticity, and thermal coefficient of expansion. Each parameter was measured at least three weeks after casting so that all the concrete parameters would have stabilized and be representative of the test slabs during all experimentation.

Phase I

Four weeks after casting, experimentation of Phase I began. Because pavement movements can be induced by both moisture and temperature variations a clear sealant was brushed onto all exposed surfaces of the slab to eliminate the former. A pair of rebar stakes were hammered far into the ground at each of the five plastic insert locations along the slab, and a horizontal bar was positioned firmly between the two stakes. This can be seen in Fig 5.14. The configurations are used as fixed supports for the instrumentation. The instrumentation consists of linear voltage distance transducers (LVDT's) and thermocouples mounted at each of the five locations along the slab. The vertical LVDT's were made by Trans-Tek with a linear range of approximately 0.6 inch. They were mounted by use of a thumb screw. The horizontal LVDT's were made by Schaevitz and were much more sensitive, with a linear range less than the width of a nickel. They were mounted by use of two nuts threaded to its housing, which surrounded a washer that had been previously tack welded to the rebar. A horizontal and vertical gage configuration can be seen in Fig 5.15. Also seen in Fig 5.15 are tiny squares mounted to the slab and plastic inserts. They were mounted after the LVDT's to aid in the zeroing and scaling processes. All of the gage wires and thermocouple wires were run from the slab to the data acquisition system as seen in Fig 5.16. Inside the data acquisition

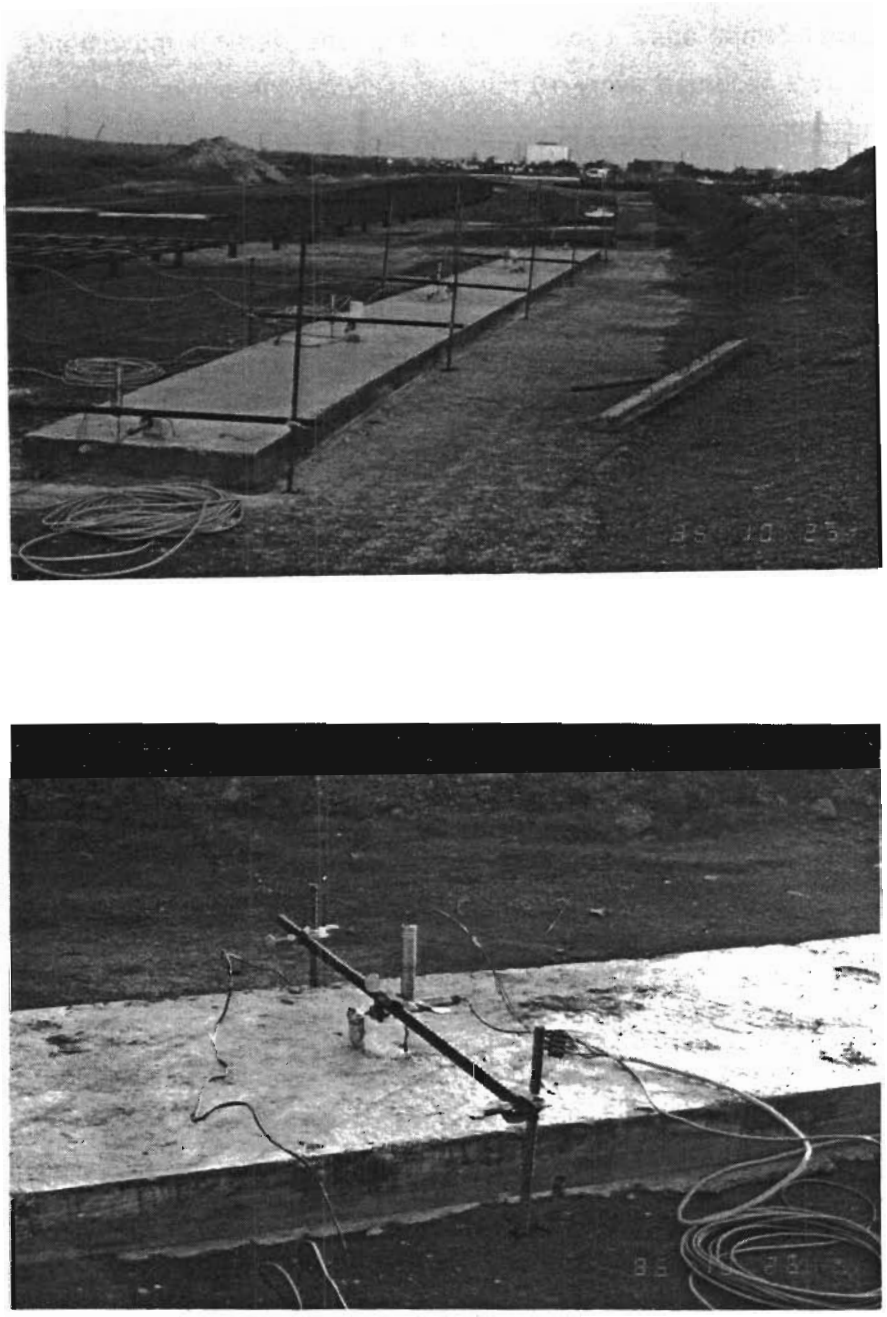

Fig 5.14. Fixed rebar supports for instrumentation.

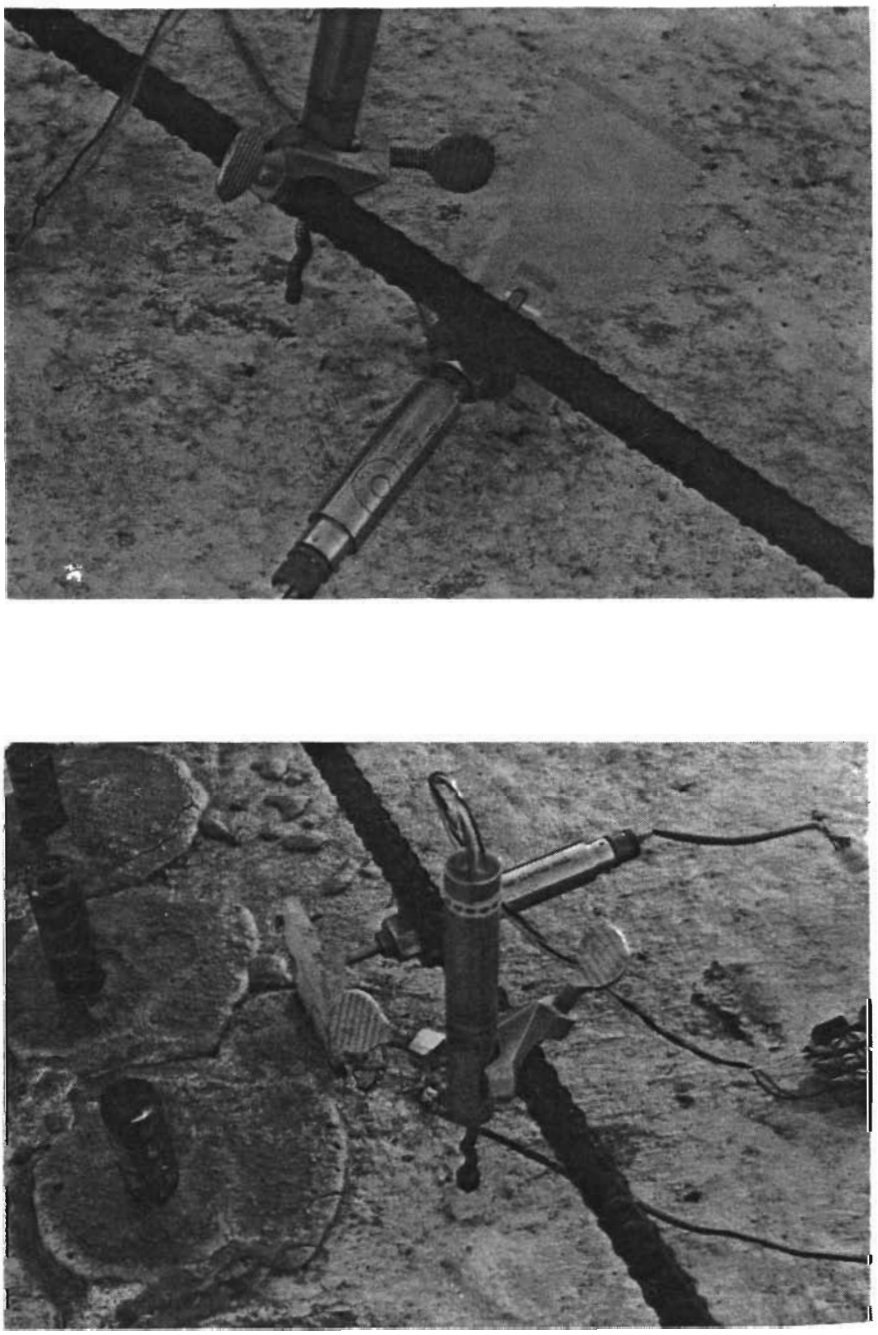

Fig 5.15. Horizontal and vertical linear voltage distance transducer configuration.

Fig 5.16. Gage and thermocouple wire from slab to data acquisition system.

system, gage and thermocouple voltages were read and converted to digits. All channels would open to a microcomputer at certain intervals to be read, converted to displacements and temperatures, and stored onto a disk. This set-up is shown in Fig 5.17. All wires can be seen leading into the back of the data acquisition system. The microcomputer is mounted on top of the data acquisition system. There are also two power supplies shown which supply the starting voltage required by the LVDT's.

Before sunrise all gages and monitoring equipment are positioned and turned on. The LVDT's are then zeroed manually one by one. They are then scaled by opening and closing the respective channel before and after a calibrated displacement block is inserted between the LVDT rod and the leveling block. The time increment is then punched into the computer and the monitoring process begins. The gages and thermocouples would then report at each time increment until mid-afternoon, when peak slab temperatures would generally occur.

Phase II

After Phase I was completed, the slab was ready to be sawed for Phase II of the experimentation. The first cut-out made was for the first push-off test and, at a later time, a second cut-out was made for a second push-off test. Each cut-out required two transverse saw cuts spaced 1 foot 3-1/2 inches apart. The piece would then be lifted out and be replaced by the mechanical instrumentation. Figure 5.18 shows the pavement saw used in cutting the slabs in Houston while Figure 5.19 shows the completion and removal of a typical sawed section. As seen in Fig 5.20, a hydraulic ram and load cell have been placed into the gap. Half-inch steel plates were used to insure concentric loading on the load cell so that accurate loads would be read. They were threaded at their centers and then screwed onto each end of the load cell. The pressure gage was added to the hydraulic ram to insure that ram and load cell capacities were not exceeded during the jacking operation. Both the hydraulic ram and the load cell were rated for twenty thousand pounds. The section areas to be pushed were 9 feet by 2 feet for the pilot slab in Austin and 14 feet by 2 feet for the test slabs in Houston. Therefore, two test sections could be pushed from each slab. Figure 5.21 shows the entire set-up for the first push-off test for the Austin test slab. The same gage configuration that was used in Phase I is used except that both LVDT's, horizontal and vertical, are the Trans-Tek models. They were used because of the large horizontal movements expected during the test. The monitoring

Fig 5.17. Monitoring devices needed for monitoring slab movements and temperatures.

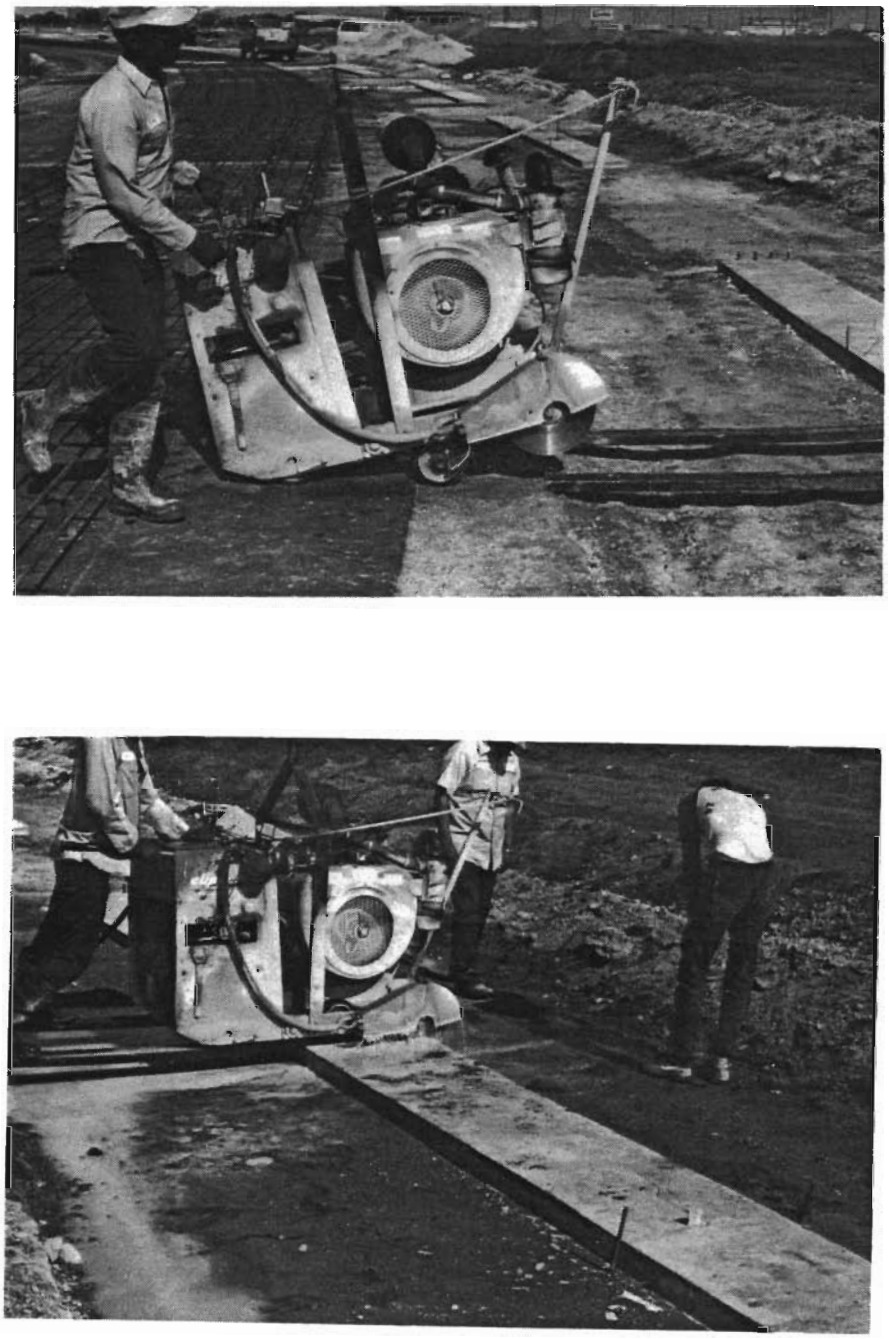

Fig 5.18. Pavement saw used to cut through the test slabs.

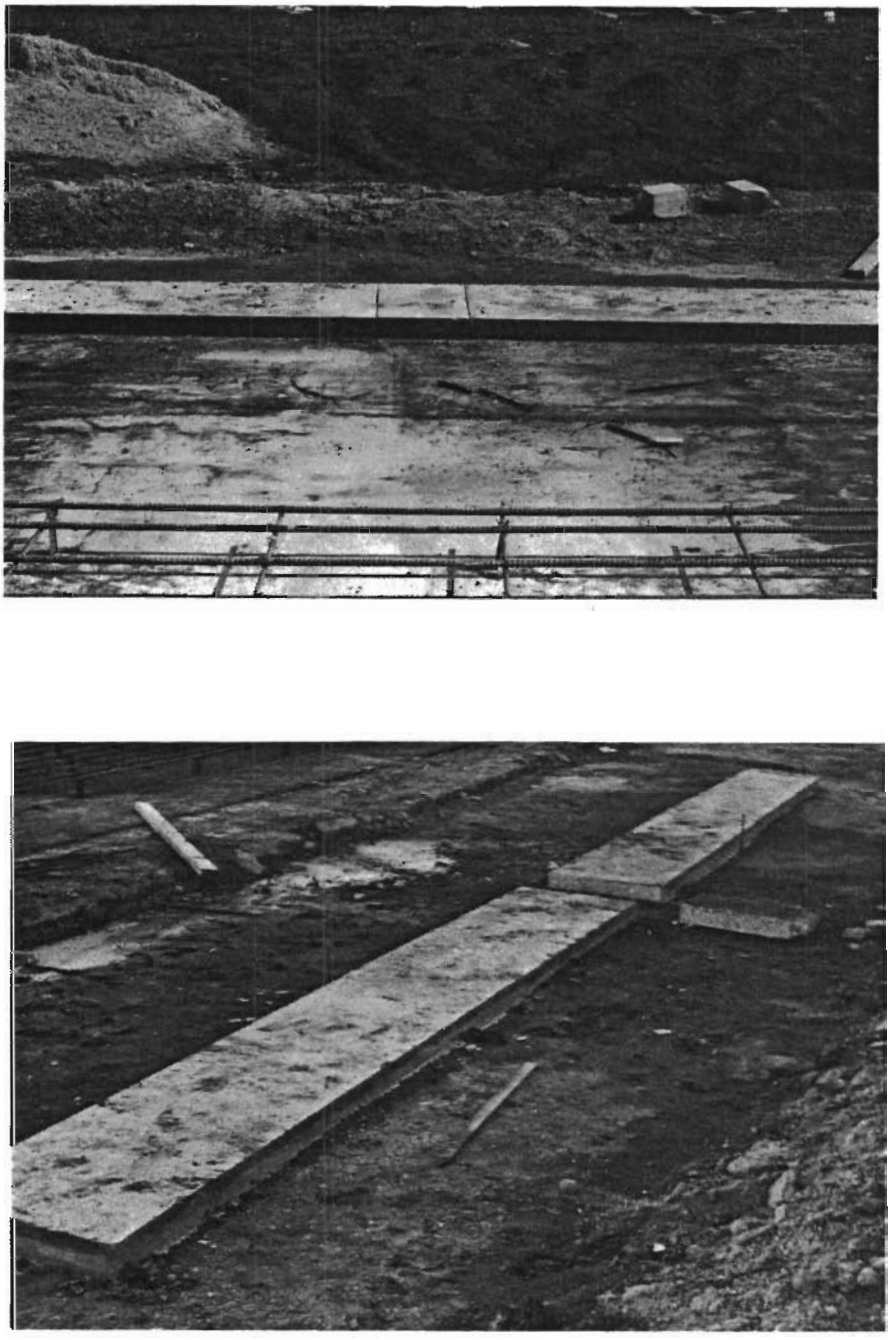

Fig 5.19. A typical sawed section needed for push-off test.

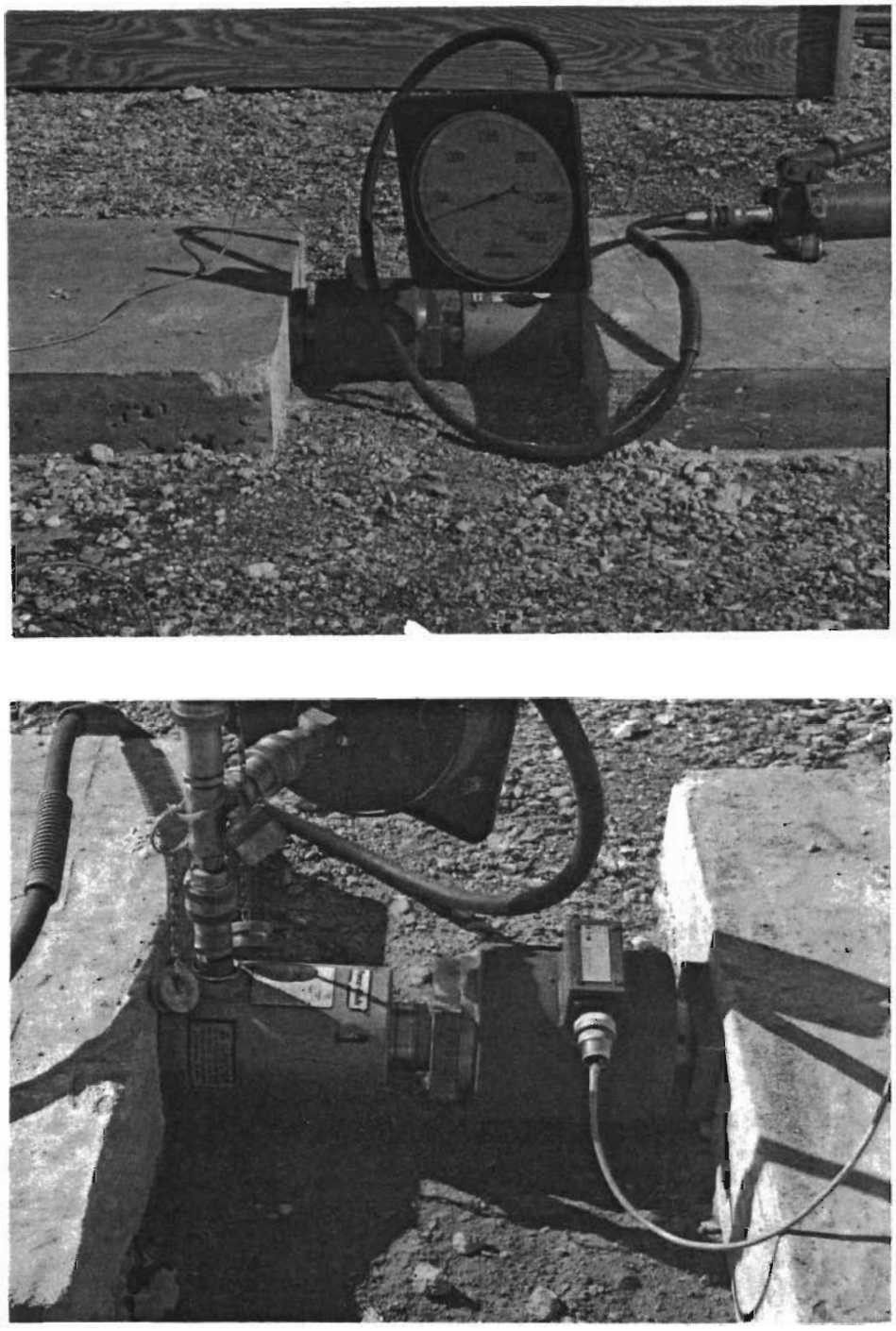

Fig 5.20. Load cell and hydraulic ram used in push-off tests.

Fig 5.21. Equipment set-up for push-off test No. 1 in Austin, Texas.

location is in the center of the slab area in order to represent the average horizontal and vertical movements of the test specimen. This is also shown in Fig 5.21.

The test is begun by again manually zeroing and scaling the two LVDT's. Then the push–off test is started. Each time pressure is applied to the ram, a reading is taken by the operator. At that instant of time, all channels of the data acquisition system are opened, recording the load cell force, slab temperature, and both displacements. Pressure is applied in 100 to 300–psi increments until sliding is induced and the monitored force has dropped off significantly from its earlier peak.

The second push-off test required another cut-out after the first push-off test was completed. This was so the pinned end could serve as a reaction for both push-off tests. Slab areas were kept the same for the second push-off test, but weight was added to simulate a thicker slab. Precast preweighed concrete blocks were stacked along the surface of the slab except where they would interfere with the gages. They in effect, turned the 4-inch slab in Austin into an 8-inch slab, and the 3-1/2-inch slab in Houston to a 7-inch slab. As mentioned in Chapter 2, this addition in weight can give a better idea of the magnitude of adhesion between the slab and its subbase. If there is little difference between the first and second push-off tests, then we can assume that the adhesion component plays a major role in the total subbase frictional resistance. Figure 5.22 shows the second push-off test run on the Austin test slab.

TESTING OF CONCRETE SPECIMENS

Two variables were measured from the concrete cylinders that had been cast during construction. They were the modulus of elasticity and the concrete's compressive strength. A stress-strain relationship was necessary so that computed movements could be compared to the actual movements obtained in Phase I of the experimentation.

Each cylinder was first capped with a sulfur-based material and then harnessed with a compressiometer. The compressiometer held two mounted dial gauges so that they could be averaged as the total strain during loading. The capping station and a mounted compressiometer can be seen in Fig 5.23. The cylinder was preloaded to seat the loading arrangement. The gauges were then zeroed and loading began. Every time the load dial reached an additional 2000–pound increment, the operator would signal for the two gauge readers to

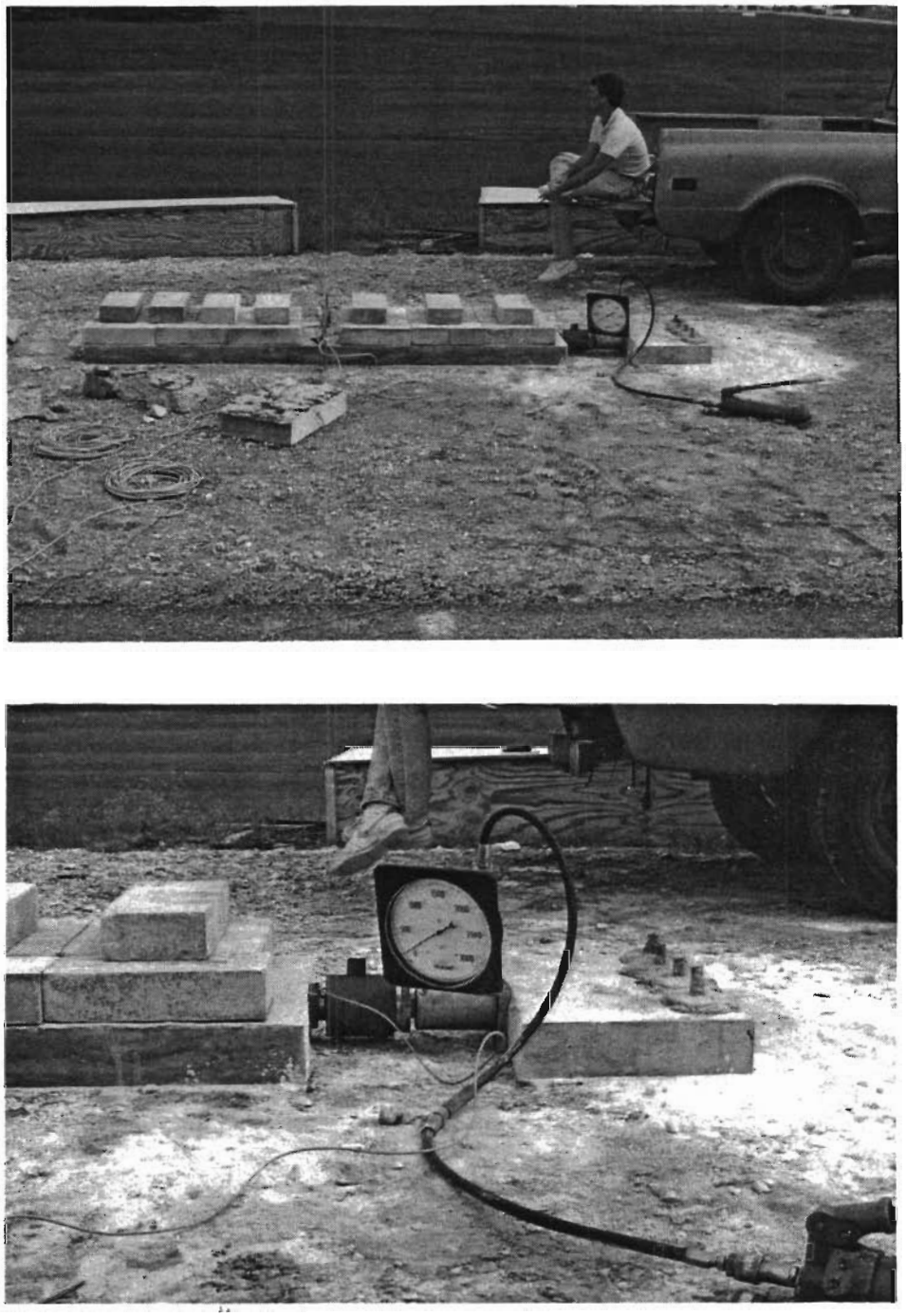

(continued)

Fig 5.22. Eight-inch simulated slab for second push-off test in Austin, Texas.

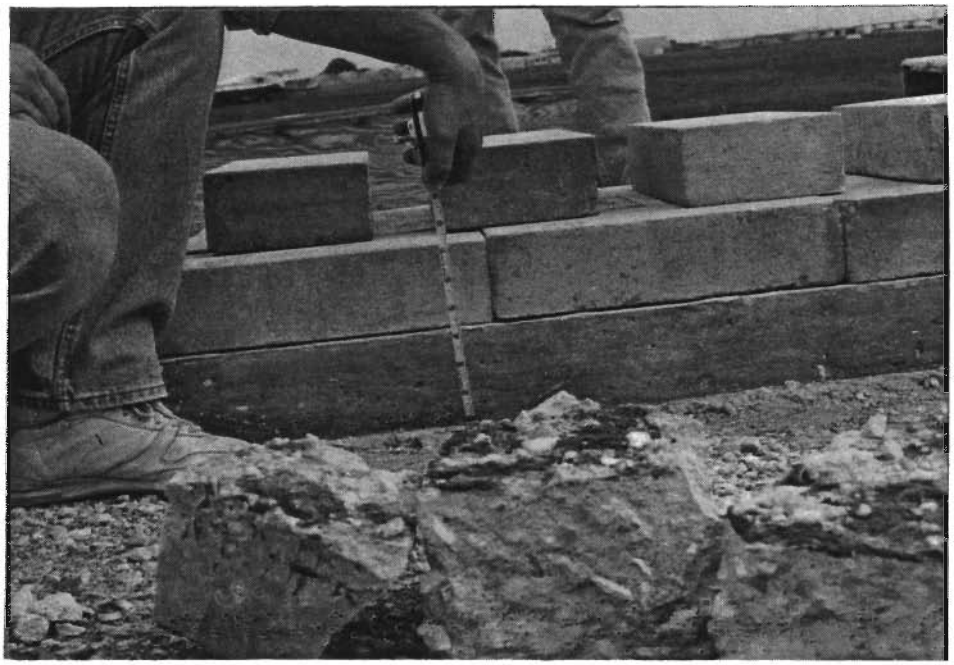

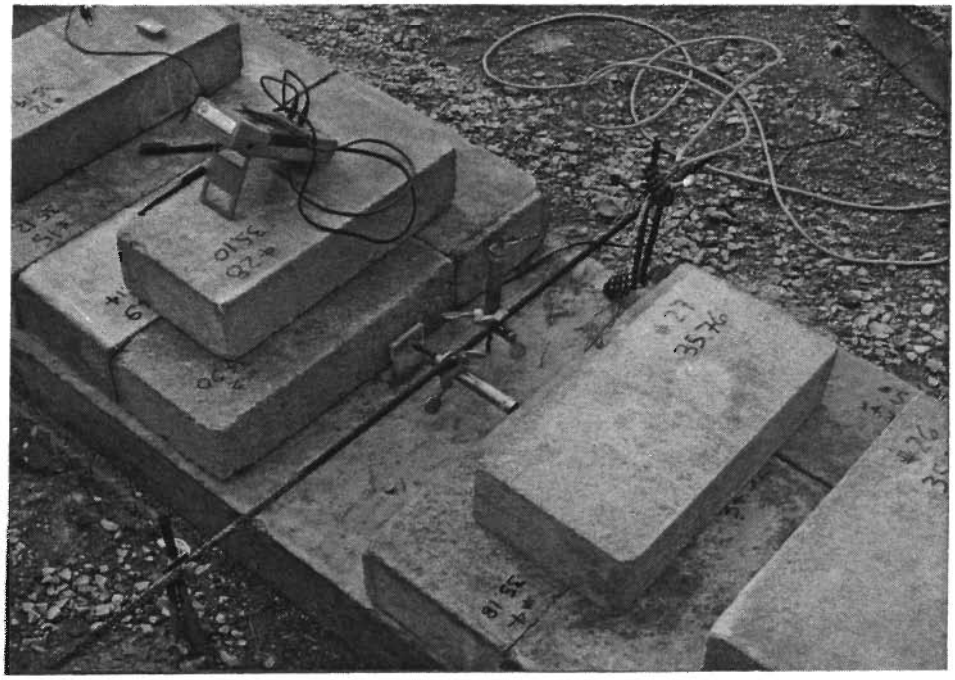

Fig 5.22. (continued).

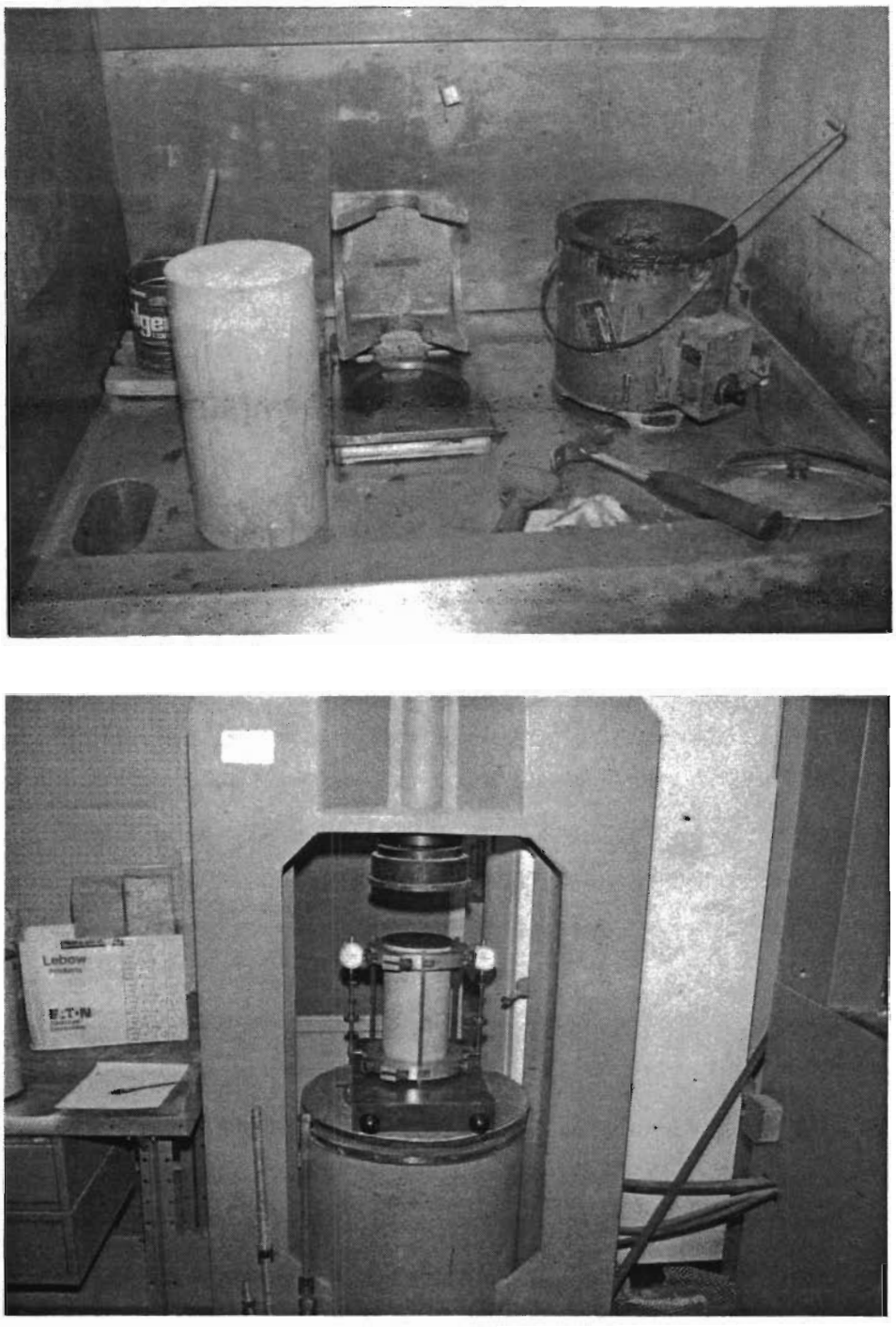

(continued)

Fig 5.23. Cylinder capping station. Modulus of elasticity test using a compressiometer.

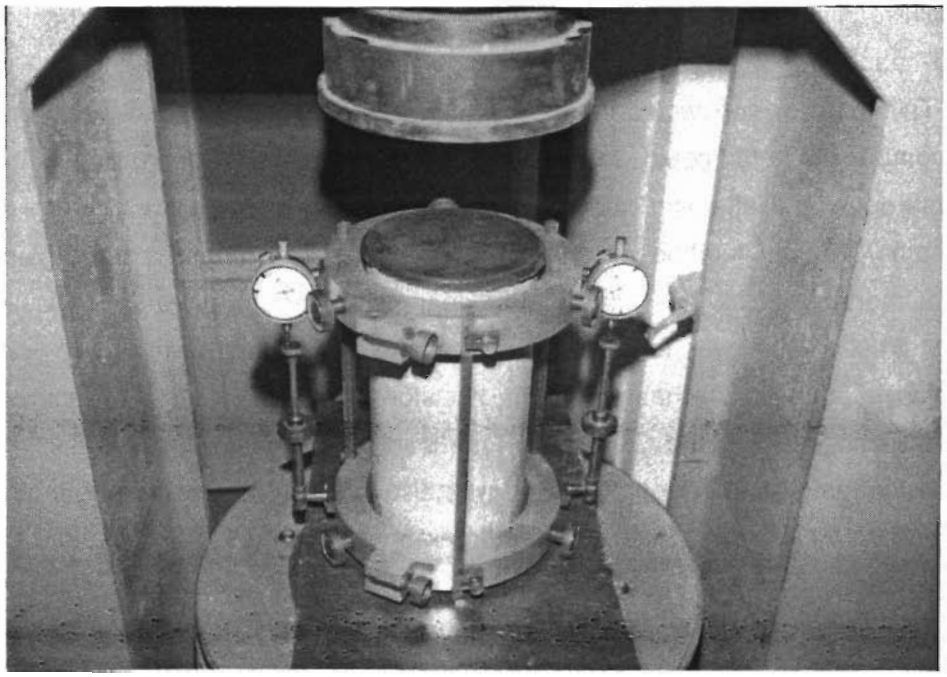

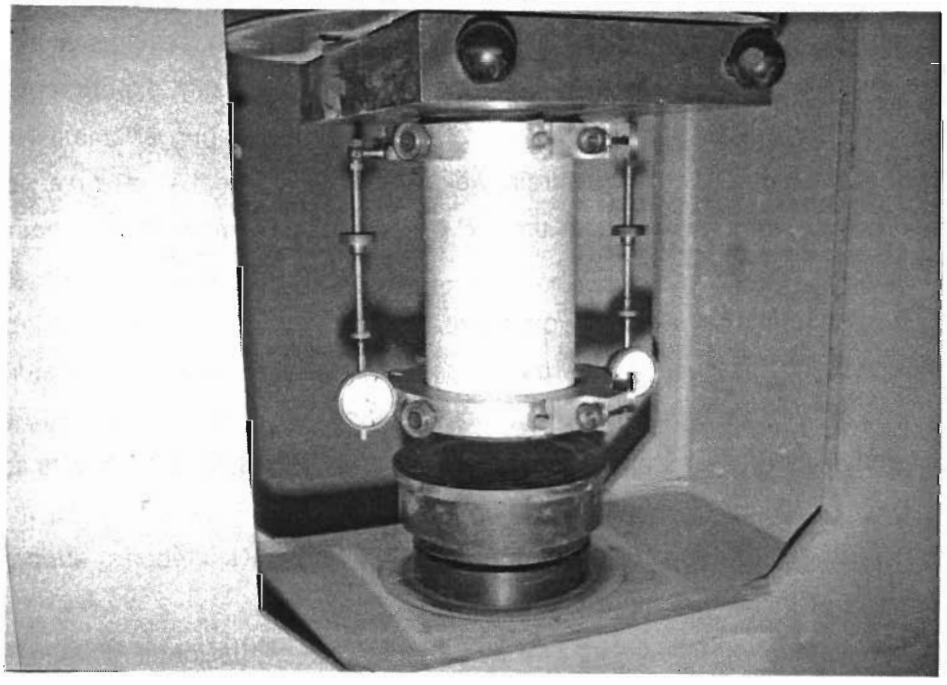

Fig 5.23. (continued).

take a strain reading. This operation can be seen in Fig 5.24. Loading would continue until the total load reached approximately one-third of the expected compressive strength of the cylinder. This mark was expected to be approximately 32 kips. The load was then taken off so that the compressiometer could be removed. The cylinder was then loaded to failure. All loading was done at a straining rate of 20 micro-strains per minute.

Another popular method for characterizing concrete strength is the flexural test. The method commonly used by the Texas State Department of Highways and Public Transportation in their construction sites was followed. The beams cast in Austin were tested using the center point loading head while the beams cast in Houston were tested using the third point loading head. This was because of the availability of the loading machines.

The thermal coefficient of expansion was also measured. Hand-made beam forms were made so that all dimensions would exceed three-and-a-half times the maximum aggregate size of the expected concrete mix. Beam dimensions were 4-1/2 inches by 4-1/2 inches by 13 inches. The longer faces were used for mounting the surface strain gages and surface thermocouple wires. During casting an internal thermocouple lead was placed so that by having internal and surface temperatures a thermal gradient could be assumed between the two. Therefore, after the gradient became constant, or stabilized, during testing, strain gage readings could be taken at that particular temperature. The basic experiment consisted of running the specimens through a temperature cycle while monitoring strains. The correlation between change in temperature and strain yields the thermal coefficient of expansion. This variable was also needed in computing the movements to be compared with those obtained in Phase I.

Since specimen movements would experience friction resistance during the test, a frictionless support for the specimens was devised to prevent resistance on these movements. A giant skateboard was designed and built for this purpose. It can be seen in Fig 5.25. The skateboard consisted of 85 all-directional roller bearings mounted on top of a plastic board. They were held in place by recessed bolts and nut in a plywood board so that the entire skateboard could lie flat during testing. Figure 5.26 shows the skateboard supporting the test specimens inside of the temperature chamber before testing.

The specimens were prepared first by sanding both of the longitudinal sides for proper mounting of 120 mm surface strain gages. Strain gage leads were then epoxied with a surface thermocouple to the specimen and soldered to the strain gage. This can be seen in Fig 5.27. All surfaces were brushed with a moisture barrier to prevent moisture variations within the

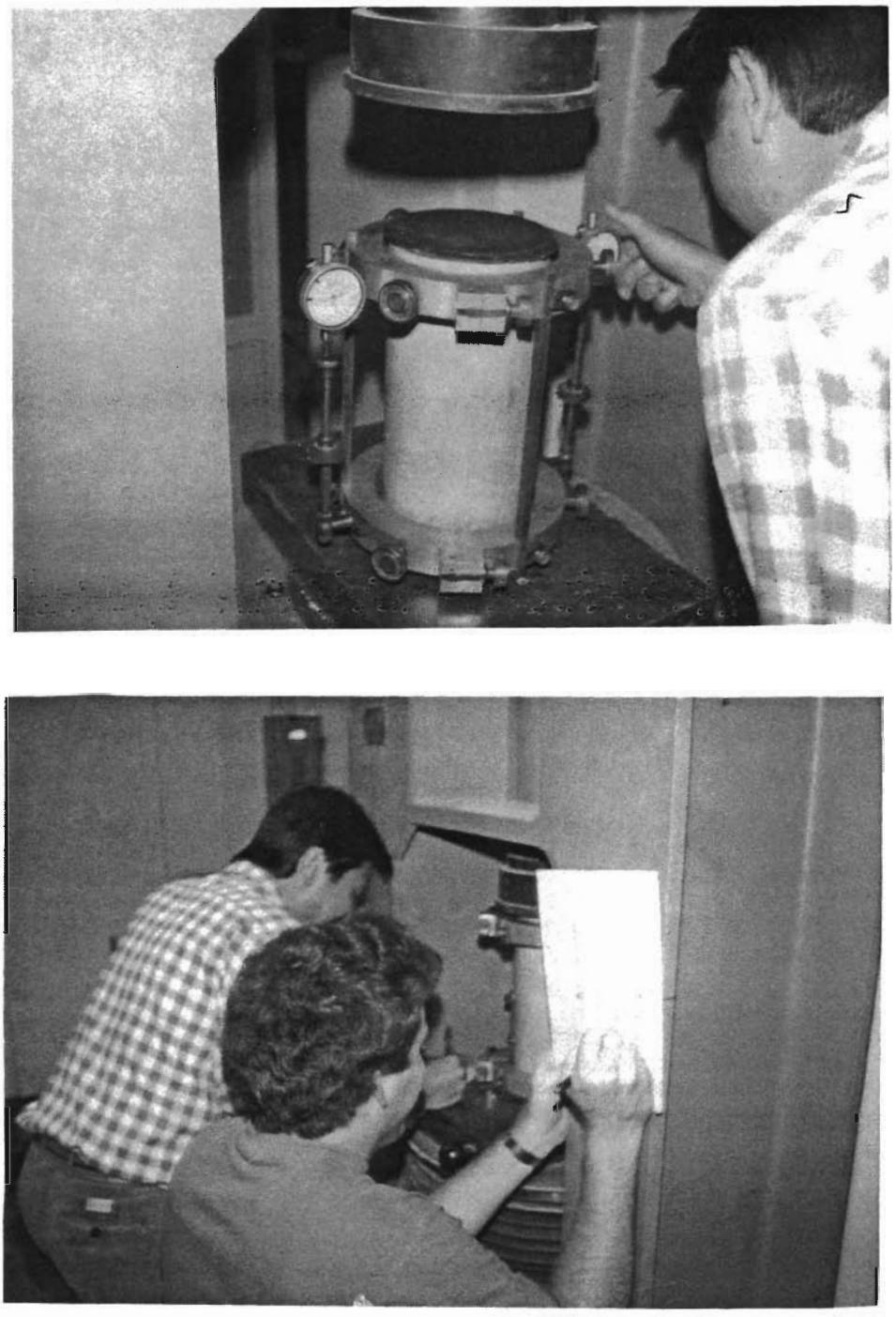

Fig 5.24. Zeroing and monitoring strain gages for modulus of elasticity tests.

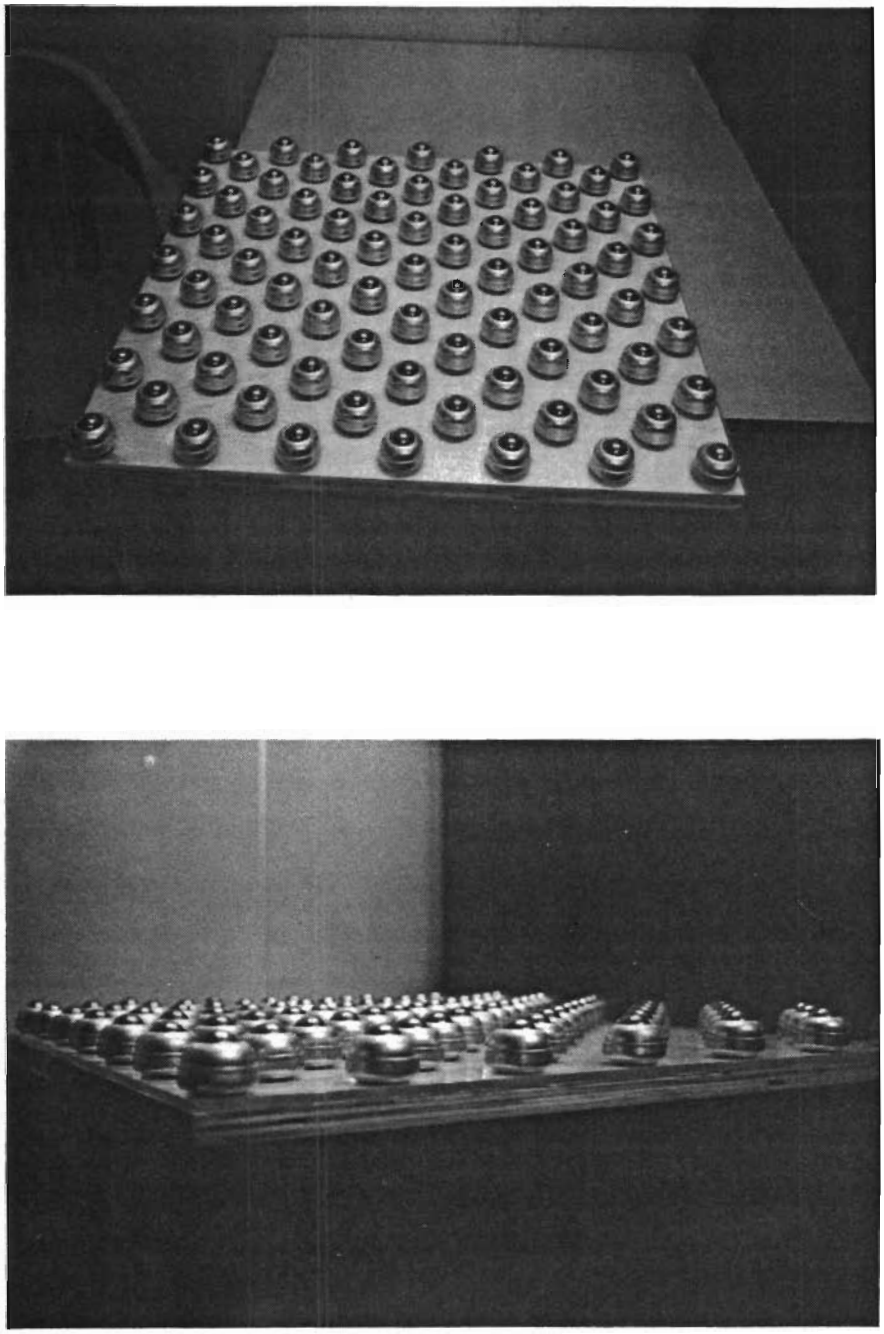

(continued)

Fig 5.25. Constructed skateboard used in thermal coefficient of expansion experiment.

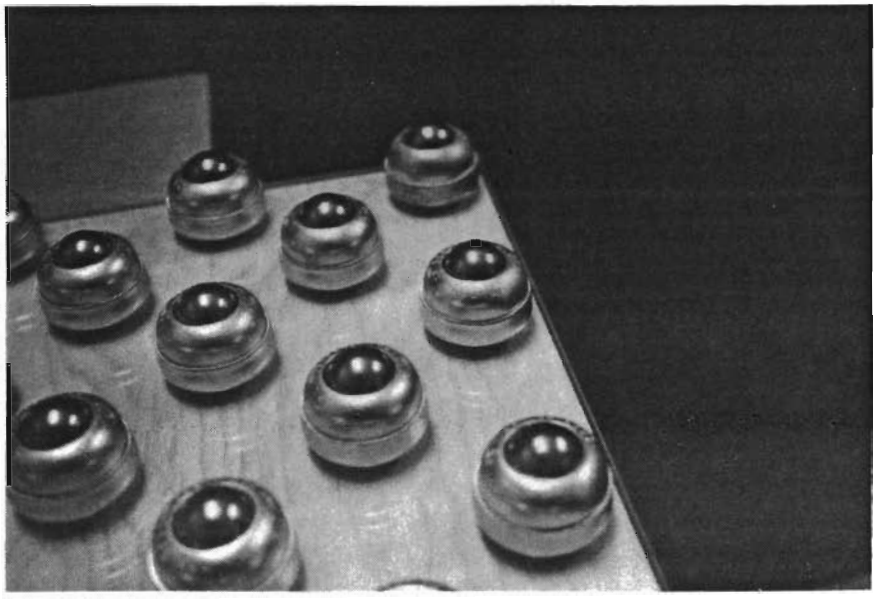

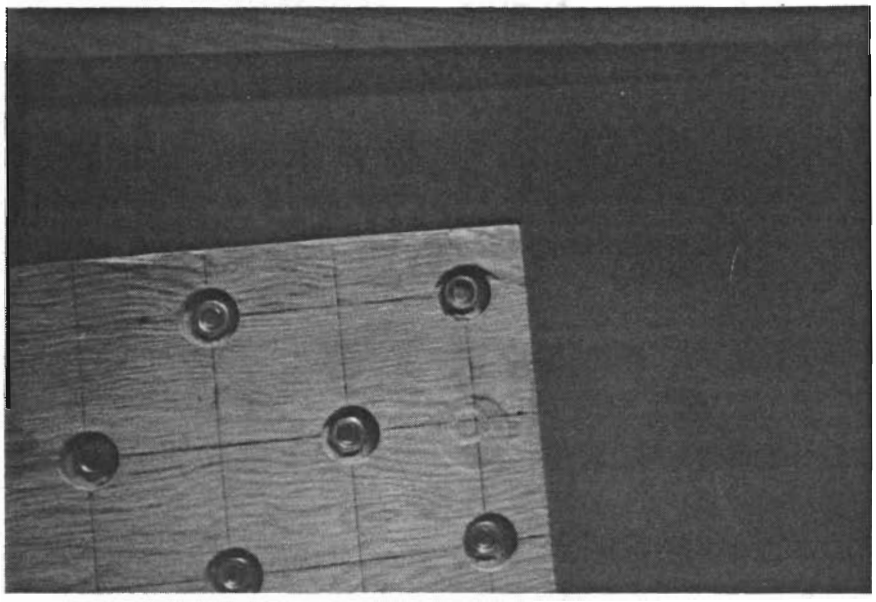

Fig 5.25. (continued).

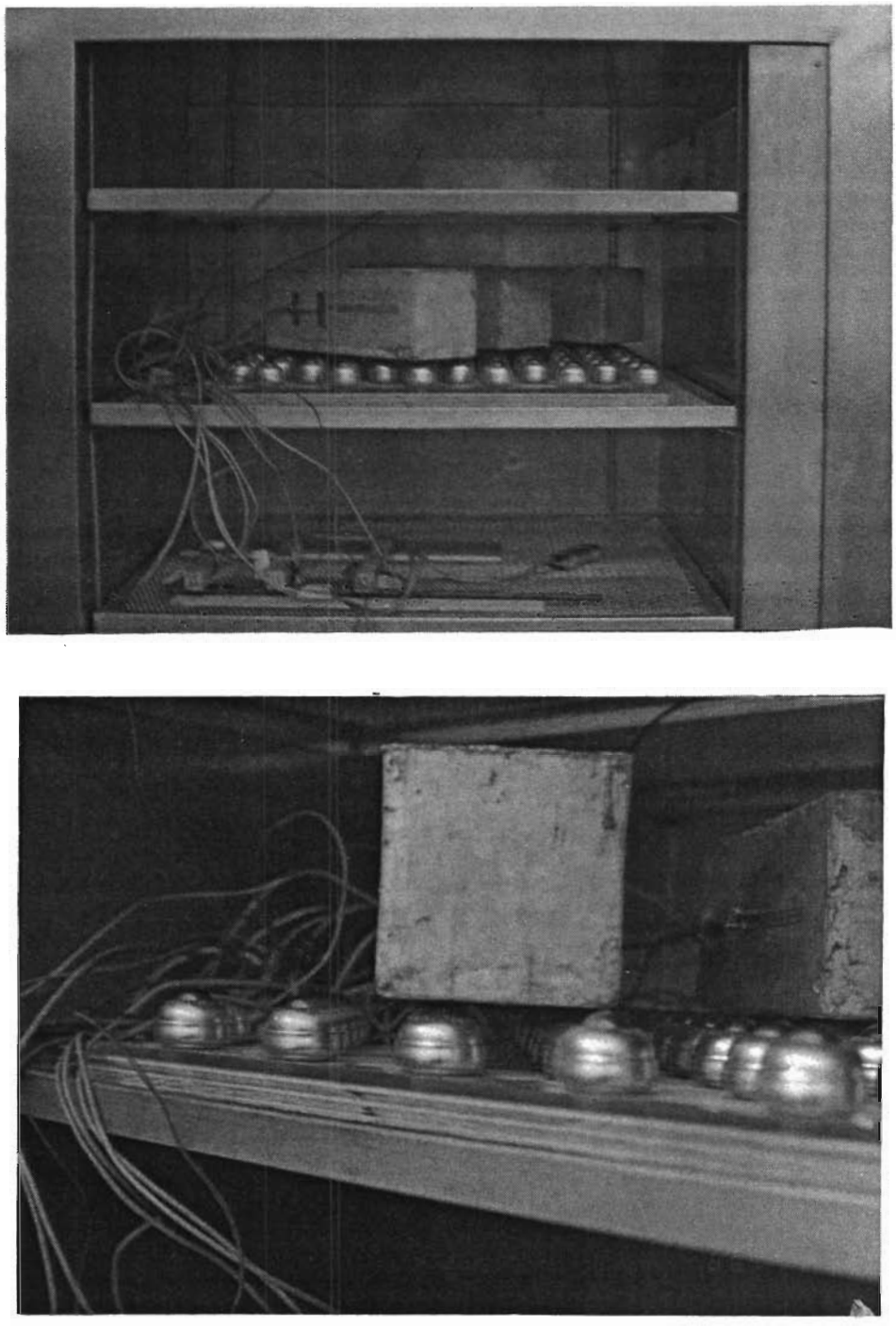

Fig 5.26. Skateboard used as frictionless support for test speciments.

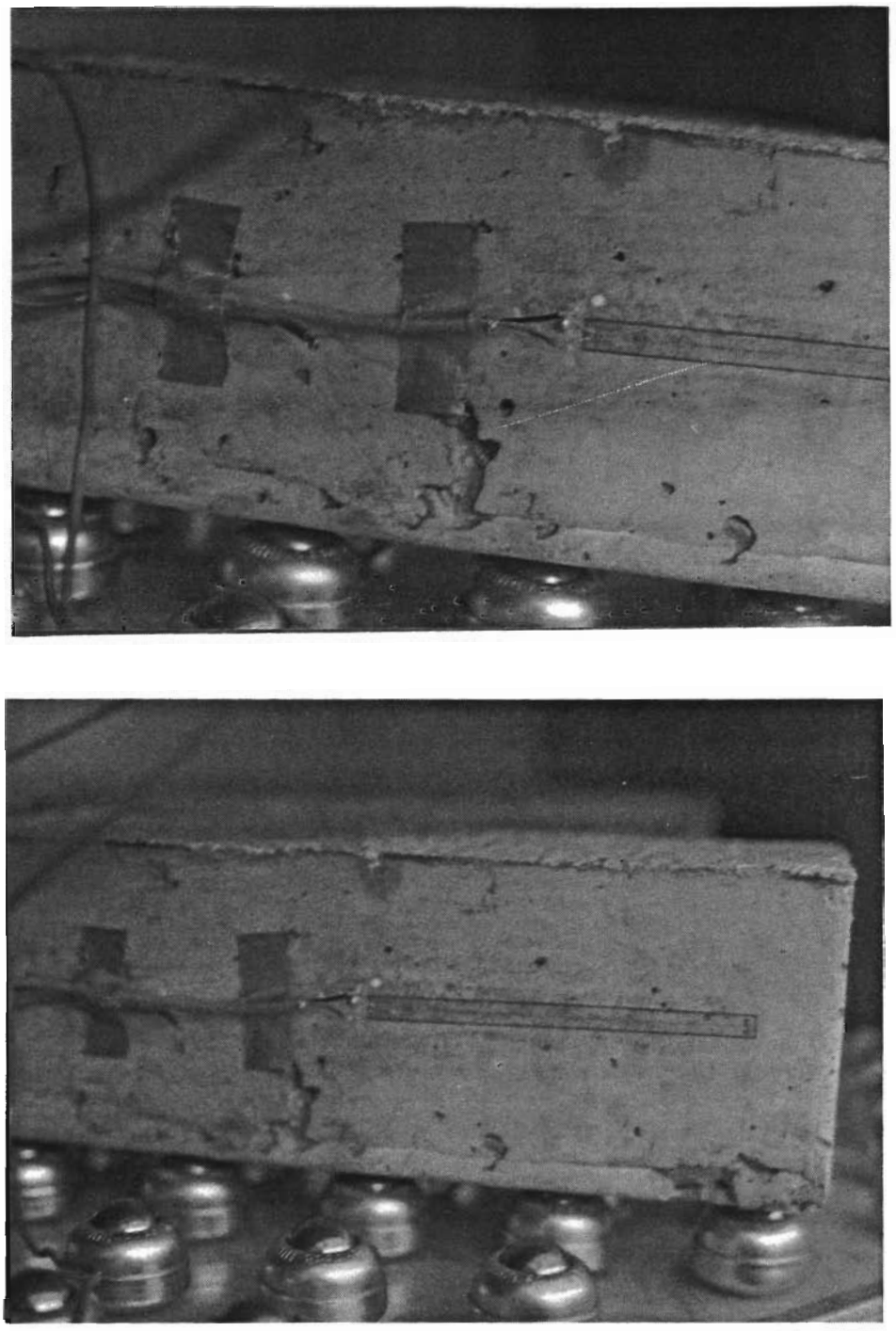

Fig 5.27. Mounted surface strain gage and thermocouple on test specimen.

specimens during testing. All wire leads were channeled through an open port inside of the temperature chamber. The strain leads were connected to a conventional check and balance box configuration while the thermocouple leads were attached to the data acquisition system also used in Phase I and Phase II. Temperatures were monitored on the screen of the micro-computer and strains were taken by reading the dial after balancing operations. These monitoring devices can be seen in Fig 5.28. The experiment consisted of closing in on a particular temperature, waiting for the surface and internal temperatures to stabilize, to be approximately equal to one another, and then taking strain readings at that temperature. The specimens were taken through a temperature cycle where strain readings were taken at approximately the 45°F, 75°F, 105°F, and 135°F marks.

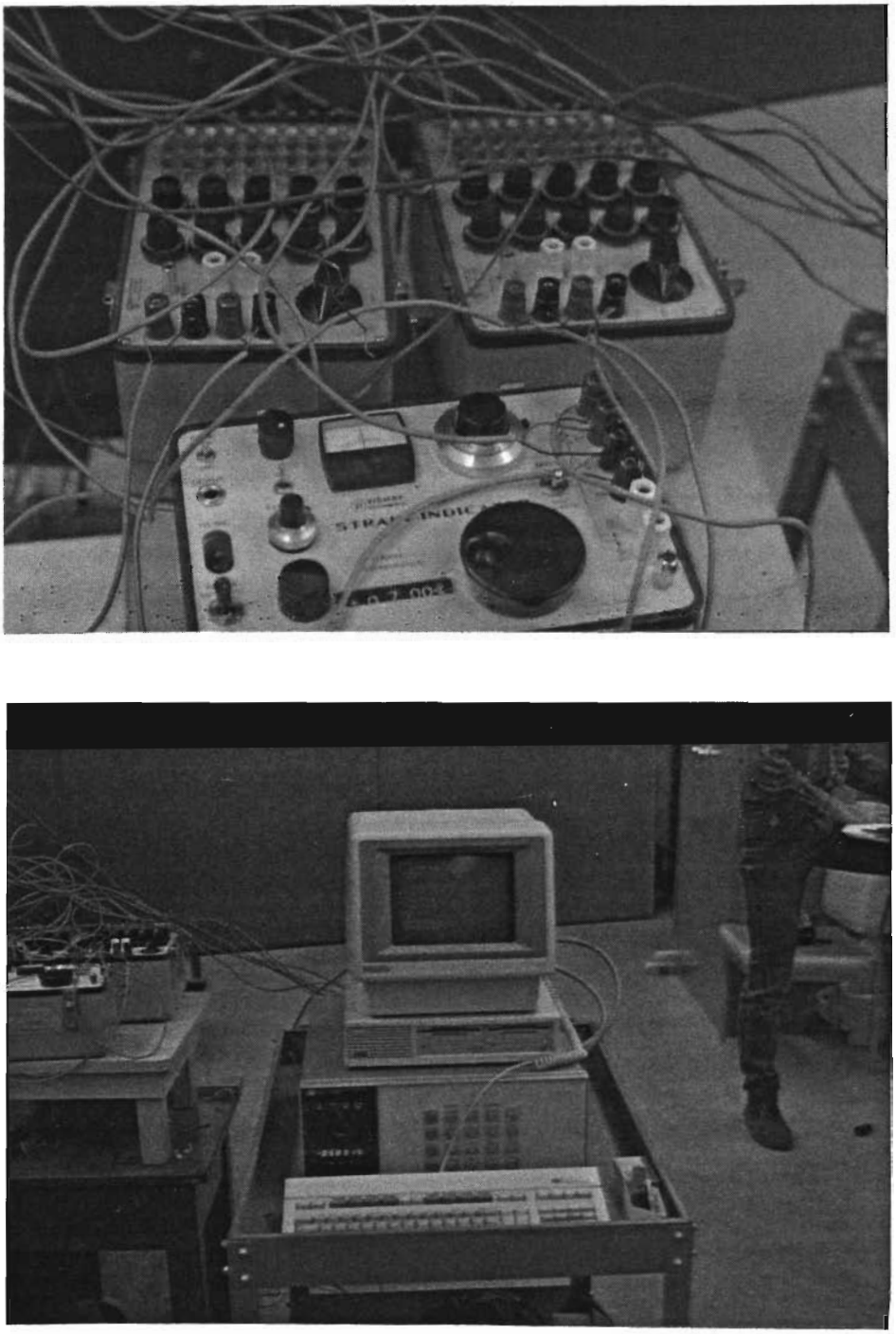

Fig 5.28. Strain and temperature monitoring devices used during thermal expansion experimentation.

CHAPTER 6. EXPERIMENTAL RESULTS

This chapter discusses the results obtained in this research project. It includes the results of Phase I, where continuous temperatures and movements were monitored over a typical daily temperature cycle. The push-off tests in Phase II are also included for the various subbases. These results precede Phase I results so that the friction-movement profiles can be used to analyze the results obtained in Phase I. Concrete properties obtained by experimentation also precede Phase I in order that they also may be used in the analysis. There are also discussions included between results to help explain them.

PHASE II

This portion of the experimentation used a mechanical device to induce movements in order that frictional information could be obtained. Concrete sections, 2 feet by 9 feet, were pushed out at the Austin site using a 4-inch and an 8-inch simulated slab depth. The Houston site used 2–foot by 14 –foot concrete sections with 3-1/2 inch and simulated 7-inch depths. The capacity of both the load cell and the hydraulic ram was reached for the push-off test on the cement stabilized subbase. Therefore, the slab was cut again so that a 2–foot by 4–foot section could be tested. Again, the smaller section could not be pushed without exceeding the capacity of the equipment. Even though the maximum frictional resistance was not determined in this case, the data obtained can still be used as an under estimation of its value.

Table 6.1 shows the results of the first push-off test at the Austin site over a flexible subbase. It gives the load cell reading, ram pressure, both horizontal and vertical movements, slab temperature, calculated frictional resistance (jacking force/contact area) and coefficient of friction, and the time span in which loading took place. These results are shown graphically in Figs 6.1 through 6.5. Figures 6.1 and 6.2, respectively, show the horizontal and vertical movements up until the peak frictional resistance. These friction profiles are important only to jointed and continuous slabs where movements rarely are greater than 0.03-inch during their service life. Figure 6.3 shows the two graphs in Figs 6.1 and 6.2 together. Figure 6.3 graph shows that the resultant direction between the two is approximately 45° since both the horizontal and vertical profiles closely follow one another. In other words, for this particular subbase, the vertical movements are of the same magnitude as the horizontal

TABLE 6.1. PUSH-OFF DATA ON 4-INCH SLAB ON FLEXIBLE SUBBASE

Push-off Test No.: 1-BRC Slab Area: 2592 in^2
Date: 16 October 1986 Slab Thickness: 4 inches
Subbase: Flexible Base

Time (Hr:Min)	Load (kips)	Ram Pressure (ksi)	Horizontal Movement (inch)	Vertical Movement (inch)	Slab Temperature (°F)	Frictional Resistance (psi)	μ
14:47	0.587	.110	.0000	.0000	83.68	.23	.67
14:49	1.672	.350	.0005	-.0003	83.77	.65	1.92
14:49	3.448	.670	.0012	-.0002	83.73	1.33	3.96
14:51	4.356	.880	.0022	.0010	83.79	1.68	5.01
14:51	4.852	1.00	.0030	.0022	83.84	1.87	5.58
14:50	5.390	1.06	.0037	.0039	83.86	2.08	6.20
14:53	6.170	1.10	.0067	.0088	83.88	2.38	7.09
14:53	6.682	1.30	.0091	.0127	83.82	2.58	7.68
14:53	7.143	1.42	.0137	.0209	83.89	2.76	8.21
14:54	7.452	1.50	.0182	.0284	83.89	2.88	8.57
14:54	7.663	1.50	.0243	.0387	83.88	2.96	8.81
14:55	7.566	1.50	.0322	.0517	83.95	2.92	8.69
14:56	7.367	1.30	.0414	.0660	83.93	2.84	8.47
14:56	7.115	1.20	.0506	.0813	83.98	2.75	8.18
14:57	6.251	1.00	.0528	.0851	83.98	2.41	7.19
14:58	5.390	1.00	.0549	.0889	84.00	2.08	6.19
14:58	4.689	0.90	.0571	.0931	84.02	1.81	5.39
14:59	4.137	0.70	.0603	.0980	84.06	1.60	4.76
14:59	3.358	0.60	.0671	.1062	84.06	1.30	3.86
14:59	2.828	0.50	.0738	.1132	84.07	1.09	3.25
15:00	2.152	0.50	.2526	.1616	84.11	0.83	2.47
15:01	2.051	0.42	.2573	.1667	84.09	0.79	2.36
15:01	1.878	0.40	.2710	.1745	84.11	0.72	2.16
15:02	1.798	0.40	.2819	.1818	84.13	0.69	2.07
15:02	1.701	0.35	.2941	.1887	84.15	0.66	1.96
15:03	1.615	0.35	.3096	.1968	84.22	0.62	1.86
15:03	1.494	0.34	.4219	.2159	84.22	0.58	1.72
15:03	1.411	0.32	.4339	.2233	84.22	0.54	1.62
15:04	1.323	0.32	.4529	.2277	84.25	0.51	1.52
15:04	1.267	0.30	.4823	.2288	84.25	0.49	1.46

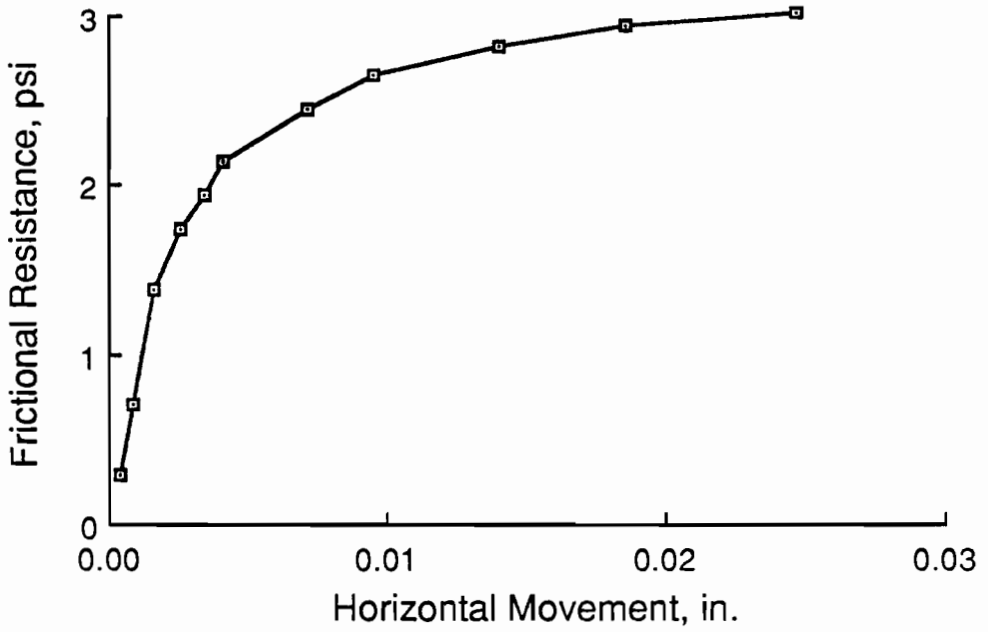

Fig 6.1. Horizontal movement to peak frictional resistance for 4-inch slab on flexible subbase.

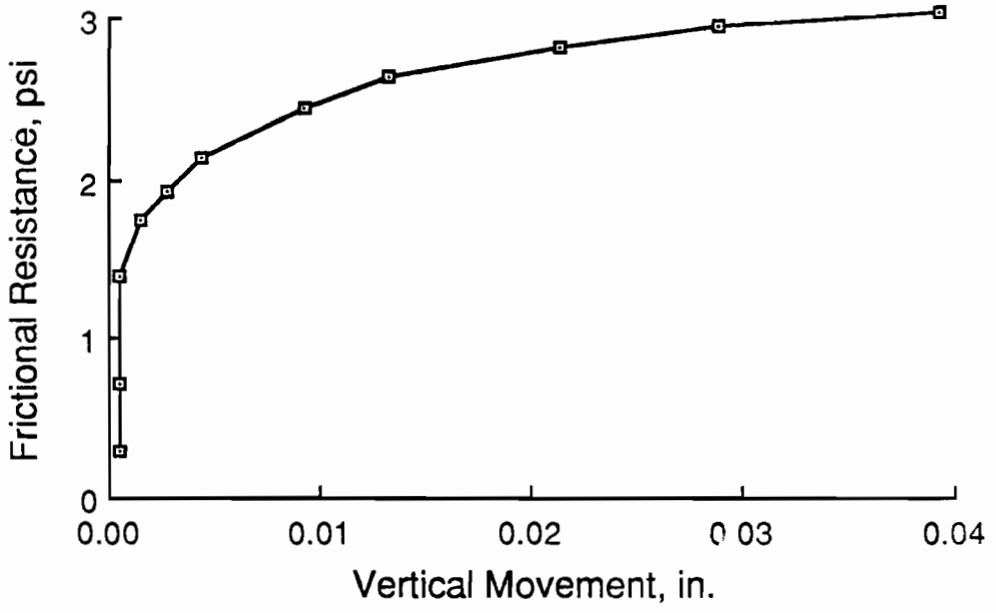

Fig 6.2. Vertical movement to peak frictional resistance for 4-inch slab on flexible subbase.

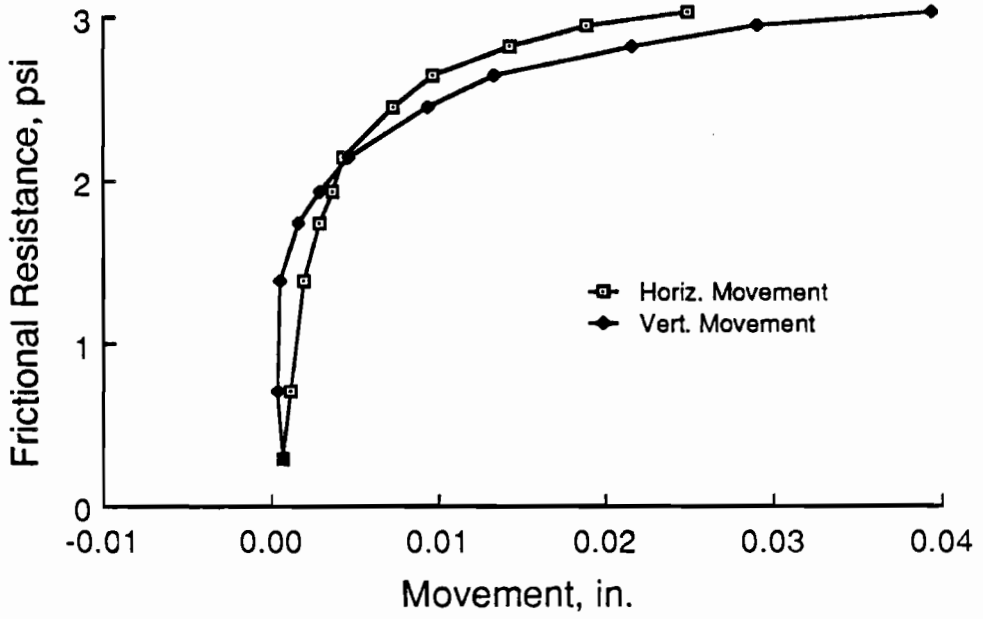

Fig 6.3. Horizontal and vertical movements to peak frictional resistance for 4-inch slab on flexible subbase.

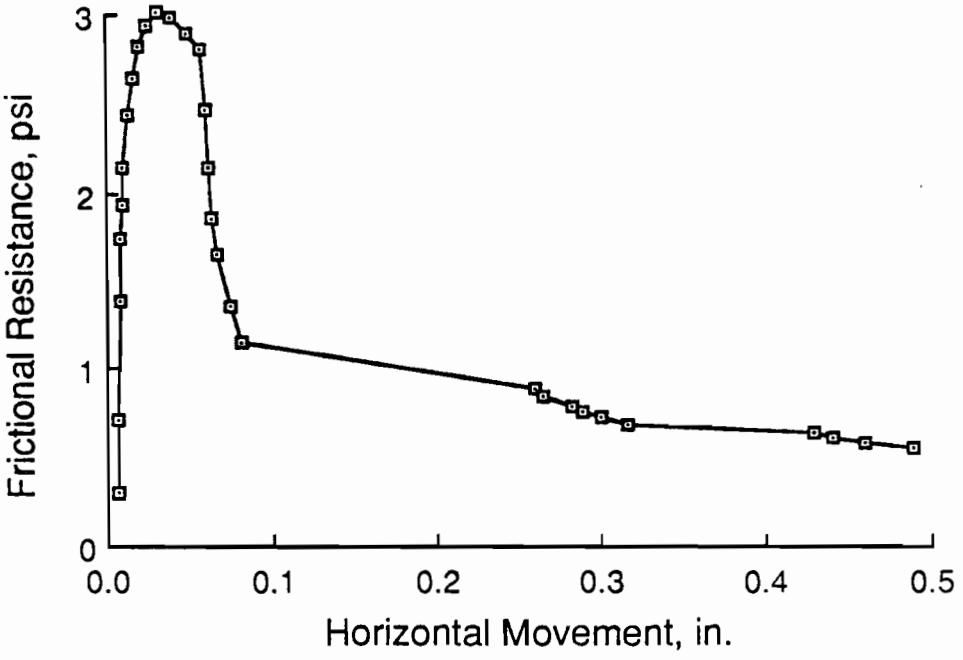

Fig 6.4. Horizontal movement for push-off test on 4-inch slab over flexible subbase.

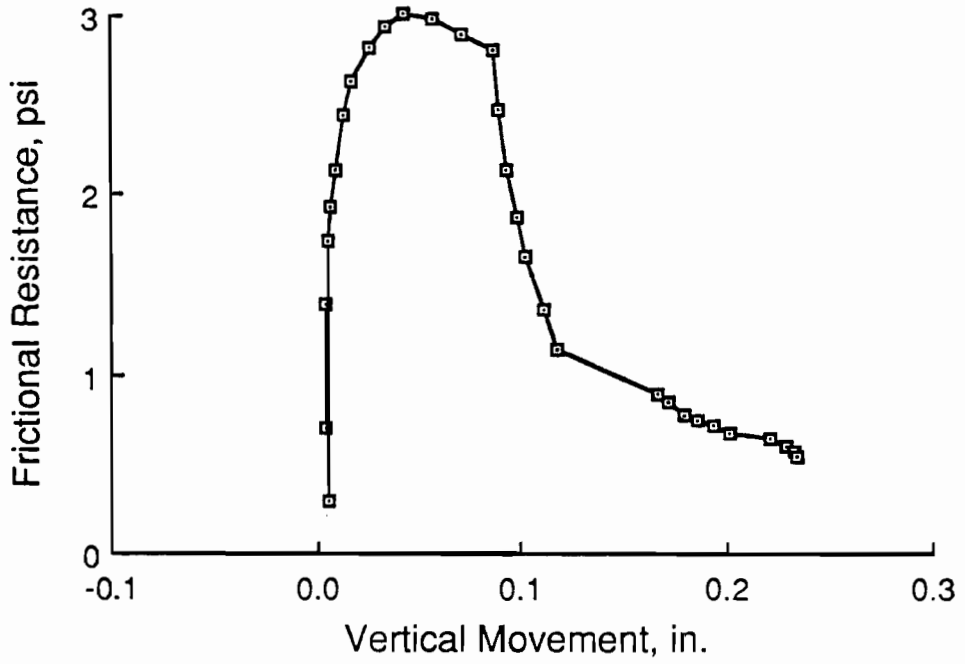

Fig 6.5. Vertical movement for push-off test on 4-inch flexible subbase.

movements up until sliding. This is a major concern for rigid pavements. Any vertical movement can cause decompaction of the subbase or even a void, which is detrimental to concrete pavements. The slightest gap between the pavement and its continuous support is considered a void, where failure by flexural cracking is possible due to vehicle loading. The last two figures, Figs 6.4 and 6.5, respectfully, show the horizontal and vertical movements up until and far beyond sliding. Movements of these magnitudes can be seen only in prestressed pavements, where additional movements are elastically induced into the pavement during post tensioning operations. Any vertical movements beyond roughly a tenth of an inch represent horizontal movements due to the vertical gage's inability to slide along the surface as it is being pushed. The slab was lifted to one side so that the failure plane could be observed. As shown in Fig 6.6 it was clear that the sliding, or the failure plane, was not at the slab-subbase interface but was down in the subbase. This important observation means that the frictional resistance is not dependent on the frictional characteristics between the pavement and its subbase as for loose unbonded subbases, but is dependent on the material strength properties of the subbase for stabilized subbases. In fact, every concrete slice that was cut and removed from the slab for the push-off equipment had subbase adhering to its bottom, except for the untreated clay. Figure 6.7 shows a few of these overturned slices.

Concrete blocks were added to the second slab to simulate an 8-inch slab to see the effect on friction of doubling the weight. Table 6.2 and Figs 6.8 through 6.12 show the results of the second push-off test at the Austin site. They are arranged in the same manner as the 4–inch–slab results. The maximum frictional restraint increased from 3.0 psi to 3.4 psi. This means that doubling the overburden pressure increased the maximum frictional restraint only 13 percent. This result agrees with the hypothesis that, for this subbase, which behaves as a stabilized subbase due to the cementing agents inherent in it, and for stabilized subbases, frictional restraint is dependent on the material strength properties of the subbase and is only a slight function of the weight of the slab.

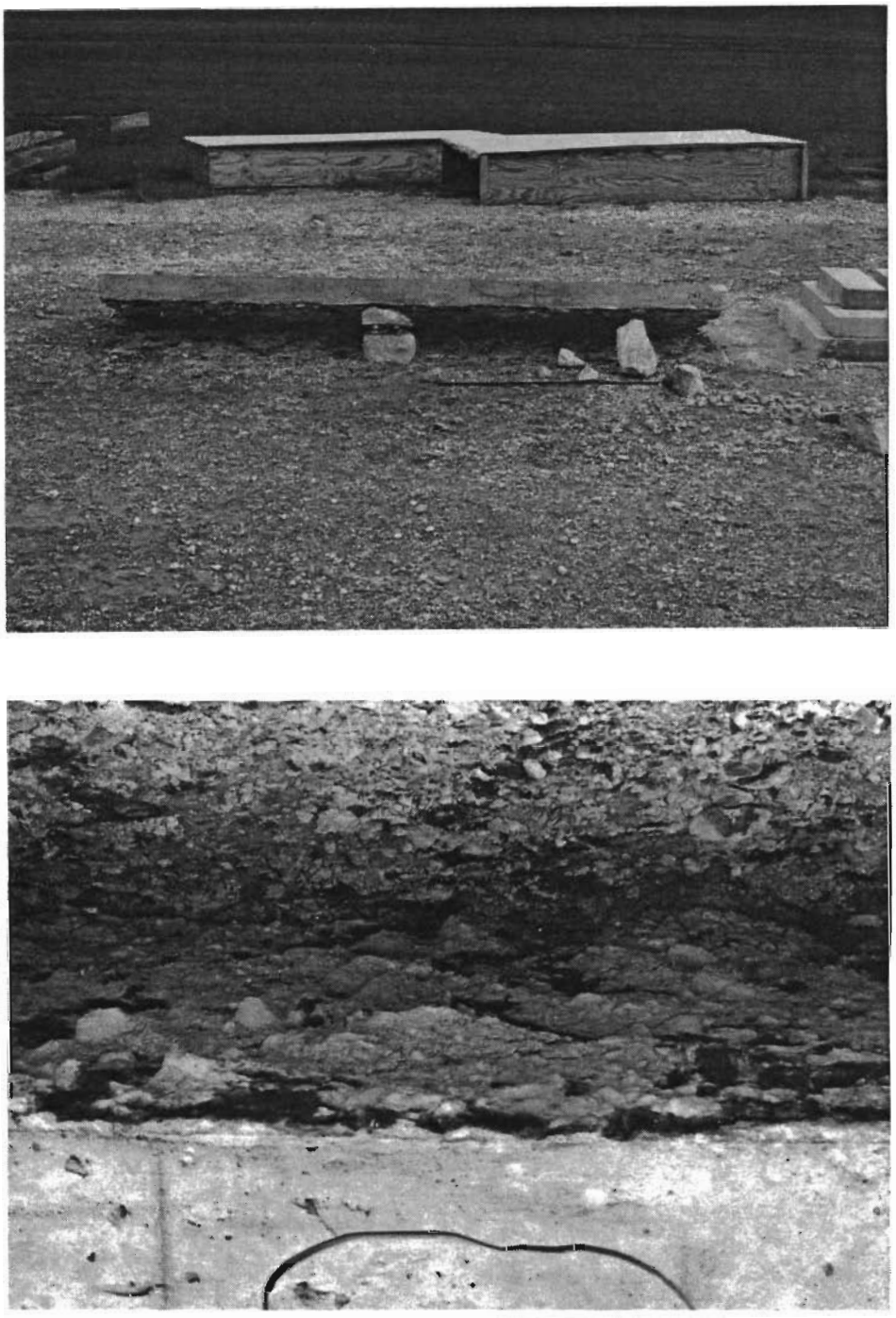

(continued)

Fig 6.6. Observation of failure plane after push-off test on 4-inch slab over a flexible subbase.

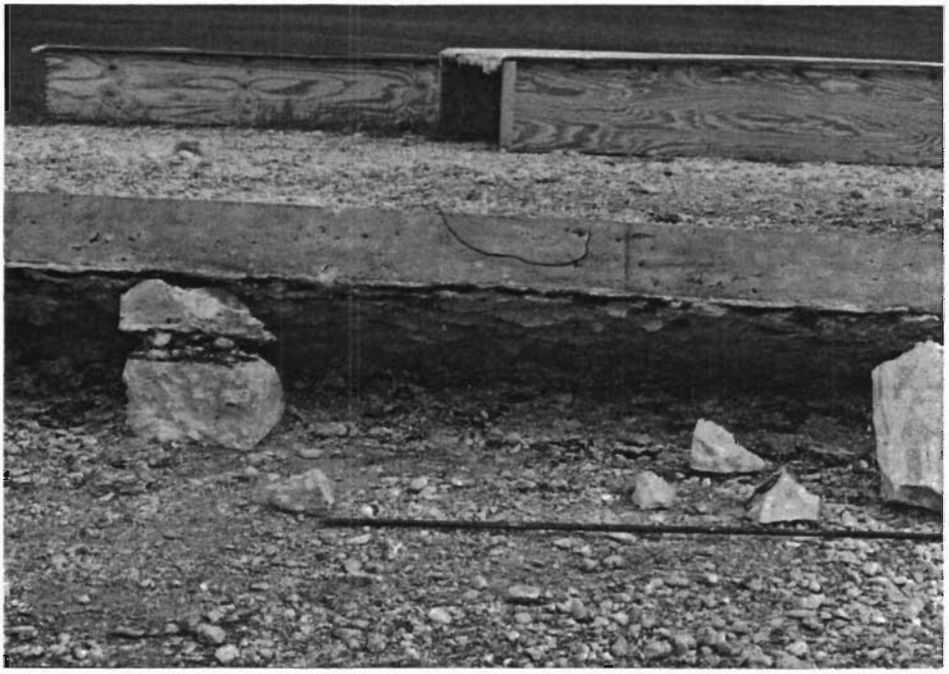

(continued)

Fig 6.6. (continued).

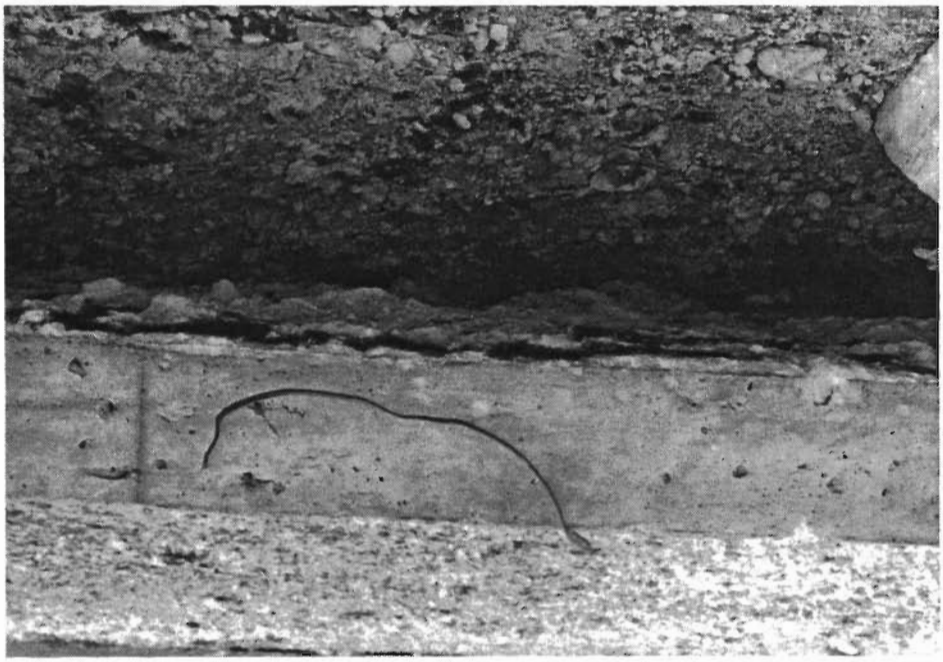

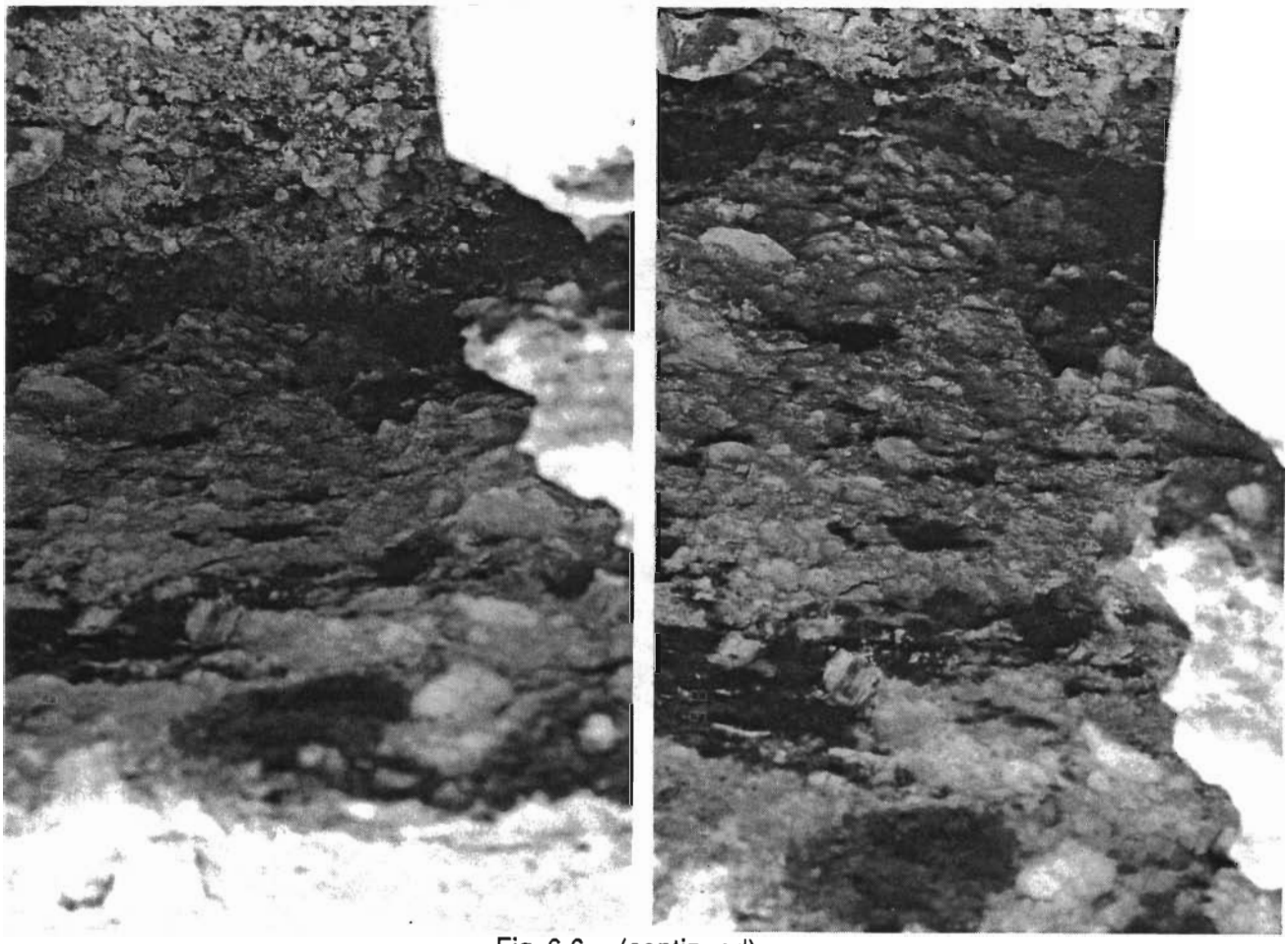

Fig 6.6. (continued).

(a) Flexible.

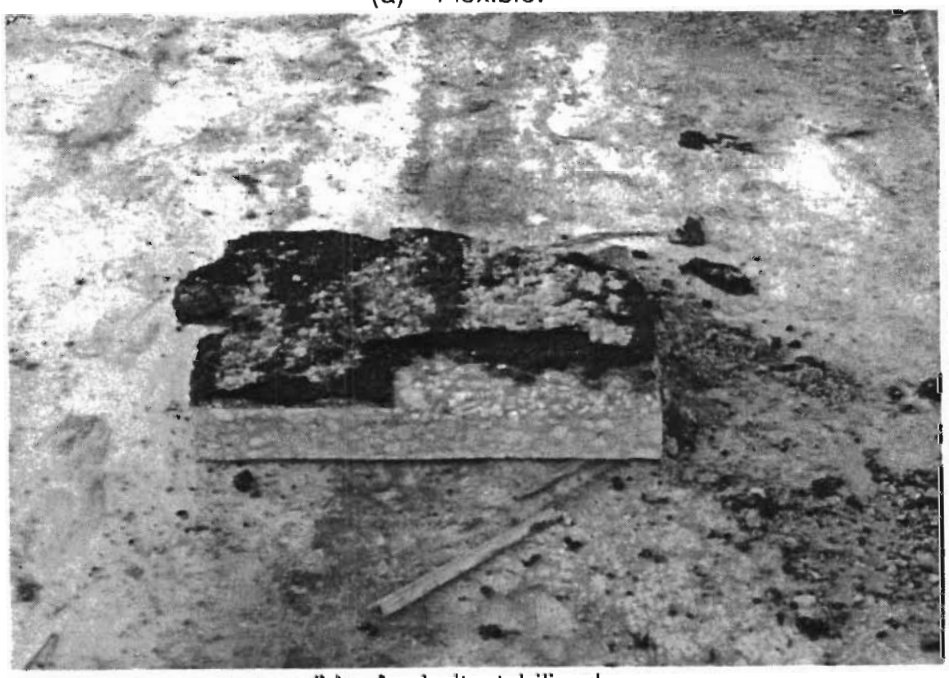

(b) Asphalt stabilized.

(continued)

Fig 6.7. Overturned slab cut-out shown subbase adhesion.

(c) Cement stabilized.

(d) Lime treated.
Fig 6.7. (continued).

TABLE 6.2. PUSH-OFF DATA ON SIMULATED 8-INCH SLAB OVER FLEXIBLE SUBBASE

Push-off Test No.: 2-BRC Slab Area: 2592 in^2
Date: 20 October 1986 Slab Thickness: 8 inches
Subbase: Flexible Base *8-in. simulated slab thickness using concrete blocks

Time (Hr:Min)	Load (kips)	Ram Pressure (ksi)	Horizontal Movement (inch)	Vertical Movement (inch)	Slab Temperature (°F)	Frictional Resistance (psi)	μ
16:07	0.386	0.02	.0000	.0000	75.04	0.15	0.22
16:08	0.387	0.02	.0000	.0000	75.00	0.15	0.22
16:08	1.429	0.28	.0000	.0001	75.00	0.55	0.82
16:09	2.163	0.44	.0000	.0001	75.00	0.83	1.25
16:09	2.777	0.58	.0002	.0001	74.97	1.07	1.60
16:10	3.559	0.74	.0004	.0000	74.91	1.37	2.05
16:10	4.488	0.92	.0008	.0001	74.97	1.73	2.58
16:10	5.322	1.09	.0013	.0000	74.97	2.05	3.06
16:11	6.077	1.24	.0017	.0001	74.98	2.34	3.50
16:11	6.970	1.42	.0028	.0003	74.89	2.69	4.01
16:11	7.539	1.54	.0046	.0021	74.95	2.91	4.34
16:12	7.940	1.62	.0070	.0049	74.95	3.06	4.57
16:12	8.154	1.70	.0112	.0112	74.91	3.15	4.69
16:12	8.579	1.76	.0149	.0168	74.91	3.31	4.93
16:13	8.722	1.78	.0198	.0252	74.91	3.37	5.02
16:13	8.705	1.80	.0362	.0586	74.91	3.36	5.01
16:13	8.686	1.90	.0519	.0882	74.93	3.35	5.00
16:14	8.015	1.70	.0697	.1084	74.93	3.09	4.61
16:14	6.766	1.40	.0952	.1350	74.89	2.61	3.89
16:15	5.178	0.90	.1527	.1805	74.86	2.00	2.98
16:17	3.832	0.80	.2613	.2372	74.84	1.48	2.21
16:17	3.679	0.80	.2626	.2372	74.84	1.41	2.12
16:17	3.182	0.65	.3643	.2768	74.80	1.23	1.83
16:18	2.813	0.60	.1778	.3047	74.86	1.09	1.62
16:18	2.583	0.55	.5938	.3250	74.86	1.00	1.49
16:18	2.394	0.50	.6616	.3280	74.86	0.92	1.38
16:19	2.192	0.50	.6643	.3502	74.82	0.85	1.26
16:19	2.052	0.40	.6667	.3503	74.82	0.79	1.18
16:19	1.917	0.40	.6682	.3546	74.82	0.74	1.10

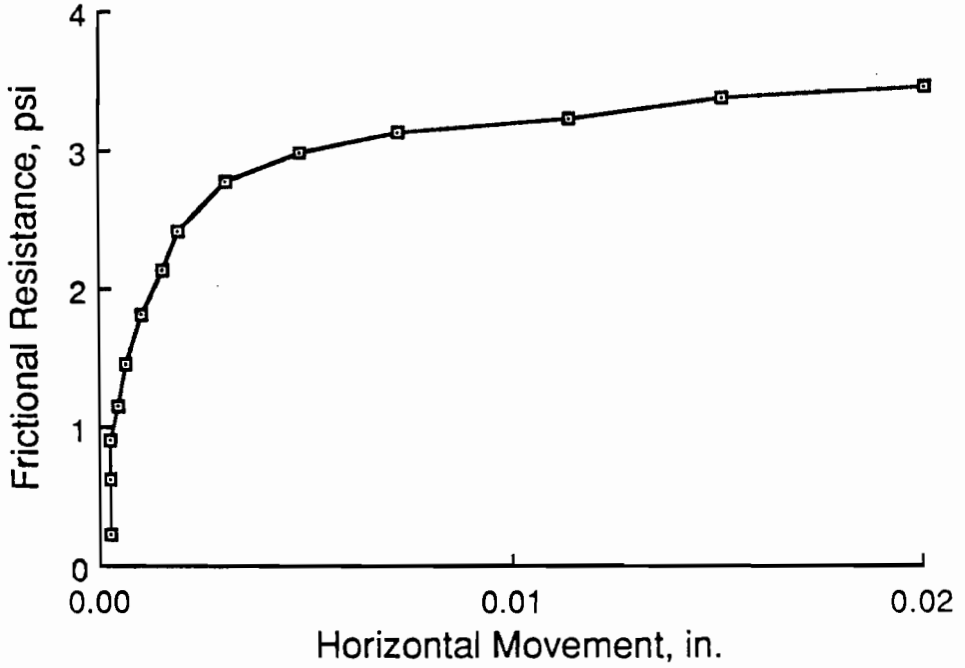

Fig 6.8. Horizontal movements to peak frictional resistance for simulated 8-inch slab on flexible subbase.

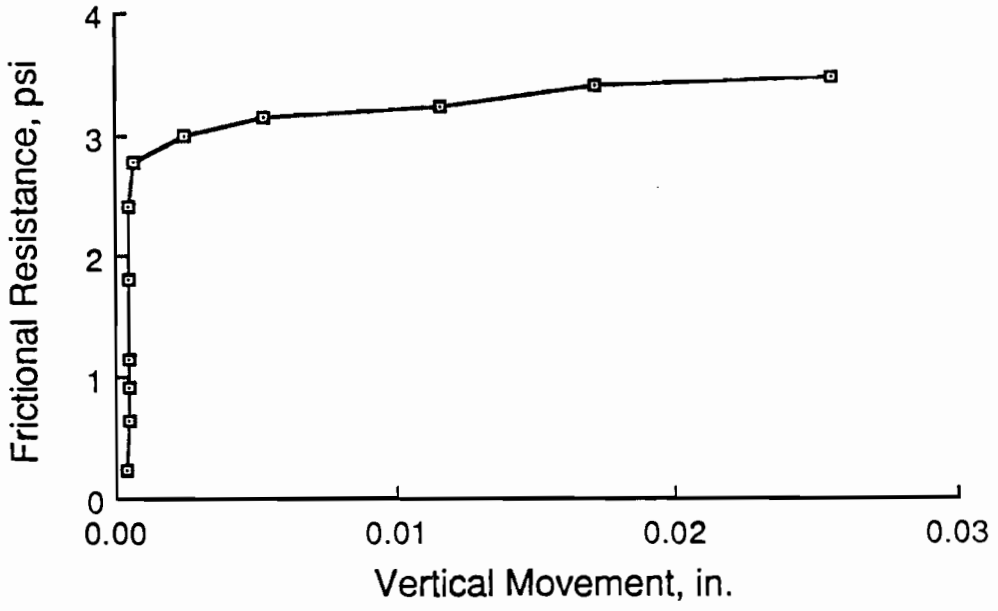

Fig 6.9. Vertical movements to peak frictional resistance for simulated 8-inch slab on flexible subbase.

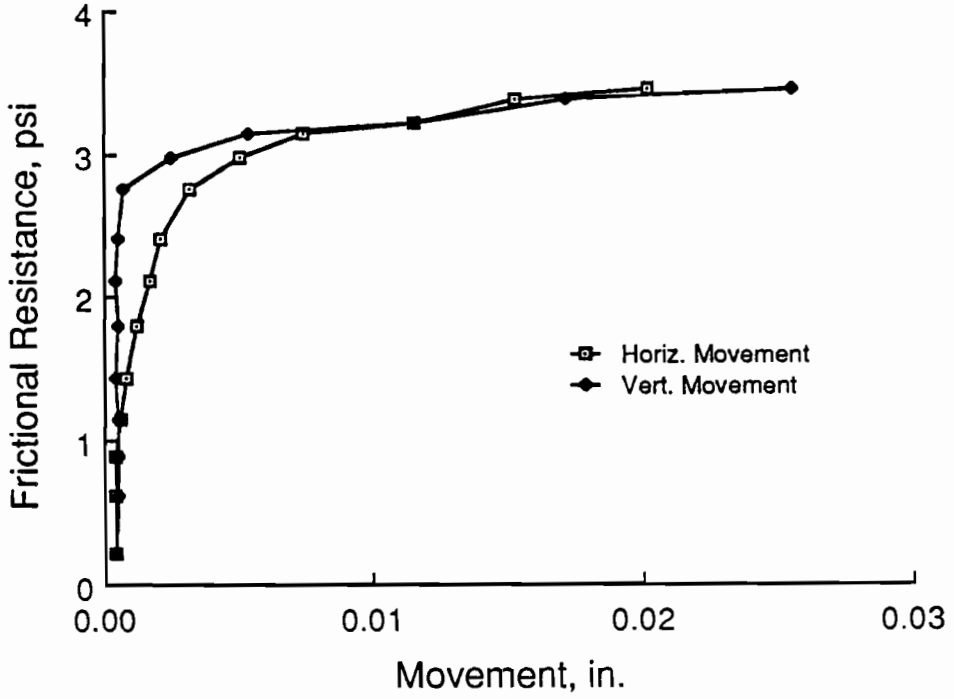

Fig 6.10. Horizontal and vertical movements to peak frictional resistance for simulated 8-inch slab on flexible subbase.

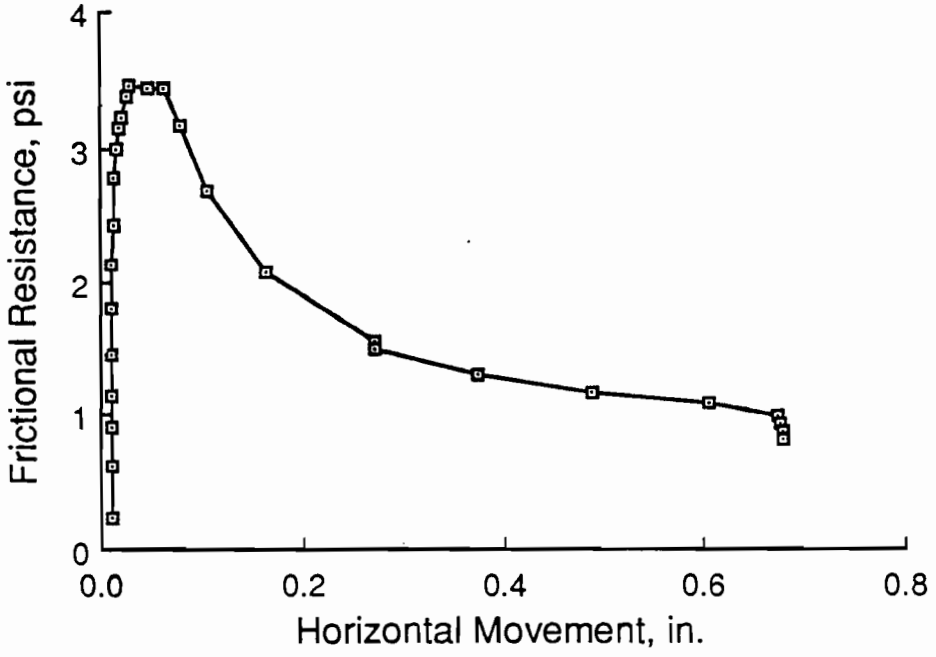

Fig 6.11. Horizontal movement for push-off tests on simulated 8-inch slab on flexible subbase.

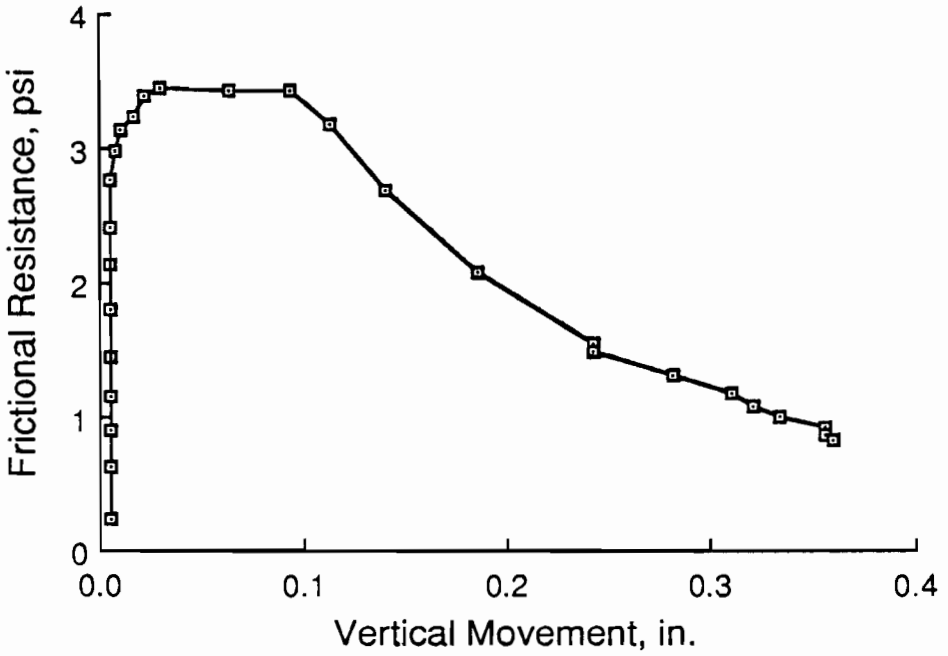

Fig 6.12. Vertical movement for push-off test on simulated 8-inch slab on flexible subbase.

Table 6.3 and Figs 6.13 through 6.17 show the results of the first push-off test on the asphalt stabilized subbase at the Houston site. The asphalt subbase was observed to be sticking to the bottom of the pavement during the test. The sliding plane seemed to occur between the 3/4-inch asphalt stabilized subbase and the cement stabilized subbase. Figure 6.18 shows the shearing and shoving of the subbase after sliding was induced. These shearing cracks went entirely through the subbase to the cement stabilized subbase, thus leading to the conclusion that the entire mass of asphalt was sliding with the pavement section. Therefore, if the supporting stabilized subbase is thin enough, frictional restraint will not be entirely dependent on the subbase's strength properties but on the frictional characteristics between the subbase and its subgrade. Table 6.4 and Fig 6.19 through 6.23 show the results of the push-off test run on a simulated 7-inch slab over the asphalt stabilized subbase. Maximum frictional restraint showed only a 35 percent increase when the weight of the slab was doubled. Vertical movements in both cases seem to be far less than in the flexible subbase tests, which can largely be attributed to the surface texture of the failure planes of the two subbases.

As previously mentioned for the cement stablized push-off test, a 2–foot by 14–foot section failed to move along with a 2–foot by 4–foot section after reaching the capacity of the loading equipment. The results of the push-off test on the 2–foot by 4–foot section are given in Table 6.5 and Figs 6.24 through 6.26. Only minimal movements were observed in the one one-thousandth of an inch range. The final frictional resistance recorded was over 15 psi. The estimated peak frictional resistance for a cement stabilized subbase could be as high as twice or three times this value. Figure 6.24 represents a very high shearing stiffness for this particular subbase when compared to other subbases. The pavement seemed to have glued itself to the cement stabilized subbase. This was also observed in the push-off tests described by Goldberg, where slabs cast on top of a troweled smooth concrete could not be loaded to failure without exceeding the capacity of the loading equipment (Ref 6).

Table 6.6 and Figs 6.27 through 6.32 give the results of the push-off tests run on the 3.5-inch slab on the lime treated clay subbase. The failure plane, again, was not at the slab-subbase interface but was slightly below, within the subbase. When the second slab was loaded to twice its weight the peak frictional resistance only increased from 1.6 psi to 1.7 psi, a 6 percent increase. Therefore, failure is again only moderately dependent on its overburden pressure from the pavement and is mostly dependent on the subbase's material strength

TABLE 6.3. PUSH-OFF DATA FOR 3-1/2 INCH SLAB ON ASPHALT STABILIZED SUBBASE

Push-off Test No.: 1-Houston Slab Area: 4032 in^2
Date: 28 October 1986 Slab Thickness: 3-1/2 inches
Subbase: Asphalt Stabilized Base

Time (Hr:Min)	Load (kips)	Ram Pressure (ksi)	Horizontal Movement (inch)	Vertical Movement (inch)	Slab Temperature (°F)	Frictional Resistance (psi)	μ
13:24	1.361	300	----	----	----	----	----
13:25	1.361	300	.0000	.0000	82.74	.34	1.15
13:27	2.679	600	-.0003	.0002	82.81	.66	2.26
13:27	3.308	710	-.0002	.0003	82.94	.82	2.79
13:28	3.266	710	-.0002	.0004	82.90	.81	2.76
13:28	3.900	850	-.0003	.0009	82.85	.97	3.29
13:29	4.344	950	.0018	.0015	83.08	1.08	3.67
13:29	4.616	1000	.0047	.0021	83.01	1.14	3.90
13:30	5.087	1100	.0079	.0032	83.01	1.26	4.29
13:30	5.776	1200	.0117	.0047	83.01	1.43	4.88
13:31	5.475	1200	.0167	.0067	83.01	1.36	4.62
13:31	6.076	1300	.0225	.0094	83.03	1.51	5.13
13:32	6.554	1400	.0298	.0137	83.03	1.63	5.54
13:32	6.402	1450	.0416	.0224	83.07	1.59	5.41
13:33	5.398	1300	.0547	.0321	83.10	1.34	4.56
13:34	5.702	1500	.0784	.0450	83.12	1.41	4.82
13:34	4.940	1600	.1073	.0618	83.12	1.23	4.17
13:34	4.638	1600	.1334	.0750	82.98	1.15	3.91
13:35	4.541	1700	.1668	.1035	82.98	1.12	3.84
13:35	4.100	1500	.1892	.1252	82.92	1.02	3.46
13:36	2.294	1500	.2281	.1212	82.96	.57	1.94
13:36	3.531	1400	.3618	.1761	82.94	.88	2.98
13:40	3.029	1400	.4861	.1426	82.99	.75	2.56
13:40	2.163	1100	.6270	-.0373	82.90	.54	1.83
13:40	2.174	1000	.7403	-.0129	82.89	.54	1.84
13:40	1.951	1000	.8556	-.0039	82.80	.48	1.65

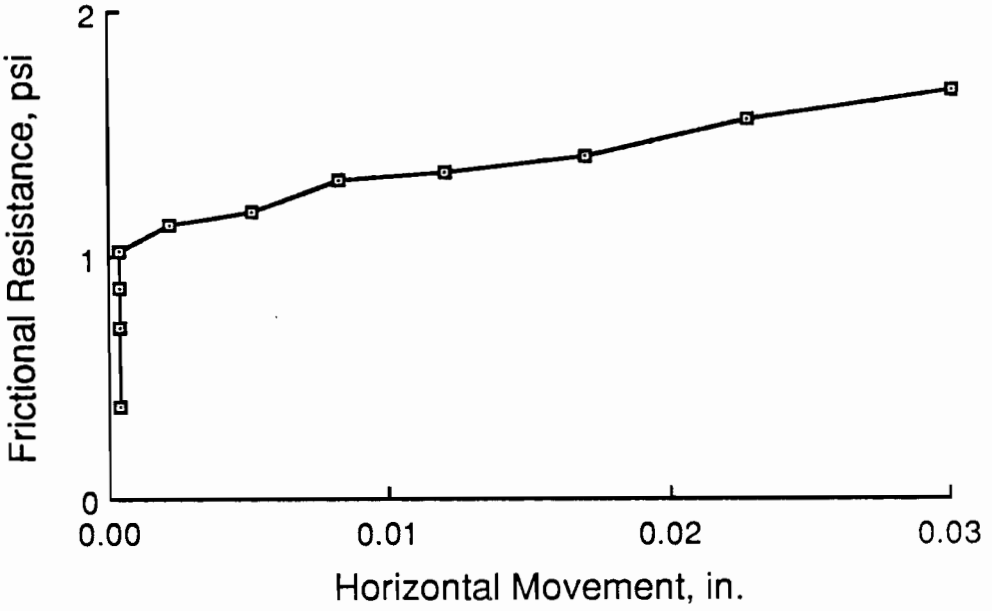

Fig 6.13. Horizontal movement to peak frictional resistance for 3.5-inch slab on asphalt stabilized subbase.

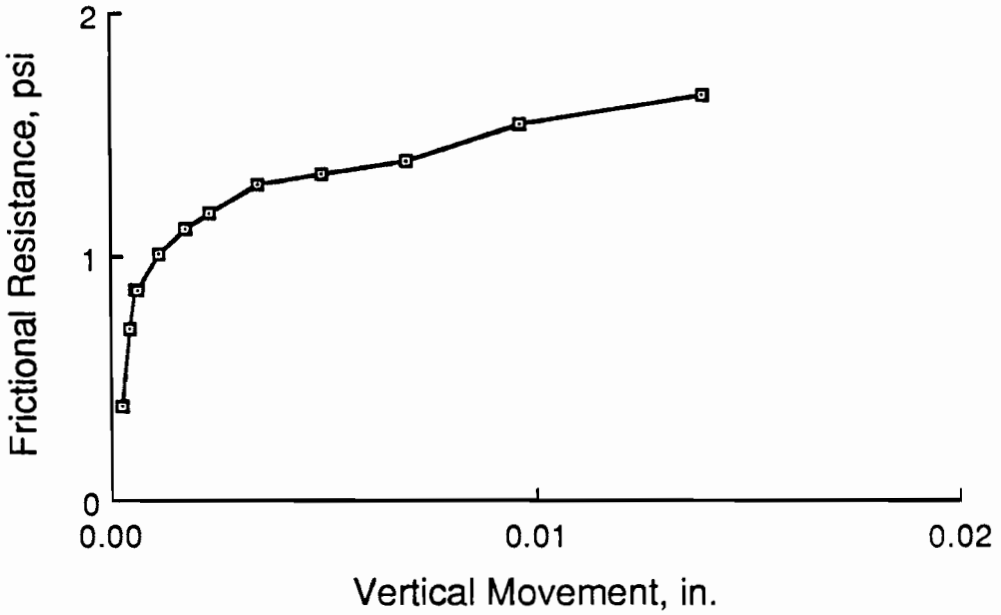

Fig 6.14. Vertical movement to peak frictional resistance for 3.5-inch slab on asphalt stabilized subbase.

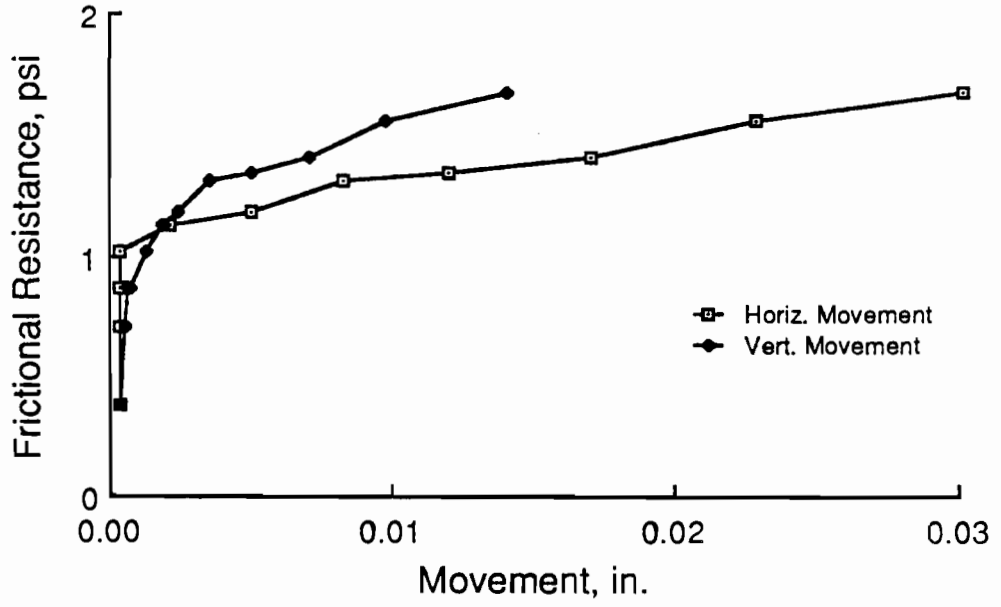

Fig 6.15. Horizontal and vertical movements to peak frictional resistance for 3.5-inch slab on asphalt stabilized subbase.

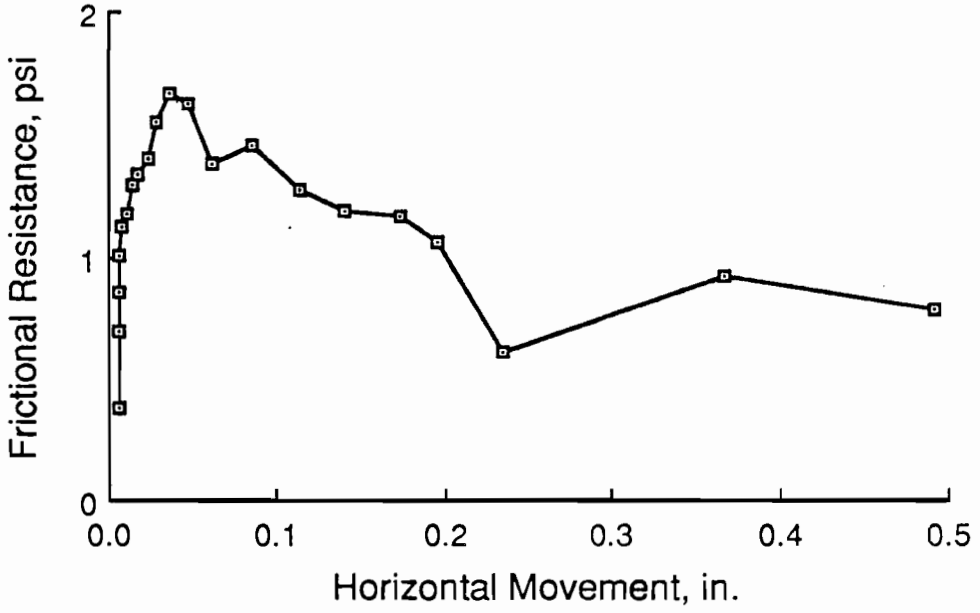

Fig 6.16. Horizontal movement for push-off test on 3.5-inch slab on asphalt stabilized subbase.

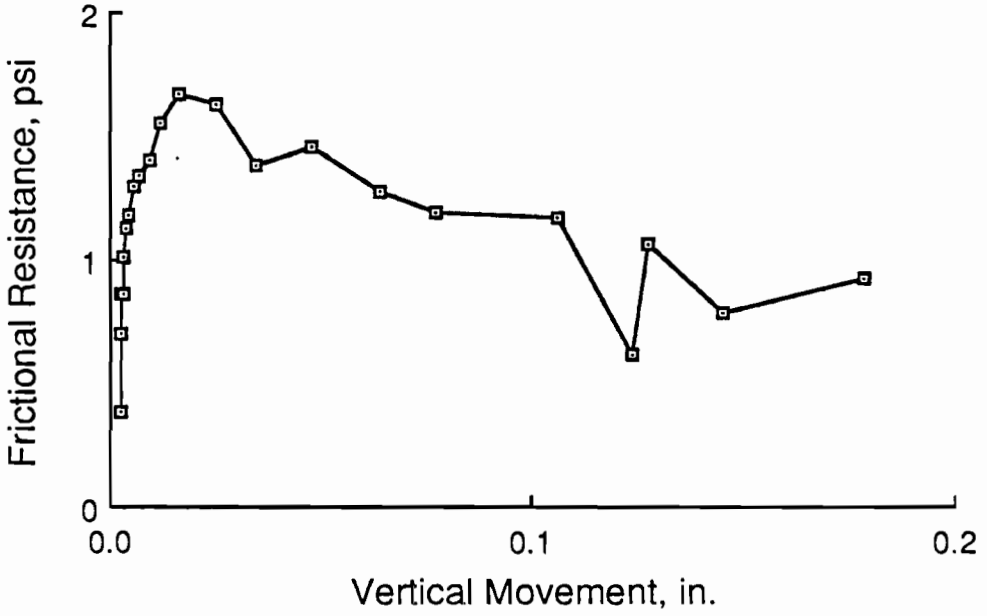

Fig 6.17. Vertical movement for push-off test on 3.5-inch slab on asphalt stabilized subbase.

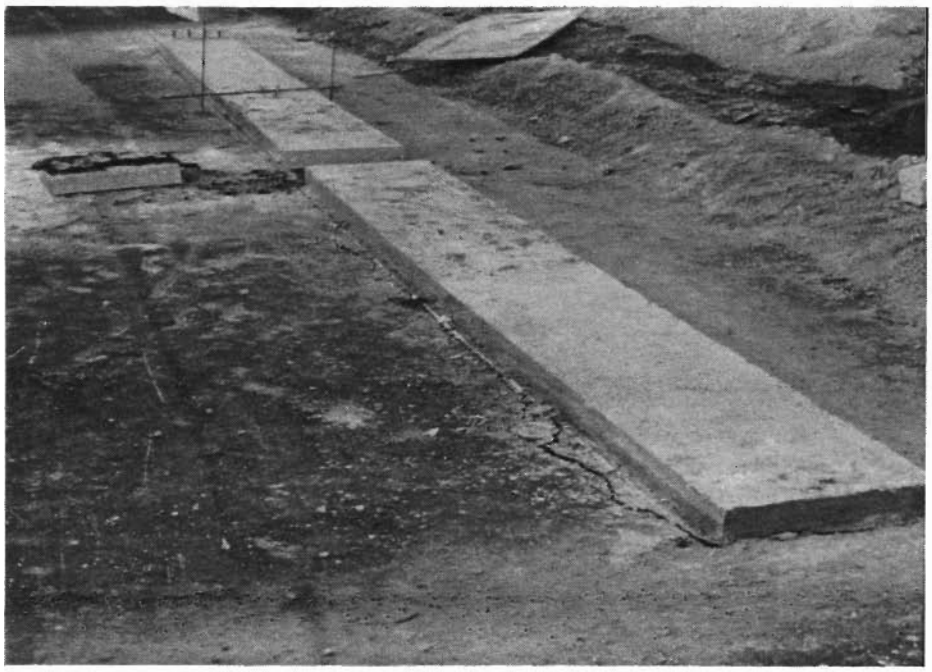

(continued)

Fig 6.18. Shearing and shoving of asphalt stabilized subbase after push-off test.

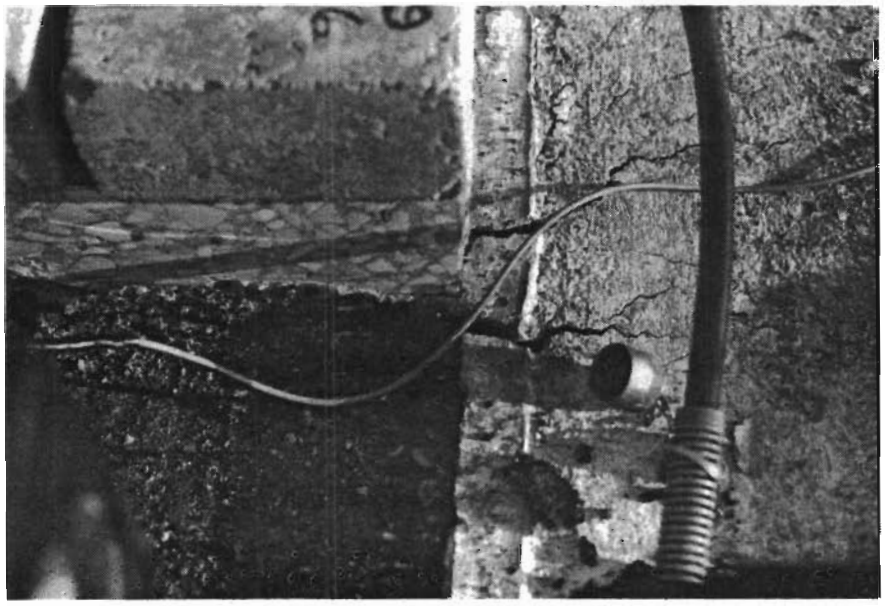

Fig 6.18. (continued).

TABLE 6.4. PUSH-OFF DATA FOR SUMULATED 7-INCH SLAB ON ASPHALT STABILIZED SUBBASE

Push-off Test No.: 2-Houston Slab Area: 4032 in^2
Date: 30 October 1986 Slab Thickness: 7–inches simulated
Subbase: Asphalt Stabilized Base

Time (Hr:Min)	Load (kips)	Ram Pressure (ksi)	Horizontal Movement (inch)	Vertical Movement (inch)	Slab Temperature (°F)	Frictional Resistance (psi)	μ
16:11	- - - -	.10	- - - -	- - - -	- - - -	- - - -	- - - -
16:12	.797	.10	0	0	82.60	.19	.34
16:13	.796	.10	-.0001	-.0004	82.56	.19	.34
16:13	1.708	.40	-.0001	0	82.54	.42	.72
16:13	3.277	.75	-.0001	0	81.97	.81	1.39
16:14	4.368	.95	.0006	.0001	82.45	1.08	1.85
16:14	4.784	1.05	.0012	.0001	82.44	1.19	2.02
16:15	5.813	1.30	.0025	.0001	82.49	1.44	2.46
16:15	6.419	1.40	.0043	.0001	82.51	1.59	2.71
16:16	7.237	1.60	.0064	.0154	82.40	1.79	3.06
16:16	7.941	1.70	.01	.0016	83.21	1.97	3.36
16:17	8.101	1.70	.0156	.0033	82.49	2.01	3.42
16:17	8.156	1.90	.0247	.0062	82.44	2.02	3.45
16:18	8.880	2.20	.0380	.0119	82.44	2.20	3.75
16:18	8.669	2.20	.0571	.0207	82.38	2.15	3.66
16:18	8.018	2.10	.0775	.0314	82.40	1.99	3.39
16:19	7.139	1.80	.1008	.0418	82.45	1.77	3.02
16:19	7.014	2.00	.1141	.0441	82.38	1.74	2.96
16:20	7.086	1.90	.1655	.0659	82.38	1.76	2.99
16:21	6.655	1.90	.2083	.0839	82.22	1.65	2.81
16:21	6.486	1.90	.2633	.0927	82.45	1.61	2.74
16:22	5.716	1.80	.3574	.1016	82.16	1.42	2.42
16:22	5.106	1.60	.4999	.1397	82.22	1.27	2.16
16:23	4.492	1.50	.6339	.1664	82.24	1.11	1.90

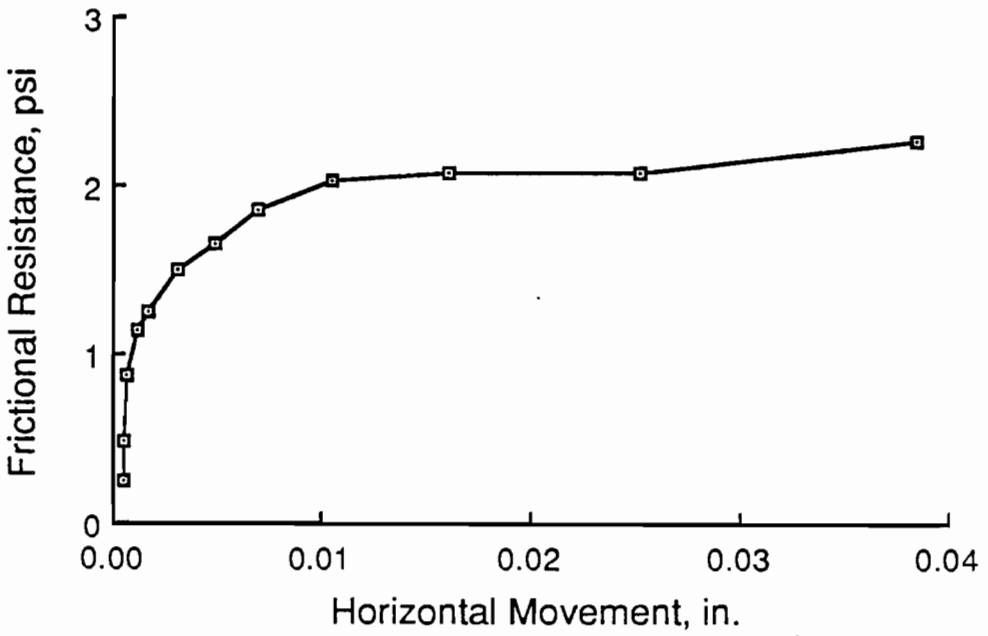

Fig 6.19. Horizontal movement to peak frictional resistance for simulated 7-inch slab on asphalt stabilized subbase.

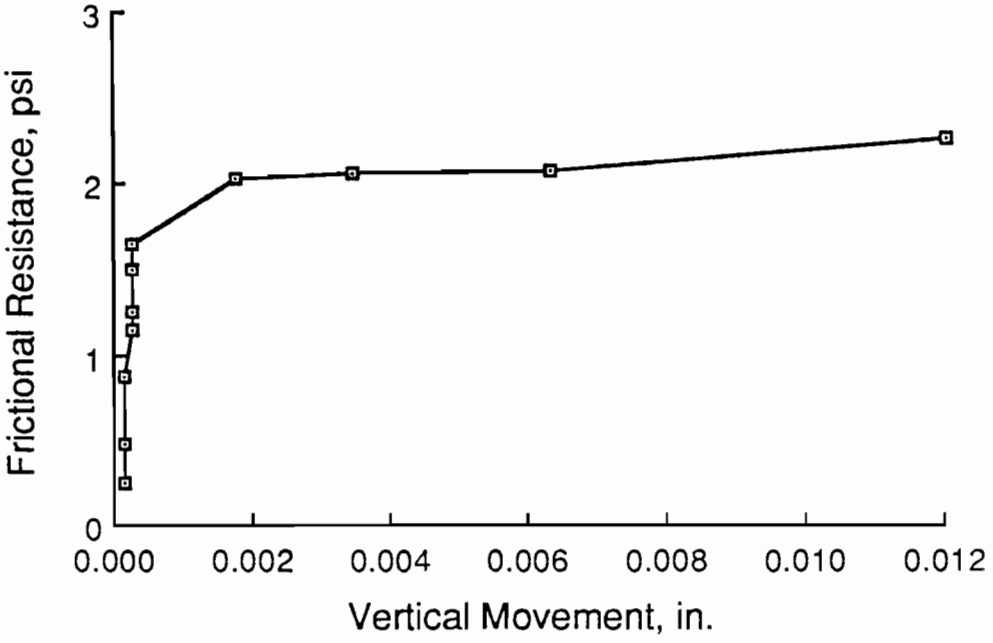

Fig 6.20. Vertical movement peak frictional resistance for simulated 7-inch slab on asphalt stabilized subbase.

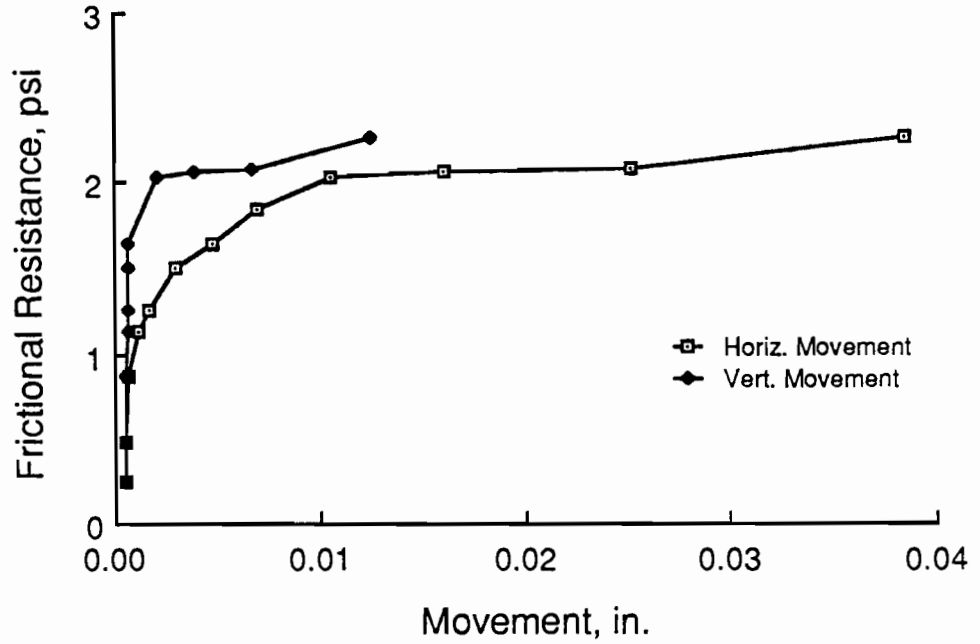

Fig 6.21. Horizontal and vertical movements to peak frictional resistance for simulated 7-inch slab on asphalt stabilized subbase.

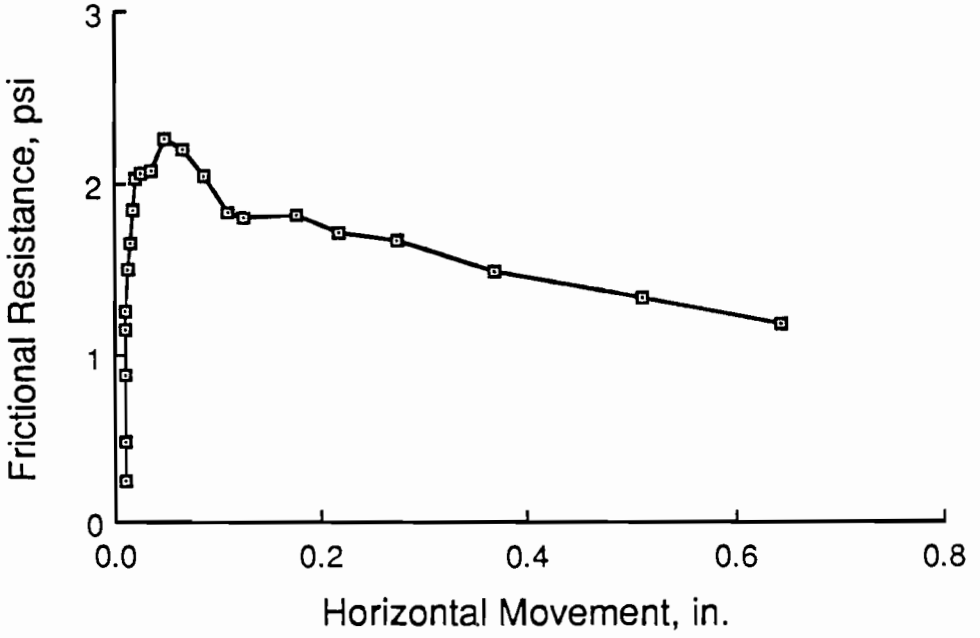

Fig 6.22. Horizontal movement for push-off tests on simulated 7-inch asphalt stabilized subbase.

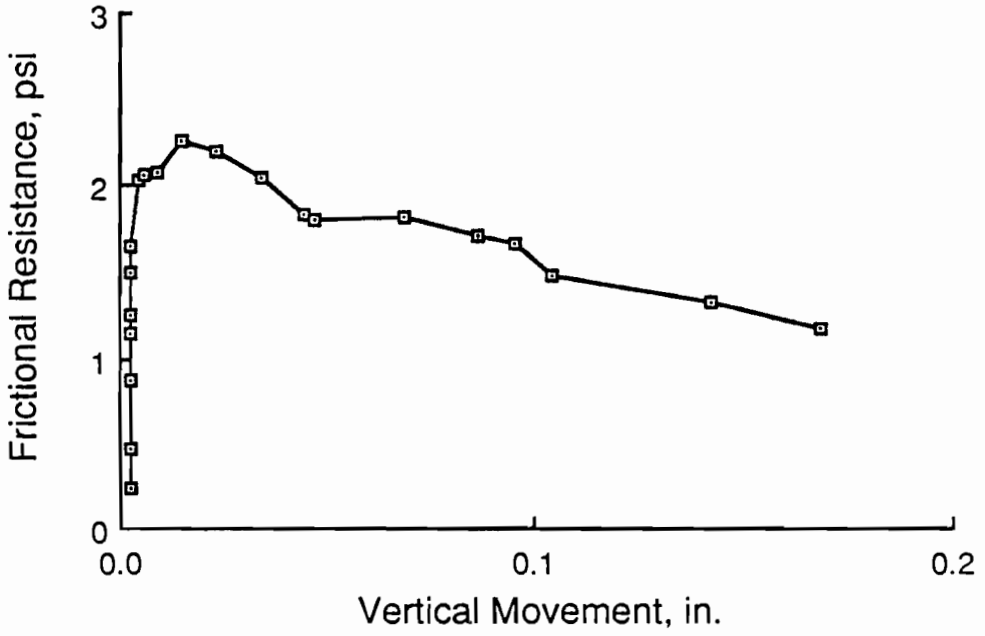

Fig 6.23. Vertical movement for push-off tests on simulated 7-inch slab on asphalt stabilized subbase.

TABLE 6.5. PUSH-OFF DATA FOR 3.5-INCH SLAB ON CEMENT STABILIZED SUBBASE

Push-off Test No.: 3-Houston Slab Area: 1152 in^2
Date: 30 October 1986 Slab Thickness: 3-1/2 inches
Subbase: Cement Stabilized Base

Time (Hr:Min)	Load (kips)	Ram Pressure (ksi)	Horizontal Movement (inch)	Vertical Movement (inch)	Slab Temperature (°F)	Frictional Resistance (psi)	μ
16:52	.791	.16	0	0	74.84	.69	2.34
16:53	1.529	.32	0	.0001	74.77	1.33	4.52
16:53	3.227	.70	.0001	.0001	74.93	2.80	9.54
16:53	5.142	1.05	.0002	.0001	74.73	4.46	15.20
16:54	7.235	1.5	.0003	.0002	74.75	6.28	21.40
16:54	9.051	1.88	.0004	.0003	74.82	7.85	26.76
16:55	10.661	2.15	.0006	.0003	74.82	9.25	31.51
16:55	12.200	2.42	.0007	.0004	74.71	10.29	36.06
16:55	13.559	2.70	.0006	.0004	74.80	11.77	40.08
16:56	14.812	2.90	.0009	.0005	74.77	12.86	43.79
16:57	17.310	3.50	.0011	.0004	74.75	15.03	51.17
16:58	17.686	3.50	.0012	.0004	74.71	15.35	52.28

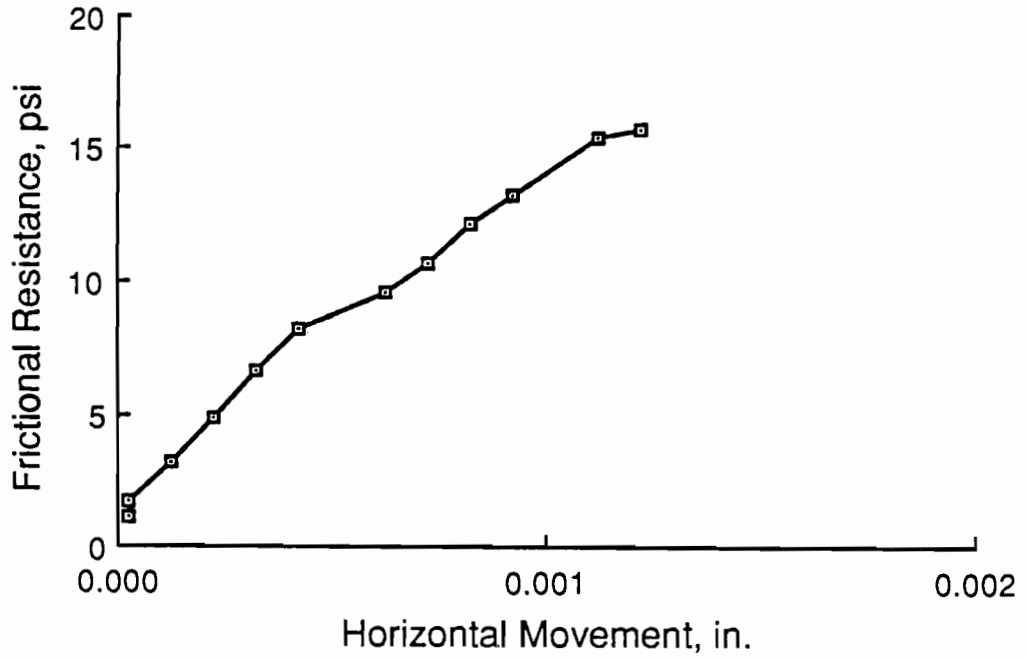

Fig 6.24. Horizontal movement for push-off test on 3.5-inch slab on cement stabilized subbase.

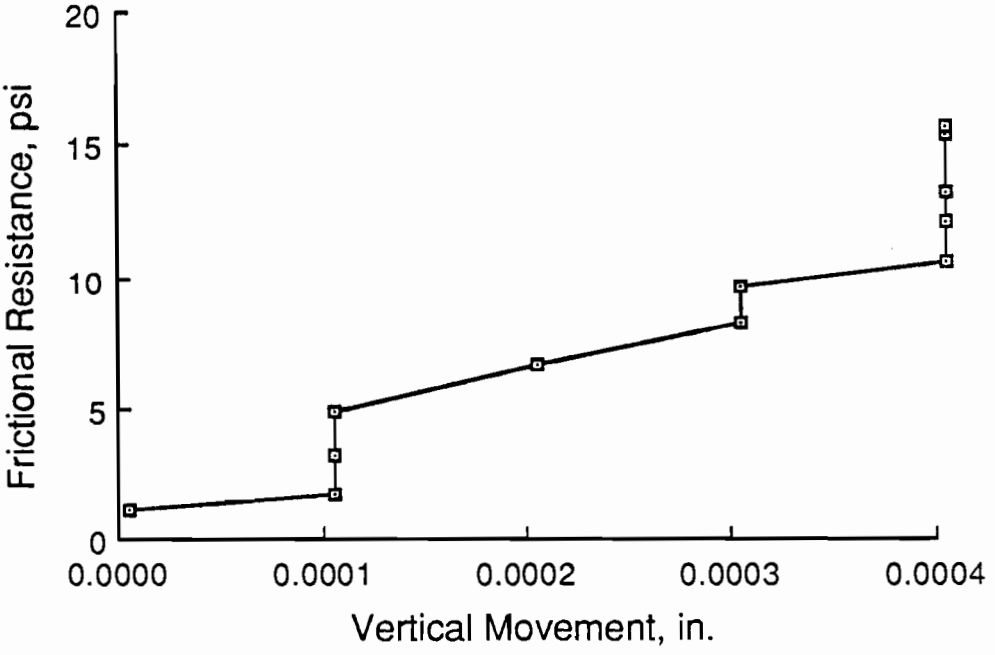

Fig 6.25. Vertical movement for push-off test on 3.5-inch slab on cement stabilized subbase.

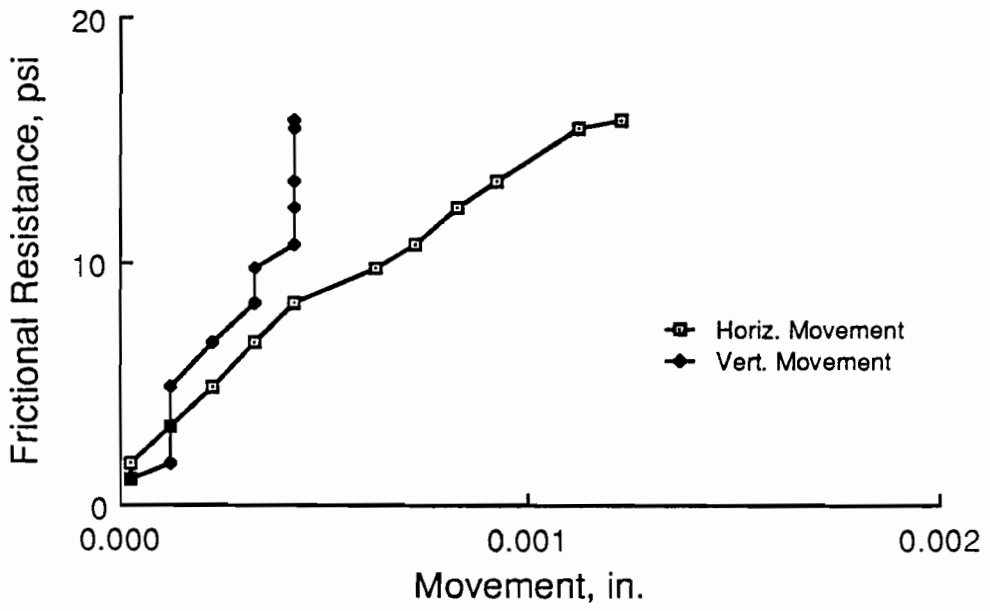

Fig 6.26. Horizontal and vertical movements for push-off test on 3.5-inch slab over cement stabilized subbase.

TABLE 6.6. PUSH-OFF DATA FOR 3.5-INCH SLAB ON LIME TREATED CLAY SUBBASE

Push-off Test No.: 4-Houston Slab Area: 4032 in^2
Date: 28 October 1986 Slab Thickness: 3-1/2 inches
Subbase: Lime–treated Subbase

Time (Hr:Min)	Load (kips)	Ram Pressure (ksi)	Horizontal Movement (inch)	Vertical Movement (inch)	Slab Temperature (°F)	Frictional Resistance (psi)	μ
16:11	- - - -	.04	- - - -	- - - -	- - - -	- - - -	- - - -
16:12	- - - -	.04	- - - -	- - - -	- - - -	- - - -	- - - -
16:12	1.465	.30	0	0	85.05	.36	1.24
16:13	1.672	.36	.0001	.0001	85.12	.41	1.41
16:13	2.404	.50	.0007	.0001	85.12	.60	2.03
16:13	3.296	.68	.0016	.0001	85.03	.82	2.78
16:14	4.221	.89	.0028	0	85.10	1.05	3.57
16:14	4.905	1.05	.0041	.0008	85.10	1.22	4.14
16:14	5.807	1.24	.0071	.0034	84.99	1.44	4.90
16:15	6.309	1.40	.0108	.0062	85.03	1.56	5.33
16:15	5.325	1.45	.0300	.0229	84.97	1.32	4.50
16:16	3.644	1.05	.0586	.0435	84.97	.90	3.08
16:16	2.706	.70	.0956	.0626	84.88	.67	2.29
16:17	2.135	.60	.1538	.0730	84.90	.53	1.80
16:18	1.901	.45	.2076	.0989	84.90	.47	1.61
16:18	1.777	.45	.2573	.1074	84.97	.44	1.50
16:19	1.639	.40	.3605	.1189	84.83	.41	1.38
16:19	1.427	.35	.5025	.1443	84.92	.35	1.21
16:20	1.389	.35	.6271	.1663	84.87	.34	1.17
16:20	1.316	.35	.7501	.1825	84.85	.33	1.11
16:21	1.314	.35	.8734	.1863	84.88	.33	1.11

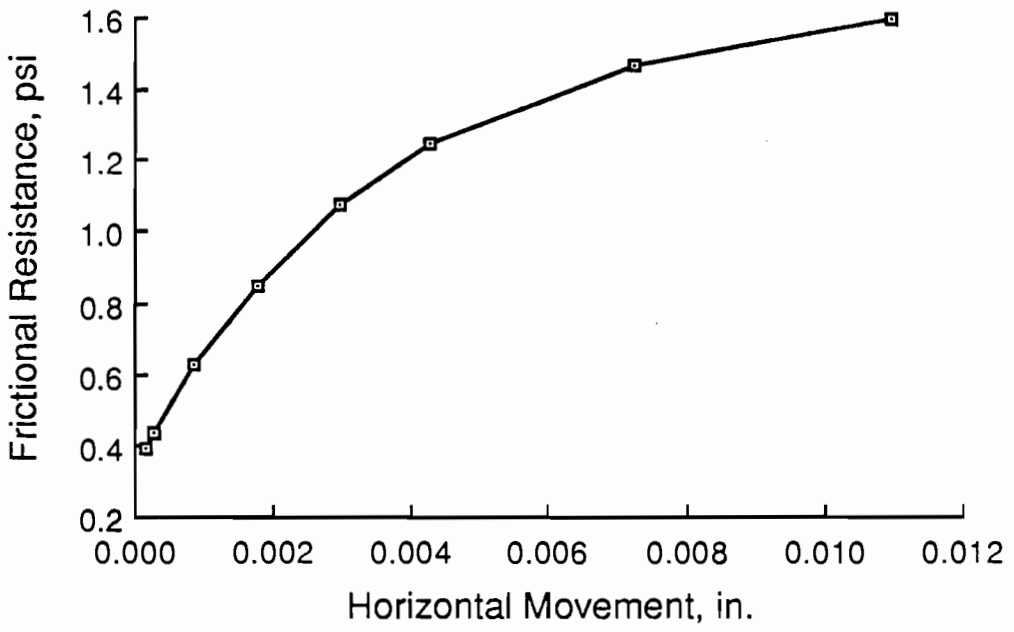

Fig 6.27. Horizontal movement to peak frictional resistance for 3.5-inch slab on lime treated clay subbase.

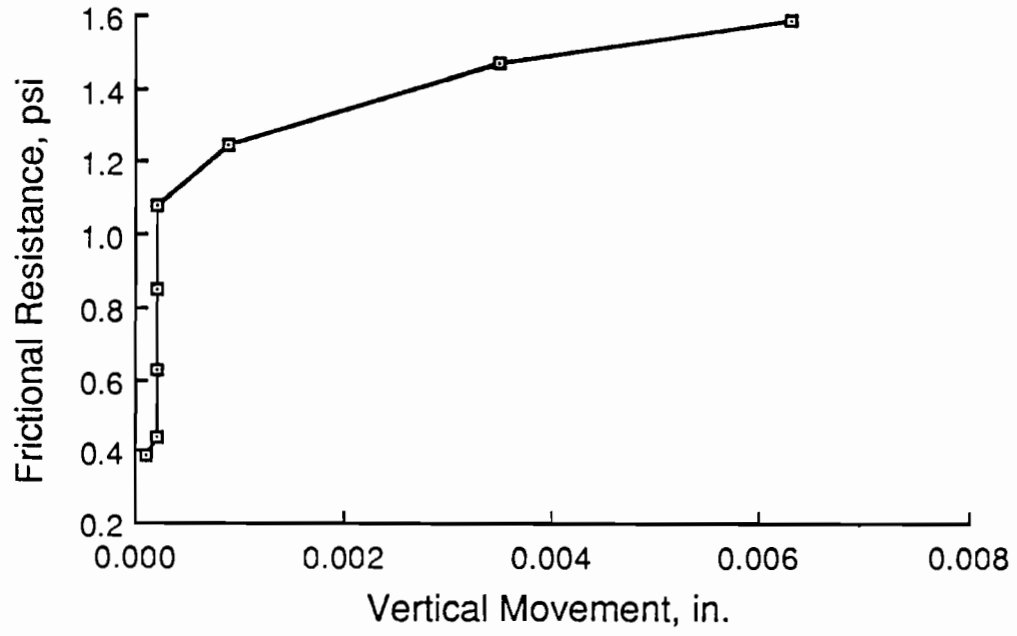

Fig 6.28. Vertical movement to peak frictional resistance for 3.5-inch slab on lime treated clay subbase.

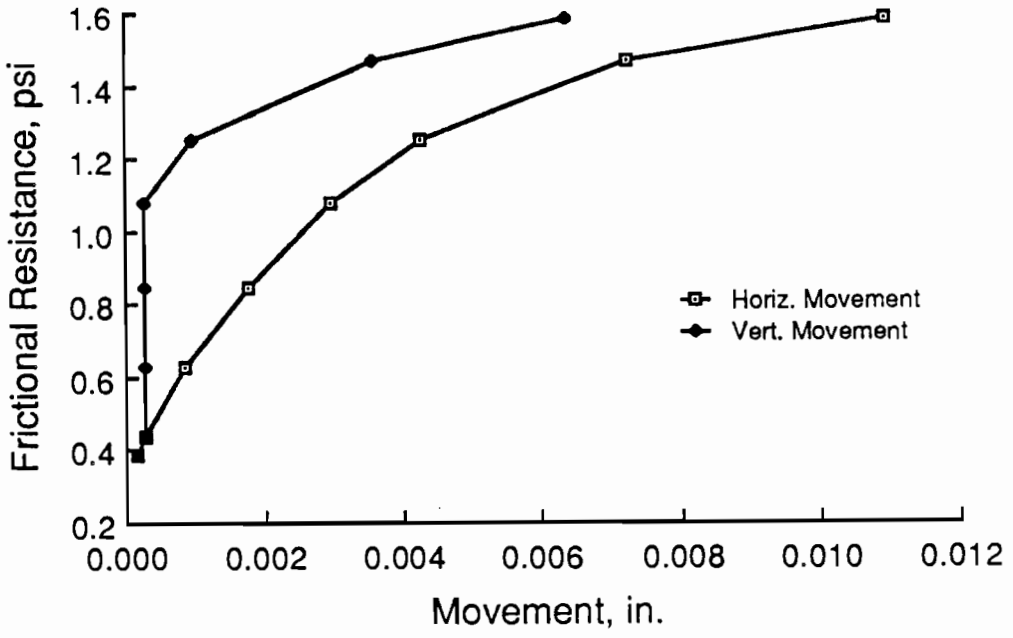

Fig 6.29. Horizontal and vertical movements to peak frictional resistance for 3.5-inch slab on lime treated clay subbase.

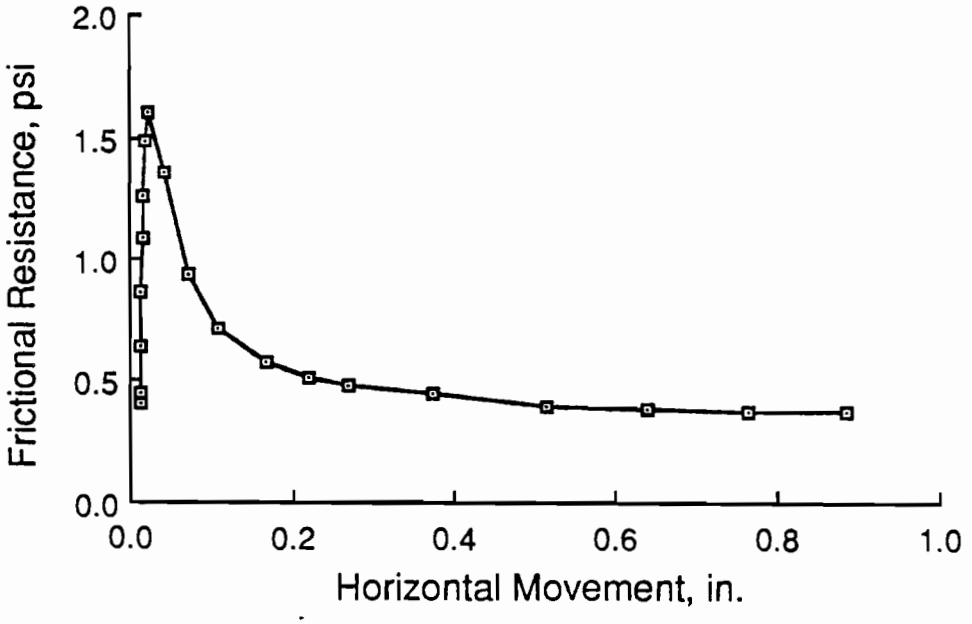

Fig 6.30. Horizontal movement for push-off test on 3.5-inch slab on lime treated clay subbase.

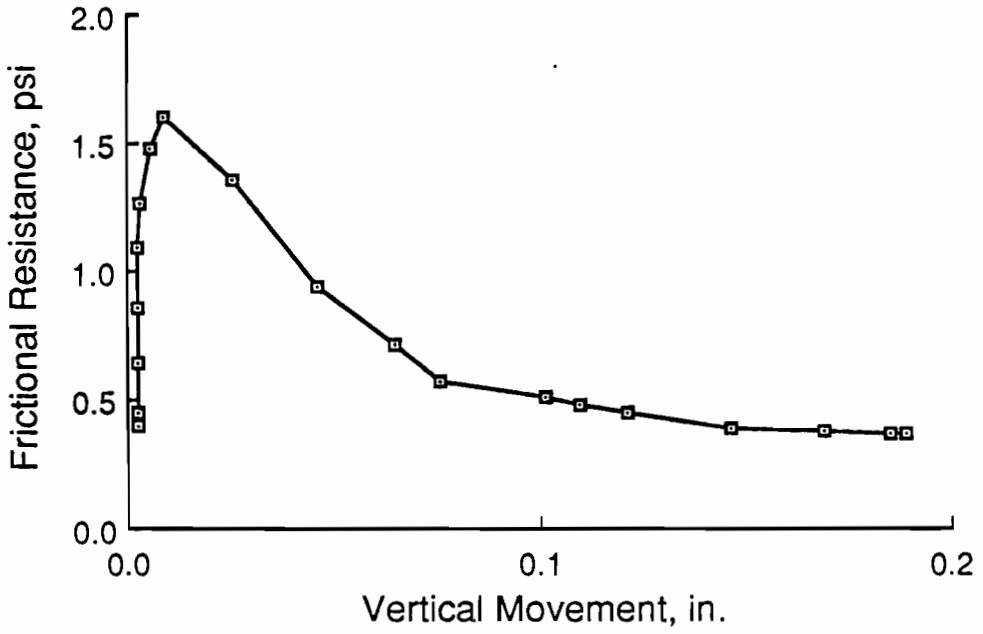

Fig 6.31. Vertical movement for push-off tests on 3.5-inch slab on lime treated clay subbase.

properties. The second test results on this subbase are found in Table 6.7 and Figs 6.32 through 6.36.

This was not the case for the untreated clay subbase. The failure was observed at the slab subbase interface and the peak frictional resistance almost doubled after the weight of the slab was doubled. The 3.5-inch and simulated 7-inch slab results are given in Table 6.8 and Figs 6.37 through 6.41 and Table 6.9 and Figs 6.42 through 6.46 respectfully. The peak frictional resistance increased from 0.6 psi to 1.1 psi, an 83 percent increase. Observation points to the fact that, for an unbonded subbase, failure occurs at the slab-subbase interface and that the magnitude of frictional resistance is linearly dependent on the slab weight. Therefore, the use of a coefficient of friction in the design of pavements is applicable for unbound subbases.

SUMMARY

Table 6.10 gives the summary of results for the push-off tests run on the various subbases. The untreated clay gave the least amount of resistance. The addition of lime to the same clay raised the peak frictional resistance from 0.6 psi to 1.6 psi for the 3.5-inch slab tested, which represents a 160 percent increase. Both the lime and asphalt stabilized subbases provided frictional resistances of approximately the same magnitude. The flexible subbase offered roughly twice as much frictional resistance as both the lime and asphalt stabilized subbases. The cement stabilized subbase glued the test slab down, offering a frictional resistance above 15 psi.

CONCRETE PROPERTIES

The concrete batches for both the Austin and the Houston test sites used approximately a five–sack mix design. Both also used crushed limestone as the aggregate. The Houston mix came from a truck used on a pavement placement at the construction site. The Houston batch was expected to give higher concrete strength properties compared to the Austin batch due to a slightly higher cement content and considerably lower water content. The slump for the Austin batch was 4 inches while the Houston batch gave only a 2–inch slump. Table 6.11

TABLE 6.7. PUSH-OFF DATA FOR 7-INCH SLAB ON LIME TREATED CLAY SUBBASE

Push-off Test No.: 5-Houston Slab Area: 4032 in^2
Date: 30 October 1986 Slab Thickness: 7 inches simulated
Subbase: Lime Treated Subbase

Time (Hr:Min)	Load (kips)	Ram Pressure (ksi)	Horizontal Movement (inch)	Vertical Movement (inch)	Slab Temperature (°F)	Frictional Resistance (psi)	μ
17:19	- - - -	.14	- - - -	- - - -	- - - -	- - - -	- - - -
17:20	- - - -	.14	- - - -	- - - -	- - - -	- - - -	- - - -
17:22	1.958	.45	0	0	79.39	.49	.83
17:22	3.163	.70	.0012	.0010	79.48	.78	1.34
17:23	4.206	.90	.0026	.0023	79.54	1.04	1.78
17:23	4.787	1.00	.0034	.0030	79.45	1.19	2.02
17:23	5.060	1.10	.0039	.0034	79.39	1.26	2.14
17:24	6.114	1.30	.0065	.0050	79.47	1.52	2.58
17:24	6.933	1.50	.0118	.0075	79.32	1.72	2.93
17:24	6.204	1.55	.0335	.0181	79.43	1.54	2.67
17:24	4.980	1.40	.0679	.0328	79.38	1.24	2.11
17:25	4.092	1.00	.1277	.0514	79.32	1.01	1.73
17:25	3.407	.85	.2622	.0748	79.36	.85	1.44
17:25	3.156	.80	.3994	.0873	79.38	.78	1.34
17:25	3.054	.75	.5393	.1078	79.32	.76	1.29
17:26	2.902	.75	.6753	.1175	79.27	.72	1.23
17:26	2.798	.75	.8110	.1249	79.30	.69	1.18
17:27	2.687	.75	.9725	.1333	79.38	.67	1.14

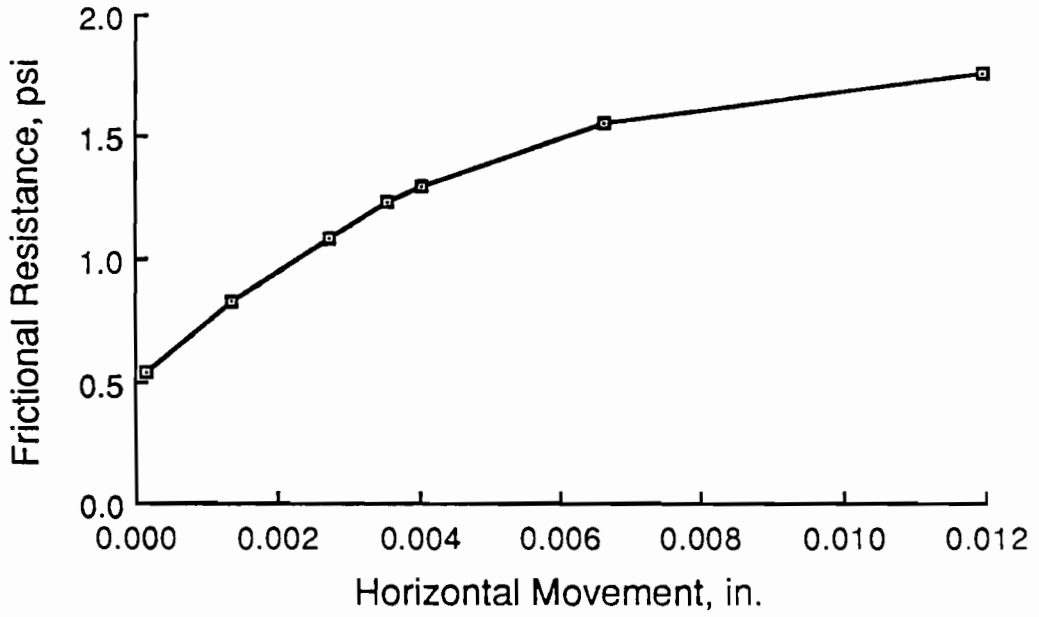

Fig 6.32. Horizontal movement to peak frictional resistance for simulated 7-inch slab on lime–treated clay subbase.

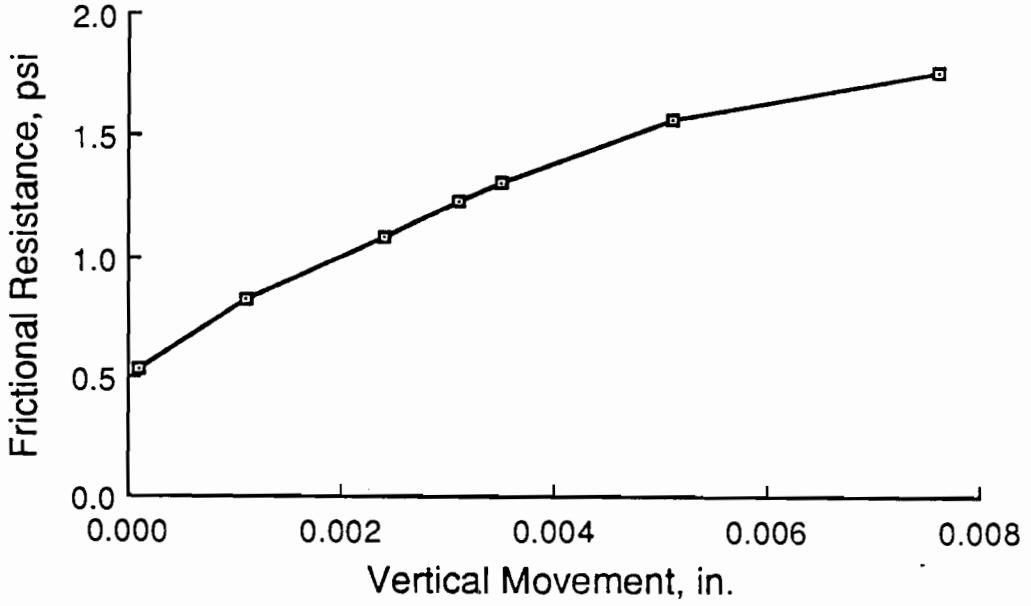

Fig 6.33. Vertical movement to peak frictional resistance for simulated 7-inch slab on lime–treated clay subbase.

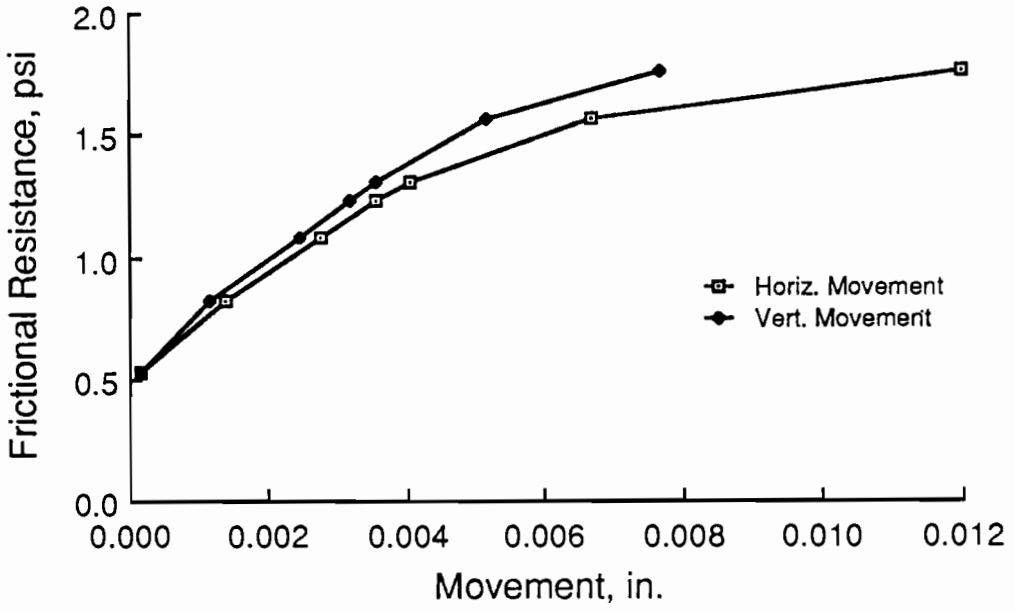

Fig 6.34. Horizontal and vertical movements to peak frictional resistance for simulated 7-inch slab on lime–treated clay subbase.

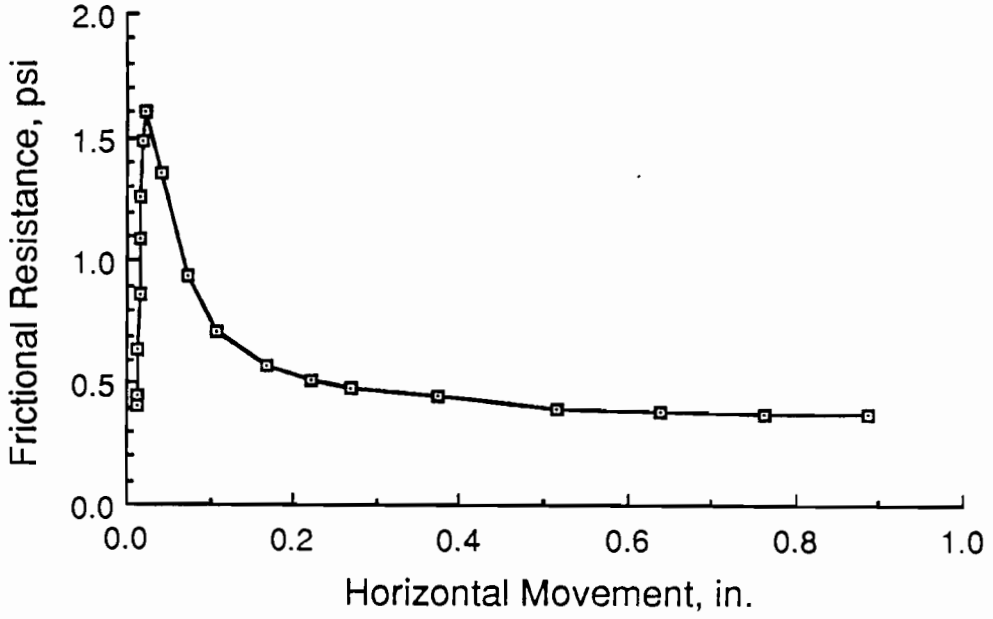

Fig 6.35. Horizontal movement for push-off test for simulated 7-inch slab on lime–treated clay subbase.

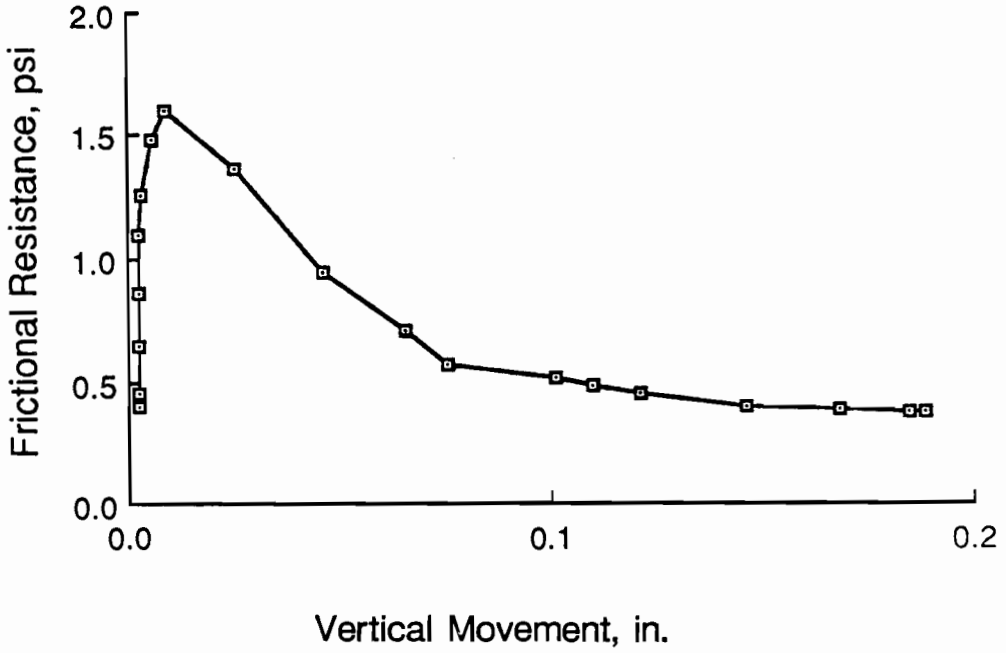

Fig 6.36. Vertical movement for push-off test on simulated 7-inch slab on lime–treated clay subbase.

TABLE 6.8. PUSH-OFF DATA FOR 3.5-INCH SLAB ON UNTREATED CLAY SUBBASE

Push-off Test No.: 6-Houston Slab Area: 4032 in^2
Date: 28 October 1986 Slab Thickness: 3-1/2 inches
Subbase: Untreated Clay

Time (Hr:Min)	Load (kips)	Ram Pressure (ksi)	Horizontal Movement (inch)	Vertical Movement (inch)	Slab Temperature (°F)	Frictional Resistance (psi)	μ
16:58	- - - -	.12	- - - -	- - - -	- - - -	- -	- - - -
16:58	- - - -	.12	- - - -	- - - -	- - - -	- -	- - - -
16:59	1.518	.30	.0	0	85.77	.38	1.28
16:59	1.800	.38	.0027	.0007	85.68	.45	1.52
17:00	2.232	.46	.0095	.0022	85.62	.55	1.89
17:00	2.442	.50	.0147	.0036	85.62	.61	2.06
17:01	2.558	.55	.0296	.0063	85.60	.63	2.16
17:01	2.548	.55	.0374	.0075	85.46	.63	2.15
17:01	2.550	.58	.0627	.0121	85.44	.63	2.15
17:02	2.508	.58	.0890	.0159	85.48	.62	2.12
17:02	2.470	.58	.1144	.0196	85.48	.61	2.09
17:02	2.267	.58	.1166	.0197	85.51	.56	1.91
17:03	2.366	.58	.2472	.0431	85.55	.59	1.99
17:03	2.276	.58	.3798	.0611	85.41	.56	1.92
17:03	2.210	.57	.5040	.0794	85.48	.55	1.87
17:04	1.970	.57	.6348	.0874	85.37	.49	1.66
17:05	2.164	.56	.7601	.1261	85.23	.54	1.83
17:05	2.139	.56	.8828	.1328	85.23	.53	1.81

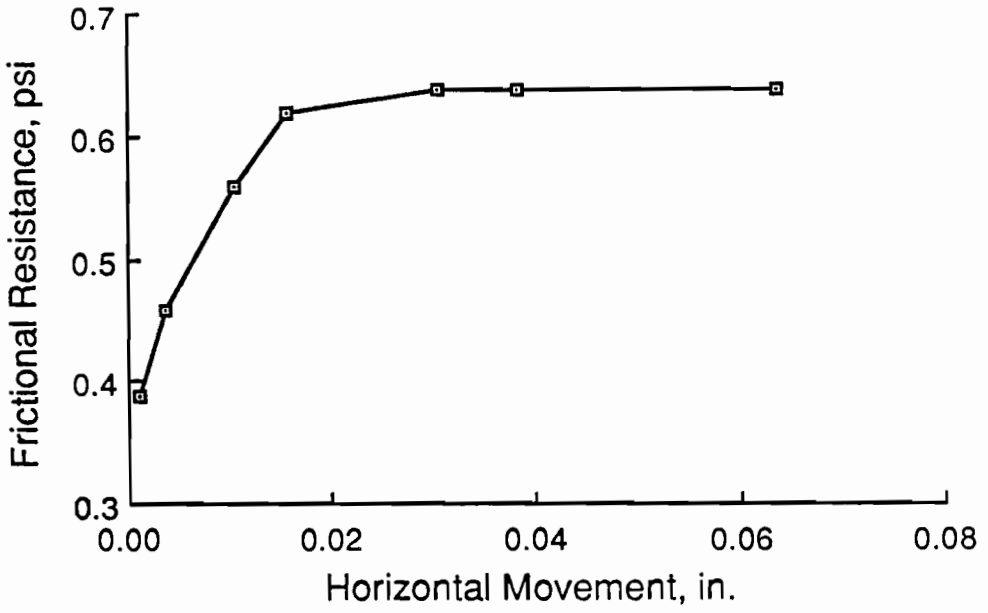

Fig 6.37. Horizontal movement to peak frictional resistance for 3.5-inch slab on untreated clay subbase.

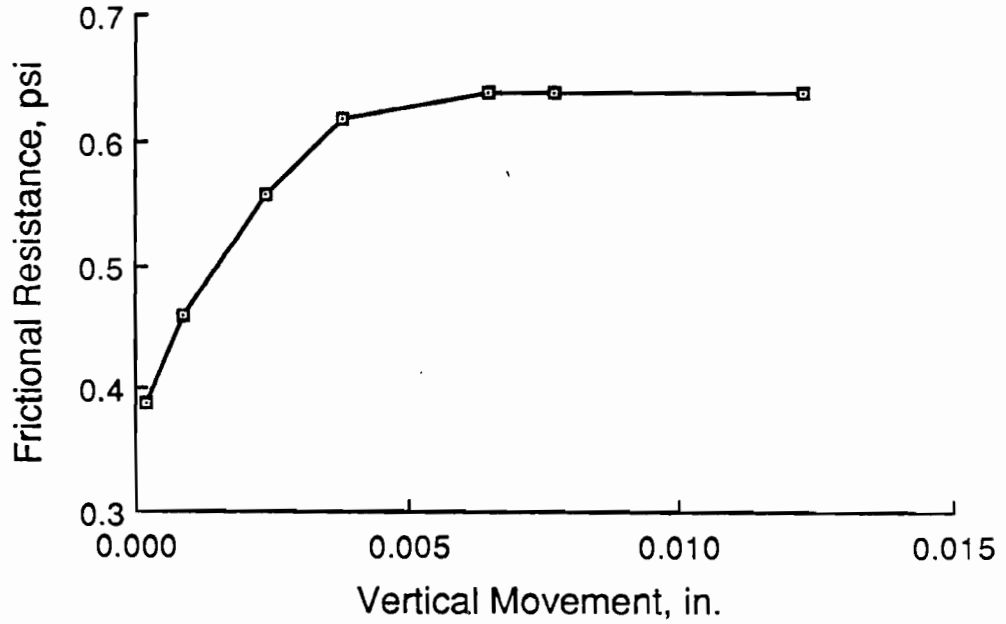

Fig 6.38. Vertical movement to peak frictional resistance for 3.5-inch slab on untreated clay subbase.

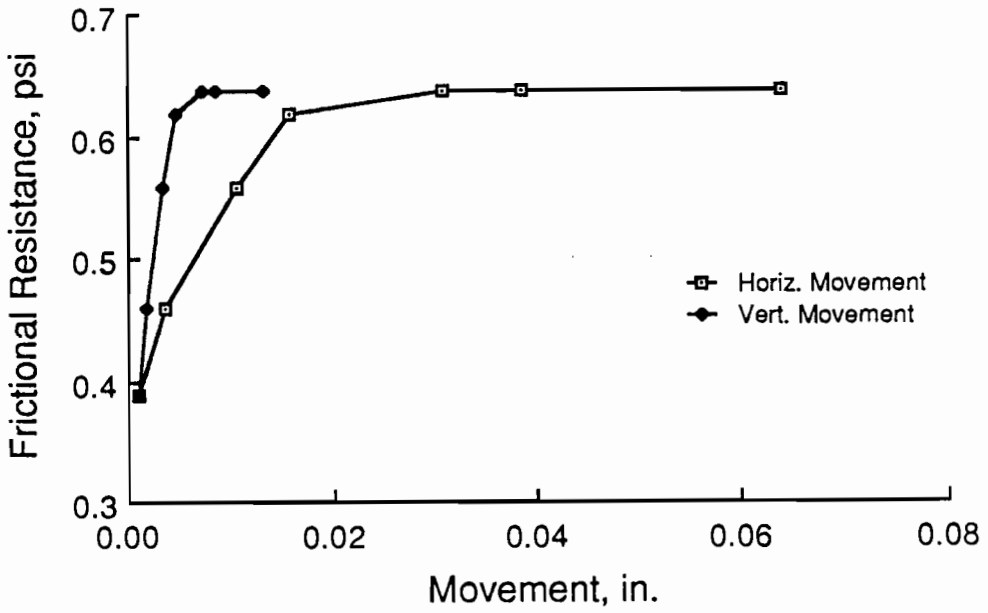

Fig 6.39. Horizontal and vertical movements to peak frictional resistance for 3.5-inch slab on untreated clay subbase.

Fig 6.40. Horizontal movement for push-off test on 3.5-inch slab on untreated clay subbase.

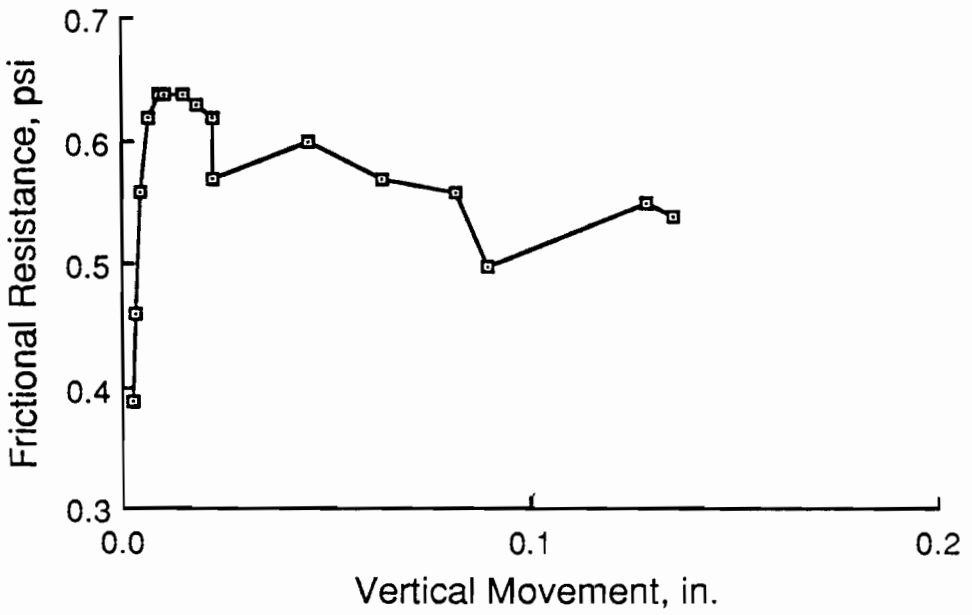

Fig 6.41. Vertical movement for push-off test on 3.5-inch slab on untreated clay subbase.

TABLE 6.9. PUSH-OFF DATA FOR SIMULATED 7-INCH SLAB ON UNTREATED CLAY SUBBASE

Push-off Test No.: 7-Houston Slab Area: 4032 in^2
Date:30 October 1986 Slab Thickness: 7 inches simulated
Subbase: Untreated Clay

Time (Hr:Min)	Load (kips)	Ram Pressure (ksi)	Horizontal Movement (inch)	Vertical Movement (inch)	Slab Temperature (°F)	Frictional Resistance (psi)	μ
17:57	- - - -	.15	- - - -	- - - -	- - - -	- - - -	- - - -
17:57	- - - -	.15	- - - -	- - - -	- - - -	- - - -	- - - -
17:57	1.627	.35	0	0	78.53	.40	.69
17:57	1.779	.38	.0002	0	78.35	.44	.75
17:58	2.099	.45	.0005	0	78.42	.52	.89
17:58	2.359	.50	.0009	0	78.39	.59	1.00
17:58	2.683	.60	.0019	0	78.37	.67	1.14
17:58	2.892	.65	.0030	.0002	78.49	.72	1.22
17:59	3.124	.72	.0044	.0004	78.48	.77	1.32
17:59	3.336	.78	.0060	.0007	78.42	.83	1.41
17:59	3.527	.82	.0077	.0010	78.33	.87	1.49
18:00	3.684	.85	.0097	.0014	78.37	.91	1.56
18:00	3.863	.90	.0119	.0018	78.28	.96	1.63
18:00	4.037	.94	.0145	.0023	78.39	1.00	1.71
18:00	4.175	1.00	.0180	.0029	78.33	1.04	1.77
18:01	4.337	1.00	.0224	.0035	78.30	1.08	1.83
18:01	4.440	1.05	.0289	.0039	78.28	1.10	1.88
18:01	4.188	1.06	.0306	.0043	78.31	1.04	1.77
18:02	4.464	1.08	.0520	.0048	78.17	1.11	1.89
18:02	4.358	1.08	.0706	.0048	78.21	1.08	1.84

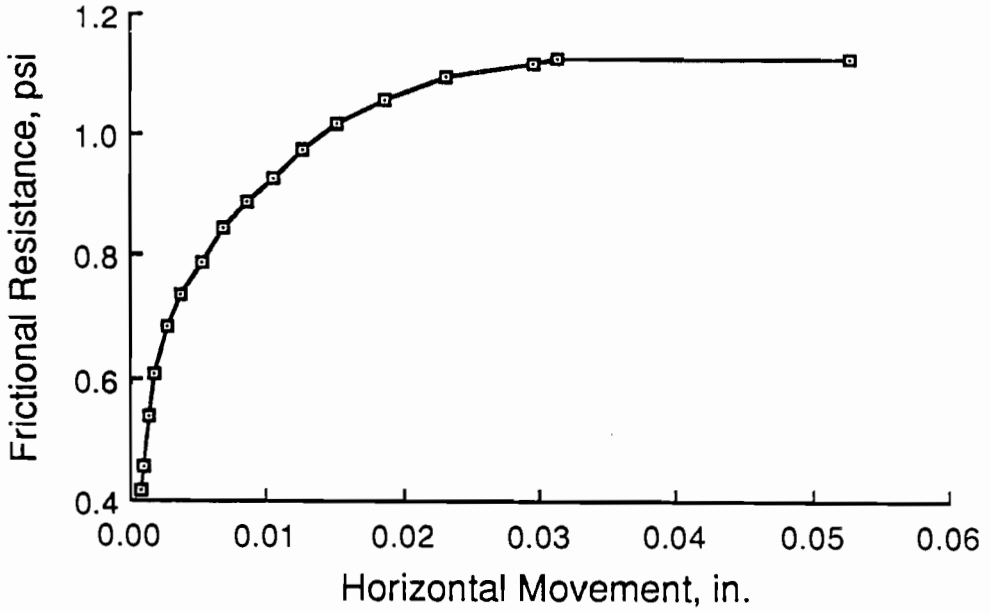

Fig 6.42. Horizontal movement to peak frictional resistance for simulated 7-inch slab on untreated clay subbase.

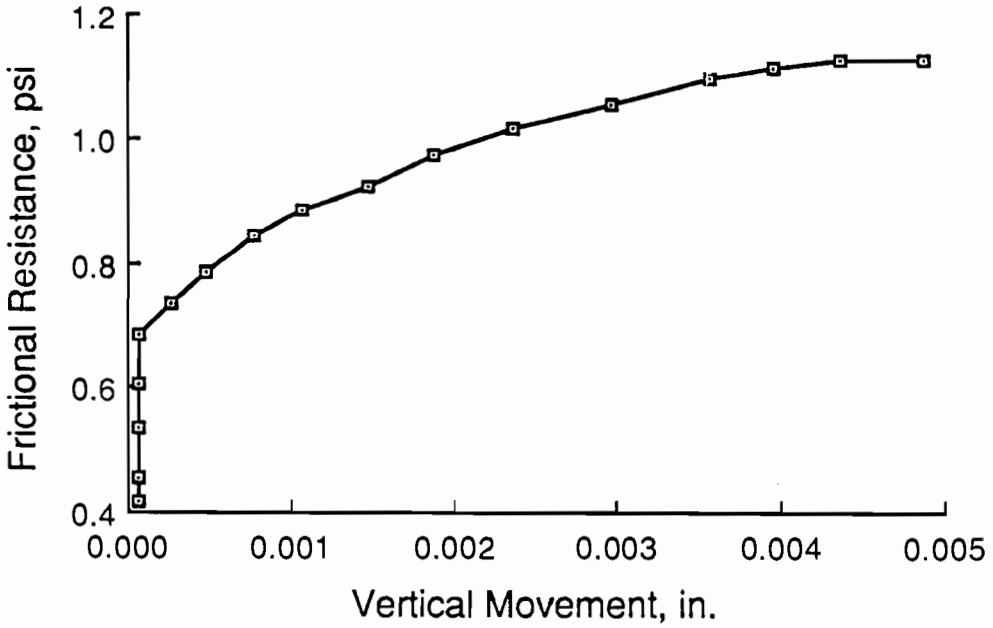

Fig 6.43. Vertical movement to peak frictional resistance for simulated 7-inch slab on untreated clay subbase.

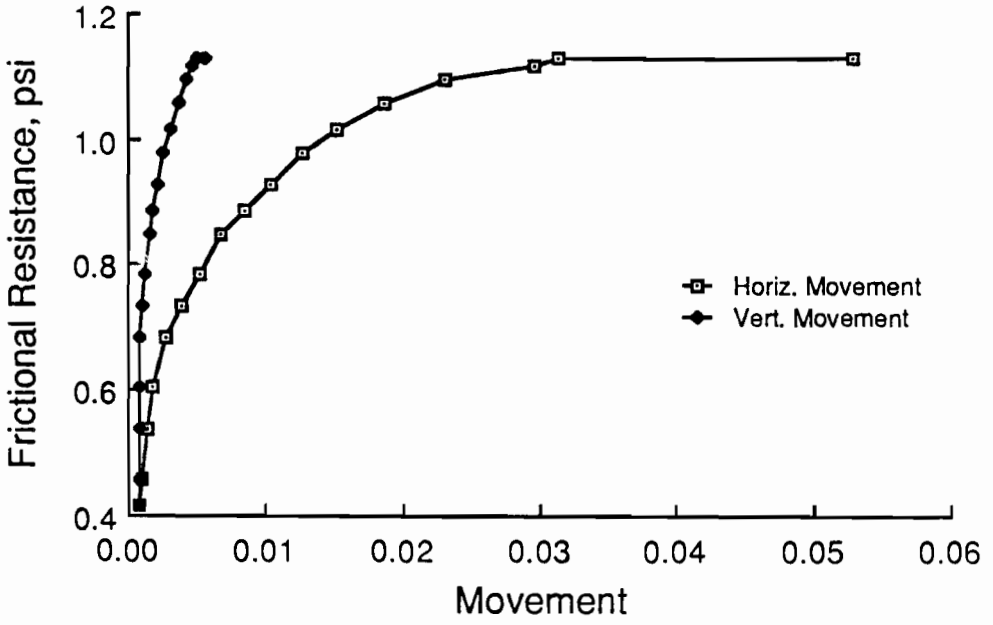

Fig 6.44. Horizontal and vertical movements to peak frictional resistance for simulated 7-inch slab on untreated clay subbase.

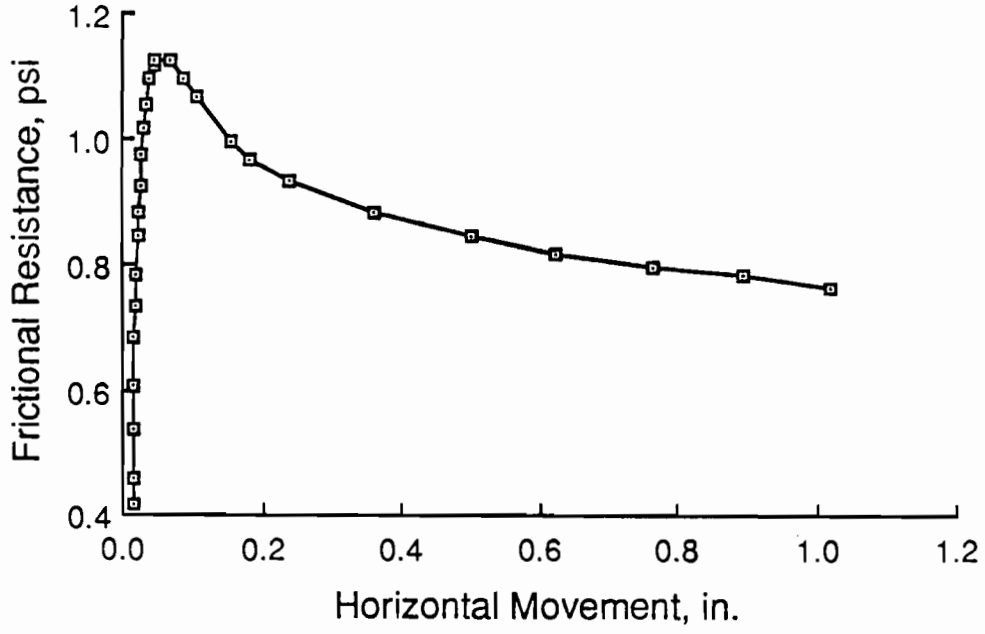

Fig 6.45. Horizontal movement for push-off test on simulated 7-inch slab on untreated clay subbase.

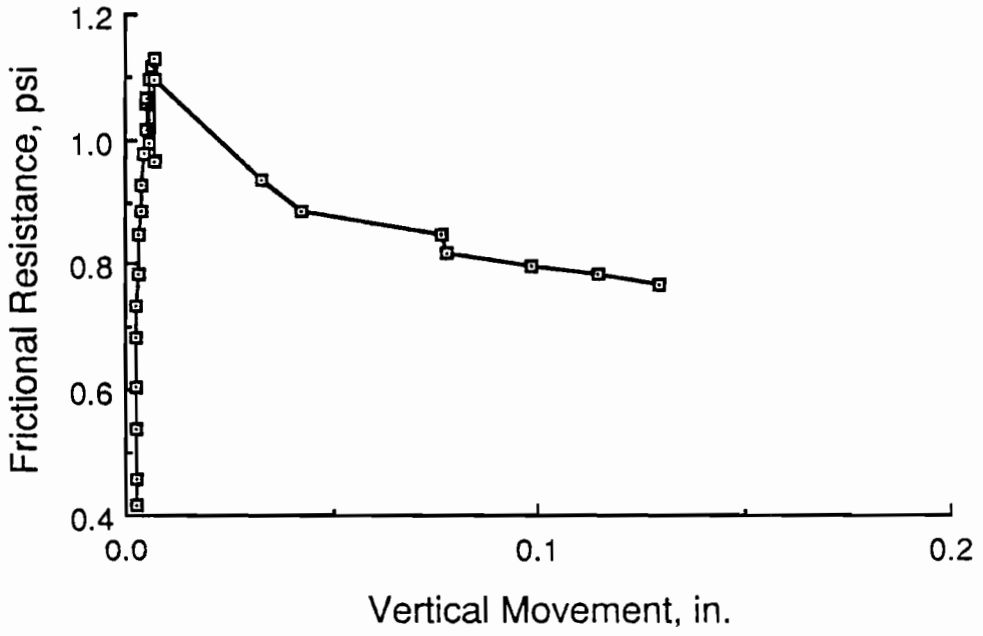

Fig 6.46. Vertical movement for push-off test on simulated 7-inch slab on untreated clay subbase.

TABLE 6.10. RESULTS OF PUSH-OFF TESTS

Subbase Type	Peak Frictional Resistance (psi)	Horizontal Movement at Sliding (inch)	Slab Depth (inches)
Flexible	3.0, 3.4	0.024, 0.020	4, 8
Asphalt Stabilized	1.6, 2.2	0.030, 0.038	3.5, 7
Cement Stabilized	15.4 +	0.001 +	3.5
Lime–treated Clay	1.6, 1.7	0.011, 0.012	3.5, 7
Untreated Clay	0.6, 1.1	0.030, 0.052	3.5, 7

TABLE 6.11. RESULTS OF CONCRETE TESTING

Concrete Property	Austin Batch*	Houston Batch*
Compressive Strength (ksi)	3.89 (0.001)	5.56 (0.13)
Flexural Strength (psi)	470 (11)	715 (14)
Modulus of Elasticity (ksi)	4,817 (203)	5,154 (82)
Coefficient of Thermal Expansion (in./in.°F)	6.48×10^{-6}	5.84×10^{-6}

*( ) Standard deviation values.

presents results of experimentation carried out on specimens cast and cured at both locations. As expected, the concrete compressive strength was higher for the Houston batch (5.6 ksi) than for the Austin batch (3.9 ksi). Flexural strengths and moduli of elasticity also followed the same pattern. All testing involved numerous specimens but results showed little scatter between each test. A stiffer mix lowers the amount of movements a concrete specimen undertakes during a change in temperature. Therefore it was expected that the coefficient of thermal expansion would be lower for the Houston batch as compared to the Austin batch. Experimental results showed a coefficient of expansion of 5.8 micro strains per degree Fahrenheit for the Houston batch and 6.5 micro strains per degree Fahrenheit for the Austin batch.

The purpose for obtaining concrete properties was to use them along with the friction movement profiles obtained in Phase II to calculate expected test slab movements for Phase I of the experimentation. Thus, actual movements obtained by experimentation can be compared to the computed movements. The computer model used to compute the expected movements is the PCP1 program developed in conjunction with a Center for Transportation Research research project (Ref 3).

PHASE I

Transverse cracking was observed in the 3/4-inch bond breaker everywhere on the construction site. The cracks were spaced roughly 20 to 30 feet apart and ran from edge to edge of prepared subbase. This is termed reflection cracking and is caused by shrinkage cracks from the cement stabilized subbase propagating up into the bond breaker. One of these reflection cracks propagated through one of the test slabs and cracked it. The failed test slab was directly on the cement stabilized subbase and the crack occurred 6 inches off the center of the slab. Theoretically the center of the slab is where the highest stresses are felt, due to frictional restraint. The crack occurred before one free end of the slab was pinned to its anchor. The transverse crack and the failed test slab can be seen in Fig 6.47. Whether the crack occurred by the propagation of the reflection crack and/or the high center span stresses induced by the frictional restraint of the cement stabilized subbase cannot be determined. Even though the test slab had failed, thus negating it for the Phase I experimentation, there is an important fact that can be learned. All movements spoken of so far in this report are

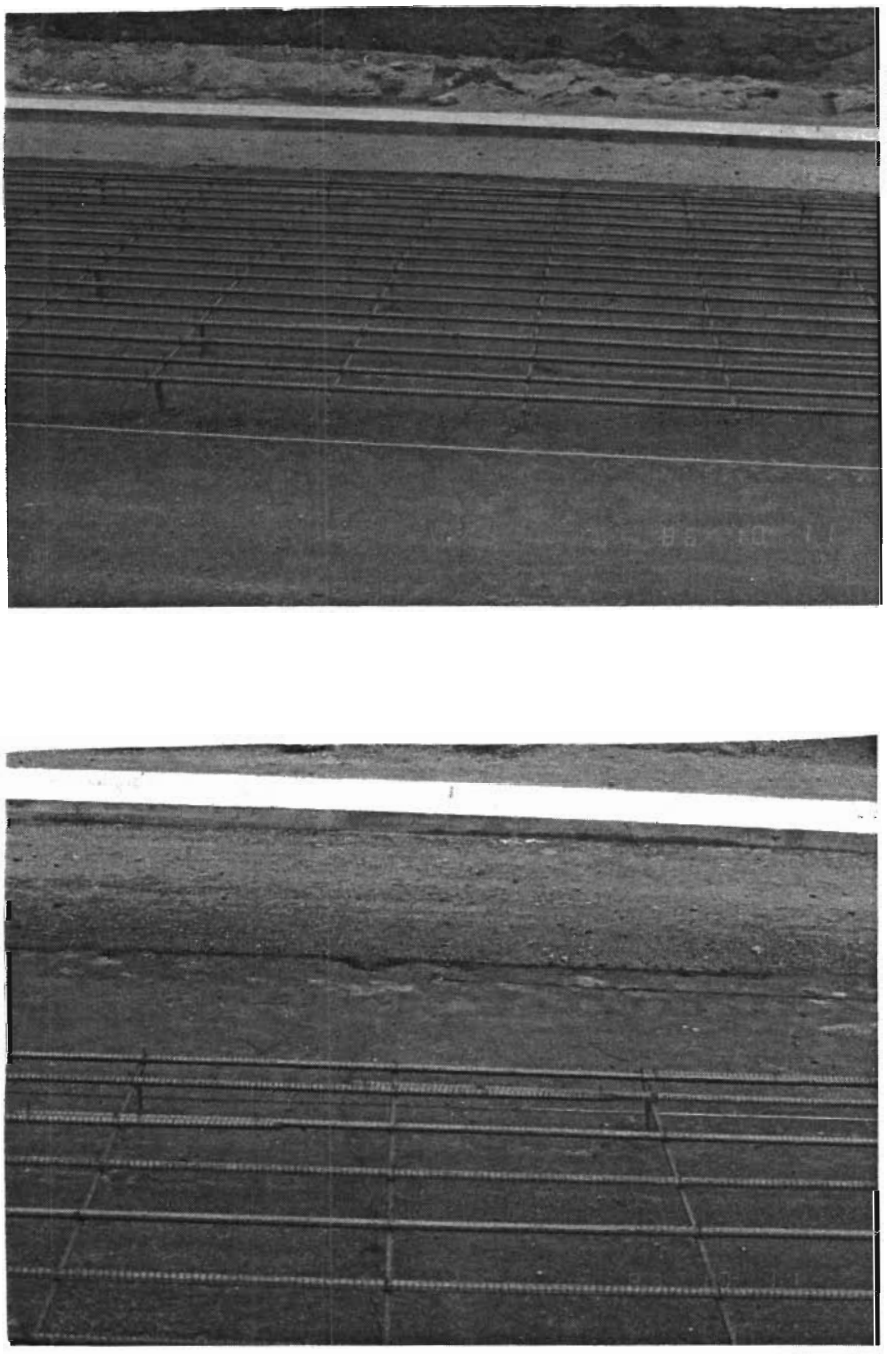

(continued)

Fig 6.47. Transverse reflection crack and failed test slab on cement stabilized subbase.

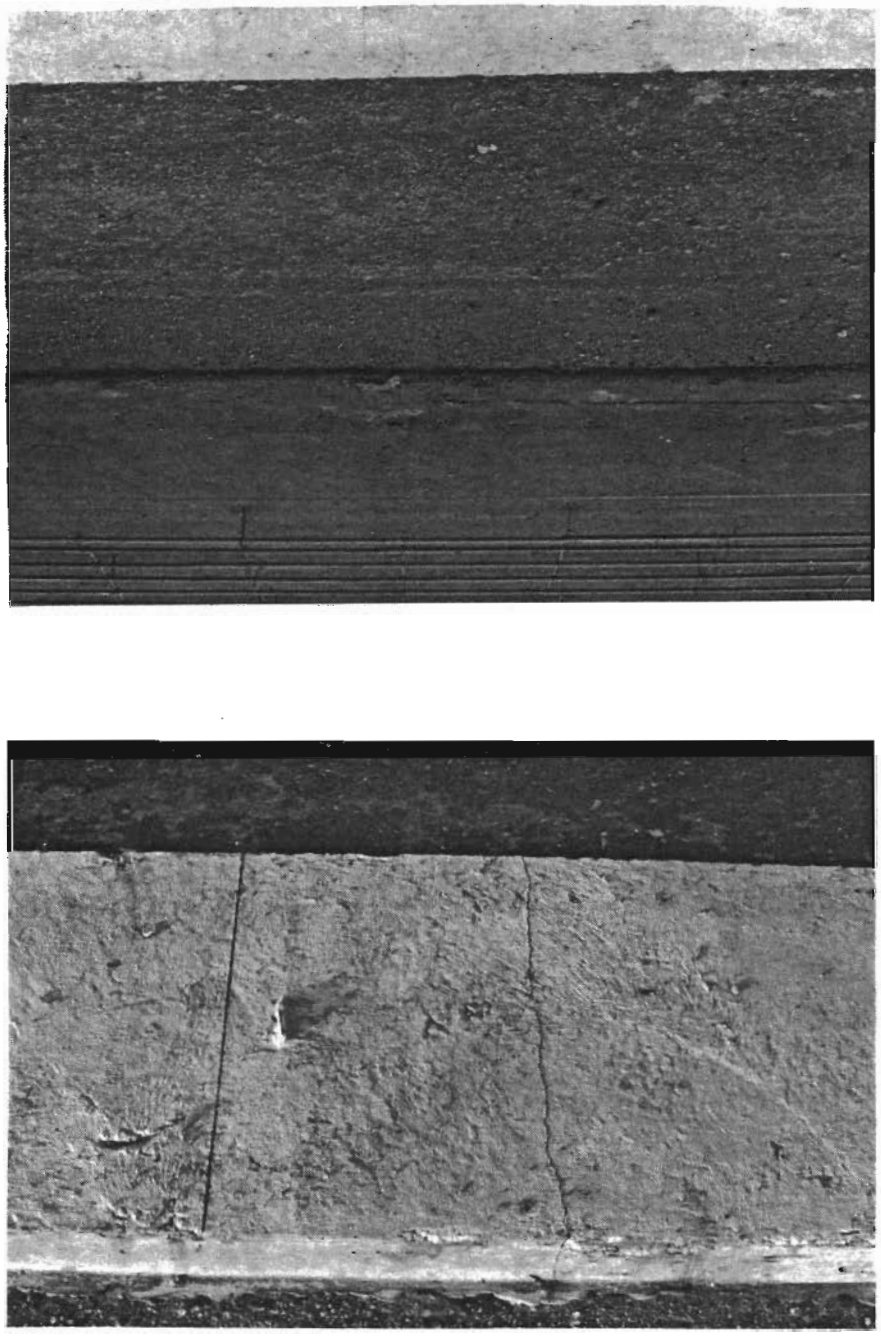

Fig 6.47. (continued).

induced movements caused by thermal and moisture variations of the pavement on its subbase; however, movements relative to the slab and its subbase can also be induced by the subbase for the same reasons.

Table 6.12 gives the results of the horizontal and vertical movements at five locations along a 22-foot slab cast on top of a flexible subbase. The change in temperature represented a 14.7°F drop. Also shown in Table 6.12 are the calculated movements without any friction for free thermal expansion using the value obtained in the concrete properties testing. The last column represents calculated movements with friction by inputing concrete properties and the friction-movement profile obtained in Phase II into the computer model. Figure 6.48 graphically displays each of the actual and calculated horizontal movements while Fig 6.49 shows the actual vertical movements. It can be seen that all actual and calculated movements with friction are relatively close, but are very small when compared to the calculated movements without friction. Any differences between the first two are largely due to the fact that the pinned anchor scheme did not work effectively in fixing one end of the slab. Anchor movements were recorded for every slab tested, as seen in Tables 6.12 through 6.15 and Figs 6.48, 6.50, 6.52, and 6.54. Therefore, the actual center of the slab was unknown. The calculated movements were all based on the pinned anchor's being the simulated center span. Although the tests were run on different subbases with different slab lengths and thermal changes, actual and calculated horizontal movements are all in the same order of magnitude. This is largely due to the fact that movements were so small that only a small initial portion of the friction-movement profiles was encountered, making it difficult to see any noticeable differences in horizontal movements. For this reason, the observation of the pinned anchor's not working properly in fixing the slab, and the different vertical slab profiles, no valid friction information can be obtained in this experimental phase.

Vertical movements, as shown in Figs 6.49, 6.51, 6.53, and 6.55, were monitored so that proper judgment, when comparing horizontal movements for the various subbases, could be made if the vertical profiles of the slabs were similar. However, as these figures show, the vertical profiles of the slabs vary, making a comparison based on the horizontal movement for frictional resistance impossible. Each slab displayed different vertical profiles, largely due to the various effects curling had on each slab.

If this test is used again to obtain subbase friction information, several things must be changed. Larger induced movements must be derived by lengthening the slab or creating larger temperature changes. If the slabs are lengthened, care must be taken so that premature

TABLE 6.12. CONTINUOUS TEST RESULTS FOR 22-FOOT SLAB ON FLEXIBLE SUBBASE (ΔT = -14.65°F)

	Distance From Pinned End (feet)	Actual Movements (mils)	Calculated Movements without Friction (mils)	Calculated Movements with Friction (mils)
Vertical	0.20	-.05	- -	- -
	6.66	0.4	- -	- -
	11.58	-1.5	- -	- -
	16.58	-0.2	- -	- -
	21.58	2.9	- -	- -
Horizontal	0.20	-0.3	-0.2	-0.1
	6.66	-0.5	-7.6	-4.5
	11.58	-0.6	-13.2	-8.4
	16.58	-3.4	-18.9	-13.0
	21.58	05.4	-24.6	-18.3

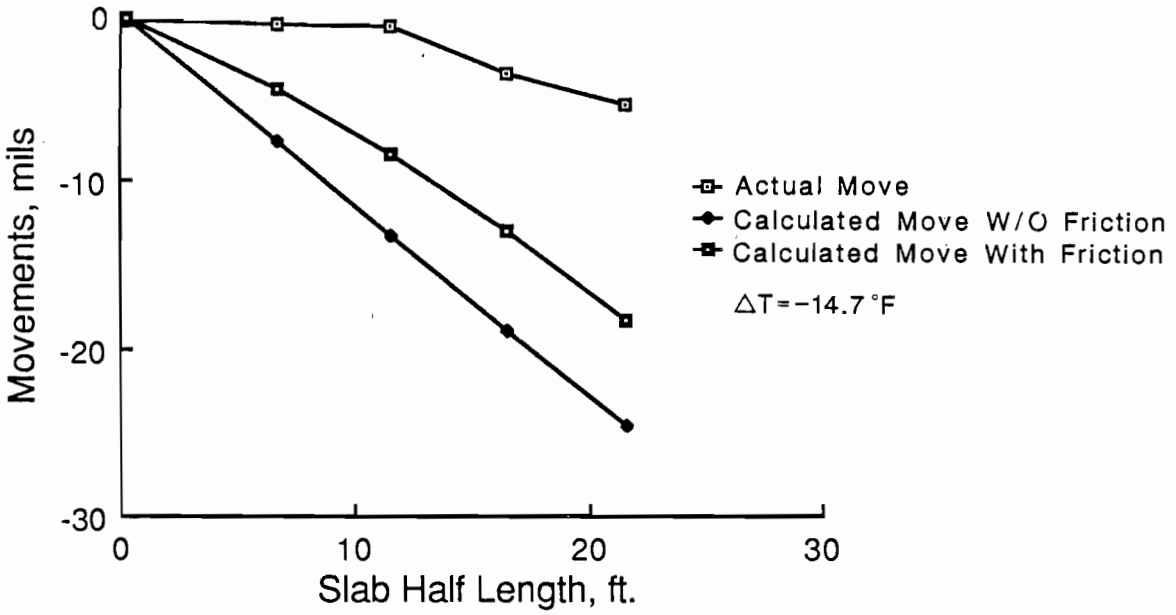

Fig 6.48. Horizontal movements for continuous test for simulated 44-foot slab on flexible subbase.

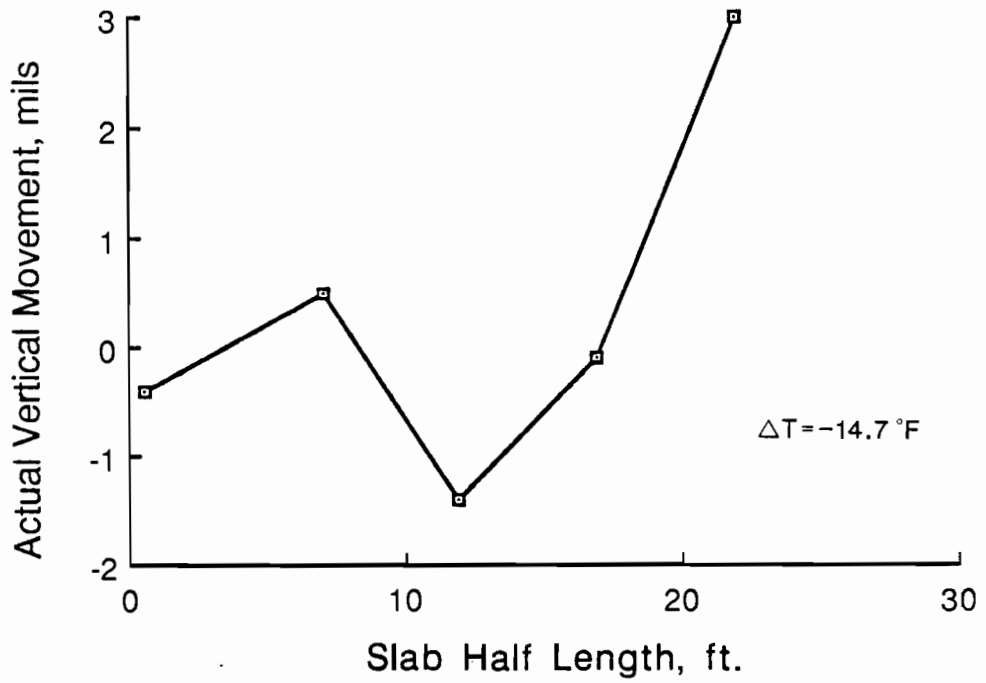

Fig 6.49. Vertical movement for continuous test for simulated 44-foot slab on flexible subbase.

TABLE 6.13. CONTINUOUS TEST RESULTS FOR 32-FOOT SLAB ON ASPHALT STABILIZED SUBBASE (ΔT = 21.72°F)

	Distance From Pinned End (feet)	Actual Movements (mils)	Calculated Movements without Friction (mils)	Calculated Movements with Friction (mils)
Vertical	0.20	-1.3	- -	- -
	10.25	-0.3	- -	- -
	17.25	-4.2	- -	- -
	24.25	-3.3	- -	- -
	31.25	-7.8	- -	- -
Horizontal	0.20	-5.1	0.3	0.2
	10.25	-9.6	15.6	11.7
	17.25	16.6	26.3	20.5
	24.25	18.4	36.9	29.9
	31.25	20.5	47.6	40.3

TABLE 6.14. CONTINUOUS TEST RESULTS FOR 32-FOOT SLAB ON LIME TREATED CLAY SUBBASE (ΔT = 23.30°F)

	Distance From Pinned End (feet)	Actual Movements (mils)	Calculated Movements without Friction (mils)	Calculated Movements with Friction (mils)
	0.20	1.1	- -	- -
	10.25	6.6	- -	- -
Vertical	17.25	-0.4	- -	- -
	24.25	-0.3	- -	- -
	31.25	-14.1	- -	- -
	0.20	-3.9	0.3	0.2
	10.25	1.4	16.7	13.2
Horizontal	17.25	-2.8	28.2	23.1
	24.25	2.1	39.6	33.7
	31.25	20.8	51.0	45.0

TABLE 6.15. CONTINUOUS TEST RESULTS FOR 32-FOOT SLAB ON UNTREATED CLAY SUBBASE (ΔT = 27.81°F)

	Distance From Pinned End (feet)	Actual Movements (mils)	Calculated Movements without Friction (mils)	Calculated Movements with Friction (mils)
	0.20	4.9	- -	- -
	10.25	0.0	- -	- -
Vertical	17.25	3.2	- -	- -
	24.25	3.3	- -	- -
	31.25	-12.4	- -	- -
	0.20	-5.5	0.4	0.4
	10.25	-1.7	20.0	18.3
Horizontal	17.25	0.0	33.6	31.2
	24.25	7.5	47.3	44.4
	31.25	20.2	60.9	58.3

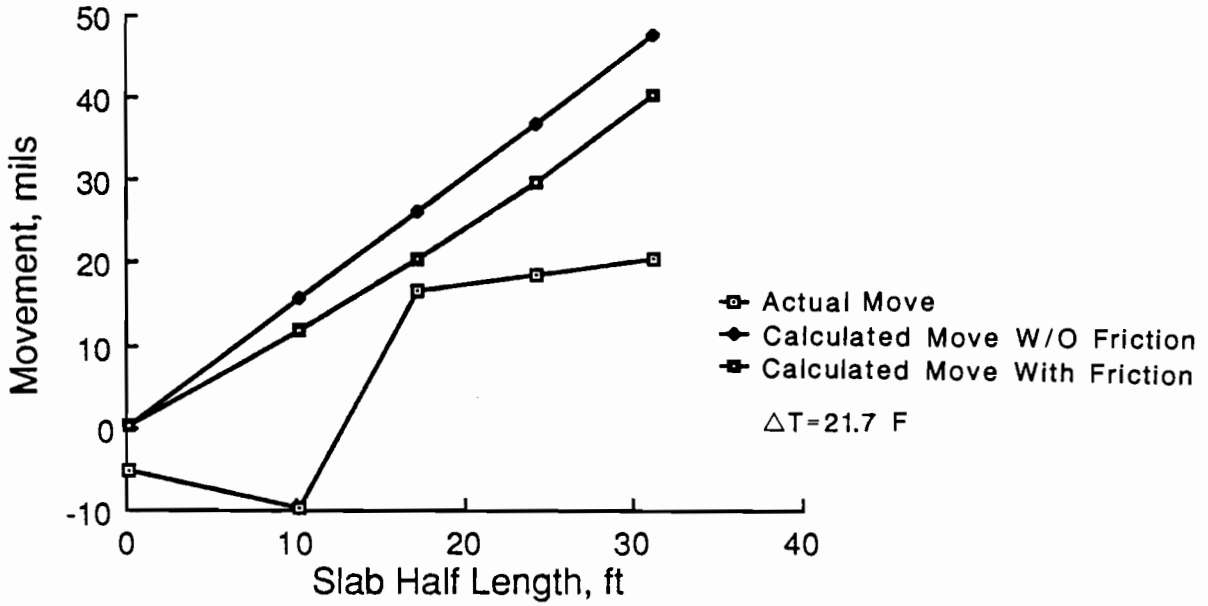

Fig 6.50. Horizontal movements for continuous tests for simulated 64-foot slab on asphalt stabilized subbase.

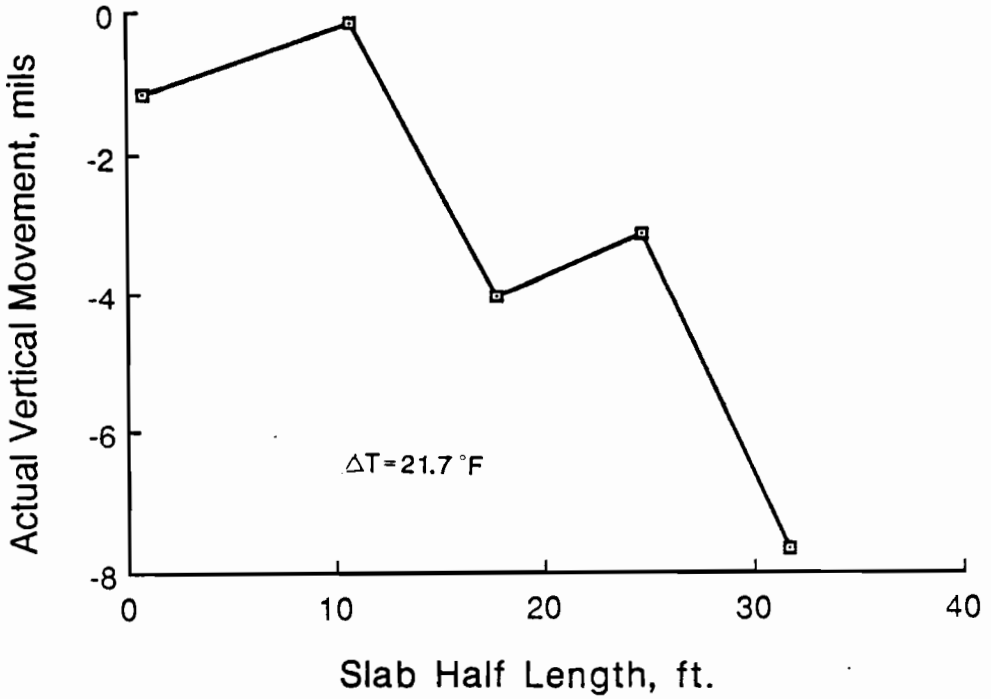

Fig 6.51. Vertical movement for continuous test for simulated 64-foot slab on asphalt stabilized subbase.

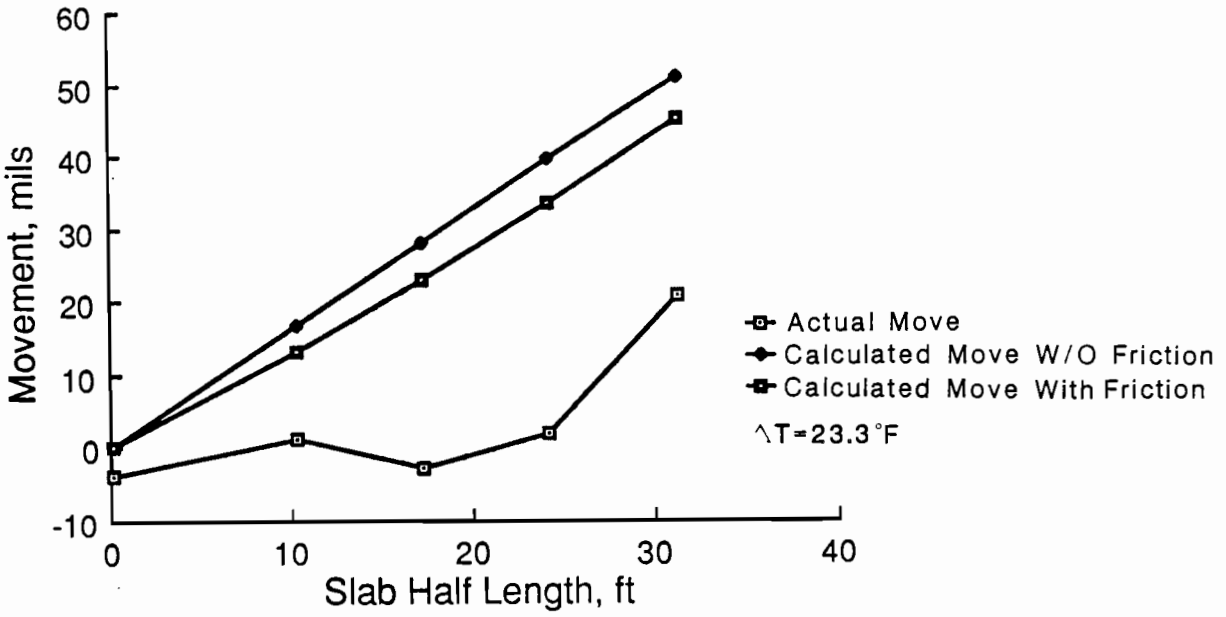

Fig 6.52. Horizontal movements for continuous test for simulated 64-foot slab on lime treated clay subbase.

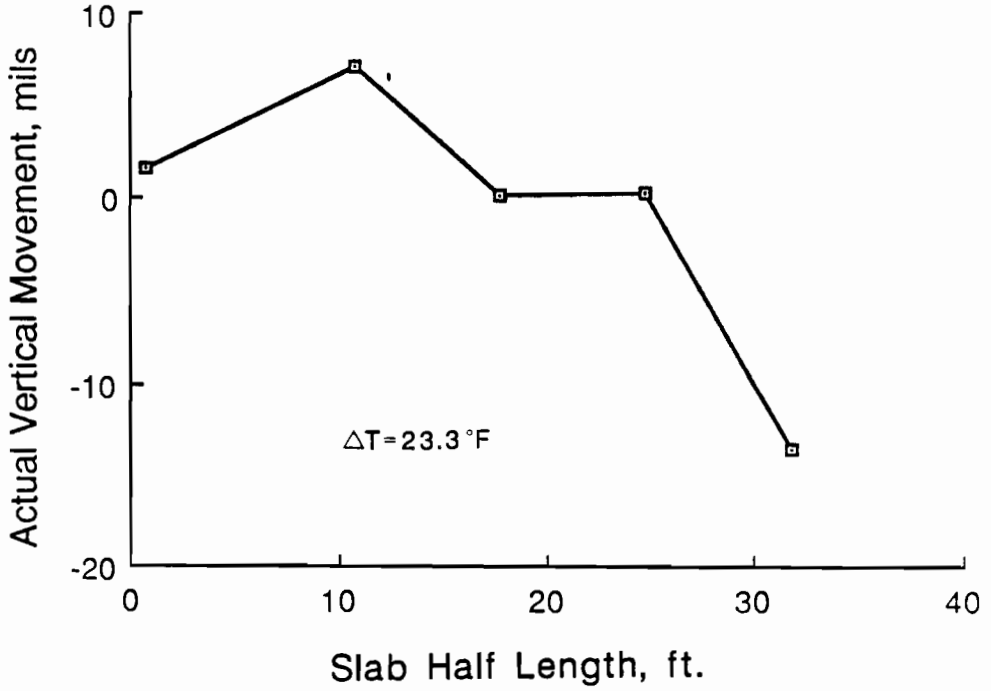

Fig 6.53. Vertical movement for continuous test for simulated 64-foot slab on lime treated clay subbase.

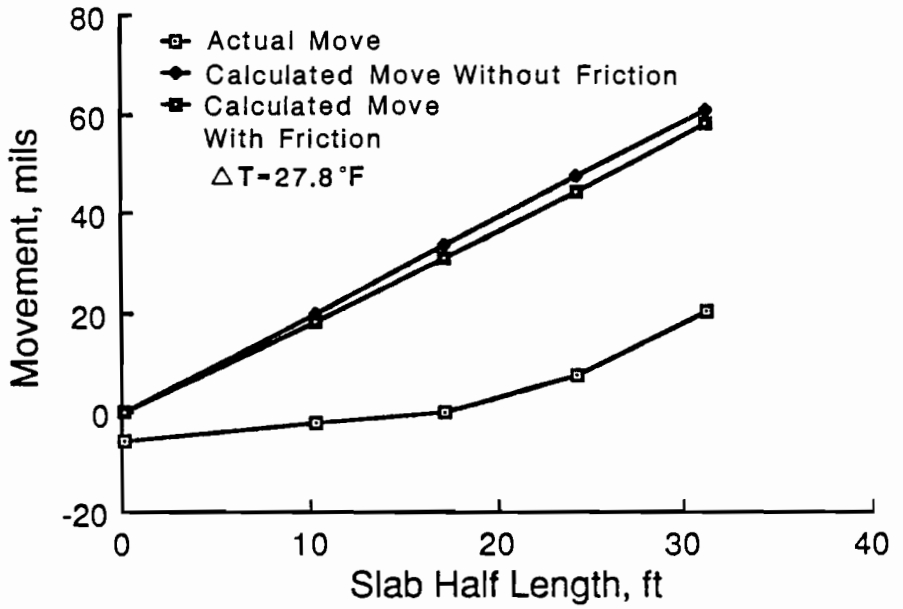

Fig 6.54. Horizontal movements for continuous test for simulated 64-foot slab on unreated clay subbase.

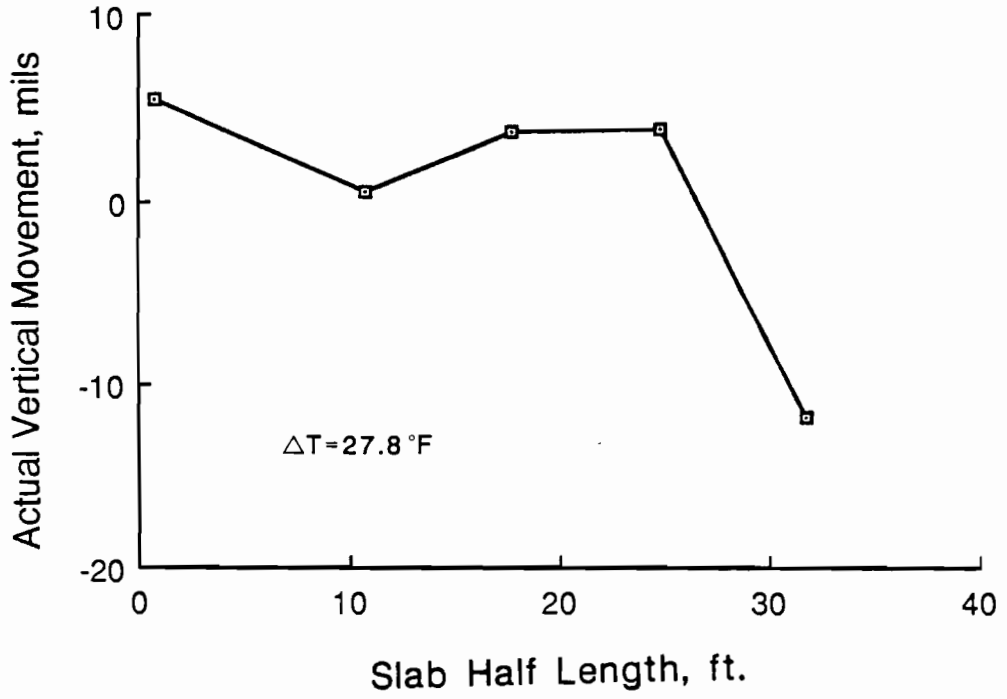

Fig 6.55. Vertical movement for continuous test on simulated 64-foot slab on untreated clay subbase.

cracking will not occur as the concrete gains strength. This can be accomplished by maintaining a constant temperature during curing of the test specimen by use of a thermal blanket or a temperature controlled insulation box, or by increasing the slab's depth, since slab weight has been proven not to have any significant effect on subbase friction for stabilized subbases. Curing effects must also be minimized if proper subbase frictional information is to be obtained. Running these tests on hot dry days did provide a large change in temperature, but it increased slab curling. This can be altered by uniform heating by, again, use of a thermal blanket or a temperature controlled box covering the entire slab.

CHAPTER 7. DISCUSSION OF EXPERIMENTAL RESULTS

The objective of this chapter is to discuss the results obtained from Phase I and Phase II of this project. Subbase resistance values are summarized and recommended for computer implementation. A comparison of computed and measured slab movements obtained from Phase I is made. Computed slab stresses are also given for each slab tested in Phase I.

PHASE II DISCUSSION

Observation of the failure plane pointed to failure within the subbase material for stabilized subbases and at the slab-subbase interface for unbound subbases. This is shown in Fig 7.1. This leads the friction analysis to a strength of materials analysis. This point can be explained further by using the results obtained from the untreated clay and lime–treated clay tests. Figure 7.2 shows the frictional resistance at sliding for both subbases using the 3.5-inch and simulated 7-inch slab results. Failure occurs at roughly the same amount of movement and frictional resistance for the lime–treated clay, which denotes a material failure within the subbase, as observed. Doubling the slab weight on the untreated clay, however, causes the point of failure to roughly double both the movement and frictional resistance at sliding. This is representative of the classic frictional behavior, where the amount of resistance is directly dependent on the nominal weight of the object when sliding occurs between two materials.

A material failure is only slightly dependent on its overburden pressure, which is supplied by the slab's weight. Frictional resistance for stabilized subbases should be looked into as a two–dimensional stress-strain problem instead of taking the classical friction approach. This can best be described by the use of Mohr's circle. Figure 7.3 depicts this by again comparing the lime–treated clay and untreated clay subbases. The magnitude of the shearing stress varies greatly for the untreated clay, depending on its principal stress, which is dependent on slab weight and stays relatively the same for the lime–treated clay, which means the shearing stress is not dependent on slab weight. Therefore, the use of the coefficient of friction is not feasible in design when a stabilized subbase is used. Every stabilized subbase tested showed minimal gain in frictional resistance after doubling the slab's weight. The friction movement profiles contained in this chapter should be the only items used in determining concrete stress due to subbase friction. The coefficient of friction needs slab

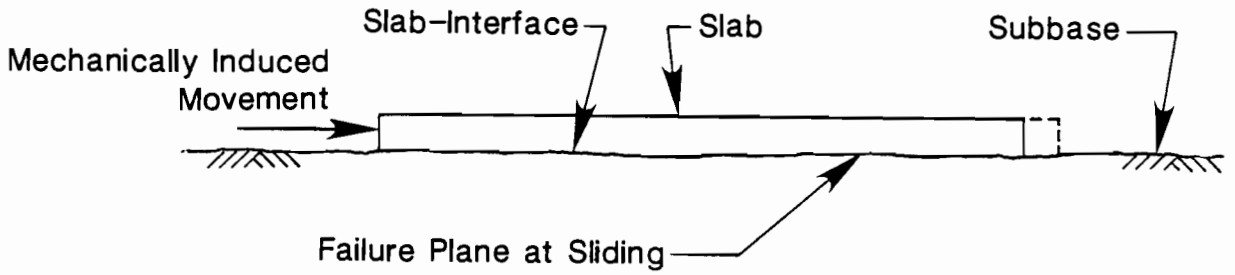

(a) Loose unbound subbase.

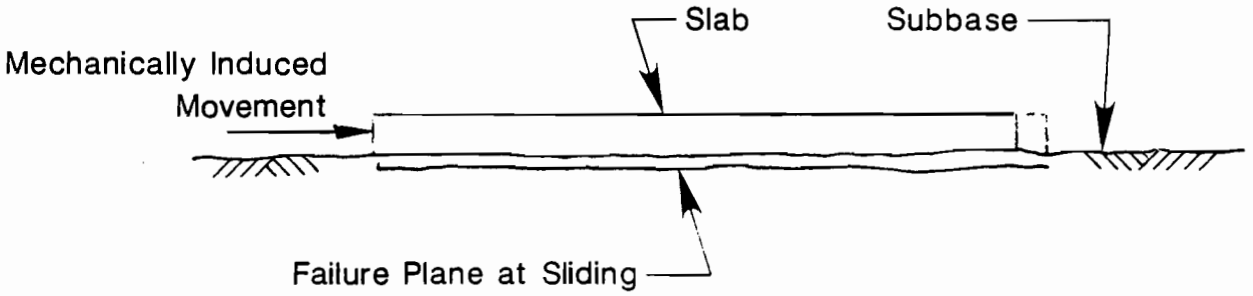

(b) Stabilized subbase.

Fig 7.1. Failure plane location for (a) loose unbound subbase and (b) stabilized subbase.

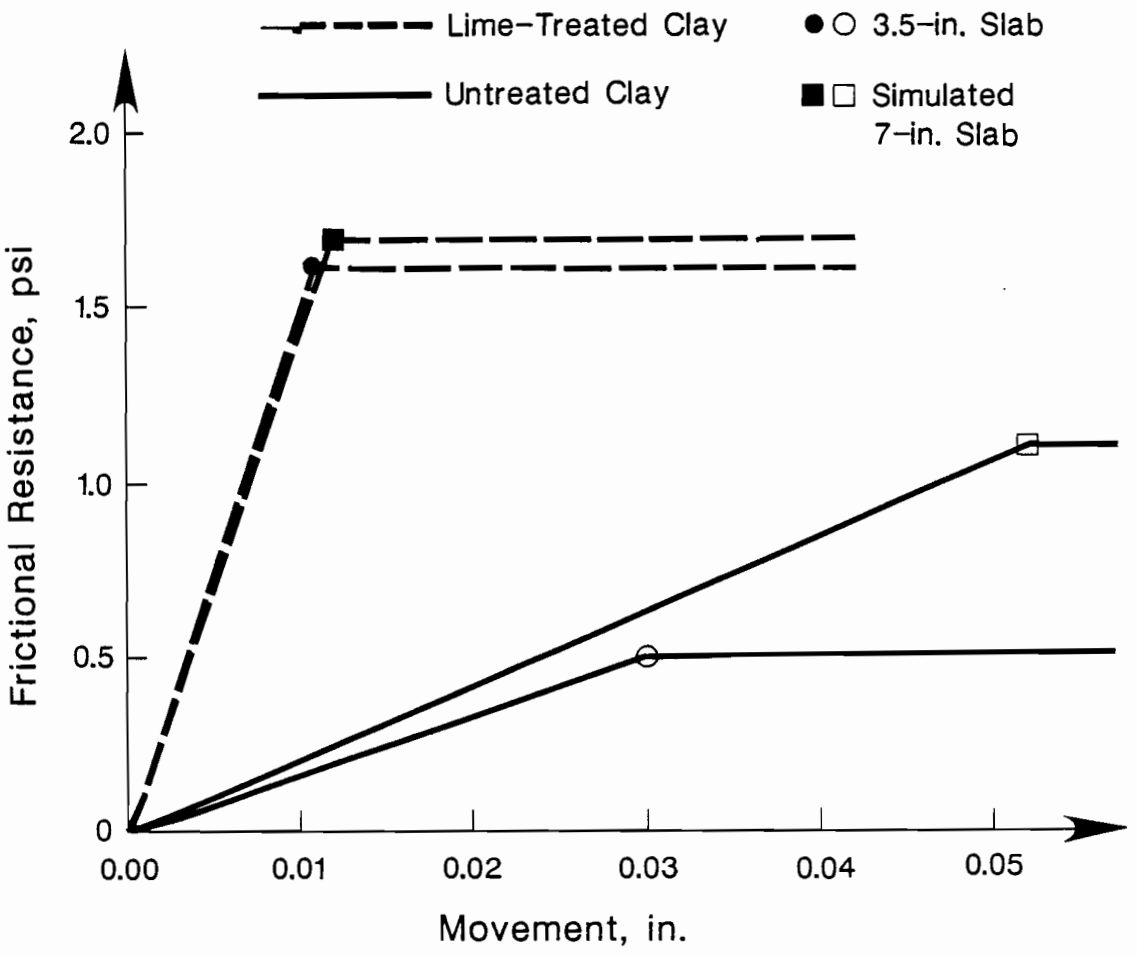

Fig 7.2. Stabilized and unbound subbase comparison using a lime–treated clay and an untreated clay.

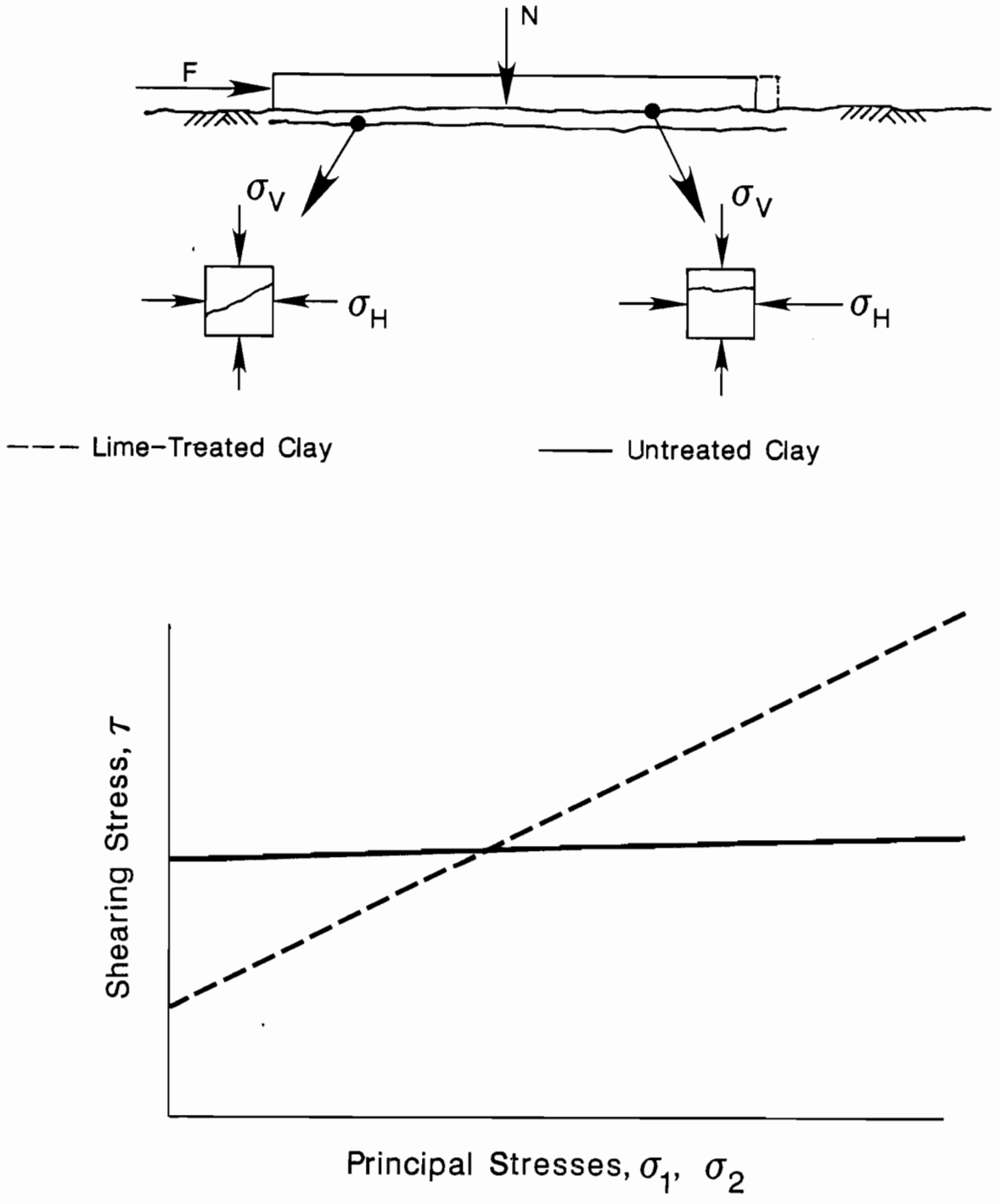

Fig 7.3. Stabilized and unbound subbase comparison on shearing stress using Mohr's circles.

weight as an additional parameter in determining frictional resistance. Because this parameter is does not affect the restraint with stabilized subbases, this can be a time saver in the design process. The graph in Fig 7.4 should be the only tool needed for determining concrete stresses due to subbase friction. A push-off test could be run on a particular stabilized subbase using a minimal depth concrete slab and a maximum depth concrete slab. All other depths that are designed for can be interpolated between the two graphs obtained in the experimentation. On the other hand, if a loose unbound subbase were to be tested and used in the design, only one push-off test could be run and a coefficient of friction could be obtained for design of slabs with any depth.

There is one more point important point that should be brought out in this study. Usually the magnitude of frictional restraint is looked upon only for comparing subbases and not the movement at which sliding is induced. The addition of stabilized agents increases the shearing stiffness of the subbases, thus reducing the movement at the point of sliding. Figure 7.5 shows schematically what would be ideal results of the push-off tests run on the lime–treated and untreated clay subbases using 3.5-inch slab sections. The shaded areas in Fig 7.5 represent stored energy in the pavement due to frictional restraint. If tip movements were equivalent for two identical slabs, the energy stored in the slab on the untreated clay would be much smaller than the energy stored in the slab on the lime–treated clay. It is recognized that the movements could never be equivalent; due to different subbase-slab interaction, but if both slabs experienced a tip movement of 0.01 inch there would be over eight times the stored energy in the slab on the lime–treated clay as in the slab on the untreated clay. Even though larger movements will occur in the slab on the untreated clay for an equivalent change in temperature, thus increasing its shaded area, the point can still be made; even though the peak frictional restraint for the lime–treated clay is twice that of the untreated clay, the point at which sliding is induced is equally as important when comparing frictional restraints for various subbases. Proper evaluation of subbases on frictional restraint should be given as shown in Figs 7.6 and 7.7, where both the peak frictional resistance and movement at sliding can be reviewed.

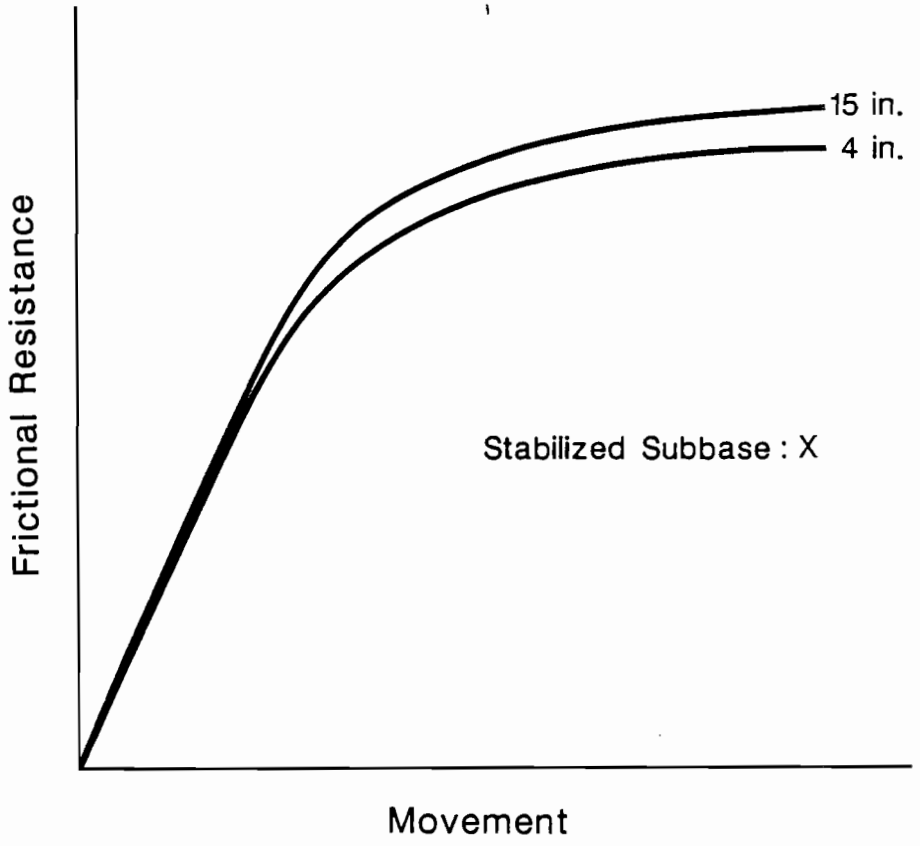

Fig 7.4. Recommended design tool for use in determining concrete stresses due to subbase friction.

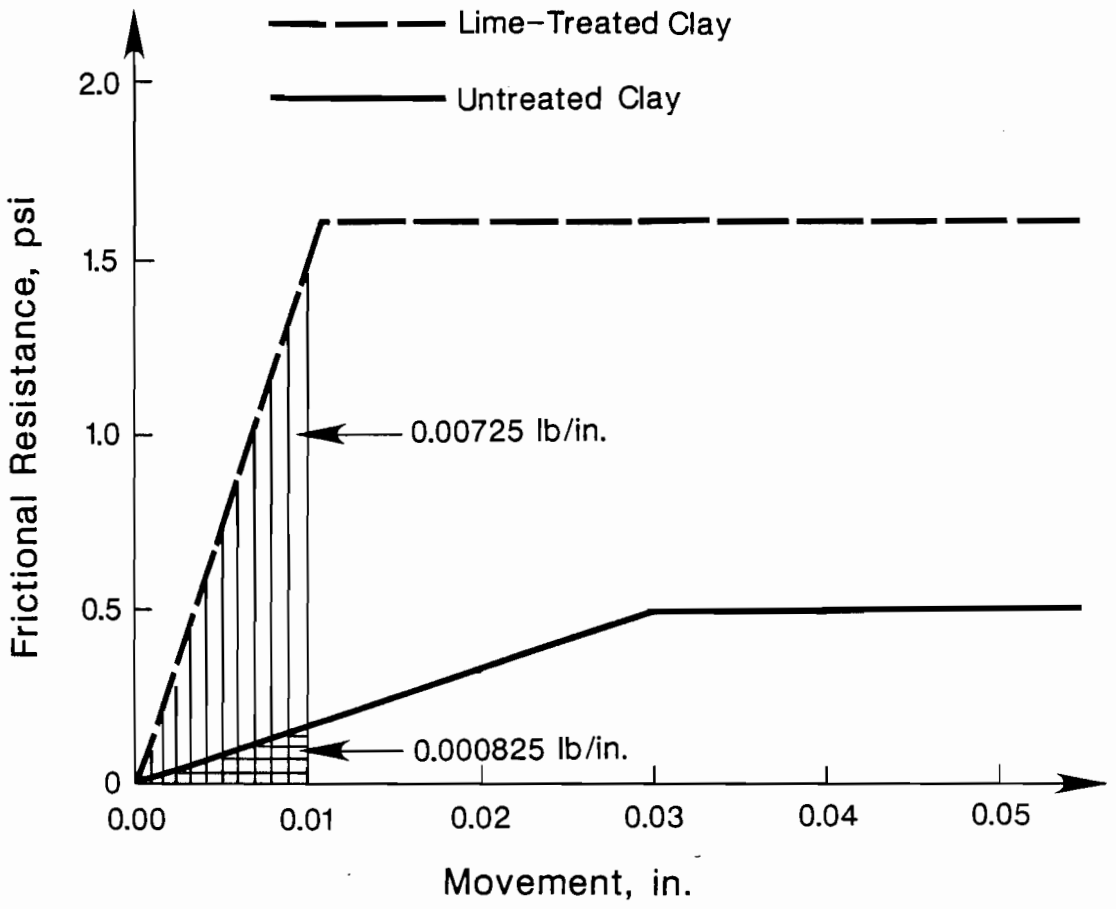

Fig 7.5. Subbase friction comparison by using an energy approach.

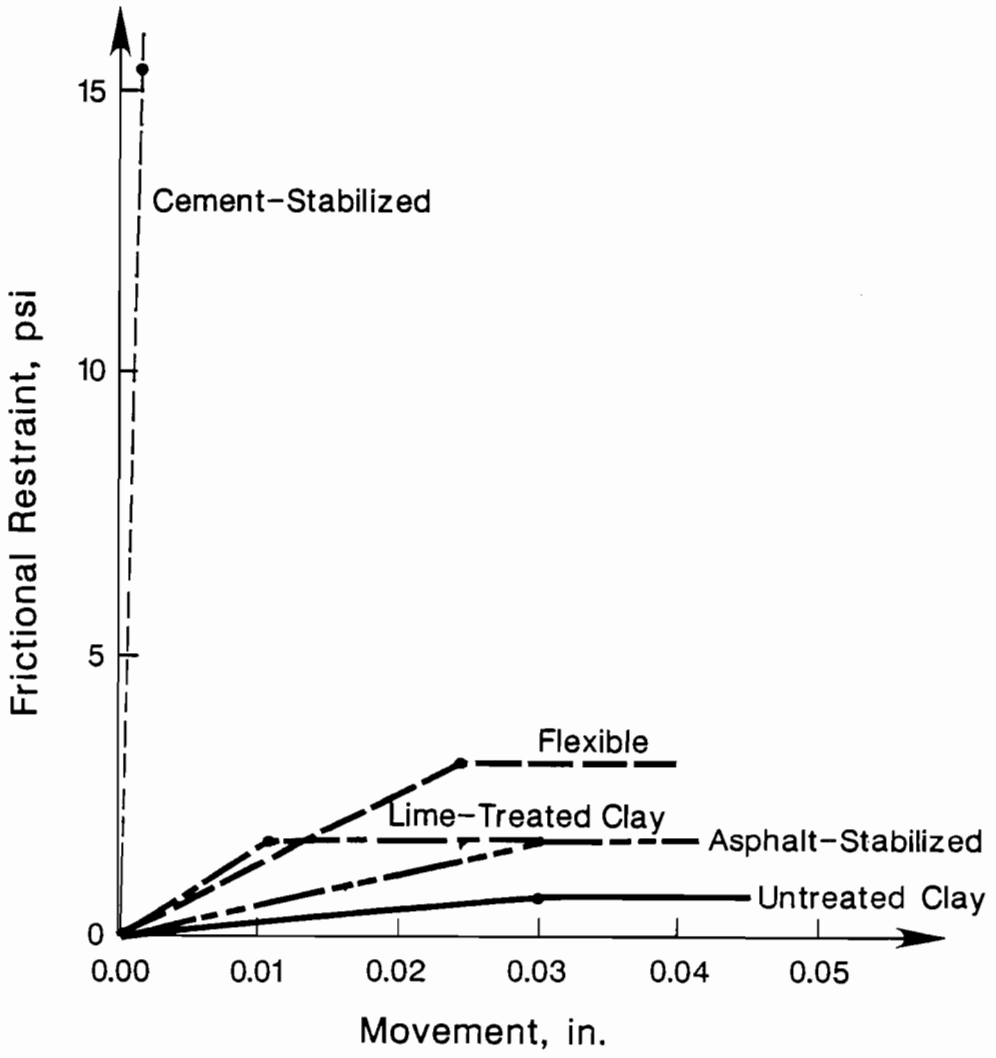

Fig 7.6. Push-off results for various subbases tested using a 3.5-inch slab.

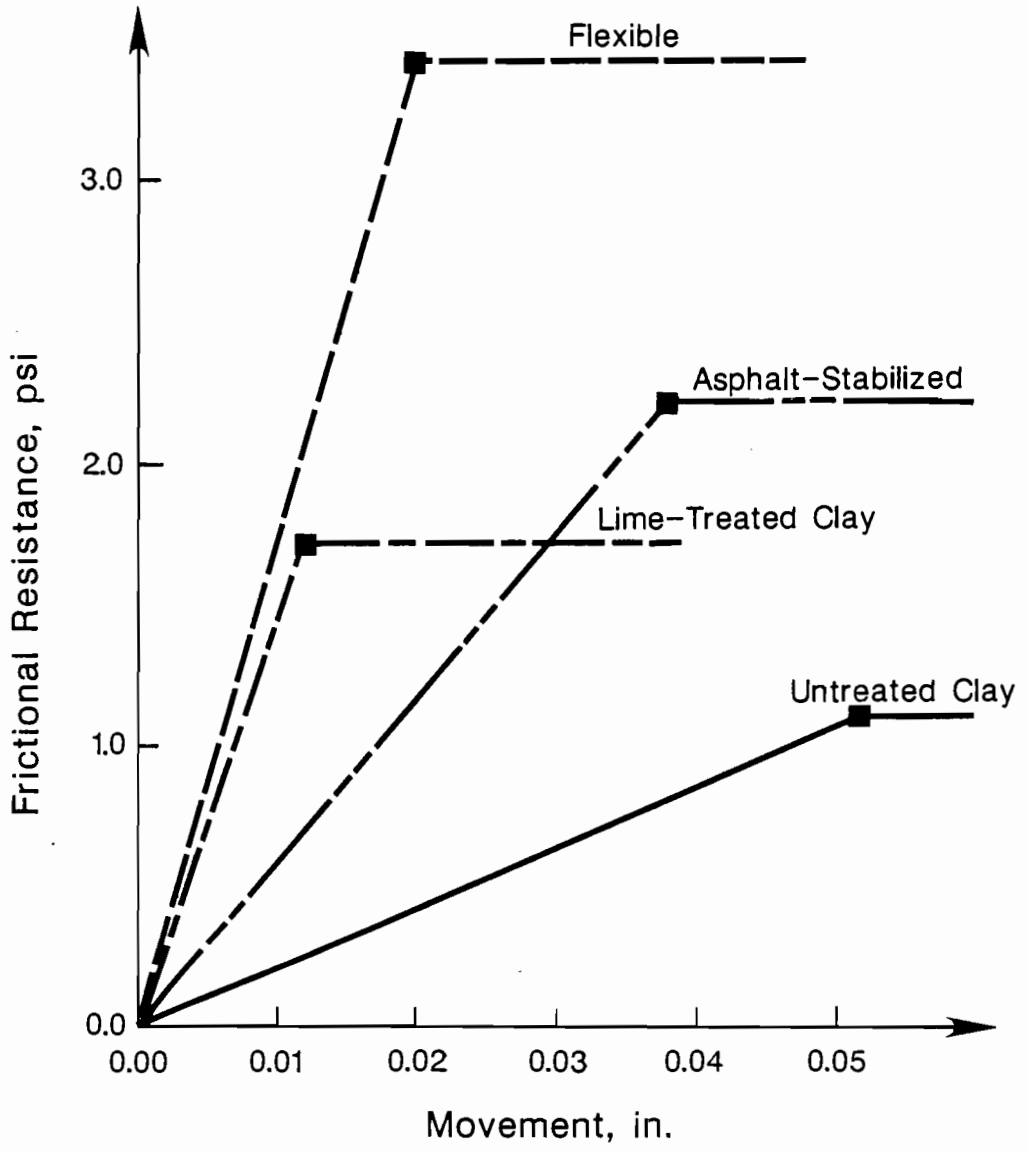

Fig 7.7. Push-off results for various subbases tested using a simulated 7-inch slab.

COMPARISON OF COMPUTED AND MEASURED SLAB MOVEMENTS

Table 7.1 shows a summary of the results for the Phase I run on the various subbases for movements at the free end of the test slabs. The vertical movements showed actual lifting due to friction resistance, but it primarily gave the curling effect results. At night, the top of the slab is cooler than the bottom, and, thus, lifting occurs at the slab's edges. This was the case for the flexible subbase continuous test where a change of 3 mils was recorded in the lifting direction. During the day time the opposite occurs. The other continuous tests showed anywhere from an 8–mil to a 14–mil drop at the free end of the slab.

Not only did the vertical slab profiles vary from slab to slab but their pinned end movements varied also. Therefore, the acting center of each slab varied. Even though the temperature gradients also varied between slabs in Phase I, it was mainly the first two reasons that keep valid subbase information from being obtained. Therefore, a comparison of slab movements between slabs would be worthless.

When comparing actual slab movements to computed slab movements, as shown in Table 7.1, there is a large difference. The actual free-end horizontal movements represent anywhere between 25 and 50 percent of the calculated free-end horizontal movements using the friction profiles obtained from Phase I for each continuous test. This large difference can best be explained by the failure of the anchor in pinning one of the slab ends. Since movements were recorded for all slabs at the pinned end, the acting center of each slab would be better represented as somewhere closer to the actual center of each slab. Thus, the computed movements would be much smaller using a shorter slab length and would compare more closely to the measured movements obtained in Phase I.

There are also important results obtained from the computer runs made using PCP1. Table 7.2 shows the major components of data taken from the outputs. It was interesting to see that, for all four slabs tested under each particular change in temperature, the resulting calculated movements were only slightly less than the calculated movements without friction, but every test had reached the maximum frictional resistance somewhere along the length of the slab. Therefore, design of jointed pavements of these or longer lengths must require frictional resistance data beyond sliding for average daily temperature cycles. The computed pinned-end stress did not seem to vary considerably among subbases. The calculated pinned-end stresses varied between 65 and 150 psi for various temperature changes. A crack will usually develop when a concrete pavement encounters a stress between 200 and 400 psi in

TABLE 7.1. SUMMARY OF CONTINUOUS TEST RESULTS FOR VARIOUS SUBBASES

Subbase Type	Slab Half Length (feet)	Temperature Gradient (°F)	Actual Free End Movements		Calculated Horizontal Movements	
			Horizontal (mils)	Vertical (mils)	w/o Friction	w/Friction
Flexible	22	-14.7	-5.4	2.9	-24.6	-18.3
Asphalt–stabilized	32	21.7	20.5	-7.8	47.6	40.3
Lime–treated Clay	32	23.3	20.8	-14.1	51.0	45.0
Untreated Clay	32	27.8	20.2	-12.4	60.9	58.3

TABLE 7.2. CALCULATED RESULTS SIMULATING CONTINUOUS TESTS USING FRICTION–MOVEMENT PROFILES OBTAINED FROM PUSH–OFF TESTS, CONCRETE PROPERTIES OBTAINED FROM EXPERIMENTATION, AND COMPUTER MODEL PCP1 (REF 3)

Subbase Type	Slab Half Length (feet)	Change in Temperature (°F)	Calculated Free End Movement (mils)	Calculated Pinned End Concrete Stress (psi)	Point of Maximum Friction From Pinned End (feet)
Flexible	22	-14.7	-18.8	-150	22.0
Asphalt Stabilized	32	21.7	41.5	153	24.5
Lime Treated Clay	32	23.3	46.3	143	8.8
Untreated Clay	32	27.8	59.8	65	16.8

tension for most concrete pavements. These stresses shown are due only to frictional restraint on an average daily temperature cycle; when stresses due to curling and traffic loading are added, the tensile capacity of the pavement can be reached. It is for this reason that the magnitude of stress due to frictional restraint should be known for proper design on concrete pavements. The smaller the slabs, as for a shorter joint spacing, the less movements and thus the less importance in distinguishing the frictional characteristics of the subbase.

SUMMARY

Table 7.3 gives peak resistance and movement at sliding values for various slab depth for the five subbases tested in this project. The first two columns are values obtained in Phase II of the experimentation. The last two columns are recommended values for thicker, more commonly used slab depths. Their values were derived by extrapolation of the friction-movement profiles in Chapter 6. Table 7.3 can be used for the recommended friction values needed for the JRCP, CRCP, and PCP computer programs. Although these values provide a more precise design for stabilized subbases it is recommended that a further step be taken. All of the computer programs listed above have several options in creating the friction profile. It is recommended that, if only the peak resistance and movement at sliding values are given, the parabolic option be chosen to fit a curve between the origin and the given data point. This better models actual slab-subbase interaction as compared to a straight line, as seen in the friction-movement profiles in Chapter 6. The furthest step in accurately defining slab-subbase interaction is to put in all of the data points that define the actual friction-movement profile for the particular subbase. This is what is most recommended because the parabolic curve induced by the program only partially simulates the actual slab-subbase interaction with friction. Loose unbound subbases seem to fit only the parabolic shape, but the stabilized subbases portray a steep initial slope and then flatten out near sliding. This behavior can be seen in all of the friction-movement profiles illustrated in Chapter 6.

TABLE 7.3. RECOMMENDED PEAK FRICTIONAL RESISTANCES AND MOVEMENT AT SLIDING FOR VARIOUS SUBBASES

	Experimental Results		Recommended Values	
Subbase Type	Slab Depth (3.5 inches)	Slab Depth (7 inches)	Slab Depth (10.5 inches)	Slab Depth (14 inches)
Flexible*	3.0 psi [0.024 in.]	3.4 psi [0.020 in.]	3.6 psi [0.015 in.]	3.7 psi [0.015 in.]
Asphalt–stabilized	1.6 psi [0.030 in.]	2.2 psi [0.038 in.]	2.5 psi [0.035 in.]	2.8 psi [0.035 in.]
Cement-stabilized	15.4+ psi [0.001+ in.]	-- [--]	30.0 psi [0.002 in.]	30.0 psi [0.002 in.]
Lime-treated	1.6 psi [0.011 in.]	1.7 psi [0.012 in.]	1.7 psi [0.012 in.]	1.8 psi [0.013 in.]
Untreated clay	0.6 psi [0.030 in.]	1.1 psi [0.052 in.]	1.5 psi [0.065 in.]	1.8 psi [0.080 in.]

* Experimental slabs were 4 inches and 8 inches; therefore recommended values will be for 12 inches and 16 inches slabs.

CHAPTER 8. CONCLUSIONS AND RECOMMENDATIONS

CONCLUSIONS

(1) The magnitude of frictional resistance and the point at which sliding occurs varies from subbase to subbase.

(2) The addition of stabilizing agents to a subbase will offer higher frictional resistance and the point at which sliding occurs will be a smaller movement as compared to an unbound subbase.

(3) The magnitude of subbase friction is dependent on three components, namely bearing, shear, and adhesion at the slab-subbase interface.

(4) If the adhesion component is high enough, the failure plane at sliding will not be at the slab-subbase interface, but within the subbase. This holds true for all stabilized subbases tested in this project.

(5) The failure plane at sliding will be at the slab-subbase interface for loose unbound subbases.

(6) If failure occurs within the subbase as for stabilized subbases, frictional information can be looked at as a two-dimensional stress analysis, where the shearing is only slightly influenced by the overburden pressure supplied by slab weight.

(7) If failure occurs at the slab-subbase interface, then the magnitude of frictional resistance is directly dependent on slab weight.

(8) A coefficient of friction can be used in design of concrete pavements for determining frictional resistances for loose unbound subbases, but not for stabilized subbases.

(9) Subbase friction for stabilized subbases must be determined by a friction–movement profile obtained through a push-off test.

(10) Push-off tests should be repeated over time due to the recognition that the initial test will yield higher frictional resistances than steady-state conditions.

(11) All friction testing in this project was done under initial conditions. Actual frictional resistances will be slightly lower due to the steady-state behavior of pavements over their subbases and slower induced loading rates.

(12) All oils and emulsifications tested in the past for reducing frictional restraint have failed.

(13) The slab cast on top of the cement-stabilized subbases appeared to be glued to it at the slab-subbase interface. As in another past experiment where a slab was cast on top of a concrete base, the slabs could not be moved without exceeding the capacity of the loading equipment.

(14) The order of frictional resistances when comparing subbases can be determined only by observing the areas under each friction-movement profile for a given free-end displacement. This can be termed as an energy approach for comparing subbase friction information.

(15) This energy approach leads to listing the cement–stabilized subbase, flexible subbase, lime-treated clay subbase, asphalt–stabilized subbase, and untreated clay subbase as offering the largest to the smallest amount of frictional resistance.

(16) The pinned anchor at one end of each test slab worked effectively as an anchor for the push-off tests but was ineffective at simulating the center-span of a slab for the continuous tests.

(17) Different vertical profiles were obtained during the continuous tests due to varying curling effects for each slab.

(18) Small horizontal movements were encountered in the continuous test, making extraction of subbase friction information difficult.

(19) Varying curling effects, anchor movements, slab lengths, and changes in temperature made it impossible to compare subbase frictional resistances.

(20) Subbase friction has a direct effect on concrete stresses, steel stresses, joint openings, and crack widths for concrete pavements.

(21) Subbase friction comes into play only when movements are induced into the pavement due to shrinkage, thermal variations, moisture variations, and Poisson's effect.

(22) The cracking of the slab cast on top of the cement stabilized subbase prompted concern over movements relative to the slab and its subbase caused by subbase movements induced by the variations discussed in Item 21.

(23) The friction-movement response of a subbase up until sliding is dependent on the elastic properties of the subbase in the shearing direction. A stabilized

subbase will offer a higher shearing stiffness due to its increased strength, and, thus, a steeper slope will be given.

(24) The point at which sliding occurs and the friction-movement response after sliding is dependent on the roughness characteristics at the slab-subbase interface if failure occurs there, or on the strength of the subbase material in shear if the failure occurs within the subbase.

(25) If the subbase is thin enough and adheres to the bottom of the pavement, sliding may be induced between the subbase and its subgrade. This was the case for the push-off test run on the 3/4-inch asphalt–stabilized subbase over the cement–stabilized subbase. Elastic response and the point at which sliding is induced may be dependent on both the subbase and its subgrade if the stabilized subbase is thin.

RECOMMENDATIONS

(1) Push-off tests should be repeated so that a steady-state condition can be established for more accurate friction information.

(2) Push-off tests should be run for various subbase thicknesses, temperatures, and moisture conditions so that these conditions can be incorporated in the friction-movement profiles.

(3) Maximum and minimum possible slab depths should be used in push-off tests so that two friction-movement profiles can be given for each subbase condition. All designed depths in between can be interpolated between the two profiles.

(4) Because failure occurs within the stabilized subbases, subbase friction information may be obtained through triaxial shear tests run on core samples taken from the subbase, thus eliminating the need for casting concrete slabs and running field experimentation. Many cores could be taken all over the state and tested in-house for subbase variability caused by varying construction techniques and materials.

(5) Direct shear tests can also be run on core samples for thin subbases on subgrades.

(6) Continuous tests should be run so that actual horizontal movements can be compared for various subbases and also to obtain good subbase friction information. Because a slab will have experienced many thermal cycles before testing, the steady-state frictional condition will have been reached. Actual loading rates would lead to more accurate friction information also.

(7) It is recommended that many modifications be undertaken if the continuous tests are undertaken again.

   (a) The pinned-anchor scheme failed at fixing one end of the slab. It is recommended that the center for the slab remain at the center and, to help insure that no movements occur at center-span, that vertical dowel bars and/or a concrete anchor be placed at center-span at casting.

   (b) A much longer slab should be cast. Care must be taken so that premature cracking will not occur as the concrete gains strength. This can be accomplished by use of a thermal blanket or a temperature–controlled insulation box during the curing stages of the slabs.

   (c) A much larger temperature change can be used. This can be induced through artificial heating and cooling inside an insulated box.

   (d) Uniform heating and cooling across the depth of the slab is important so that curling effects will be eliminated. If the vertical profiles are not similar, then horizontal movements cannot be properly compared for various subbases. This can be accomplished through slow heating and cooling, using sophisticated temperature control equipment.

(8) If similar vertical slab profiles are encountered in the field using daily heating and cooling, then a comparison can be made between various subbases with respect to subbase friction when actual curling effects are present.

REFERENCES

1. Noble, C. S., B. F. McCullough, and W. R. Hudson, "Summary and Recommendations for the Implementation of Rigid Pavement Design, Construction, and Rehabilitation Techniques," Research Report 177-22F, Center for Transportation Research, The University of Texas at Austin, September 1979.
2. Klingner, Richard E. , "Theory of Concrete Behavior," CE383L Class Notes, The University of Texas at Austin, Fall 1986.
3. Mendoza-Diaz, Alberto, B. Frank McCullough, and Ned H. Burns, "Behavior of Long Prestressed Pavement Slabs and Design Methodology," Research Report 401-3, Center for Transportation Research, The University of Texas at Austin, November 1986.
4. Chia, Way Seng, B. Frank McCullough, and Ned H. Burns, "Field Evaluation of Subbase Friction Characteristics," Research Report 401-5, Center for Transportation Research, The University of Texas at Austin, November 1986.
5. Stott, J. P., "Tests on Materials for Use as Sliding Layers Under Concrete Road Slabs," Road Research Laboratory, DSIR, 1961.
6. Goldbeck, A. T., "Friction Tests of Concrete on Various Subbases," Public Roads, United States Department of Agriculture, July 1924.
7. Timms, A. G., "Evaluating Subbase Friction Reducing Mediums for Rigid Pavements," Highway Research Record 60, Highway Research Board, Washington, D. C., 1963.
8. Friberg, B. F., "Frictional Resistance Under Concrete Pavements and Restraint Stresses in Long Reinforced Slabs," Proceedings, Highway Research Board, Vol 33, 1934.
9. McCullough, B. Frank, and Alberto Mendoza, "Report on a Mechanistic Analysis of the PCC Aprons at King Fahd International Airport, Kingdom of Saudi Arabia," Austin Research Engineers, October 1985.
10. Westergaard, H. M., "Analysis of Stresses in Concrete Roads Caused by Variations of Temperature," Public Roads, May 1927.
11. Guide Specifications for Highway Construction, American Association of State Highway and Transportation Officials, 1985.

12. Standard Specifications for Construction of Roads and Bridges on Federal Highway Projects, Unites States Department of Transportation, 1979.

13. Construction Report, Texas State Department of Highways and Public Transportation, Construction Division, March 1, 1986.